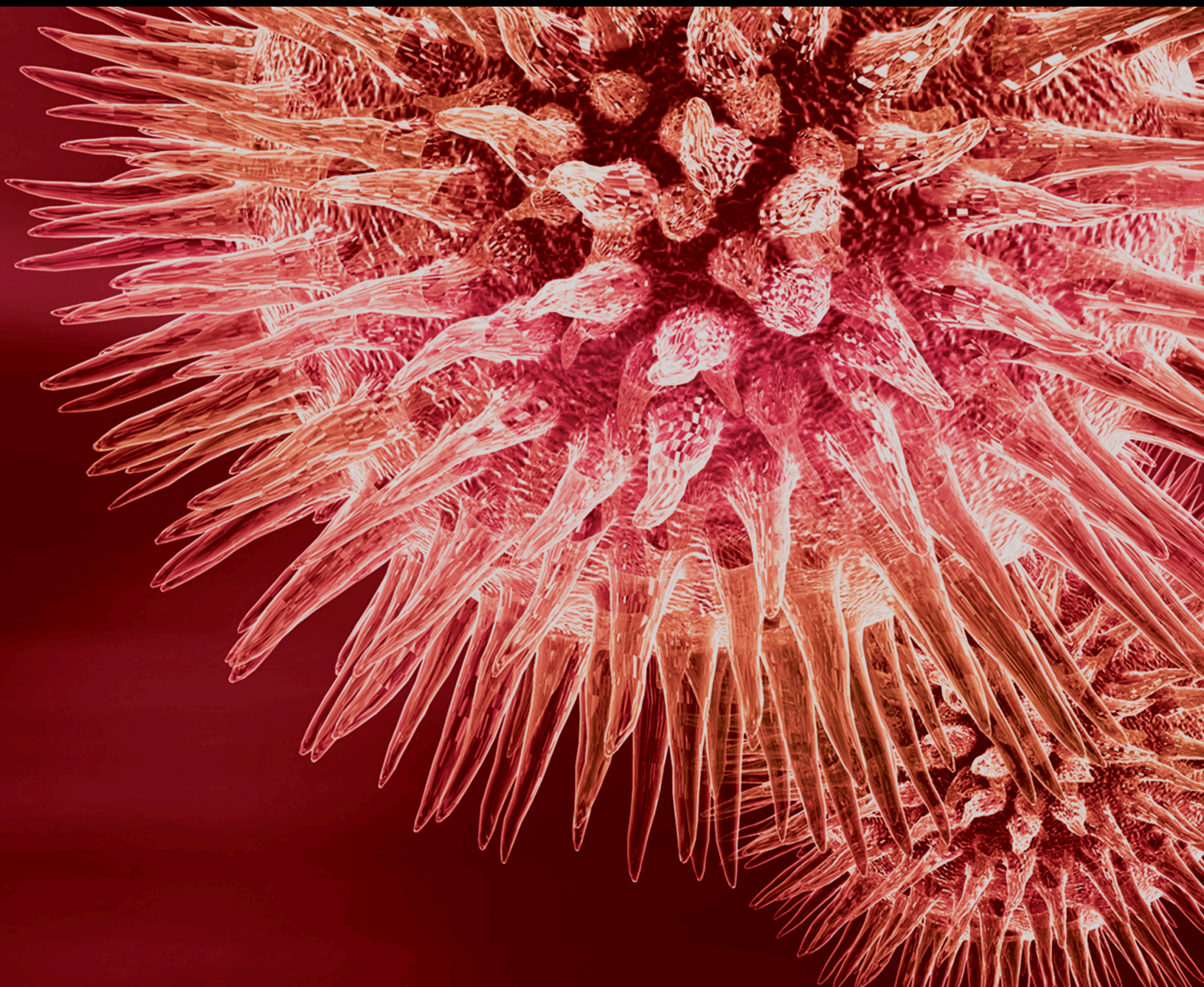# New Biomaterials and Regenerative Medicine Strategies in Periodontology, Oral Surgery, Esthetic and Implant Dentistry 2018

Lead Guest Editor: David M. Dohan Ehrenfest
Guest Editors: Adriano Piattelli, Gilberto Sammartino, and Hom-Lay Wang

New Biomaterials and Regenerative Medicine Strategies in Periodontology, Oral Surgery, Esthetic and Implant Dentistry 2018

New Biomaterials and Regenerative Medicine Strategies in Periodontology, Oral Surgery, Esthetic and Implant Dentistry 2018

Lead Guest Editor: David M. Dohan Ehrenfest
Guest Editors: Adriano Piattelli, Gilberto Sammartino, and Hom-Lay Wang

Editorial Board

Contents

Editorial

New Biomaterials and Regenerative Medicine Strategies in Periodontology, Oral Surgery, Esthetic and Implant Dentistry 2018

David M. Dohan Ehrenfest (ID),[1,2,3] **Adriano Piattelli,**[4]
Gilberto Sammartino,[5] **and Hom-Lay Wang** (ID)[2]

[1]*Department of Oral and Maxillofacial Surgery, The University of Michigan Health System, Ann Arbor, Michigan, USA*
[2]*Department of Periodontics and Oral Medicine, The University of Michigan, School of Dentistry, Ann Arbor, Michigan, USA*
[3]*LoB5 Research Unit, School of Dentistry & Research Center for Biomineralization Disorders, Chonnam National University, Gwangju, Republic of Korea*
[4]*Department of Medical, Oral and Biotechnological Sciences, G. D'Annunzio University of Chieti-Pescara, Chieti, Italy*
[5]*Department of Oral Surgery, Faculty of Medicine, University of Naples Federico II, Naples, Italy*

Correspondence should be addressed to David M. Dohan Ehrenfest; lob5@mac.com

The development of new biomaterials and regenerative medicine strategies appears as a major field of research in periodontology, oral surgery, and esthetic and implant dentistry (the POSEID disciplines) in the current era of tissue engineering and quest for tissue regeneration. Biomaterial research remains the core science of all these opportunities of regenerative treatments of the maxilla and improvement of oral rehabilitation [1].

In our previous special issues in 2015 and 2016, we selected a series of articles with new data on a wide range of topics in biomaterials and regenerative research in periodontology, oral surgery, and esthetic and implant dentistry, and we highlighted how these interconnected fields of research are both transversal (multidisciplinary) and translational (from basic sciences to clinical applications). In this 2018 special issue, we selected articles with the same insight and wished to illustrate the complexity of this research field.

In our previous editorials in 2015 and 2016, we described particularly the strength, weakness, opportunities, and threats on these disciplines and how research in implantable materials, particularly dental implants (new implant design and surfaces) [2], bone materials, or surgical adjuvants [3], is affected by not only scientific bias and misunderstandings, but also industrial and financial interferences, creating many inaccuracies in the literature. Despite the incredible potential and revolution these disciplines are supporting for patients and the clinical approach of oral rehabilitation, there is also a major threat to the credibility of this field.

In the 2016 editorial of this special issue, we described particularly some ethical and legal issues related to this field, especially concerning the lack of transparency and control in dental implants (with so many illegal pirate productions or the lack of quality controls in general) or through the dramatic example of L-PRF (leukocyte- and platelet-rich fibrin) and related blood derivatives (with many providers marketing kits and devices for blood concentrates without any legal authorization in many countries, for example, A-PRF and i-PRF) [4]. These major issues were creating confusion in the mind of users, but also in the literature some researchers received undisclosed funding to write articles about techniques or materials [5], which sometimes were marketed but not even legally authorized! This was one of the major threats to this research field: how the credibility of some research topics was affected by the lack of ethics of some authors and merchants [5].

In 2018, unfortunately, very little has evolved. As a strange matter of fact, the development of these new biomaterials and regenerative medicine strategies seems to have reached a plateau that no one seemed to expect so early, before any major breakthrough or revolution of the clinical paradigms. As we can observe in the current literature, research topics seem to be permanently turning around, and we see currently very little major developments.

In this 2018 special issue on new biomaterials and regenerative medicine strategies in periodontology, oral surgery, and esthetic and implant dentistry, we continued our task to gather a meaningful corpus of relevant articles. More than before, a better control of the specialized literature is needed.

Conflicts of Interest

The editors declare that they have no conflicts of interest regarding the publication of this special issue.

Acknowledgments

David M. Dohan Ehrenfest
Adriano Piattelli
Gilberto Sammartino
Hom-Lay Wang

References

[1] L. M. Wisniewska, D. M. D. Ehrenfest, P. Galindo-Moreno et al., "Molecular, cellular and pharmaceutical aspects of biomaterials in dentistry and oral and maxillofacial surgery. An internationalization of higher education and research perspective," *Current Pharmaceutical Biotechnology*, vol. 18, no. 1, pp. 10–18, 2017.

[2] D. M. D. Ehrenfest, P. G. Coelho, B.-S. Kang, Y.-T. Sul, and T. Albrektsson, "Classification of osseointegrated implant surfaces: materials, chemistry and topography," *Trends in Biotechnology*, vol. 28, no. 4, pp. 198–206, 2010.

[3] D. M. D. Ehrenfest, L. Rasmusson, and T. Albrektsson, "Classification of platelet concentrates: from pure platelet-rich plasma (P-PRP) to leucocyte- and platelet-rich fibrin (L-PRF)," *Trends in Biotechnology*, vol. 27, no. 3, pp. 158–167, 2009.

[4] D. M. D. Ehrenfest, N. R. Pinto, A. Pereda et al., "The impact of the centrifuge characteristics and centrifugation protocols on the cells, growth factors, and fibrin architecture of a leucocyte- and platelet-rich fibrin (L-PRF) clot and membrane," *Platelets*, vol. 29, no. 2, pp. 171–184, 2018.

[5] D. M. D. Ehrenfest, C. Q. Zhang, N. R. Pinto, and T. Bielecki, "Merchants shall be expelled from the Temple: the PRGF((R)) (Plasma-Preparation Rich in Growth Factors)-Endoret((R)) case," *Muscles, Ligaments and Tendons Journal*, vol. 4, pp. 473–477, 2014.

Research Article

One-Piece Implants with Smooth Concave Neck to Enhance Soft Tissue Development and Preserve Marginal Bone Levels: A Retrospective Study with 1- to 6-Year Follow-Up

Jean-Pierre Axiotis,[1] Paolo Nuzzolo [iD],[2] Carlo Barausse,[3] Roberta Gasparro [iD],[2] Paolo Bucci,[2] Roberto Pistilli,[4] Gilberto Sammartino [iD],[2] and Pietro Felice[3]

[1] *"Centre of Implantology and Dental Aesthetics", Région Stéphanoise, France*
[2] *Department of Neurosciences, Reproductive Sciences and Dental Sciences, University Federico II of Naples, Italy*
[3] *Department of Biomedical and Neuromotor Sciences, Unit of Periodontology and Implantology, University of Bologna, Bologna, Italy*
[4] *Oral and Maxillofacial Unit, San Camillo Hospital, Rome, Italy*

Correspondence should be addressed to Gilberto Sammartino; gilberto.sammartino@unina.it

Academic Editor: Elena Landi

Novel one-piece implants with concave smooth neck have been introduced to promote the formation of a thick mucosal layer and preserve marginal bone. A retrospective study on 70 patients with 1- to 6-year follow-up was carried out. Cumulative survival rates were assessed. Variations of marginal bone level were measured on periapical radiographs as distance of the implant-abutment junction from the bone crest. Influence of different variables on treatment outcome was evaluated. Cumulative success rate after 6 years was 99.4 % at implant level and 98.6 % at patient level. Marginal bone level changed in a significant way over time. After 4 months, an increase of radiographic bone level of 0.173 ± 1.088 mm at implant level and 0.18 ± 1.019 mm at patient level was recorded. Mean marginal bone loss after 5 years was 0.573 ± 0.966 mm at implant level and 0.783 ± 1.213 mm at patient level. Age, sex, smoking habits, implant sites, implant lengths and diameters, prosthetic retentions, and timing of loading did not influence marginal bone remodeling in a statistically significant way. At 4-year follow-up partial restorations lost a mean of 0.96 mm of more marginal bone compared with single restorations. This difference was statistically significant.

1. Introduction

The maintenance of peri-implant marginal bone level is the key to long-term functional and esthetic outcome of implant-supported restorations. Together with the absence of pain, inflammation, mobility, and radiographic radiolucency between implant and bone, a marginal bone loss lower than 2 mm is a mandatory criterion of success [1].

Many factors have been advocated to explain marginal bone resorption around a healthy osseointegrated implant: the establishment of a biological width, the occlusal trauma, the gingival biotype, the surgical trauma, the micromovements of the abutment, retrieved cycles of connection and disconnection of the abutment, the bacterial colonization of the implant-abutment junction (IAJ), the distance of the IAJ

from the bone crest, and the implant micro- and macrogeometry [2–6]. Still, the etiological factors underlying marginal bone loss have not been fully established [5, 7]. Implant neck morphology has been widely investigated in order to find designs that would promote bone ingrowth or limit bone loss and favour the creation of a steady mucosal seal [8].

Implant neck surface characteristics have also proven some relevance on the soft and hard tissues architecture [9]. The question whether a polished or a rough surface is more favourable for bone preservation is still debated [10–12]. More recently, one-piece implants have been introduced with a novel neck design, in which the transmucosal component has a narrower diameter than the implant body and a concave smooth surface meant promoting soft tissue creeping and the formation of a thick mucosal layer, which develops in a

FIGURE 1: Twinkon implant with concave smooth transmucosal neck.

horizontal plane and, as such, is not created at the expenses of the underlying marginal bone. With respect to traditional flared implant necks, this new design provides more space for soft tissues ingrowth and organization.

Given the encouraging preclinical data, the aim of the present retrospective study was to analyse the long-term marginal bone preservation around 167 implants with a concave transmucosal design placed in 70 patients with 1 to 6 years of follow-up.

2. Materials and Methods

The investigation design was a retrospective study. Clinical and radiographic documentation of 70 patients that had been treated with the placement of a total of 167 commercially available sand blasted Ti-6Al-4V implants with concave smooth neck (Twinkon®, Global D, Brignais, France) was collected and analysed. This implant has a one-piece design with external conical connection, which is protected with a PEEK plastic ring. The concave transmucosal part is 1.5 mm high and 1.73 mm long (Figure 1). The horizontal inward mismatch between the implant body and the transmucosal component is 0.4 mm. The sandblasted surface (sprayed with corundum micropowder) extends to the apical portion (0.20 mm high) of the transmucosal neck. The coronal portion of the transmucosal neck is machined (1.3 mm high). The selection criteria for the cases were the availability of periapical radiographs at baseline and at follow-up/s, clinical information about sex, age, smoking habits, implant site/s, insertion torque (< or > 25N/cm), implant/s length/s and diameter/s, postextractive or delayed placement, single, partial, or full-arch restorations, screw-retained or cemented prostheses, months of healing before prosthetic load, and report of complications. Files were excluded if incomplete or shorter than one year of follow-up and if radiographic identification of the bone crest level was questionable. All the patients displayed good general health without systemic or local contraindications to oral surgery and did not suffer from active periodontitis at the time of implant placement. Patients received proper information about the surgical procedures,

risks and alternative solutions, and signed an informed consent for the analysis and divulgation of their clinical information for scientific purposes. The principles outlined in the Declaration of Helsinki (64th revision) on clinical research involving human subjects were adhered to.

2.1. Surgical and Prosthetic Procedures. Following proper clinical and radiographic evaluation, the patients underwent professionally delivered oral hygiene and, if required, scaling and root planning, prior to implant placement. Patients were given prophylactic antibiotic therapy with 2 g of amoxicillin plus clavulanic acid (or clindamycin 600 mg, if allergic to penicillin) 1 h before the intervention and postoperatively 1 g amoxicillin plus clavulanic acid twice a day, for 5 days, or 300 mg clindamycin twice a day, for 7 days. The surgical procedure was performed under local anaesthesia. After a full-thickness crestal incision, a mucoperiosteal flap was elevated, and implant tunnels were realized with drills of increasing diameter under generous sterile saline irrigation. All implants were placed in native bone. Implants were placed to a depth varying on the clinical situation: as a general rule, in case of a delayed positioning in a healed ridge, the implant shoulder was placed at a crestal level, while in postextractive sockets it was placed 1,5 mm subcrestally, i.e., with the coronal end of the concave neck at a crestal level, according to standard manufacturer's protocol. Flaps were carefully sutured with resorbable sutures. X-rays were taken after implant placement to verify the correct implant position.

Ibuprofen (600 mg) was prescribed to be taken as needed. A cold and soft diet was recommended for 2 weeks and oral hygiene instructions were given. Patients were instructed to rinse twice daily with 0.12% chlorhexidine digluconate for the first 2 weeks. Sutures were removed 7 days after the surgery.

Depending on surgical and prosthetic considerations, immediate, early, or delayed loading was chosen to rehabilitate the patients. Provisional resin restorations were delivered immediately after implant placement in the case of immediate loading protocols or few weeks after abutment connection in the cases of delayed loading protocols. Definitive metal-ceramic restorations were cemented or screwed 2 to 4 months after provisional delivery.

All the patients were scheduled in a maintenance program with clinical and radiographic evaluation and oral hygiene recalls every 3 to 6 months.

2.2. Measurements. The primary outcome was the marginal bone level (MBL), measured on periapical radiographs, as linear distance in mm from the implant-abutment junction (IAJ) of the most coronal radiographic bone-implant contact (rx-fBIC). This distance was calculated on the mesial and distal aspect of each implant and given a positive sign if the rx-fBIC was coronal to the IAJ and a negative sign if it was apical to the IAJ. The measurements were realized using the Osirix software (Pixmeo Sarl, Bernex, Switzerland). As radiographs were not taken with a previously standardized technique, the biometric evaluations were calibrated on each radiograph using the height of the concave neck of the implant as known dimension (1,5 mm). Measurements were made to the nearest 0,1 mm. Variations of MBL from baseline were calculated on

radiographs taken after 4 months and 1, 2, 4, 5, and/or 6 years, depending on the availability of data, and expressed as means and standard deviations.

Subgroup analyses were carried out to assess the influence on the changes in MBL of these variables: sex, age, smoking habits, implant sites, insertion torque (< or > 25N/cm), implant length and diameter, postextractive or delayed placement, single, partial, or full-arch restoration, screw- retained or cemented prosthesis, and months of healing before prosthetic load.

The analysis was carried out at patient level and implant level.

Implant survival and success rate were assessed following the guidelines for studies on endosseous implants [13–15]: absence of pain, mobility, suppuration, mucosal redness and swelling, foreign body sensation, presence of plaque, and marginal bone loss. If all the parameters were satisfied and marginal bone loss was lesser than 1,5 mm in the first year of function and 0,2 mm for the following year, the case outcome was considered as success otherwise as survival. Rates were calculated as percentages in each time-frame considered.

2.3. Statistical Analysis. Descriptive statistics were used to summarize data: frequencies were used for nominal-level variables; means, standard deviations, and ranges were used for ordinal and continuous data. A log rank test was run to investigate differences in the implant and prosthetic survival distribution with respect to implant location (maxillary or mandibular arch, anterior or posterior site, and postextractive or not postextractive site), timing of loading (immediate or delayed), prosthesis type (single or partial), and implant-supported restoration type (screwed or cemented).

Marginal bone levels differences over time were investigated at site level (mesial and distal measurements), at implant level (mean between mesial and distal measurements), and at patient level (mean among the different implants of the same subject). At patient level a repeated measures ANOVA was used, whereas a repeated measures analysis including both fixed (time) and random effects (subject) was performed at site and implant level to account for the within-subject inner correlation.

Marginal bone levels changes between the different time points and baseline were calculated. They were compared with respect to implant location (maxillary or mandibular arch, anterior or posterior site, and postextractive or not postextractive site), timing of loading (immediate or delayed), prosthesis type (single or partial), and implant-supported restoration type (screwed or cemented) through t-tests at patient level and through nested ANOVAs at site and implant level (clustered data).

All statistical analyses were conducted using the Statistical Package for Social Sciences Software (SPSS Statistics Release 21, IBM, New York, USA). P < 0.05 was set as the level for statistical significance.

3. Results

Patient and intervention characteristics are summarized in Table 1. A total of 70 patients (45 females, 25 males; age

Table 1: Patient and intervention characteristics.

# Patients	70
# Females	45 (64.3%)
Mean age at recruitment (range)	55.64 (22-77)
Smokers	12 (17.1%)
smoking ≤ 10 cigarettes	6 (8.6%)
smoking > 10 cigarettes	6 (8.6%)
# implants	167
# implants received by patient	
# patients receiving 1 implant	23 (32.9%)
# patients receiving 2 implants	23 (32.9%)
# patients receiving 3 implants	10 (14.3%)
# patients receiving 4 implants	7 (10.0%)
# patients receiving 5 implants	4 (5.7%)
# patients receiving 6 implants	1 (1.4%)
# patients receiving 7 implants	2 (2.9%)
Arch	
# implants placed in Maxilla	17 (24.3%)
# implants placed in Mandible	51 (72.9%)
Both	2 (2.9%)
Site	
Anterior	30 (17.8%)
Posterior	139 (82.2%)
# implants placed with ≤ 25 Ncm torque	5 (3.0%)
Mean implant length (mm)	9.74±1.66
Mean implant diameter (mm)	4.25±0.8
Post-extractive implants	33
# patients receiving 1 post-extractive implant	8
# patients receiving 2 post-extractive implants	5
# patients receiving 3 post-extractive implants	1
# patients receiving 4 post-extractive implants	3
Prosthesis	
Single	29
Partial	40
Both	1
Implant supported restorations	
Screwed	15
Cemented	50
Not reported	5
Months before loading	3.58±2.32

range: 22 to 77 years, mean age at the beginning of the treatment: 56 years) were treated with 167 implants. The patients were treated between 2009 and 2012 by the same experienced surgeon. A small proportion of patients (17.1%) were smokers; half of the smokers were classified as heavy smokers (more than 10 cigarettes/day). The majority of the patients received 1 to 2 implants (65.8%), with a range from 1 to 7 implants per patient. The mandibular arch alone was the most often treated (72.9 % of the implants), and implants were placed in the posterior sectors of the upper and lower jaws in 82.2 % of the cases. Mean implant length and

TABLE 2: Implant and prosthetic failures.

	4-month follow-up	1-year follow-up	2-year follow-up	4-year follow-up	5-year follow-up	6-year follow-up
# implant failures	n=87	n=9	n=1	n=100	n=59	n=1
	0 (0.0%)	0 (0.0%)	0 (0.0%)	1 (1.0%)	0 (0.0%)	0 (0.0%)
# prosthetic failures	n=42	n=6	n=1	n=55	n=31	n=1
	0 (0.0%)	0 (0.0%)	0 (0.0%)	1 (1.82%)	0 (0.0%)	0 (0.0%)

TABLE 3: Mean peri-implant marginal bone at baseline, at loading, at 4 months, and at 1, 4, and 5 years.

	Baseline Mean±SD	4-month follow-up Mean±SD	1-year follow-up Mean±SD	4-year follow-up Mean±SD	5-year follow-up Mean±SD	Sig	Post
Implant level*	n=163	n=85	n=8	n=99	n=55	0.000	∘ # § $^{\phi}$ ∧
	0.026 ± 0.775	0.173 ± 1.088	-0.386 ± 1.421	-0.383 ± 1.150	-0.573 ± 0.966		
Patient level**	n=70	n=38	n=6	n=41	n=27	0.002	§ ∧
	0.018 ± 0.734	0.182 ± 1.019	-0.295 ± 1.611	-0.184 ± 0.990	-0.783 ± 1.213		

Data are presented as mean ± standard deviation. SD: standard deviation; Sig: significance; post: significant post hoc comparisons; ∘baseline vs 1 year; #baseline vs 4 years; §baseline vs 5 years; ∗4 months vs 4 years; ∧4 months vs 5 years.
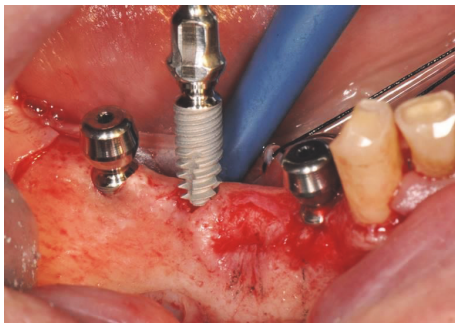
FIGURE 2: Implant placement in healed ridge for a partial restoration in posterior mandible. The smooth concave neck is left above the bony crest to allow soft tissues maturation.

diameter were 9.74±1.66 and 4.25±0.8, respectively. A total of 33 postextractive implants were placed in 17 patients. All but five implants were placed with a torque > 25 Ncm. A total of 30 single and 41 partial prostheses were delivered, while no full-arch rehabilitation was realized. Regarding prosthetic retention, 50 restorations were cemented, while 15 were screw-retained; in 3 cases the information was not reported. A mean time of 3.58±2.32 months before prosthetic loading was calculated. Data from 4-month, 1-year, 2-year, 4-year, 5-year, and 6-year follow-up were collected when available. Due to the limited number of records, 2-year and 6-year follow-up data were included in the computation of survival and failure rates but excluded from other statistical analyses (Figure 2). Implant and prosthetic failures are summarized in Table 2.

Of all the implants placed, one was lost for peri-implantitis after 4 years (cumulative success rate: 99.4 % at implant level; 98.6 % at patient level). The failed implant had been placed in a healed ridge (not postextractive) and had been loaded after 3 months, supporting a partial prosthesis of four elements on four implants in the posterior mandible.

No significant influence in treated arch, site (anterior or posterior), prosthetic rehabilitation (single or partial), timing of placement, and loading on the occurrence of implant failure was detected. Similarly variables as age, sex, smoking habit, implant length, and diameter did not influence these rates in a statistically significant way. Two minor prosthetic complications (screw loosening) were also recorded.

Mean peri-implant marginal bone level changes are shown in Table 3. MBL changed in a significant way over time, at site level, at implant level, and at patient level (p: 0.00, 0.00, and 0.002, respectively). After 4 months, a slight increase of radiographic level was recorded (mean value: 0.18 mm ± 1.019 at patient level) with respect to baseline, even though it did not reach statistical significance. At site level, mesial sites showed significant changes after 4 years and 5 years with respect to baseline and 4-month follow-up; distal sites showed significant changes after 1 year, 4 years, and 5 years with respect to baseline and after 4 years and 5 years with respect to 4-month follow-up. At implant level, significant changes were recorded after 1 year, 4 years, and 5 years with respect to baseline and after 4 years and 5 years with respect to 4-month follow-up. At patient level, significant changes were recorded at 5 years with respect to baseline and 4-month follow-up. Mean marginal bone loss after 5 years was 0.573 ± 0.966 mm at implant level and 0.783 ± 1.213 mm at patient level (Figure 3). The influence of different variables on marginal bone level changes was assessed (data not shown). No statistically significant differences in marginal bone level changes in relation to the arch treated and location in the arch (anterior or posterior) were detected. Prosthetic retention, screwed or cemented, had no significant influence on marginal bone remodeling, while a significant difference was found between single and partial restorations for changes after 4 years with respect to baseline at implant level and patient level (p value: 0.002, 0.003, and 0.003, respectively). Partial restorations were found to be subject to more bone resorption than single restorations (mean difference:
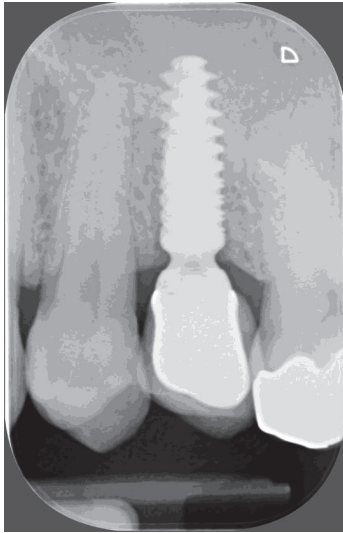
Figure 3: Radiographic 5-year follow-up of a single restoration. Some bone growth over the shoulder of the implant can be detected.

0,96 mm at patient level) after 4 years. The timing of loading had no significant influence on marginal bone remodeling, while the timing of implant placement was found to be determinant in a significant way only for distal sites after 4 years with respect to baseline: postextractive implants lost a mean of 1.003 mm more than not postextractive implants on the distal side (p= 0.03).

Variables as age, sex, smoking habits, implant length, and diameter did not influence marginal bone remodeling in a statistically significant way.

4. Discussion

The aim of this study was to assess the short- and long-term alterations of the hard tissues around one-piece implants with concave smooth neck. Marginal bone is the part of the peri-implant tissues at major risk of resorption. It has been shown that masticatory stresses are concentrated at this level, and bone loss can occur as a response to mechanical trauma [13, 16–18]. Furthermore, implant-abutment junction is located in this area, and it is the weakest part of the implant-restoration complex, both from a mechanical point of view and, mostly, from a biological standpoint. Irrespective of the kind of connection, a microgap between implant and abutment will always be present [14] and as a consequence bacterial microleakage will turn out into marginal bone loss [15, 19, 20]. Finally, even before prosthetic loading, when the implant is connected to a prosthetic or healing abutment, the soft tissues will always need a space to create a connective-epithelial seal around the transmucosal component. This biological width will be created at the expenses of the bony tissue if sufficient contact area is not provided [3].

The novel neck configuration analysed in this retrospective study has several advantages: the one-piece implant has a transmucosal neck, which brings the IAJ (and its microgap) in the soft tissues, away from marginal bone. The concave neck provides an increased space for soft tissues maturation and the establishment of a biological width. The incremented contact area provided by the concave design also provides major volume; it has been shown that, besides being shorter, the soft tissue seal around the implant is thicker [21]. The distance of 1,5 mm between the IAJ and the implant shoulder can be considered as a "safe distance" that prevents potentially harmful periodontal flora, which is known to extend apically from the epithelial junction to a maximum of 1,1 mm [22], from reaching the first bone to implant contact. Besides, the smooth surface of the neck prevents bacterial accumulation and the onset and progression of a peri-implantitis [23].

Three histologic studies showed promising results in terms of crestal bone preservation and soft tissues maturation with this concave transmucosal design. Bolle et al., in a histometric study on dogs, found evidence of some bone apposition on the implant shoulder during the healing: the marginal bone was at the level of the implant shoulder after 3 weeks and 0,18 mm above it after 18 weeks [21]. On the other hand, there have been controversial results about the dimensions of the biological width around this neck configuration: according to Huh and Bolle, this dimension is lower in the vertical plane compared to flared neck designs, while Kim et al. found no differences. In any case, it appears clear that a concave profile provides wider surface area given the same vertical dimension [21, 24, 25].

Monje et al. have shown that, together with factors as the quality of surgery, peri-implant bone thickness, and patient's habits, both the thickness of soft tissue and the location and characteristics of the IAJ are crucial for the preservation of peri-implant marginal bone [26]. The influence of implant geometry and surface on marginal bone remodeling has been stated in a meta-analysis by Laurell et al., in which a pooled mean bone loss varying from 0.24 mm to 0.75 mm was found, depending on the implant system [27].

Histologic evidence that implant design and surface are determinants in marginal bone level preservation has also been provided [28]. On the other side, Esposito et al. found no statistically significant difference in marginal bone preservation among different implant systems, even though the authors complained about a lack of well-designed RCTs for a proper meta-analysis [29].

In a retrospective multicenter radiographic evaluation of 596 dental implants, Cochran et al. found mean marginal bone loss of 2.84 ± 1.63 mm after 5 years. The authors also noted that 86% of the total mean bone loss had already occurred before prosthetic loading, so it should be ascribed to the healing pattern around the implants rather than to biomechanical factors [30].

In our study, mean peri-implant bone loss was of 0.57 mm after 5 years. More interestingly, peri-implant marginal bone did not resorb but rather overgrew on the implant shoulder to some extent after 4 months.

With this novel neck configuration, the formation of a mucosal attachment to the implant does not seem to happen at the expenses of the bony tissue; in fact, bony overgrowth seems to be promoted. The inevitable but acceptable bone loss over the years might still be related to biomechanical and/or microbiological factors, but the thickening of the soft tissues

around the concave neck and the distance of the IAJ from the bone might have acted as protective factors that limited the extent of such resorption.

Even though the importance of soft tissue thickness for maintenance of peri-implant health has not been clearly defined yet [31], a review by Suárez-López Del Amo et al. demonstrated that marginal bone loss can be limited by thicker peri-implant mucosa [32]. Furthermore, implant dimensions, the arch treated and location (anterior or posterior), the kind of prosthetic span and retention, timing of placement and loading, and smoking habit did not influence success rate or marginal bone loss, with the exception of partial prostheses at 4-year follow-up and postextractive implants at 4-year follow-up.

This observation is in accordance with previous data in literature about the lack of influence on the implant therapy outcome of different implant sizes [33], single and partial rehabilitation [34], timing of restoration [35, 36], postextractive or delayed placement [37, 38], and cemented or screw-retained prosthesis [39]. While there is some evidence that smoking habits have a negative impact on the therapy outcomes [40, 41], we could find no difference between smokers and nonsmokers in our study. One possible explanation could be that a very limited number of patients enrolled in our study were heavy smokers.

In any case, this lack of interference of factors of different nature on the outcome of the therapy makes the implant evaluated in our study a viable solution for a vast range of different clinical situations.

5. Conclusions

Within the limits of this retrospective study, one-piece implants with concave smooth neck seem to ensure satisfactory success rates and long-term marginal bone preservation, irrespective of the implant dimensions, timing of placement and loading, and kind of rehabilitation. Further investigations, possibly in the form of well-designed RCTs, are needed to confirm the findings of this study.

Data Availability

Please contact professor Pietro Felice, email: pietro.felice@ unibo.it.

Disclosure

This work is self-funded.

Conflicts of Interest

The authors declare that they have no conflicts of interest.

References

[1] C. E. Misch, M. L. Perel, H.-L. Wang et al., "Implant success, survival, and failure: the international congress of oral implantologists (ICOI) pisa consensus conference," *Implant Dentistry*, vol. 17, no. 1, pp. 5–15, 2008.

[2] G. Sammartino, H. L. Wang, R. Citarella, M. Lepore, and G. Marenzi, "Analysis of occlusal stresses transmitted to the inferior alveolar nerve by multiple threaded implants," *Journal of Periodontology*, vol. 84, no. 11, pp. 1655–1661, 2013.

[3] T. Berglundh and J. Lindhe, "Dimension of the periimplant mucosa. Biological width revisited," *Journal of Clinical Periodontology*, vol. 23, no. 10, pp. 971–973, 1996.

[4] I. Ericsson, L. G. Persson, T. Berglundh, C. P. Marinello, J. Lindhe, and B. Klinge, "Different types of inflammatory reactions in peri-implant soft tissues," *Journal of Clinical Periodontology*, vol. 22, no. 3, pp. 255–261, 1995.

[5] F. Hermann, H. Lerner, and A. Palti, "Factors influencing the preservation of the periimplant marginal bone," *Implant Dentistry*, vol. 16, no. 2, pp. 165–175, 2007.

[6] J. S. Hermann, J. D. Schoolfield, P. V. Nummikoski, D. Buser, R. K. Schenk, and D. L. Cochran, "Crestal Bone Changes Around Titanium Implants: A Methodologic Study Comparing Linear Radiographic with Histometric Measurements," *The International Journal of Oral & Maxillofacial Implants*, vol. 16, no. 4, pp. 475–485, 2001.

[7] L. Prosper, S. Redaelli, M. Pasi, F. Zarone, G. Radaelli, and E. F. Gherlone, "A randomized prospective multicenter trial evaluating the platform-switching technique for the prevention of postrestorative crestal bone loss," *The International Journal of Oral & Maxillofacial Implants*, vol. 24, no. 2, pp. 299–308, 2009.

[8] Y. Yamanishi, S. Yamaguchi, S. Imazato, T. Nakano, and H. Yatani, "Effects of the implant design on peri-implant bone stress and abutment micromovement: Three-dimensional finite element analysis of original computer-aided design models," *Journal of Periodontology*, vol. 85, no. 9, pp. e333–e338, 2014.

[9] J. Schrotenboer, Y.-P. Tsao, V. Kinariwala, and H.-L. Wang, "Effect of microthreads and platform switching on crestal bone stress levels: A finite element analysis," *Journal of Periodontology*, vol. 79, no. 11, pp. 2166–2172, 2008.

[10] A. Aloy-Prósper, L. Maestre-Ferrín, D. Peñarrocha-Oltra, and M. Peñarrocha-Diago, "Marginal bone loss in relation to the implant neck surface: An update," *Medicina Oral Patología Oral y Cirugía Bucal*, vol. 16, no. 3, Article ID 16969, pp. 365–368, 2011.

[11] M. Esposito, P. Felice, C. Barausse, R. Pistilli, G. Grandi, and M. Simion, "Immediately loaded machined versus rough surface dental implants in edentulous jaws: One-year postloading results of a pilot randomised controlled trial," *European Journal of Oral Implantology*, vol. 8, no. 4, pp. 387–396, 2015.

[12] J. Cosyn, M. M. Sabzevar, P. De Wilden, and T. De Rouck, "Two-piece implants with turned versus microtextured collars," *Journal of Periodontology*, vol. 78, no. 9, pp. 1657–1663, 2007.

[13] S. Hansson, "Implant-abutment interface: biomechanical study of flat top versus conical.," *Clinical Implant Dentistry and Related Research*, vol. 2, no. 1, pp. 33–41, 2000.

[14] M. Esposito, H. Maghaireh, and R. Pistilli, "Dental implants with internal versus external connections: 1-year post-loading results from a pragmatic multicenter randomised controlled trial," *European Journal of Oral Implantology*, vol. 8, no. 4, pp. 331–344, 2015.

[15] A. Piattelli, G. Vrespa, G. Petrone, G. Iezzi, S. Annibali, and A. Scarano, "Role of the microgap between implant and abutment: a retrospective histologic evaluation in monkeys," *Journal of Periodontology*, vol. 74, no. 3, pp. 346–352, 2003.

[16] L. Pierrisnard, F. Renouard, P. Renault, and M. Barquins, "Influence of implant length and bicortical anchorage on implant

stress distribution," *Clinical Implant Dentistry and Related Research*, vol. 5, no. 4, pp. 254–262, 2003.

[17] F. Isidor, "Influence of forces on peri-implant bone," *Clinical Oral Implants Research*, vol. 17, supplement 2, pp. 8–18, 2006.

[18] L. B. Lum, "A biomechanical rationale for the use of short implants," *Journal of Oral Implantology*, vol. 17, no. 2, pp. 126–131, 1991.

[19] N. Broggini, L. M. McManus, J. S. Hermann et al., "Peri-implant inflammation defined by the implant-abutment interface," *Journal of Dental Research*, vol. 85, no. 5, pp. 473–478, 2006.

[20] T. Tsuge, Y. Hagiwara, and H. Matsumura, "Marginal fit and microgaps of implant-abutment interface with internal anti-rotation configuration," *Dental Materials*, vol. 27, no. 1, pp. 29–34, 2008.

[21] C. Bolle, M.-P. Gustin, D. Fau, P. Exbrayat, G. Boivin, and B. Grosgogeat, "Early periimplant tissue healing on 1-piec implants with a concave transmucosal design: A histomorphometric study in dogs," *Implant Dentistry*, vol. 24, no. 5, pp. 598–606, 2015.

[22] J. Waerhaug, "Subgingival plaque and loss of attachment in periodontosis as observed in autopsy material," *Journal of Periodontology*, vol. 47, no. 11, pp. 636–642, 1976.

[23] M. Sánchez-Siles, D. Muñoz-Cámara, N. Salazar-Sánchez, J. F. Ballester-Ferrandis, and F. Camacho-Alonso, "Incidence of peri-implantitis and oral quality of life in patients rehabilitated with implants with different neck designs: a 10-year retrospective study," *Journal of Cranio-Maxillo-Facial Surgery*, vol. 43, no. 10, pp. 2168–2174, 2016.

[24] J.-B. Huh, G.-B. Rheu, Y.-S. Kim, C.-M. Jeong, J.-Y. Lee, and S.-W. Shin, "Influence of Implant transmucosal design on early peri-implant tissue responses in beagle dogs," *Clinical Oral Implants Research*, vol. 25, no. 8, pp. 962–968, 2014.

[25] S. Kim, K.-C. Oh, D.-H. Han et al., "Influence of transmucosal designs of three one-piece implant systems on early tissue responses: a histometric study in beagle dogs," *International Journal of Oral and Maxillofacial Implants*, vol. 25, no. 2, pp. 309–314, 2010.

[26] A. Monje, F. Suarez, P. Galindo-Moreno, A. García-Nogales, J.-H. Fu, and H.-L. Wang, "A systematic review on marginal bone loss around short dental implants (<10 mm) for implant-supported fixed prostheses," *Clinical Oral Implants Research*, vol. 25, no. 10, pp. 1119–1124, 2014.

[27] L. Laurell and D. Lundgren, "Marginal bone level changes at dental implants after 5 years in function: a meta-analysis," *Clinical Implant Dentistry and Related Research*, vol. 13, no. 1, pp. 19–28, 2011.

[28] P. Valderrama, M. M. Bornstein, A. A. Jones, T. G. Wilson Jr., F. L. Higginbottom, and D. L. Cochran, "Effects of implant design on marginal bone changes around early loaded, chemically modified, sandblasted acid-etched-surfaced implants: A histologic analysis in dogs," *Journal of Periodontology*, vol. 82, no. 7, pp. 1025–1034, 2011.

[29] M. Esposito, M. G. Grusovin, P. Coulthard, P. Thomsen, and H. V. Worthington, "A 5-year follow-up comparative analysis of the efficacy of various osseointegrated dental implant systems: A systematic review of randomized controlled clinical trials," *The International Journal of Oral & Maxillofacial Implants*, vol. 20, no. 4, pp. 557–568, 2005.

[30] D. L. Cochran, P. V. Nummikoski, J. D. Schoolfield, A. A. Jones, and T. W. Oates, "A prospective multicenter 5-year radiographic evaluation of crestal bone levels over time in 596 dental implants placed in 192 patients," *Journal of Periodontology*, vol. 80, no. 5, pp. 725–733, 2009.

[31] W. Martin, E. Lewis, and A. Nicol, "Local risk factors for implant therapy," *International Journal of Oral and Maxillofacial Implants*, pp. 24–28, 2009.

[32] F. S.-L. Del Amo, G.-H. Lin, A. Monje, P. Galindo-Moreno, and H.-L. Wang, "Influence of soft tissue thickness on peri-implant marginal bone loss: A systematic review and meta-analysis," *Journal of Periodontology*, vol. 87, no. 6, pp. 690–699, 2016.

[33] B. S. Sotto-Maior, E. G. F. Mercuri, P. M. Senna, N. M. S. P. Assis, C. E. Francischone, and A. A. Del Bel Cury, "Evaluation of bone remodeling around single dental implants of different lengths: a mechanobiological numerical simulation and validation using clinical data," *Computer Methods in Biomechanics and Biomedical Engineering*, vol. 19, no. 7, pp. 699–706, 2016.

[34] C. T. Firme, M. V. Vettore, M. Melo, and G. M. Vidigal Jr., "Peri-implant bone loss around single and multiple prostheses: systematic review and meta-analysis," *The International Journal of Oral & Maxillofacial Implants*, vol. 29, no. 1, pp. 79–87, 2014.

[35] M. Esposito, M. G. Grusovin, M. Willings, P. Coulthard, and H. V. Worthington, "The effectiveness of immediate, early, and conventional loading of dental implants: a cochrane systematic review of randomized controlled clinical trials," *The International Journal of Oral & Maxillofacial Implants*, vol. 22, no. 6, pp. 893–904, 2007.

[36] F. Suarez, H.-L. Chan, A. Monje, P. Galindo-Moreno, and H.-L. Wang, "Effect of the timing of restoration on implant marginal bone loss: A systematic review," *Journal of Periodontology*, vol. 84, no. 2, pp. 159–169, 2013.

[37] B. R. Chrcanovic, T. Albrektsson, and A. Wennerberg, "Dental implants inserted in fresh extraction sockets versus healed sites: a systematic review and meta-analysis," *Journal of Dentistry*, vol. 43, no. 1, pp. 16–41, 2015.

[38] P. Felice, E. Soardi, M. Piattelli, R. Pistilli, M. Jacotti, and M. Esposito, "Immediate non-occlusal loading of immediate post-extractive versus delayed placement of single implants in preserved sockets of the anterior maxilla: 4-month post-loading results from a pragmatic multicentre randomised controlled trial," *European Journal of Oral Implantology*, vol. 4, no. 4, pp. 329–344, 2011.

[39] M. L. De Brandão, M. V. Vettore, and G. M. Vidigal Júnior, "Peri-implant bone loss in cement- and screw-retained prostheses: Systematic review and meta-analysis," *Journal of Clinical Periodontology*, vol. 40, no. 3, pp. 287–295, 2013.

[40] V. Moraschini and E. D. P. Barboza, "Success of dental implants in smokers and non-smokers: a systematic review and meta-analysis," *International Journal of Oral and Maxillofacial Surgery*, vol. 45, no. 2, pp. 205–215, 2016.

[41] S. Sayardoust, K. Gröndahl, E. Johansson, P. Thomsen, and C. Slotte, "Implant survival and marginal bone loss at turned and oxidized implants in periodontitis-susceptible smokers and never-smokers: A retrospective, clinical, radiographic case-control study," *Journal of Periodontology*, vol. 84, no. 12, pp. 1775–1782, 2013.

Clinical Study

Comparative Histological and Histomorphometric Results of Six Biomaterials Used in Two-Stage Maxillary Sinus Augmentation Model after 6-Month Healing

Gerardo La Monaca (iD),[1] **Giovanna Iezzi,**[2] **Maria Paola Cristalli** (iD),[3] **Nicola Pranno,**[4]
Gian Luca Sfasciotti,[4] **and Iole Vozza** (iD)[4]

[1]*Department of Sense Organs, Sapienza University of Rome, Rome, Italy*
[2]*Department of Medical, Oral and Biotechnological Sciences, University of Chieti-Pescara, Chieti Scalo, Italy*
[3]*Department of Biotechnologies and Medical Surgical Sciences, Sapienza University of Rome, Rome, Italy*
[4]*Department of Oral and Maxillofacial Sciences, Sapienza University of Rome, Rome, Italy*

Correspondence should be addressed to Gerardo La Monaca; gerardo.lamonaca@uniroma1.it

Objectives. To evaluate the performances of six different bone substitute materials used as graft in maxillary sinus augmentation by means of histological and histomorphometric analysis of bone biopsies retrieved from human subjects after a 6-month healing period. *Materials and Methods*. Six consecutive patients (3 males, 3 females, aged 50-72 years), healthy, nonsmokers, and with good oral hygiene, presenting edentulous posterior maxilla with a residual bone crest measuring ≤ 4 mm in vertical height and 3 to 5 mm in horizontal thickness at radiographic examination, were selected to receive sinus augmentation and delayed implant placement. Under randomized conditions, sinus augmentation procedures were carried out using mineralized solvent-dehydrated bone allograft (MCBA), freeze-dried mineralized bone allograft (FDBA), anorganic bovine bone (ABB), equine-derived bone (EB), synthetic micro-macroporous biphasic calcium-phosphate block consisting of 70% beta-tricalcium phosphate and 30% hydroxyapatite (HA-β-TCP 30/70), or bioapatite-collagen (BC). After 6 months, bone core biopsies were retrieved and 13 implants were placed. Bone samples were processed for histological and histomorphometric analysis. CT scans were taken before and after surgery. After 4 months of healing, patients were restored with a provisional fixed acrylic resin prosthesis, as well as after further 2-4 months with a definitive cemented zirconia or porcelain-fused-to-metal crowns. *Results*. There were no postoperative complications or implant failures. The histological examination showed that all biomaterials were in close contact with newly formed bone, surrounding the graft granules with a bridge-like network. No signs of acute inflammation were observed. The histomorphometry revealed 20.1% newly formed bone for MCBA, 32.1% for FDBA, 16.1% for ABB, 22.8% for EB, 20.3% for HA-β-TCP 30/70, and 21.4% for BC. *Conclusions*. Within the limitations of the present investigation, all the six tested biomaterials showed good biocompatibility and osteoconductive properties when used in sinus augmentation procedures, although the FDBA seemed to have a better histomorphometric result in terms of newly formed bone and residual graft material. This trial is registered with ClinicalTrials.gov Identifier (Registration Number): NCT03496688.

1. Introduction

The lack of adequate bone height and thickness negatively affects implant-supported rehabilitation in the edentulous posterior maxilla. Therefore, bone-grafting procedures are needed to increase the available bone volume and to provide structural and mechanical support for the placement of dental implants.

Among graft materials, autologous bone is considered the gold standard due to its osteogenic, osteoinductive, and osteoconductive properties [1–3]. However, the use of autogenous bone has significant drawbacks such as a limited

TABLE 1: Patient characteristics at study baseline.

N	Sex	Age	Implant location	Type of implant	
				Length	Diameter
1	M	72	1.4	10	3.75
			1.6	11.5	5
2	F	62	2.6	10	5
			2.7	10	5
3	F	54	1.4	13	5.5
			1.6	13	5.5
4	F	50	2.4	10	4.3
			2.6	13	5.5
5	M	57	1.3	13	4
			1.5	10	4
			1.7	11.5	5
6	M	63	2.4	13	4
			2.6	10	5

intraoral supply, the need of general anesthesia in case of extraoral harvesting, donor site morbidity, increased operating time, need of two surgical sites, tendency to partial resorption and potential intraoperative, and postoperative complications [2, 4–7].

To overcome these disadvantages, a large number of biomaterials have been used alone or in combination with autografts in augmentation procedures [8–19]. Among the osteoconductive materials, allografts (fresh-frozen bone, freeze-dried bone, demineralized freeze-dried bone), xenografts (of bovine, equine, or porcine origin), and alloplastic materials (different combination of calcium-phosphate, bioactive glasses, polymers) were described in the dental literature as being able to enhance bone formation. Furthermore, several studies have shown that the biomaterials may not adversely influence clinical outcomes and implant survival when compared to autogenous bone [20, 21].

The two-stage sinus lift augmentation with delayed implant insertion was considered a good clinical model to evaluate the performance of graft materials, because bone formation occurs within an enclosed space and with a minimal interference from external factors. In addition, this procedure is highly predictable and allows collecting bone biopsy specimens during implant insertion avoiding any additional discomfort for the patients [17, 20].

The aim of the present study was to evaluate the performances of six different bone substitute materials used as graft in maxillary sinus augmentation, by means of histological and histomorphometric analysis of bone biopsies retrieved from human subjects after a healing period of 6 months.

2. Materials and Methods

2.1. Patient Selection. Six patients (3 males, 3 females, aged 50–72 years) who were healthy, nonsmokers, and with good oral hygiene were recruited in this study among those referred to Department of Oral and Maxillofacial Sciences, Sapienza University of Rome, for implant-supported

rehabilitation in the posterior atrophic maxilla (Table 1). Inclusion criteria were maxillary partial edentulism in the premolar/molar areas, with a residual bone crest measuring ≤ 4 mm in vertical height and 3 to 5 mm in horizontal thickness as measured on computerized tomography (CT) scan. Exclusion criteria were being pregnant or lactating females, patients with impaired systemic conditions, smoking habit, and maxillary sinus pathology. After clinical and radiographic evaluation, the patients signed a written informed consent form to study participation.

All the clinical procedures were performed in accordance with the Declaration of Helsinki and the Good Clinical Practice Guidelines. The protocol of the study was approved by the Ethical Committee of the Sapienza University of Rome (n. 3447).

2.2. Surgical and Restorative Procedures. The preoperative antibiotic and analgesic therapy with Amoxicillin 875 mg + Clavulanic acid 125 mg (Augmentin, GlaxoSmithKline, Belgium) and Ketoprofene 200 mg (Ibifen, 200 mg, IBI Lorenzini, Aprilia, Italy) was given orally 1 hour prior to surgery. Immediately prior to surgery, patients rinsed with a chlorhexidine digluconate solution 0.2% (Corsodyl, GlaxoSmithKline, Belgium) for 2 min, to be continued for 2 weeks postoperatively.

Surgery was performed under sterile conditions and local anesthesia (mepivacaine 2% with epinephrine 1:100.000, Carbocaine, AstraZeneca, Italy). A lateral window technique was used for sinus floor elevation. A slightly palatal crestal incision and two vertical releasing incisions were made mesial and distal on the buccal mucosa according to the sinus anatomy to elevate a mucoperiosteal flap (Figure 1(a)). On the lateral side of the sinus wall, the oval-shaped bony window was performed, with the inferior border about 5 mm from the alveolar crest and the superior portion left intact, to create a trapdoor effect (Figure 1(b)). The sinus membrane was carefully raised and, together with the bony window, was rotated inward and upward (Figure 1(c)). The
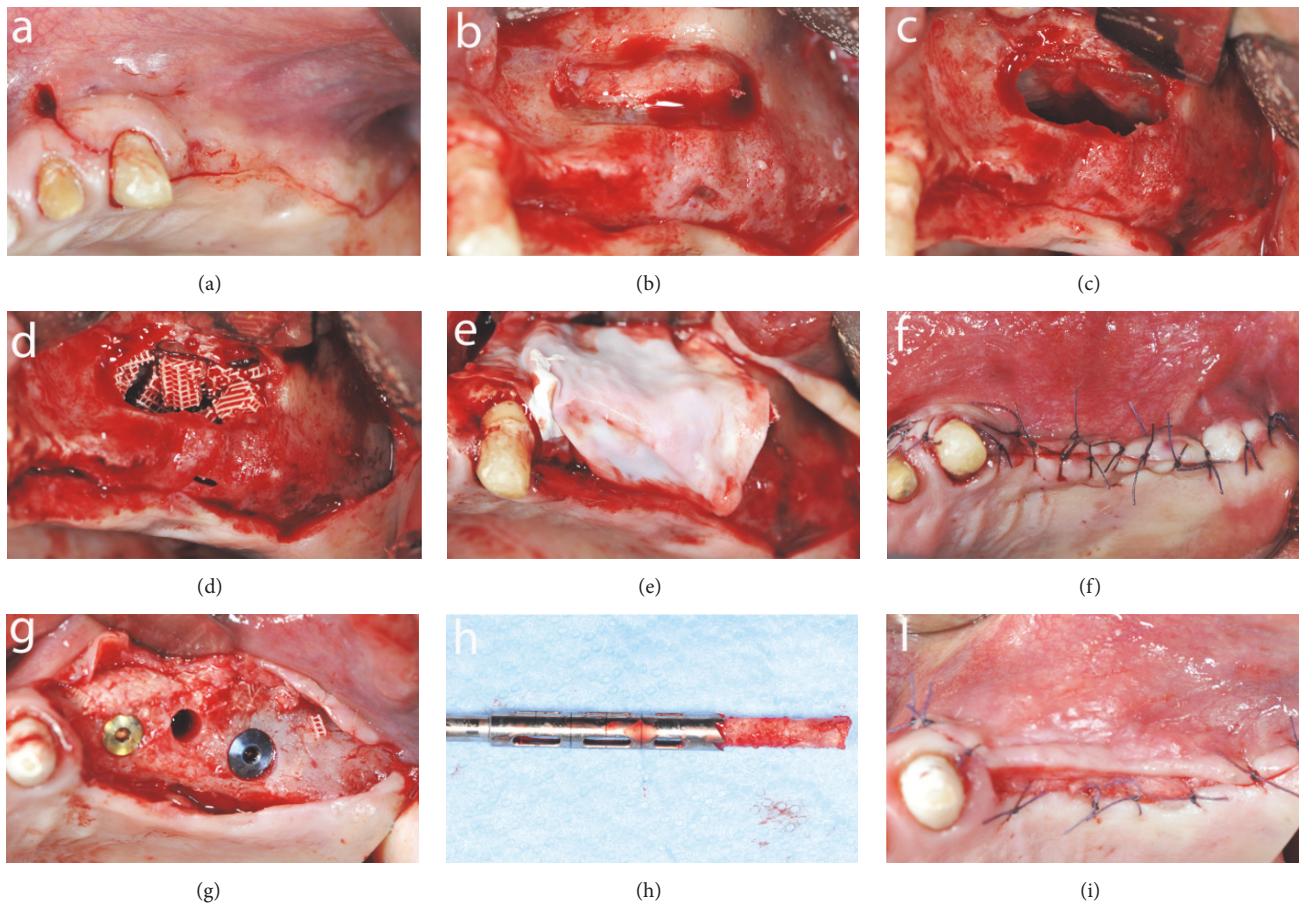
Figure 1: Intraoperative views of the sinus augmentation procedure: (a) mobilization of the mucoperiosteal flap; (b) oval-shaped bony window; (c) sinus membrane elevation; (d) graft material in place; (e) resorbable membrane over the lateral window; (f) suture; (g) bone core biopsy and implant placement; (h) trephine bur and harvested specimen; (i) suture.

subantral cavity was packed with the graft material (Figure 1(d)) and a resorbable membrane (Bio-Gide, Geistlich Biomaterials Italy S.r.l.) was placed over the lateral wall defect (Figure 1(e)). The mucoperiosteal flap was replaced and stabilized with resorbable interrupted sutures (5-0 Vicryl, Johnson & Johnson Medical, Norderstedt, Germany), which were removed after 2 weeks (Figure 1(f)). Postoperatively, the antibiotic therapy was prescribed for 1 week (Amoxicillin 875 mg + Clavulanic acid 125 mg twice a day) and, if necessary, the analgesic therapy was continued with Ketoprofene 200 mg.

After 6 months clinical and radiographic examinations were performed and each patient was reappointed for biopsy and implant placement in the same location. Under local anesthesia, a full thickness flap was raised and a bone biopsy was performed using a 3.5 mm trephine bur under sterile saline solution irrigation, guided by the radiographic/surgical template in the selected implant site. A total of six bone samples were retrieved from the occlusal aspect of the alveolar crest, one from each augmented site and at least two implants (NobelParallel CC or NobelSpeedy, Nobel Biocare Italiana S.r.l., Italy), were placed according to the manufacturer's indications (Figures 1(g), 1(h), and 1(i)).

To identify crestal bone during histologic and histomorphometric procedures, the harvested specimens were marked with toluidine blue stain on the occlusal side.

After 4 months of healing, patients were provisionally restored with a fixed acrylic resin prosthesis and after 2 to 4 months of function, the definitive prosthetic rehabilitation was applied with cemented zirconia or porcelain-fused-to-metal crowns.

Under randomized conditions, each sinus augmentation procedure was carried out using one of the following six commercial bone substitute materials: mineralized solvent-dehydrated bone allograft (MCBA, Puros®; Zimmer Dental GmbH, Freiburg, Germany); freeze-dried mineralized bone allograft (FDBA, Organizzazione Toscana Trapianti, Azienda Ospedaliero-Universitaria Careggi, Florence, Italy); anorganic bovine bone (ABB, Bio-Oss®, Geistlich Biomaterials Italia S.r.l.); equine-derived bone (EB osteOXenon®- Bioteck S.p.A., Arcugnano (VI), Italy); synthetic micro-macroporous biphasic calcium-phosphate block consisting of 70% beta-tricalcium phosphate and 30% hydroxyapatite (HA-β-TCP 30/70, BioCer Entwicklungs GmbH, Bayreuth, Germany); and bioapatite-collagen (BC, Biostite™, GABA Vebas San Giuliano Milanese, MI, Italy).

MCBA is cancellous or cortical mineralized solvent-dehydrated bone allograft obtained from cadaveric bone by a processing technique (Tutoplast Process, RTI Biologics, Alachua, FL), which preserves the bone architecture maintaining its biomechanical properties and minimizing antigenicity and infective potential [8, 9, 22].

FDBA is freeze-dried mineralized bone allograft processed using lyophilization; it maintains both the organic and the inorganic component (salts of calcium and phosphate), and when used as a graft material, the mineral content is broken down by osteoclasts, becoming osteoinductive proteins available to induce new bone formation. However, to release osteoinductive proteins from the FDBA organic matrix, a prolonged osteoclast mediated demineralization is needed [23].

ABB is a xenogenic material formed by deproteinized sterilized bovine cancellous bone with 75% porosity and a crystal size of about 10 μm in the form of granules. Its native crystal-line structure is chemically and physically highly similar to human bone and its porous nature promotes the initial biologic processes of cell adhesion and proliferation [19]. This material is well documented and has been shown to be well integrated into host bone tissue in different clinical and histological results [24–26].

EB is an equine-derived bone tissue deantigenated by a proteolytic low temperature process that preserves type 1 bone collagen and makes it anorganic although it conserves unaltered its mineral structure of hydroxyapatite saving the resorption potential [10, 27–29].

HA-β-TCP 30/70 is a new bioceramic with reticular structure, which seems to have a better resorption and an increased bone formation due to the levels of released calcium and phosphorous ions able to stimulate new bone formation [8, 16, 30–33]. Indeed, HA seems to act as scaffold and TCP as the resorbable component.

BC is hydroxyapatite associated with type I bovine collagen plus glucosamine. Different studies showed its efficacy as human bone substitute material in the sinus augmentation procedure [34, 35]. The presence of collagen accelerates fibrin formation of the clot while glucosamine improves the bone mineralization progression.

2.3. Histological Procedure. The bone cores were retrieved and were immediately stored in 10% buffered formalin and processed to obtain thin ground sections. The specimens were processed using the Precise 1 Automated System (Assing, Rome, Italy) [35]. The specimens were dehydrated in a graded series of ethanol rinses and embedded in a glycol methacrylate resin (Technovit 7200 VLC, Kulzer, Wehrheim, Germany). After polymerization, the specimens were sectioned, along their longitudinal axis, with a high precision diamond disk at about 150 μ m, and ground down to about 30 μm with a specially designed grinding machine Precise 1 Automated System (Assing, Rome, Italy). Three slides were obtained from each specimen. These slides were stained with acid fuchsin and toluidine blue and examined with transmitted light Leitz Laborlux microscope (Leitz, Wetzlar, Germany).

Histomorphometry of the percentages of newly formed bone, residual grafted material, and marrow spaces was carried out using a light microscope (Laborlux S, Leitz, Wetzlar, Germany) connected to a high-resolution video camera (3CCD, JVCKY-F55B, JVC, Yokohama, Japan) and interfaced with a monitor and PC (Intel Pentium III 1200 MMX, Intel, Santa Clara, CA, USA). This optical system was associated with a digitizing pad (Matrix Vision GmbH, Oppenweiler, Germany) and a histometry software package with image capturing capabilities (Image-Pro Plus 4.5, Media Cybernetics Inc., Immagini & Computer Snc, Milan, Italy).

3. Results

3.1. Clinical Results. The healing process after sinus augmentation procedures was uneventful. No postoperative complications were present. In no case there was perforation of the sinus membrane. No clinical sign of sinus pathology was observed. Six months after sinus augmentation, the radiographic evaluation of all patients showed the presence of dense bone in the maxillary sinuses where the biomaterials were inserted (Figure 2).

Primary stability of the implants was achieved in all cases independently of the use of bone substitute material (insertion torque value was at least 35 N). All 13 implants placed during the biopsy retrieval had no complications and were osseointegrated at the end of prosthetic rehabilitation. No failures and no dropouts occurred.

3.2. Histological and Histomorphometric Results. Mineralized solvent-dehydrated bone (MCBA). At low magnification, trabecular bone with large marrow spaces and biomaterial particles was observed (Figure 3(a)). The biomaterial particles showed different sizes and they were partially surrounded by newly formed bone. Newly formed bone was characterized by large osteocyte lacunae and bridged up greatest part of the biomaterial particles (Figure 3(b)). In some fields, osteoblasts were observed in the process of apposing bone directly on the particle surface. In the marrow spaces only few inflammatory cells were detected. Histomorphometry showed that newly formed bone represented 20.1%, marrow spaces 57.5% and the residual graft material 22.4%.

Freeze-dried mineralized bone allograft (FDBA). At low power magnification, newly formed bone with marrow spaces and particles of residual biomaterial was present. In a marginal portion of the sample, preexisting bone with small remodeling areas could be observed (Figure 4(a)). At high power magnification, in some fields, the biomaterial particles were completely osseointegrated and areas of bone neoformation could be observed also inside the particles. Some of the biomaterial particles showed irregular margins, typical of a resorption process (Figure 4(b)). Bone neoformation areas could be seen both in contact with the biomaterial particles and in the marrow spaces, where few spindle cells could also be detected. Histomorphometry showed that newly formed bone represented 32.1%, marrow spaces 47.8%, and the residual graft material 20.1%.

(a)

(b)

(c)
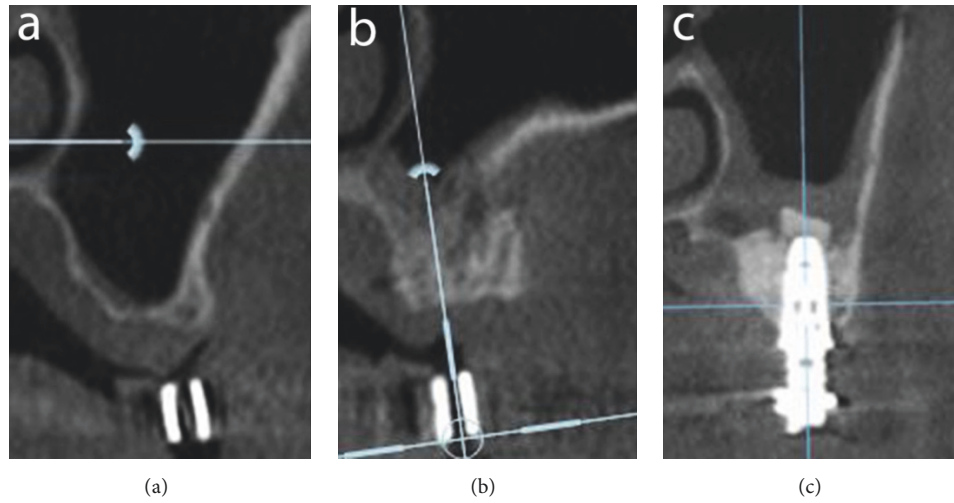
Figure 2: Radiographic evaluation: (a) CT scan before surgery; (b) CT scan after 6 months of graft healing; (c) CT scan after implant placement.

(a)

(b)
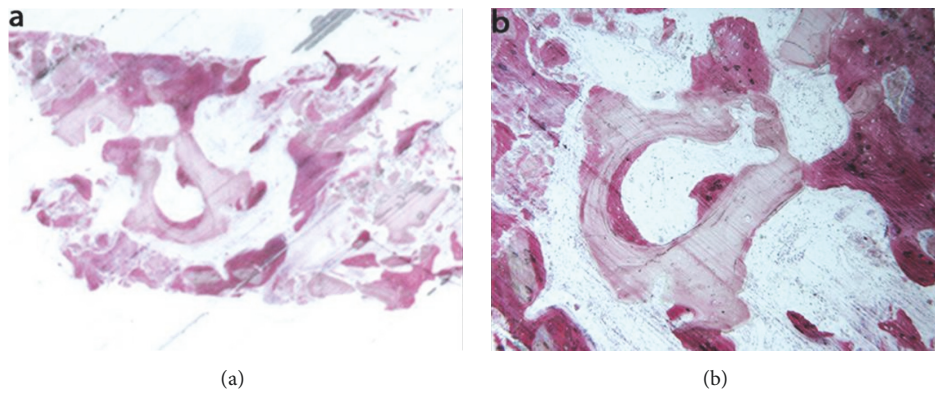
Figure 3: Mineralized solvent-dehydrated bone (toluidine blue and acid fuchsin): (a) trabecular bone with large marrow spaces and biomaterial particles was observed (original magnification 12X); (b) the biomaterial particles showed different sizes and they were partially surrounded by newly formed bone that was characterized by large osteocyte lacunae (original magnification 40X).

(a)

(b)
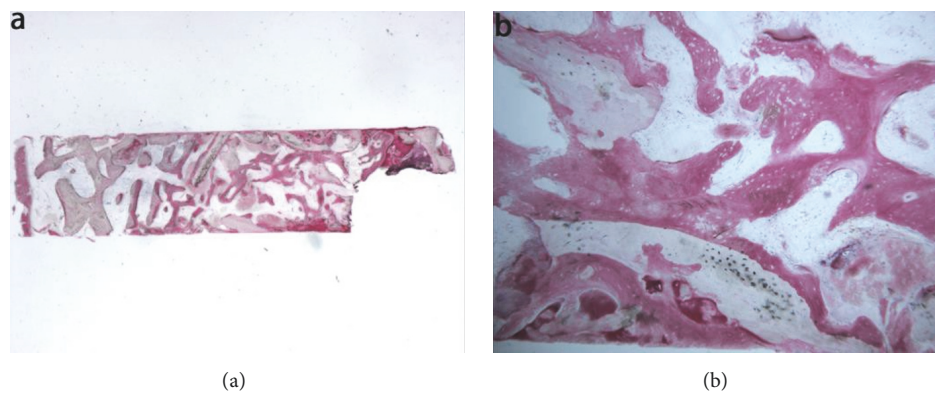
Figure 4: Freeze-dried mineralized bone allograft (toluidine blue and acid fuchsin): (a) newly formed bone with marrow spaces and particles of residual biomaterial was present. In a marginal portion of the sample, preexisting bone with small remodeling areas could be observed (original magnification 12X); (b) the biomaterial particles, showing areas of bone neoformation in their inner part, could be observed. Some of the biomaterial particles showed irregular margins, typical of a resorption process (original magnification 40X).

(a)

(b)
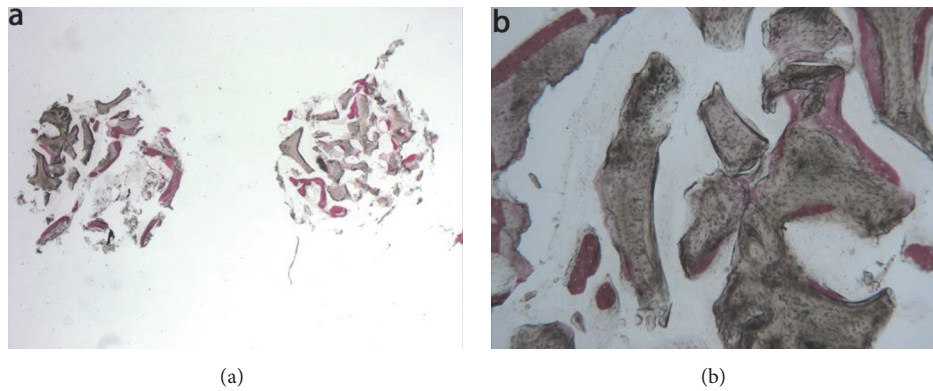
FIGURE 5: Anorganic bovine bone (toluidine blue and acid fuchsin): (a) the specimen appeared to be constituted by two separate fragments, where several particles of residual biomaterial were evident (original magnification 12X); (b) the areas of bone neoformation in tight contact with the biomaterial surface were present. In some fields, new bone formation inside the biomaterial particles could be observed (original magnification 40X).

(a)

(b)
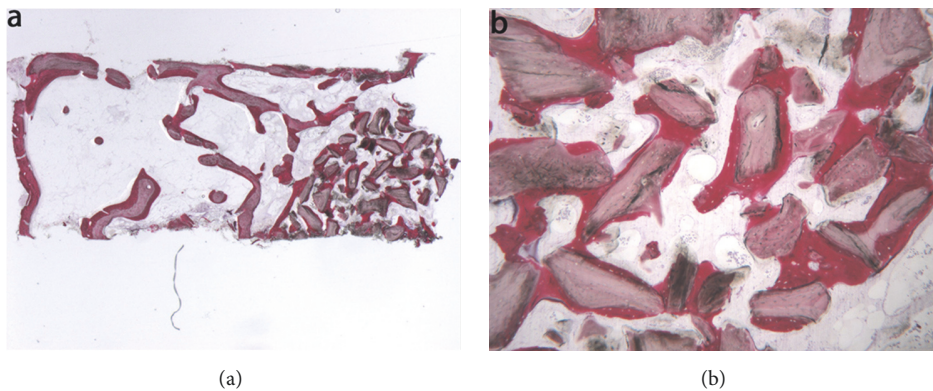
FIGURE 6: Equine-derived bone (toluidine blue and acid fuchsin): (a) trabecular bone with large marrow spaces and biomaterial particles was observed. The biomaterial particles were located in the apical portion of the biopsy and they were surrounded by new bone (original magnification 12X); (b) the bone was in close contact with the granules and in some areas osteoblasts were observed in the process of apposing bone directly on the particle surface (original magnification 40X).

Anorganic bovine bone (ABB). At low power magnification, the specimen appeared to be formed by two separate fragments, each presenting several residual biomaterial particles (Figure 5(a)). At high power magnification, most of the biomaterial particles showed areas of bone neoformation in tight contact with the biomaterial surface (Figure 5(b)). The newly formed bone in contact with the biomaterial particles showed wide osteocyte lacunae, typical of a young bone. In some fields, new bone formation inside the biomaterial particles could be observed. Histomorphometry showed that newly formed bone represented 16.1%, marrow spaces 46.7% and the residual biomaterial 37.2%.

Equine-derived bone (EB). At low magnification, trabecular bone with large marrow spaces and biomaterial particles was observed (Figure 6(a)). The particles were located in the apical portion of the biopsy and they were surrounded by new bone. In many fields the bone was in strict contact with the granules and in some areas osteoblasts were observed in the process of apposing bone directly on the particle surface (Figure 6(b)). Many large vessels could be detected. No inflammatory cells, or multinucleated giant cells, were present around the biomaterial or at the interface with bone. Histomorphometry showed that newly formed bone represented 22.8%, marrow spaces 47.1%, and the residual graft material 30.1%.

Synthetic micro-macroporous biphasic calcium-phosphate (HA-β-TCP 30/70). In the examined sample, newly formed trabecular bone and preexisting bone with marrow spaces and residual biomaterial could be observed (Figure 7(a)). At low power magnification, the residual biomaterial was surrounded by newly formed bone and no gaps were present at the bone biomaterial interface. In some portions of the specimen the graft seemed to undergo resorption (Figure 7(b)). No inflammatory cells or multinucleated giant cells were present around the biomaterial or at the interface with bone. Many small and large sized vessels could be observed. Histomorphometry showed that newly formed bone represented 20.3%, marrow spaces 41.8%, and the residual graft material 37.9%.

(a)

(b)
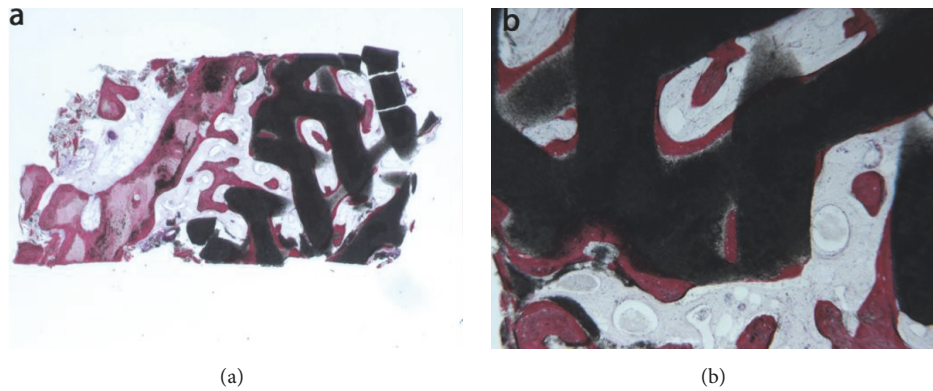
FIGURE 7: Synthetic micro-macroporous biphasic calcium-phosphate (HA-β-TCP 30/70) (toluidine blue and acid fuchsin): (a) trabecular bone with marrow spaces and residual biomaterial, located in the apical portion of the sample, could be observed (original magnification 12X); (b) the residual biomaterial was surrounded by newly formed bone and no gaps were present at the bone biomaterial interface. In some fields, the graft seemed to undergo resorption. Many large blood vessels could be seen (original magnification 40X).

(a)

(b)

(c)
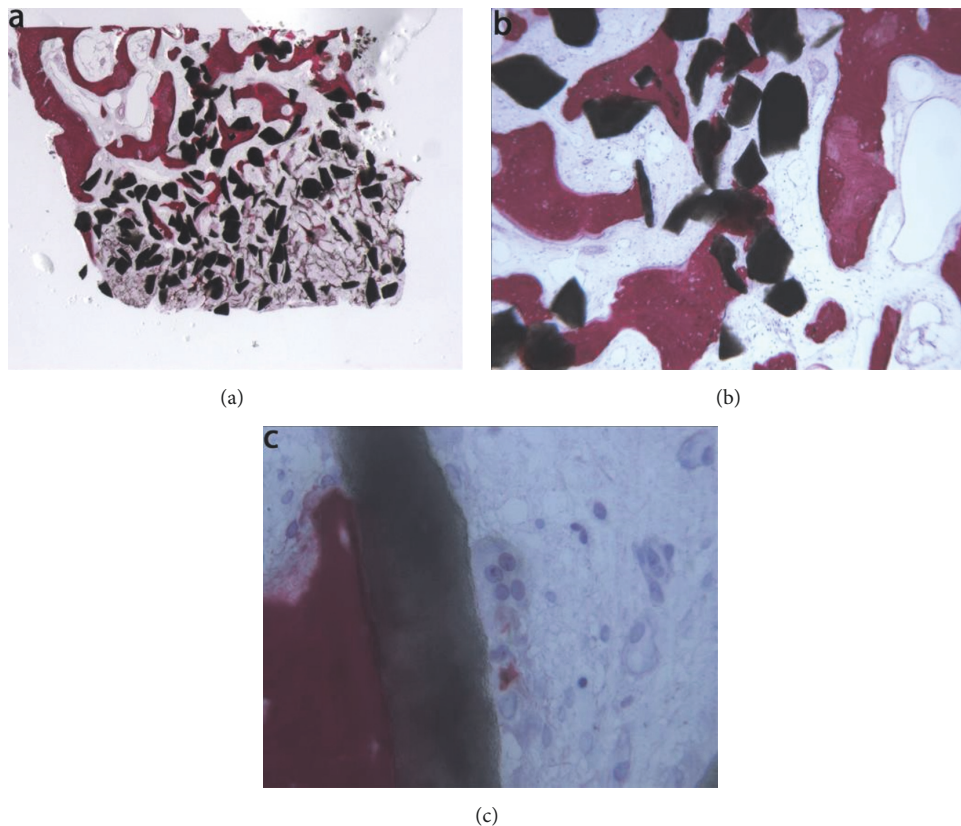
FIGURE 8: Bioapatite-collagen (toluidine blue and acid fuchsin): (a) trabecular bone with marrow spaces and residual biomaterial particles was observed (original magnification 12X); (b) osteoblasts were observed in the process of apposing bone directly on the particle surface. Marrow spaces were colonized by small and large blood vessels in close proximity to the new bone and to the particles (original magnification 40X); (c) moderate inflammatory infiltrate and multinucleated giant cells, probably osteoclasts, were observed directly on the biomaterial particles surface (original magnification 400X).

Bioapatite-collagen (BC). In the examined sample, trabecular bone with marrow spaces and residual biomaterial was observed (Figure 8(a)). Specifically, half of the sample was formed by residual biomaterial surrounded by newly formed bone, while in an apical portion of the sample many particles were partially covered by connective tissue. The new bone produced a network, "bridging" between the particles (Figure 8(b)). In a few fields, osteoblasts were observed in the process of apposing bone directly on the particle surface. Marrow spaces were colonized by small

TABLE 2: Histomorphometric results of bone biopsies retrieved from sinuses augmented.

	MCBA (%)	FDBA (%)	ABB (%)	EB (%)	HA-β-TCP 30/70 (%)	BC (%)
Newly formed bone	20.1	32.1	16.1	22.8	20.3	21.4
Marrow spaces	57.5	47.8	46.7	47.1	41.8	53.3
Residual graft material	22.4	20.1	37.2	30.1	37.9	25.3

MCBA: mineralized solvent-dehydrated bone
FDBA: freeze-dried mineralized bone allograft
ABB: anorganic bovine bone
EB: equine-derived bone
HA-β-TCP 30/70: synthetic micro-macroporous biphasic calcium-phosphate
BC: Bioapatite-collagen.

and large blood vessels in close proximity to the new bone and the biomaterial particles. Moderate inflammatory infiltrate and multinucleated giant cells, probably osteoclasts, were observed directly on the biomaterial particles surface (Figure 8(c)). Histomorphometry showed that newly formed bone represented 21.4 %, marrow spaces 53.3%, and the residual graft material 25.3%.

The histomorphometric results of bone biopsies are summarized in Table 2.

4. Discussion

Sinus augmentation is a well-documented technique for creating adequate bone volume to successfully place dental implants in resorbed maxillary posterior regions [36]. However clinical and histological outcomes regarding bone substitute materials still remain open areas of investigation because an ideal grafting material should provide biologic stability, ensure volume maintenance, and induce a high rate of formation of vital bone and bone remodeling [19]. Although numerous studies have compared grafting materials after sinus augmentation [7, 9, 16, 19, 27, 37–39], no one has compared histological and histomorphometric results of MCBA, FDBA, ABB, EB, HA-TCP (30/70), BC, using a standardized two-stage sinus augmentation model.

Within the limits of the present investigation, whose results referred to a limited number of patients, the histological and histomorphometric analysis of the regenerated tissues might provide useful information regarding the nature and amount of newly formed bone of the six tested biomaterials.

At histologic examination all biomaterials were in close contact with newly formed bone and showed the same pattern of bone formation surrounding the graft granules and producing a bridge-like network between the grafted particles.

From the present histologic investigation, the MCBA sample showed the highest biocompatibility, because no signs of acute inflammation were present, which was furthermore affirmed by the ability to form and maintain new bone bridging the greatest part of the biomaterial particles, as reported by other previous studies [9, 22, 38]. The use of MCBA tends to result in a slightly lower level of new bone formation compared to autologous bone, even if this tendency was not significant in a meta-analysis [3]. At the histomorphometric examination the percentage of new bone (20.1%) was lower than the percentage found by Schmitt et al. (35.41%) [8], while

the residual biomaterial (22.4%) was comparable to the value reported for other graft materials [40]. Moreover, our results agreed with histologic examination of NOUMBISSI et al. [41], in which the graft turnover (resorption and replacement by new bone) occurred more rapidly in MCBA.

Histomorphometry of FDBA sample showed that newly formed bone represented 32.1%, the highest value among the compared biomaterials. This data was similar to results of Kolerman et al. [42], who reported 27.5%, but lower than 41.1% described by Cammack et al. [43] and confirmed the capability to form a larger volume of bone in shorter times during clinical trials, as reported by other investigations [10, 44]. Sbordone et al. found that FDBA had similar outcomes compared to autogenous bone in sinus grafting procedure even when the residual floor thickness was less than 3 mm [45]. Furthermore, the evidence of resorption phenomena in our histology confirms that this material could influence long-term results in regenerated sites [23].

ABB was used as grafting material in a great number of studies, taking advantage of its well-known osteoconductive properties [44]. Some authors showed that microvascular density at 6 months in sinus augmented with ABB was not significantly different from microvascular density in sites augmented with autogenous bone [46]. In the present investigation ABB sample showed areas of new bone formation in close contact with the biomaterial surface and no signs of inflammation, suggesting a neutral interaction of the grafted particles with the new bone tissue. Moreover, compared to the other biomaterials at the histomorphometric examination, ABB showed the lowest percentage of newly formed bone (16.1%) and a higher amount of remaining biomaterial (37.2%). This no homogenous bone structure could, avoiding bone resorption, guarantee long-term stability of the augmented maxillary sinus [8]. Indeed, Mordenfeld et al. [15] showed long-term maintenance of these results after 9 years and Traini et al. [47] after 11 years.

Compared to ABB, EB showed a greater amount of newly formed bone (22.8%) and lower residual graft material (30.1%), in accordance with the results of a randomized clinical trial, which evaluated samples harvested 6 months after sinus augmentation with both of these materials [29]. This higher resorption could be influenced by a deantigenation process to which EB is subjected.

The presence, observed in our sample, of new bone surrounding the biomaterial particles, of many large vessels and in some fields of osteoblasts apposing bone directly on

the particle surface is comparable to other studies [27, 47]. The ability of EB to achieve a more rapid and intense vascularization could promote long-term implant osseointegration and predictability of rehabilitation in regenerated sites.

The HA-β-TCP 30/70 blocks used in the present investigation had a reticular structure, manufactured by a rapid prototyping (RP) technique offering a precise control of the porosity and external shape of a Ha-TCP ratio ceramic bone substitute [16] so as to influence bone formation.

Indeed, the use of HA-β-TCP 30/70, whose degradation can be tailored by varying its chemical composition together with the incorporation of pores, seems to be a good strategy to overcome the low degradation rate of CaP ceramics, which represents a limitation of these materials [16].

On 3D reconstruction and quantitative analysis, the HA/TCP scaffolds exhibited good performances in terms of both bone regeneration and vascularization, independently of the specific scaffold morphology (i.e., granules or blocks) [47]. However, Giuliani et al. reported that the scaffold morphology could influence the long-term kinetics of bone regeneration by showing that block-based specimens presented better results than granule-based samples [48]. The data of the present study is in agreement with other investigations concerning bone formation in maxillary sinus augmentation with HA-beta-TCP (30/70), after a healing period of 6 months [34, 37].

The histological and histomorphometric aspects of BC sample were similar to those of the other materials tested and confirm the osteoconductive property of this biomaterial as shown in previous studies [34, 35]. Moreover, the plastic and spongy consistency of this biomaterial renders it very easy to handle and to shape with scissors, allowing it to be used in sinus augmentation procedures without any membrane, in contrast to granular grafts, as suggested by some authors [49, 50]. Lastly the presence of collagen and glucosamine improves, respectively, fibrin formation and bone mineralization process as confirmed by Maiorana et al. [51, 52].

5. Conclusion

Within the limitations of the present investigation, all the six biomaterials tested in two-stage maxillary sinus augmentation model showed good biocompatibility and osteoconductive properties and could be used successfully in sinus augmentation procedure. Although, the FDBA seemed to have the best histomorphometric result in terms of newly formed bone and residual graft material. Nevertheless, longer term histological studies will be needed to understand better resorption times and modalities [53, 54].

Data Availability

The histological data used to support the findings of this study are included within the article.

Conflicts of Interest

The authors declare that there are no conflicts of interest regarding the publication of this paper.

References

[1] S. P. Pilipchuk, A. B. Plonka, A. Monje et al., "Tissue engineering for bone regeneration and osseointegration in the oral cavity," *Dental Materials*, vol. 31, no. 4, pp. 317–338, 2015.

[2] L. Castagna, W. D. Polido, L. G. Soares, and E. M. B. Tinoco, "Tomographic evaluation of iliac crest bone grafting and the use of immediate temporary implants to the atrophic maxilla," *International Journal of Oral and Maxillofacial Surgery*, vol. 42, no. 9, pp. 1067–1072, 2013.

[3] R. J. Klijn, G. J. Meijer, E. M. Bronkhorst, and J. A. Jansen, "A meta-analysis of histomorphometric results and graft healing time of various biomaterials compared to autologous bone used as sinus floor augmentation material in humans," *Tissue Engineering—Part B: Reviews*, vol. 16, no. 5, pp. 493–507, 2010.

[4] S. A. Zijderveld, E. A. J. M. Schulten, I. H. A. Aartman, and C. M. Ten Bruggenkate, "Long-term changes in graft height after maxillary sinus floor elevation with different grafting materials: Radiographic evaluation with a minimum follow-up of 4.5 years," *Clinical Oral Implants Research*, vol. 20, no. 7, pp. 691–700, 2009.

[5] C. M. Misch, "Autogenous bone: is it still the gold standard?" *Implant Dentistry*, vol. 19, no. 5, p. 361, 2010.

[6] G. Bavetta and M. E. Licata, "The use of human allogenic graft (HBA) for maxillary bone regeneration: Review of literature and case reports," *Current Pharmaceutical Design*, vol. 18, no. 34, pp. 5559–5568, 2012.

[7] S. A. Danesh-Sani, S. S. Wallace, A. Movahed et al., "Maxillary Sinus Grafting with Biphasic Bone Ceramic or Autogenous Bone: Clinical, Histologic, and Histomorphometric Results from a Randomized Controlled Clinical Trial," *Implant Dentistry*, vol. 25, no. 5, pp. 588–593, 2016.

[8] C. M. Schmitt, H. Doering, T. Schmidt, R. Lutz R, F. W. Neukam, and K. A. Schlegel, "Histological results after maxillary sinus augmentation with Straumann, BoneCeramic, Bio-Oss, Puros, and autologous bone. A randomized controlled clinical trial," *Clinical Oral Implants Research*, vol. 24, no. 5, pp. 576–585, 2013.

[9] S. Annibali, M. P. Cristalli, G. La Monaca et al., "Human maxillary sinuses augmented with mineralized, solvent-dehydrated bone allograft: a longitudinal case series," *Implant Dentistry*, vol. 20, no. 6, pp. 445–454, 2011.

[10] M. Nevins, F. Heinemann, and U. W. Janke, "Equine-derived bone mineral matrix for maxillary sinus floor augmentation: a clinical, radiographic, histologic, and histomorphometric case series," *The International journal of periodontics & restorative dentistry*, vol. 33, no. 4, pp. 483–489, 2013.

[11] S. Tetè, R. Vinci, V. L. Zizzari et al., "Maxillary sinus augmentation procedures through equine-derived biomaterial or calvaria autologous bone: immunohistochemical evaluation of OPG/RANKL in humans," *European Journal of Histochemistry*, vol. 57, no. 1, p. e10, 2013.

[12] J. Bassil, N. Naaman, R. Lattouf et al., "Clinical, histological, and histomorphometrical analysis of maxillary sinus augmentation using inorganic bovine in humans: preliminary results," *Journal of Oral Implantology*, vol. 39, no. 1, pp. 73–80, 2013.

[13] D. Z. Lee, S. T. Chen, and I. B. Darby, "Maxillary sinus floor elevation and grafting with deproteinized bovine bone mineral: a clinical and histomorphometric study," *Clinical Oral Implants Research*, vol. 23, no. 8, pp. 918–924, 2012.

[14] T. Chackartchi, G. Iezzi, M. Goldstein et al., "Sinus floor augmentation using large (1-2mm) or small (0.25-1mm) bovine

bone mineral particles: A prospective, intra-individual controlled clinical, micro-computerized tomography and histomorphometric study," *Clinical Oral Implants Research*, vol. 22, no. 5, pp. 473–480, 2011.

[15] A. Mordenfeld, M. Hallman, C. B. Johansson, and T. Albrektsson, "Histological and histomorphometrical analyses of biopsies harvested 11 years after maxillary sinus floor augmentation with deproteinized bovine and autogenous bone," *Clinical Oral Implants Research*, vol. 21, no. 9, pp. 961–970, 2010.

[16] C. Mangano, B. Sinjari, J. A. Shibli et al., "A Human clinical, histological, histomorphometrical, and radiographical study on biphasic ha-beta-tcp 30/70 in maxillary sinus augmentation," *Clinical Implant Dentistry and Related Research*, vol. 17, no. 3, pp. 610–618, 2015.

[17] Z. Mazor, R. A. Horowitz, M. del Corso, H. S. Prasad, M. D. Rohrer, and D. M. D. Ehrenfest, "Sinus floor augmentation with simultaneous implant placement using Choukroun's platelet-rich fibrin as the sole grafting material: a radiologic and histologic study at 6 months," *Journal of Periodontology*, vol. 80, no. 12, pp. 2056–2064, 2009.

[18] T. R. Dinato, M. L. Grossi, E. R. Teixeira, J. C. Dinato, F. S. Sczepanik, and S. A. Gehrke, "Marginal bone loss in implants placed in the maxillary sinus grafted with anorganic bovine bone: a prospective clinical and radiographic study," *Journal of Periodontology*, vol. 87, no. 8, pp. 880–887, 2016.

[19] G. Iezzi, M. Degidi, A. Piattelli et al., "Comparative histological results of different biomaterials used in sinus augmentation procedures: a human study at 6 months," *Clinical Oral Implants Research*, vol. 23, no. 12, pp. 1369–1376, 2012.

[20] S. A. Danesh-Sani, S. P. Engebretson, and M. N. Janal, "Histomorphometric results of different grafting materials and effect of healing time on bone maturation after sinus floor augmentation: a systematic review and meta-analysis," *Journal of Periodontal Research*, vol. 52, no. 3, pp. 301–312, 2016.

[21] M. Chiapasco, P. Casentini, and M. Zaniboni, "Bone augmentation procedures in implant dentistry," *The International Journal of Oral & Maxillofacial Implants*, vol. 24, supplement, pp. 237–259, 2009.

[22] S. J. Froum, S. S. Wallace, N. Elian, S. C. Cho, and D. P. Tarnow, "Comparison of mineralized cancellous bone allograft (Puros) and anorganic bovine bone matrix (Bio-Oss) for sinus augmentation: histomorphometry at 26 to 32 weeks after grafting," *International Journal of Periodontics and Restorative Dentistry*, vol. 26, no. 6, pp. 543–551, 2006.

[23] R. A. Wood and B. L. Mealey, "Histologic comparison of healing after tooth extraction with ridge preservation using mineralized versus demineralized freeze-dried bone allograft," *Journal of Periodontology*, vol. 83, no. 3, pp. 329–336, 2012.

[24] S. J. Froum, S. S. Wallace, S.-O. Cho, N. Elian, and D. P. Tarnow, "Histomorphometric comparison of a biphasic bone ceramic to anorganic bovine bone for sinus augmentation: 6- to 8-month postsurgical assessment of vital bone formation. A Pilot Study," *International Journal of Periodontics and Restorative Dentistry*, vol. 28, no. 3, pp. 273–281, 2008.

[25] G. Cannizzaro, P. Felice, M. Leone, P. Viola, and M. Esposito, "Early loading of implants in the atrophic posterior maxilla: lateral sinus lift with autogenous bone and Bio-Oss versus crestal mini sinus lift and 8-mm hydroxyapatite-coated implants. A randomised controlled clinical trial," *European Journal of Oral Implantology*, vol. 2, no. 1, pp. 25–38, 2009.

[26] G. Iezzi, A. Scarano, C. Mangano, B. Cirotti, and A. Piattelli, "Histologic results from a human implant retrieved due to

fracture 5 years after insertion in a sinus augmented with anorganic bovine bone," *Journal of Periodontology*, vol. 79, no. 1, pp. 192–198, 2008.

[27] D. A. Di Stefano, G. Gastaldi, R. Vinci et al., "Bone formation following sinus augmentation with an equine-derived bone graft: A retrospective histologic and histomorphometric study with 36-month follow-up," *The International Journal of Oral & Maxillofacial Implants*, vol. 31, no. 2, pp. 406–412, 2016.

[28] S. Tetè, V. L. Zizzari, R. Vinci et al., "Equine and porcine bone substitutes in maxillary sinus augmentation: A histological and immunohistochemical analysis of VEGF expression," *The Journal of Craniofacial Surgery*, vol. 25, no. 3, pp. 835–839, 2014.

[29] D. A. L. Di Stefano, G. Gastaldi, R. Vinci, L. Cinci, L. Pieri, and E. Gherlone, "Histomorphometric Comparison of Enzyme-Deantigenic Equine Bone and Anorganic Bovine Bone in Sinus Augmentation: A Randomized Clinical Trial with 3-Year Follow-Up," *The International journal of oral & maxillofacial implants*, vol. 30, no. 5, pp. 1161–1167, 2015.

[30] L. Artese, A. Piattelli, D. A. Di Stefano et al., "Sinus lift with autologous bone alone or in addition to equine bone: an immunohistochemical study in man," *Implant Dentistry*, vol. 20, no. 5, pp. 383–388, 2011.

[31] S. Raynaud, E. Champion, J. P. Lafon, and D. Bernache-Assollant, "Calcium phosphate apatites with variable Ca/P atomic ratio III. Mechanical properties and degradation in solution of hot pressed ceramics," *Biomaterials*, vol. 23, no. 4, pp. 1081–1089, 2002.

[32] C. Mangano, V. Perrotti, J. A. Shibli et al., "Maxillary sinus grafting with biphasic calcium phosphate ceramics: clinical and histologic evaluation in man," *The International Journal of Oral & Maxillofacial Implants*, vol. 28, no. 1, pp. 51–56, 2013.

[33] N. Broggini, D. D. Bosshardt, S. S. Jensen, M. M. Bornstein, C.-C. Wang, and D. Buser, "Bone healing around nanocrystalline hydroxyapatite, deproteinized bovine bone mineral, biphasic calcium phosphate, and autogenous bone in mandibular bone defects," *Journal of Biomedical Materials Research Part B: Applied Biomaterials*, vol. 103, no. 7, pp. 1478–1487, 2015.

[34] G. Garlini, M. Redemagni, M. Donini, and C. Maiorana, "Maxillary Sinus Elevation With an Alloplastic Material and Implants: 11 Years of Clinical and Radiologic Follow-Up," *Journal of Oral and Maxillofacial Surgery*, vol. 68, no. 5, pp. 1152–1157, 2010.

[35] L. Trombelli, L. Penolazzi, E. Torreggiani et al., "Effect of hydroxyapatite-based biomaterials on human osteoblast phenotype." *Minerva stomatologica*, vol. 59, no. 3, pp. 103–115, 2010.

[36] M. del Fabbro, G. Rosano, and S. Taschieri, "Implant survival rates after maxillary sinus augmentation," *European Journal of Oral Sciences*, vol. 116, no. 6, pp. 497–506, 2008.

[37] Y. K. Kim, P. Y. Yun, S. G. Kim, and S. C. Lim, "Analysis of the healing process in sinus bone graft- ing using various grafting materials," *Oral Surg Oral Med Oral Pathol OralRadiol Endod*, vol. 107, pp. 204–211, 2009.

[38] S. Annibali, G. Iezzi, G. L. Sfasciotti et al., "Histological and histomorphometric human results of HA-Beta-TCP 30/70 compared to three different biomaterials in maxillary sinus augmentation at 6 months: A preliminary report," *BioMed Research International*, vol. 2015, Article ID 156850, 2015.

[39] A. Monje, F. O'Valle, F. Monje-Gil et al., "Cellular, vascular, and histomorphometric outcomes of solvent-dehydrated vs freeze-dried allogeneic graft for maxillary sinus augmentation: A randomized case series," *The International Journal of Oral & Maxillofacial Implants*, vol. 32, no. 1, pp. 121–127, 2017.

[40] A. Scarano, M. Degidi, G. Iezzi et al., "Maxillary sinus augmentation with different biomaterials: a comparative histologic and histomorphometric study in man," *Implant Dentistry*, vol. 15, no. 2, pp. 197–207, 2006.

[41] S. S. Noumbissi, J. L. Lozada, P. J. Boyne et al., "Clinical, histologic, and histomorphometric evaluation of mineralized solvent-dehydrated bone allograf (Puros) in human maxillary sinus grafts.," *Journal of Oral Implantology*, vol. 31, no. 4, pp. 171–179, 2005.

[42] R. Kolerman, J. Nissan, M. Rahmanov, H. Vered, O. Cohen, and H. Tal, "Comparison between mineralized cancellous bone allograft and an alloplast material for sinus augmentation: A split mouth histomorphometric study," *Clinical Implant Dentistry and Related Research*, vol. 19, no. 5, pp. 812–820, 2017.

[43] G. V. Cammack II, M. Nevins, D. S. Clem III, J. P. Hatch, and J. T. Mellonig, "Histologic evaluation of mineralized and demineralized freeze-dried bone allograft for ridge and sinus augmentations," *International Journal of Periodontics and Restorative Dentistry*, vol. 25, no. 3, pp. 231–237, 2005.

[44] V. L. Zizzari, S. Zara, G. Tetè, R. Vinci, E. Gherlone, and A. Cataldi, "Biologic and clinical aspects of integration of different bone substitutes in oral surgery: a literature review," *Oral Surgery, Oral Medicine, Oral Pathology, Oral Radiology, and Endodontology*, vol. 122, no. 4, pp. 392–402, 2016.

[45] C. Sbordone, P. Toti, F. Guidetti, L. Califano, G. Pannone, and L. Sbordone, "Volumetric changes after sinus augmentation using blocks of autogenous iliac bone or freeze-dried allogeneic bone. A non-randomized study," *Journal of Cranio-Maxillo-Facial Surgery*, vol. 42, no. 2, pp. 113–118, 2014.

[46] A. Piattelli, M. Degidi, D. A. Di Stefano, C. Rubini, M. Fioroni, and R. Strocchi, "Microvessel Density in Alveolar Ridge Regeneration with Autologous and Alloplastic Bone," *Implant Dentistry*, vol. 11, no. 4, pp. 370–375, 2002.

[47] T. Traini, P. Valentini, G. Iezzi, and A. Piattelli, "A histologic and histomorphometric evaluation of anorganic bovine bone retrieved 9 years after a sinus augmentation procedure," *Journal of Periodontology*, vol. 78, no. 5, pp. 955–961, 2007.

[48] A. Giuliani, A. Manescu, E. Larsson et al., "In vivo regenerative properties of coralline-derived (Biocoral) scaffold grafts in human maxillary defects: demonstrative and comparative study with beta-tricalcium phosphate and biphasic calcium phosphate bu synchrotron radiation x-ray microtopograph," *Clinical Implant Dentistry and Related Research*, vol. 16, no. 5, pp. 736–750, 2014.

[49] S. S. Wallace, S. J. Froum, S.-C. Cho et al., "Sinus augmentation utilizing anorganic bovine bone (Bio-Oss) with absorbable and nonabsorbable membranes placed over the lateral window: histomorphometric and clinical analyses," *International Journal of Periodontics & Restorative Dentistry*, vol. 25, no. 6, pp. 551–559, 2005.

[50] P. Sibilla, A. Sereni, G. Aguiari et al., "Effects of a hydroxyapatite-based biomaterial on gene expression in osteoblast-like cells," *Journal of Dental Research*, vol. 85, no. 4, pp. 354–358, 2006.

[51] C. Maiorana, D. Sigurtà, A. Mirandola, G. Garlini, and F. Santoro, "Bone resorption around dental implants placed in grafted sinuses: Clinical and radiologic follow-up after up to 4 years," *The International Journal of Oral & Maxillofacial Implants*, vol. 20, no. 2, pp. 261–266, 2005.

[52] C. Maiorana, D. Sigurtà, A. Mirandola, G. Garlini, and F. Santoro, "Sinus elevation with alloplasts or xenogenic materials and implants: An up-to-4-year clinical and radiologic follow-up," *The International Journal of Oral & Maxillofacial Implants*, vol. 21, no. 3, pp. 426–432, 2006.

[53] L. Marinucci, S. Balloni, E. Becchetti et al., "Effects of hydroxyapatite and biostite® on osteogenic induction of hMSC," *Annals of Biomedical Engineering*, vol. 38, no. 3, pp. 640–648, 2010.

[54] M. Paknejad, S. Emtiaz, A. Rokn, B. Islamy, and A. Safiri, "Histologic and histomorphometric evaluation of two bone substitute materials for bone regeneration: An experimental study in sheep," *Implant Dentistry*, vol. 17, no. 4, pp. 471–479, 2008.

Research Article

Bone Regeneration of Peri-Implant Defects Using a Collagen Membrane as a Carrier for Recombinant Human Bone Morphogenetic Protein-2

Yoo-Kyung Sun,[1] Jae-Kook Cha,[1] Daniel Stefan Thoma,[2] So-Ra Yoon [iD],[1] Jung-Seok Lee,[1] Seong-Ho Choi [iD],[1] and Ui-Won Jung [iD],[1]

[1]*Department of Periodontology, Research Institute for Periodontal Regeneration, College of Dentistry, Yonsei University, Seoul, Republic of Korea*
[2]*Clinic for Fixed and Removable Prosthodontics and Dental Material Science, University of Zurich, Zurich, Switzerland*

Correspondence should be addressed to Ui-Won Jung; drjew@yuhs.ac

This study is designed to determine the effect of collagen membrane (CM) soaked with bone morphogenetic protein-2 (rhBMP-2) for the treatment of peri-implant dehiscence defects. *Material and Methods*. Three treatment groups were allocated at each defect in 5 dogs: (i) collagenated synthetic bone (OC) and CM soaked with rhBMP-2 (BMP group), (ii) OC and CM soaked with saline (nonBMP group), and (iii) no further treatment (control group). Titanium pins were used to stabilize the membranes in two dogs. Radiographic and histomorphometric analyses were performed 4 weeks later. *Results*. The median augmented volumes were 4.27 mm^3, 6.24 mm^3, and 2.75 mm^3 in the BMP, nonBMP, and control groups, respectively; the corresponding median first bone-to-implant contact (fBIC) distances were 3.25 mm, 3.08 mm, and 2.56 mm ($P > 0.05$). The placement of pins (with the BMP and nonBMP groups pooled) significantly improved bone regeneration: the augmented volumes were 17.60 mm^3 with pins and 3.68 mm^3 without pins ($P = 0.024$), with corresponding fBIC distances of 2.25 mm and 3.31 mm, respectively ($P < 0.001$). *Conclusions*. The addition of rhBMP-2 to CM failed to improve bone regeneration of peri-implant dehiscence defects compared to using an unsoaked CM after 4 weeks. However, the stabilization of CMs using pins positively influenced the outcomes.

1. Introduction

Guided bone regeneration (GBR) using collagen membrane (CM) is a well-documented treatment modality for augmenting localized peri-implant bone defects, with many clinical and preclinical studies demonstrating that exposed implant surfaces can be successfully augmented [1–5]. However, this type of resorbable membrane appears to result in insufficient space maintenance, which is reportedly due to the pressure from the covering flap resulting in membrane collapse [3, 6]. Recent research has focused on techniques and materials to overcome these drawbacks [7–9].

Recombinant human bone morphogenetic protein-2 (rhBMP-2) has well-documented osteogenic properties that significantly improve bone regeneration [10–13]. Recent reviews have also considered rhBMP-2 to be the most promising bioactive molecules for bone regeneration [14–16].

Clinical considerations mean that dental implants need to be placed in prosthetically ideal positions, which often results in buccal dehiscence defects. Several preclinical and clinical studies have evaluated rhBMP-2 in combination with various bone-substitute materials for localized bone regeneration for this type of peri-implant defect [10, 11, 17, 18]. RhBMP-2 was combined with the bone-substitute material in all of these studies; although this resulted in successful treatment outcomes and superiority compared to control groups, the outcomes were to some extent controversial and limited by the clinical applicability of soaking bone-substitute materials

with rhBMP-2. One option would be to use a CM as a carrier for rhBMP-2, since this would potentially be advantageous in being closer to the highly osteogenic periosteum containing abundant mesenchymal cells. In addition, a rapid bone formation on the outer side of the defect might result in a more stable augmented area. Based on this assumption, Chang and colleagues used a CM as a carrier for rhBMP-2 for primary horizontal bone augmentation, demonstrating a proof of concept [18]. However, this combination has not previously been evaluated for the clinically more common peri-implant defects.

Therefore, the aim of the present study was to determine the effect of a CM soaked with rhBMP-2 for the treatment of peri-implant dehiscence defects.

2. Material and Methods

2.1. Study Design. The present experiments were designed as a controlled preclinical study involving five mongrel dogs. The dogs were aged 12–15 months and a mean body weight of 30 kg. They had no systemic disease and showed a healthy periodontium and intact dentition. The study was performed in accordance with the Animal Care and Use Committee, Yonsei Medical Center, Seoul, Korea (permission no. 2011-0188).

2.2. Experimental Materials. The following materials were used in the study:

(1) Titanium implants with a sandblasted and acid-etched surface (3.8 mm in diameter and 8 mm long) (Implantium®, Dentium, Seoul, Korea).

(2) A collagenated synthetic bone (OC; OSTEON™ Collagen, Dentium) consisting of a particulate bone-substitute material [70% hydroxyapatite (HA) and 30% β-tricalcium phosphate] and a type I collagen.

(3) A resorbable CM containing HA particles (HA collagen membrane, GENOSS, Suwon, Korea).

(4) rhBMP-2 (Cowellmedi, Busan, Korea) at a concentration of 0.5 mg/ml, which was obtained by reconstituting and diluting rhBMP-2 in a buffer solution. The HA-containing CMs were soaked in 0.2 ml of rhBMP-2 solution for 15 minutes at room temperature.

2.3. Surgical Procedures. Oral prophylaxis was applied to all dogs prior to the surgical intervention. Details of the surgical procedures are available elsewhere [19]. In brief, general anesthesia as well as local infiltration anesthesia at the surgical sites was applied. Crevicular incisions were then made from the second premolar to the first molar, and two vertical incisions were made on the buccal gingiva. Following hemisectioning, the second, third, and fourth premolars and the first molar were extracted on one side of the mandible. The buccal bone plates were removed, resulting in an acute defect with dimensions of 5 mm (apico-coronal width) by 5 mm (bucco-oral depth) and extending from the second to the fourth premolar. Primary wound closure was then performed. The sutures were removed 10 days later.

2.4. Implant Placement and Guided Bone Regeneration. Twelve weeks later, dental implants were placed and simultaneous GBR was performed (Figure 1). Following flap reflection, the healed ridge was flattened and three implants were placed with their platforms flush with the lingual bone crest. This resulted in a peri-implant dehiscence defect with a height of 3 mm at the buccal aspect (Figure 2(a)). The cortical bone plate was perforated in the vicinity of the implants, and GBR was performed. The following three treatment modalities were applied (Figure 2(c)):

(1) OC and a CM containing HA particles soaked with rhBMP-2 (BMP group).

(2) OC and a CM containing HA particles soaked with sterile saline (nonBMP group).

(3) No GBR (control group).

The control group was always located at the center implant site to minimize the influence of the BMP molecule on adjacent groups, while the BMP and nonBMP groups were allocated to the mesial or distal implant sites randomly.

In group BMP, the OC was grafted on the peri-implant defect and covered with a CM containing HA particles soaked with rhBMP-2. In group nonBMP, the OC was grafted on the peri-implant defect and then covered with a CM containing HA particles soaked with saline. No overaugmentation was attempted in either of these groups. In two of the five dogs, two titanium pins (Frios® membrane tacks, DENTSPLY Implants, Mannheim, Germany) were used to stabilize the membranes in the BMP and nonBMP groups, while no fixation pins were applied in the remaining three dogs. In addition, the CM was perforated on top of the implant and immobilized by a cover screw. No graft material or membrane was used on the control group.

Periosteal releasing incisions were subsequently made and primary wound closure was achieved using a resorbable suture material (Monosyn® 4.0 Glyconate Monofilament, B. Braun, Tuttlingen, Germany). The sutures were removed 10 days later. The dogs were sacrificed by an overdose of sodium pentobarbital 4 weeks after implant placement and GBR surgery.

2.5. Radiographic Analysis. The specimens were scanned using micro-CT (SkyScan 1072, SkyScan, Aartselaar, Belgium) and the total augmented volume (TAV, mm^3) was measured, which represented the regenerated tissue surrounding the implant. Mineralized tissue was considered to be indicated in the images by grayscale values from 39 to 52 (defined as radiopaque tissue). The lower border of the TAV was located 3 mm below the implant platform, and the coronal border was defined by the most-coronal location of radiopaque tissue. The buccolingual extension of the TAV ranged from the center of the implant to the most-buccal radiopaque tissue (at an angle of 90° to the implant surface). The mesiodistal borders of the TAV were confined by vertical lines 7 mm from the center of the implant surface (Figure 3). The implant itself was excluded from the TAV.

Cross-sectional images of each group are presented in Figure 4. The total augmented materials were painted using
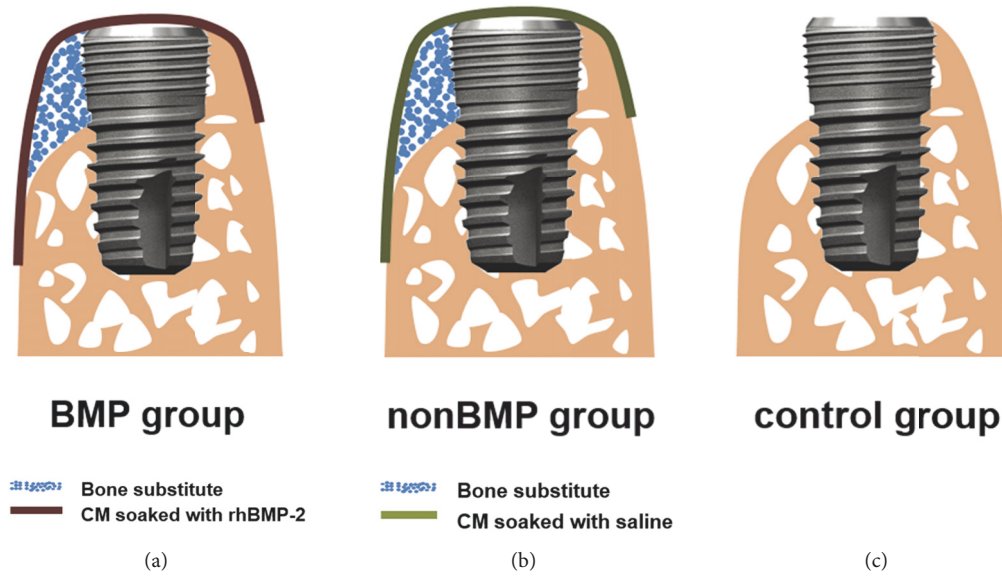
FIGURE 1: Schematic drawings of the surgery design: (a) BMP group, (b) nonBMP group, and (c) control group. Blue circles, bone-substitute materials; dark-red line, CM soaked with rhBMP-2; green line, CM soaked with saline; BMP group, cylinder-type bone-substitute material covered by CM soaked with rhBMP-2; nonBMP group, cylinder-type bone-substitute material covered by CM soaked with saline; control group, no further treatment.
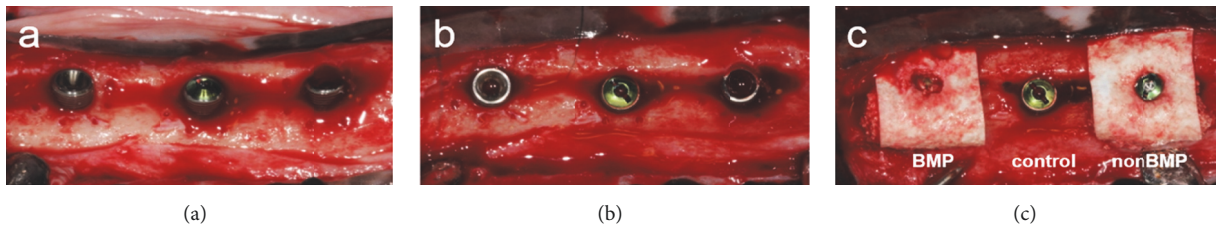
FIGURE 2: Clinical photographs of the bone augmentation procedure applied to peri-implant dehiscence defects: (a) buccal and (b) occlusal views after implant placement and (c) GBR treatment performed on dehiscence defects according to group assignment. The control group was placed at the center implant site, and the BMP and nonBMP groups were randomly allocated to the mesial and distal implant sites.
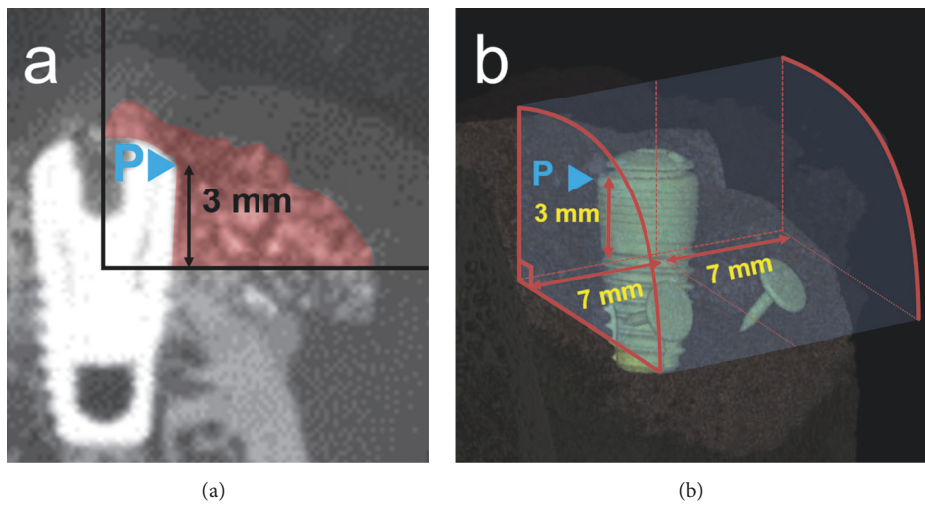
FIGURE 3: Schematic configuration of the TAV (mm^3). (a) The lower border of the TAV was located 3 mm below the implant platform. The coronal border was defined by the most-coronal location of radiopaque tissue. The buccolingual extension of the TAV ranged from the center of the implant to the most-buccal radiopaque tissue (at an angle of $90°$ to the implant surface). (b) The mesiodistal borders of the TAV were confined by vertical lines 7 mm from the center of the implant surface. The implant itself was excluded from the TAV. P, implant platform.
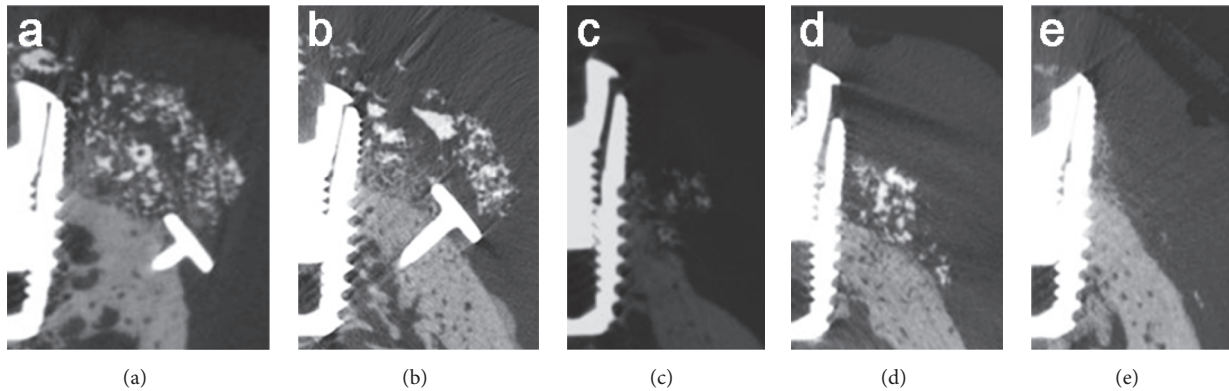
FIGURE 4: Cross-sectional radiographic images demonstrating variations both between and within the groups: (a) BMP group with pins, (b) nonBMP group with pins, (c) BMP group without pins, (d) nonBMP group without pins, and (e) control group. In the BMP and nonBMP groups, the shape of the augmented region appeared to be predominantly influenced by the use of pins.
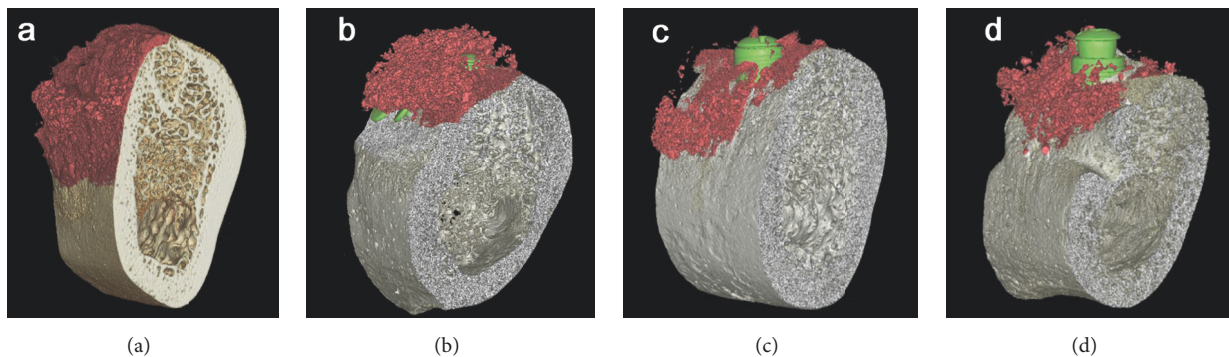
FIGURE 5: Three-dimensional reconstructed color-coded images of the total augmented area: (a) BMP group with pins, (b) nonBMP group with pins, (c) BMP group without pins, and (d) nonBMP group without pins. No remaining peri-implant defects were observed in the specimens with pins, in contrast with the sites without pins and control sites without GBR.

OnDemand 3D software (Cybermed, Seoul, Korea) to facilitate identification of the bone regeneration (Figure 5).

2.6. Histologic Analysis. Block specimens were harvested that included the implants and grafted sites with surrounding hard and soft tissues, and they were fixed in 10% neutral buffered formalin for 10 days. The specimens were then trimmed and dehydrated in ethanol before being embedded in methyl methacrylate. Specimens were cut in the center of the implant sites in a buccolingual plane and stained with hematoxylineosin and Masson's trichrome. The final thickness of the sections was 20 μm.

2.7. Descriptive Histology. The histology sections were examined under a light microscope (BX-50, Olympus Optical, Tokyo, Japan) to identify relevant structures such as the implants, new bone formation, bone-substitute material, nonmineralized tissue, and the remaining peri-implant defect.

2.8. Histomorphometric Analysis. Histomorphometric measurements were made at the buccal aspect of all implants.

An image-analysis program (Adobe Photoshop CS6, Adobe Systems, San Jose, CA, USA) was used to assess the following landmarks: implant platform (P), the first bone-to-implant contact (B), and the most-coronal buccal bone (BC) (Figure 6).

2.8.1. Linear Measurements. The following linear measurements were made:

(1) Distance between the implant platform (P) and the first bone-to-implant contact (B) (fBIC, mm).

(2) Vertical distance between the most-coronal buccal bone (BC) and the implant platform (P) (P-BC, mm).

(3) The bone-to-implant contact (BIC, %), measured along the implant surface between the implant platform (P) and extending 4 mm apically.

2.8.2. Area/Surface Measurements. A rectangular area of interest (AOI) was defined on the buccal side of the implants and included the following dimensions: coronal (implant platform), apical (4 mm apically toward the implant platform), and horizontal (2 mm from the implant surface).
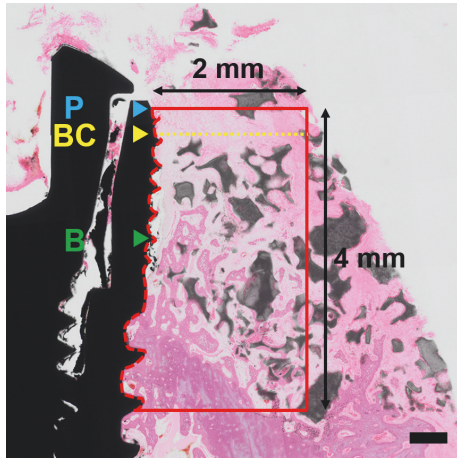
FIGURE 6: Schematic configuration for the histomorphometric analysis. P, implant platform; BC, most-coronal buccal bone; B, first bone-to-implant contact; red box, AOI. Scale bar = 500 μm.

The ratios of the following outcomes to the AOI area were measured:

(1) Newly formed bone (NB, %).

(2) Residual bone-substitute material (RBS, %).

(3) Nonmineralized tissue (NMT, %).

2.9. Statistical Analysis. Mean and standard deviation values were calculated in each group. One-way analysis of variance and the Bonferroni post hoc test were used to assess the clinical benefit of soaking the CM with the rhBMP-2 solution. The independent t-test was used to identify differences among groups related to the use of pins. The cutoff for statistical significance was $P < 0.05$.

3. Results

3.1. Clinical Findings. All of the dogs remained healthy, with no wound dehiscence or membrane exposure being detected throughout the experiments. All of the obtained samples were included in the analyses.

3.2. Radiographic Analysis. The cross-sectional images demonstrated variations both between and within the groups (Figure 4). In the BMP and nonBMP groups, the shape of the augmented region appeared to be predominantly influenced by the use of pins. No remaining peri-implant defects were observed in the specimens with pins, in contrast with the sites without pins and control sites without GBR (Figure 5).

The median TAV values were 4.27 mm^3, 6.24 mm^3, and 2.75 mm^3 in the BMP, nonBMP, and control groups, respectively (all $P > 0.05$) (Table 1). When the groups were divided according to the presence or absence of fixation pins, the median TAV was significantly higher in the group with pins (17.60 mm^3) than in that without pins (3.68 mm^3) ($P = 0.024$) (Table 2).

TABLE 1: Measured the total augmented volume (TAV) values. P value for intergroup comparison = 0.376. n = number of sites/dogs.

Group	TAV (mm^3)
BMP group	4.27 (3.08–18.23)
with pins ($n = 2$)	20.87 (19.55–22.20)
without pins ($n = 3$)	3.08 (1.68–3.68)
nonBMP group	6.24 (5.71–7.52)
with pins ($n = 2$)	12.25 (9.88–14.62)
without pins ($n = 3$)	5.71 (3.15–5.98)
Control group	2.75 (1.98–4.80)

Data are median (interquartile range) values.

3.3. Histologic Observations and Histomorphometric Analysis. In the two GBR groups (i.e., BMP and nonBMP), bone formation was generally observed along the implant surfaces (Figure 7). However, defect resolution was not consistent, with some specimens in both groups exhibiting complete regeneration and others with remaining peri-implant bone defects. In control sites, the size of the peri-implant defects appeared to be similar to that prior to augmentation. Complete resolution of the dehiscence defects was consistently observed in the histology specimens of the BMP and nonBMP groups using pins, with new bone having formed at the apical border of the bone defect and around the bone-substitute particles. In contrast, the positioning of the bone-substitute particles was disrupted and bone regeneration did not occur uniformly in the group without pins.

The median fBIC distances were 3.25 mm, 3.08 mm, and 2.56 mm in the BMP, nonBMP, and control groups, respectively, with corresponding median BIC values of 11.90%, 18.24%, and 21.96%.

Within the AOI, the median NBs were 12.84%, 8.06%, and 21.75% in the BMP, nonBMP, and control groups, respectively. The median RBS was 1.31% in the BMP group and 12.43% in the nonBMP group. There were no significant intergroup differences ($P > 0.05$). All of the data are reported in Table 3.

All of the measured histomorphometric and radiographic values (except for RBS in histomorphometric analyses) differed significantly with the presence or absence of pins when 10 specimens were divided according to the use of pins (Table 2). The median NB was 37.03% with pins and 4.87% without pins in the BMP group and 47.18% with pins and 7.90% without pins in the nonBMP group. BIC was higher in both the BMP and nonBMP groups with pins (40.38% and 33.19%, respectively) than without pins (10.49% and 10.69%, respectively) (Table 3).

4. Discussion

This study has revealed that (i) the addition of rhBMP-2 to a CM does not significantly improve peri-implant bone regeneration and (ii) fixation of the CM using pins significantly increases bone regeneration compared to using a CM without pins.

This study was designed to evaluate the usefulness of a CM as a carrier for rhBMP-2 for guided bone regeneration at

(a)   (b)   (c)   (d)   (e)
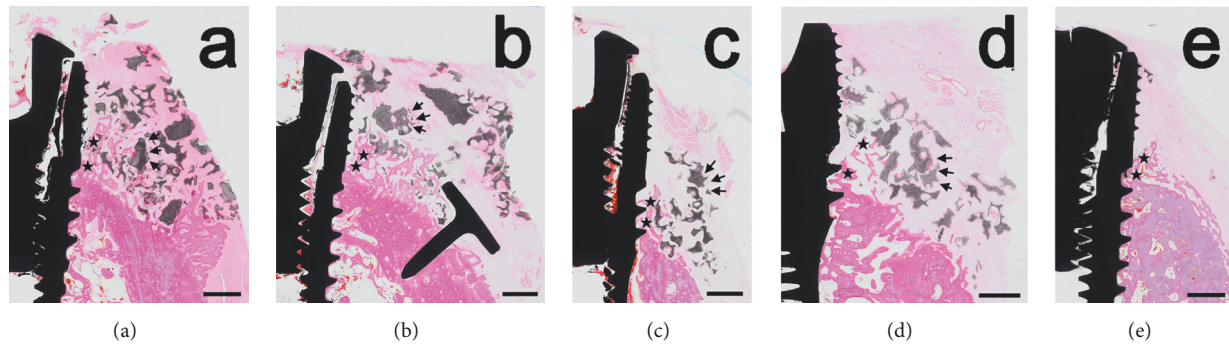
FIGURE 7: Histologic views presenting the results of GBR: (a) BMP group with pins, (b) nonBMP group with pins, (c) BMP group without pins, (d) nonBMP group without pins, and (e) control group. The results for defect resolution were not consistent, as demonstrated by some specimens in both the BMP and nonBMP groups exhibiting complete regeneration and others with remaining peri-implant bone defects. Complete resolution of the dehiscence defects was consistently observed in the histology specimens of the BMP and nonBMP groups using pins, while the positioning of bone-substitute particles was disrupted and bone regeneration did not occur uniformly in the group without pins. In the control sites, the size of the peri-implant defects appeared to be similar to the situation prior to augmentation. Asterisk, newly formed bone; arrow, residual bone-substitute material. Scale bar = 1 mm.

TABLE 2: Radiographic and histomorphometric outcomes, with data for the BMP and nonBMP groups pooled according to the use of pins.

		With pins ($n = 4$)	Without pins ($n = 6$)	P
Radiographic volume	TAV, mm^3	17.60 (7.52–23.52)	3.68 (0.27–5.71)	0.024
Linear measurements	BIC, %	40.38 (18.24–48.15)	10.59 (2.61–26.12)	0.027
	fBIC, mm	2.25 (1.95–2.38)	3.31 (3.08–0.87)	<0.001
	P-BC, mm	0.59 (0.00–1.27)	2.91 (2.51–3.44)	0.001
Measurements in the AOI	NB, %	42.54 (28.69–54.66)	6.56 (3.40–12.84)	0.006
	RBS, %	8.03 (0.00–19.01)	6.86 (0.00–23.66)	0.908
	NMT, %	53.46 (32.92–56.66)	84.94 (68.29–95.29)	0.002

Data are median (interquartile range) values.
n = number of sites/dogs. TAV (mm^3) = the total augmented volume; BIC (%) = the bone-to-implant contact; fBIC (mm) = distance between the implant platform and the first bone-to-implant contact; P-BC (mm) = vertical distance between the most-coronal buccal bone and the implant platform; NB (%) = newly formed bone; RBS (%) = residual bone-substitute material; NMT (%) = nonmineralized tissue.

TABLE 3: Histomorphometric measurements.

	Linear measurements			Measurements in the AOI		
Group	BIC, %	fBIC, mm	P-BC, mm	NB, %	RBS, %	NMT, %
BMP group	11.90 (10.49–34.65)	3.25 (2.29–3.36)	2.64 (1.27–2.75)	12.84 (4.87–28.69)	1.31 (0.00–12.42)	82.71 (54.63–87.16)
with pins ($n = 2$)	40.38 (37.52–43.25)	2.25 (2.23–2.27)	0.64 (0.32–0.95)	37.03 (32.86–41.20)	9.51 (4.75–14.26)	53.46 (52.88–54.05)
without pins ($n = 3$)	10.49 (6.55–11.20)	3.36 (3.31–3.62)	2.75 (2.70–3.04)	4.87 (4.14–8.86)	1.31 (0.65–6.86)	87.16 (84.94–91.22)
nonBMP group	18.24 (10.69–26.12)	3.08 (2.38–3.17)	2.51 (0.65–3.06)	8.06 (7.90–39.71)	12.43 (3.63–19.56)	68.29 (56.66–75.23)
with pins ($n = 2$)	33.19 (25.72–40.67)	2.17 (2.06–2.27)	0.59 (0.56–0.62)	47.18 (43.45–50.92)	8.03 (5.83–10.23)	44.79 (38.85–50.73)
without pins ($n = 3$)	10.69 (10.33–18.41)	3.17 (3.13–3.31)	3.06 (2.79–3.25)	7.90 (6.56–7.98)	19.56 (9.78–21.61)	75.2 (71.76–83.66)
Control group	21.96 (8.16–5.04)	2.56 (2.55–3.74)	2.04 (1.60–3.56)	21.75 (3.19–22.91)	0.00	78.25 (77.09–96.81)
P	0.873	0.664	0.679	0.550	0.313	0.152

Data are median (interquartile range) values.
n = number of sites/dogs.
None of the outcome measured differed significantly between the three groups ($P > 0.05$).

peri-implant dehiscence defects. Previous experiments that employed a similar protocol using animals and 30-mm peri-implant defects demonstrated that this model can serve as a valid alternative to clinical studies [20, 21].

Various preclinical models have demonstrated that rhBMP-2 improves bone regeneration by accelerating osteogenesis predominantly at the early stage of wound healing [22, 23]. In addition, the healing time is reportedly twofold shorter in dogs than in humans [24], and so earlier observation periods were established in this present study when evaluating the efficacy of rhBMP-2 compared to the previous experiments. In the present study, the bone formation at 4 weeks was greater in the GBR groups (by up to 47%) than at the untreated control sites (22%). This is in line with the reporting greater bone formation for GBR groups compared to the control sites, although those results were for longer healing periods of 8 and 16 weeks [21]. However, the addition of rhBMP-2 to a CM in the present study was not beneficial to bone regeneration compared to a CM soaked in saline at the early stage of healing of 4 weeks.

The other main difference between these two studies—apart from the healing period—was in the type of carrier material used. Various carrier materials have been used for rhBMP-2 [25–27]. It was speculated that using a CM as a carrier for rhBMP-2 could enhance the osteoinductivity of the periosteum due to the close proximity of the membrane and the periosteum. It was also speculated that an rhBMP-2 carrier in such a location would result in faster bone regeneration at the borders of the defect area, thereby ideally leading to shell-like bone formation, which could further compensate the disadvantages of a resorbable nonspace-maintaining membrane. However, this outcome was not observed in the present study, with no shell-like bone formation observed in any of the samples. In a preliminary study that used a GBR protocol and materials similar to those in the present study [18], histomorphometric analyses revealed that new bone formed closer to the membrane in the group with an rhBMP-2-loaded membrane than in the group with rhBMP-2 loaded on the bone-substitute material. This was observed as the new bone formed directly underneath the membrane in the group with rhBMP-2 loaded membrane. The differences in the observed bone regeneration pattern between these two studies might have been due to different healing periods (8 weeks versus 4 weeks), the placement of implants versus GBR alone, and the use of fixation pins.

Stability of the surgical site and space maintenance are considered to be essential for successful bone regeneration. The stabilization of a GBR site appears to be the critical factor governing the amount of bone formation. In a clinical study, it was found that bone formation was superior when using fixation pins [4]. This was subsequently supported by two in vitro studies that evaluated the effect of wound closure on the stability of GBR sites using various material combinations [6, 28], which found that the bone-substitute material moved apically upon wound closure. However, CMs were used at all sites, and it is well known that this type of membrane is weak mechanically and so may not be able to resist compressive

forces. This can result in collapse of the membrane and the above-mentioned displacement of bone-substitute material. However, the studies have demonstrated that applying additional fixation pins can reduce the membrane displacement by 50% at the level of the implant shoulder. The clinical recommendation was to add fixation pins when CMs are used in combination with particulate graft materials [6]. Fixation pins were used in two of the five dogs in the present study. The failure to standardize the experimental method was due to not being possible to fix the pins on thick, rigid cortical bone without deformation. The results demonstrate the beneficial bone formation at sites where pins are used. However, it could be considered to use alternative fixation materials, such as miniscrews which have better strength than pins in case of performing GBR on a rigid bony plate.

Apart from the fixation pins, more-rigid barrier membranes [29] or more-stable grafting materials provide further advantages in stabilizing the augmented site [30]. This was implemented in the present study by combining a cylindrical type of synthetic bone-substitute material with a type I collagen matrix and HA-coated CMs. This bone-substitute material incorporating a collagen matrix was considered to resist compressive forces and to support the augmented ridge volume [31]. An in vitro study using a similar membrane coated with HA demonstrated a significantly enhanced chemical stability and an improved mechanical structure of the membrane [32]. Moreover, the cross-linked chemical structure stiffened the CM and thereby reduced the risk of collapse [33]. Such a membrane theoretically exhibits all the characteristics necessary to support space maintenance. However, in clinical experiments the increased stiffness resulted in major difficulties in handling the membrane and applying it properly to the defect site, which meant that displacement of the graft material could not be avoided.

The outcomes of this study are limited by several factors, including the relatively small number of experimental animals, the use of pins in only two of the five dogs, the handling difficulties with the membrane resulting in suboptimal clinical outcomes, and the short observation period. Further studies involving larger numbers of animals and appropriate statistical analyses are required to confirm the results of this study.

5. Conclusion

The use of rhBMP-2 soaked on a CM as a carrier material did not result in superior bone formation compared to control sites without rhBMP-2. However, the use of fixation pins to stabilize the CMs did exert a positive effect on peri-implant bone regeneration.

Data Availability

The data used to support the findings of this study are available from the corresponding author upon request.

Disclosure

Conflicts of Interest

The authors have no conflicts of interest related to this article to report.

Authors' Contributions

Yoo-Kyung Sun and Jae-Kook Cha contributed equally to this study.

Acknowledgments

References

[1] D. Brocard, P. Barthet, E. Baysse et al., "A multicenter report on 1,022 consecutively placed ITI implants: a 7-year longitudinal study," *The International Journal of Oral & Maxillofacial Implants*, vol. 15, no. 5, pp. 691–700, 2000.

[2] N. U. Zitzmann, R. Naef, and P. Schärer, "Resorbable versus nonresorbable membranes in combination with Bio-Oss for guided bone regeneration," *International Journal of Oral & Maxillofacial Implants*, vol. 12, no. 6, pp. 844–852, 1997.

[3] T. J. Oh, S. J. Meraw, E. J. Lee, W. V. Giannobile, and H. L. Wang, "Comparative analysis of collagen membranes for the treatment of implant dehiscence defects," *Clinical Oral Implants Research*, vol. 14, no. 1, pp. 80–90, 2003.

[4] L. Carpio, J. Loza, S. Lynch, and R. Genco, "Guided bone regeneration around endosseous implants with anorqanic bovine bone mineral. a randomized controlled trial comparing bioabsorbable versus non-resorbable barriers," *Journal of Periodontology*, vol. 71, no. 11, pp. 1743–1749, 2000.

[5] J. J. Sevor, R. M. Meffert, and R. Jack Cassingham, "Regeneration of dehisced alveolar bone adjacent to endosseous dental implants utilizing a resorbable collagen membrane: Clinical and histologic results," *International Journal of Periodontics and Restorative Dentistry*, vol. 13, no. 1, pp. 71–83, 1993.

[6] J. Mir-Mari, H. Wui, R. E. Jung, C. H. F. Hämmerle, and G. I. Benic, "Influence of blinded wound closure on the volume stability of different GBR materials: An in vitro cone-beam computed tomographic examination," *Clinical Oral Implants Research*, vol. 27, no. 2, pp. 258–265, 2016.

[7] D. S. Thoma, U. W. Jung, J. Y. Park, S. P. Bienz, J. Hüsler, and R. E. Jung, "Bone augmentation at peri-implant dehiscence defects comparing a synthetic polyethylene glycol hydrogel matrix vs. standard guided bone regeneration techniques," *Clinical Oral Implants Research*, vol. 28, no. 7, pp. e76–e83, 2017.

[8] I. A. Urban, J. L. Lozada, B. Wessing, F. Suarez-Lopez del Amo, and H. L. Wang, "Vertical bone grafting and periosteal vertical mattress suture for the fixation of resorbable membranes and stabilization of particulate grafts in horizontal guided bone regeneration to achieve more predictable results: A technical report," *International Journal of Periodontics and Restorative Dentistry*, vol. 36, no. 2, pp. 153–159, 2016.

[9] G. Iglhaut, F. Schwarz, M. Gründel, I. Mihatovic, J. Becker, and H. Schliephake, "Shell technique using a rigid resorbable barrier system for localized alveolar ridge augmentation," *Clinical Oral Implants Research*, vol. 25, no. 2, pp. e149–e154, 2014.

[10] R. E. Jung, R. Glauser, P. Schärer, C. H. F. Hàmmerle, H. F. Sailer, and F. E. Weber, "Effect of rhBMP-2 on guided bone regeneration in humans: a randomized, controlled clinical and histomorphometric study," *Clinical Oral Implants Research*, vol. 14, no. 5, pp. 556–568, 2003.

[11] R. E. Jung, S. I. Windisch, A. M. Eggenschwiler, D. S. Thoma, F. E. Weber, and C. H. F. Hämmerle, "A randomized-controlled clinical trial evaluating clinical and radiological outcomes after 3 and 5 years of dental implants placed in bone regenerated by means of GBR techniques with or without the addition of BMP-2," *Clinical Oral Implants Research*, vol. 20, no. 7, pp. 660–666, 2009.

[12] J. K. Cha, J. S. Lee, M. S. Kim, S. H. Choi, K. S. Cho, and U. W. Jung, "Sinus augmentation using BMP-2 in a bovine hydroxyapatite/collagen carrier in dogs," *Journal of Clinical Periodontology*, vol. 41, no. 1, pp. 86–93, 2014.

[13] J. W. Jang, J. H. Yun, K. I. Lee et al., "Osteoinductive activity of biphasic calcium phosphate with different rhBMP-2 doses in rats," *Oral Surgery, Oral Medicine, Oral Pathology, Oral Radiology, and Endodontology*, vol. 113, no. 4, pp. 480–487, 2012.

[14] P. C. Bessa, M. Casal, and R. L. Reis, "Bone morphogenetic proteins in tissue engineering: the road from laboratory to clinic, part II (BMP delivery)," *Journal of Tissue Engineering and Regenerative Medicine*, vol. 2, no. 2-3, pp. 81–96, 2008.

[15] H. Cheng, W. Jiang, F. M. Phillips et al., "Osteogenic activity of the fourteen types of human bone morphogenetic proteins (BMPs)," *The Journal of Bone & Joint Surgery*, vol. 85, no. 8, pp. 1544–1552, 2003.

[16] X. Ji, D. Chen, C. Xu, S. E. Harris, G. R. Mundy, and T. Yoneda, "Patterns of gene expression associated with BMP-2-induced osteoblast and adipocyte differentiation of mesenchymal progenitor cell 3T3-F442A," *Journal of Bone and Mineral Metabolism*, vol. 18, no. 3, pp. 132–139, 2000.

[17] F. Schwarz, D. Rothamel, M. Herten, D. Ferrari, M. Sager, and J. Becker, "Lateral ridge augmentation using particulated or block bone substitutes biocoated with rhGDF-5 and rhBMP-2: an immunohistochemical study in dogs," *Clinical Oral Implants Research*, vol. 19, no. 7, pp. 642–652, 2008.

[18] Y. Y. Chang, J. S. Lee, M. S. Kim, S. H. Choi, J. K. Chai, and U. W. Jung, "Comparison of collagen membrane and bone substitute as a carrier for rhBMP-2 in lateral onlay graft," *Clinical Oral Implants Research*, vol. 26, no. 1, pp. e13–e19, 2015.

[19] I. K. Lee, H. C. Lim, J. S. Lee, J. Y. Hong, S. H. Choi, and U. W. Jung, "Layered approach with autogenous bone and bone substitute for ridge augmentation on implant dehiscence defects in dogs," *Clinical Oral Implants Research*, vol. 27, no. 5, pp. 622–628, 2016.

[20] K. Ito, Y. Yamada, R. Ishigaki, K. Nanba, T. Nishida, and S. Sato, "Effects of guided bone regeneration with non-resorbable and bioabsorbable barrier membranes on osseointegration around hydroxyapatite-coated and uncoated threaded titanium dental implants placed into a surgically-created dehiscence type defect in rabbit tibia: a pilot study," *Journal of oral science*, vol. 43, no. 1, pp. 61–67, 2001.

[21] D. S. Thoma, J. K. Cha, V. M. Sapata, R. E. Jung, J. Hüsler, and U. W. Jung, "Localized bone regeneration around dental implants using recombinant bone morphogenetic protein-2 and platelet-derived growth factor-BB in the canine," *Clinical Oral Implants Research*, vol. 28, no. 11, pp. 1334–1341, 2017.

[22] J. Y. Hong, M. S. Kim, H. C. Lim, J. S. Lee, S. H. Choi, and U. W. Jung, "A high concentration of recombinant human bone morphogenetic protein-2 induces low-efficacy bone regeneration in sinus augmentation: a histomorphometric analysis in rabbits," *Clinical Oral Implants Research*, vol. 27, no. 12, pp. e199–e205, 2016.

[23] U. M. E. Wikesjö, M. Qahash, G. Polimeni et al., "Alveolar ridge augmentation using implants coated with recombinant human bone morphogenetic protein-2: histologic observations," *Journal of Clinical Periodontology*, vol. 35, no. 11, pp. 1001–1010, 2008.

[24] H. Burchardt, "The biology of bone graft repair," *Clinical Orthopaedics and Related Research*, vol. 174, pp. 28–42, 1983.

[25] M. P. Kelly, O. L. A. Vaughn, and P. A. Anderson, "Systematic review and meta-analysis of recombinant human bone morphogenetic protein-2 in localized alveolar ridge and maxillary sinus augmentation," *Journal of Oral and Maxillofacial Surgery*, vol. 74, no. 5, pp. 928–939, 2016.

[26] H. Schliephake, "Clinical efficacy of growth factors to enhance tissue repair in oral and maxillofacial reconstruction: a systematic review," *Clinical Implant Dentistry and Related Research*, vol. 17, no. 2, pp. 247–273, 2015.

[27] C. H. Lai, L. Zhou, Z. L. Wang, H. B. Lu, and Y. Gao, "Use of a collagen membrane loaded with recombinant human bone morphogenetic protein-2 with collagen-binding domain for vertical guided bone regeneration," *Journal of Periodontology*, vol. 84, no. 7, pp. 950–957, 2013.

[28] J. Mir-Mari, G. I. Benic, E. Valmaseda-Castellón, C. H. F. Hämmerle, and R. E. Jung, "Influence of wound closure on the volume stability of particulate and non-particulate GBR materials: an in vitro cone-beam computed tomographic examination. Part II," *Clinical Oral Implants Research*, vol. 28, no. 6, pp. 631–639, 2017.

[29] N. Naenni, D. Schneider, R. E. Jung, J. Hüsler, C. H. Hämmerle, and D. S. Thoma, "Randomized clinical study assessing two membranes for guided bone regeneration of peri-implant bone defects: clinical and histological outcomes at 6 months," *Clinical Oral Implants Research*, vol. 28, no. 10, pp. 1309–1317, 2017.

[30] G. I. Benic, D. S. Thoma, F. Muñoz, I. Sanz Martin, R. E. Jung, and C. H. F. Hämmerle, "Guided bone regeneration of peri-implant defects with particulated and block xenogenic bone substitutes," *Clinical Oral Implants Research*, vol. 27, no. 5, pp. 567–576, 2016.

[31] U. W. Jung, J. S. Lee, W. Y. Park et al., "Periodontal regenerative effect of a bovine hydroxyapatite/collagen block in one-wall intrabony defects in dogs: A histometric analysis," *Journal of Periodontal & Implant Science*, vol. 41, no. 6, pp. 285–292, 2011.

[32] J. H. Song, H. E. Kim, and H. W. Kim, "Collagen-apatite nanocomposite membranes for guided bone regeneration," *Journal of Biomedical Materials Research Part B: Applied Biomaterials*, vol. 83, no. 1, pp. 248–257, 2007.

[33] I. Darby, "Periodontal materials," *Australian Dental Journal*, vol. 56, no. 1, pp. 107–118, 2011.

Research Article

Clinical Influence of Micromorphological Structure of Dental Implant Bone Drills

Gaetano Marenzi [ID],[1] **Josè Camilla Sammartino,**[2]
Giuseppe Quaremba [ID],[3] **Vincenzo Graziano,**[4] **Andrea El Hassanin,**[5] **Med Erda Qorri,**[6]
Gilberto Sammartino,[1] **and Vincenzo Iorio-Siciliano**[7]

[1]*Division of Oral Surgery, Department of Neurosciences, Reproductive and Odontostomatological Sciences, University "Federico II",*
 Via Pansini 5, Naples, Italy
[2]*Department of Biology and Biotechnology, University "L. Spallanzani", Via Ferrata 9, Pavia, Italy*
[3]*Department of Industrial Engineering, University of Naples "Federico II", Via Claudio 21, Naples, Italy*
[4]*Department of Advanced Biomedical Sciences, University "Federico II", Via Pansini 5, Naples, Italy*
[5]*Department of Chemical, Materials and Production Engineering, University "Federico II", Piazzale Tecchio 80, Naples, Italy*
[6]*Division of Oral and Maxillofacial Surgery, Department of Dentistry, Albanian University. Str. Durres, Tirana, Albania*
[7]*Department of Periodontology, University of Catanzaro "Magna Graecia", Viale Europa, Loc. Germaneto, Catanzaro, Italy*

Correspondence should be addressed to Gaetano Marenzi; gaetano.marenzi@tiscali.it

Background. Considerations about heat generation, wear, and corrosion due to some macrostructural bur components (e.g., cutting lips, rake angle, flute, and helix angle) have been widely reported. However, little is known about how the microstructural components of the implant drill surface can influence the implant drill lifetime and clinical performance. *Aim.* To investigate accurately the surface morphology of surgical bone drill, by means of multivariate and multidimensional statistical analysis, in order to assess roughness parameters able to predict the evolution of tribological phenomena linked to heat development, wear, and corrosion occurring in clinical use. *Materials and Methods.* The surfaces of implant drills approximately 2.0mm in diameter made by five manufacturers were examined by means of confocal microscope with white light laser interferometry, obtaining several surface roughness parameters. Statistical multivariate analysis based on discriminant analysis showed, for each cut-off, the parameters which discriminate the manufacturers. *Results.* The microstructural parameters used by discriminant analysis evidenced several differences in terms of drill surface roughness between the five manufacturers. *Conclusions.* The observed surface roughness difference of drills is able to predict a different durability and clinical performance especially in heat generation and wear onset.

1. Introduction

Minimally traumatic preparation of the implant socket is critical for predictability and enhanced osseointegration [1]. The preservation of the original bony microstructure, especially of the cancellous bone and its high osteogenic potency, will benefit the bone healing process [2]. Although osteotomy site preparation has been studied for decades, there remains a remarkable lack of consensus on what constitutes an optimal method to cut bone. Major problems faced during bone drilling were thermal necrosis, bur deformation, and the generation of microcracks on the inner surface of the drilled holes that can detrimentally affect osteosynthesis and healing [3, 4]. In clinical practice, to perform osteotomies for dental implant placement, rotary cutting instruments (burs) are used and efforts have been made to develop implant drills with improved mechanical proprieties [5–10]. Many aspects can significantly affect their cutting efficiency and durability: design, diameter, composition and surface treatment, mechanical properties, drill rotational speed, axial

drilling forces, cooling, and the sterilization process [1, 5, 10–15]. Some authors evidenced also the drill corrosion as a potential key factor in determining lifespan of the implant burs [1, 12, 16, 17].

Many of these drilling parameters also play a primary role in controlling the temperature generated during the osteotomy [1, 5, 11–14, 18, 19]. Their bone damage is related to the magnitude of the temperature elevation and the time during which the tissue is subjected to damaging temperature, identified as 47°C for 1 min [1, 9, 10, 13]. The heat generated during the implant site preparation is related to the surface cutting power [2, 15] and hence to the manufacturer's precision [2, 3]. Magnification of the cutting tip of the drills showed many differences in the manufacturing of the drills. The two-fluted drill was correlated to less heat generation whereas the three-fluted drill showed somewhat favorable cutting efficiency [2]. Heat generation, as evidenced by Matthews and Hirsch [20], can be also influenced by the manufacturer's precision (sharpness of the cutting tool) [15] and the surface deformation and roughness showed by the worn burs that cause a more significant and continuous temperature rise than new burs [5, 12, 14, 21]. No clear suggestion is made on the number of times that the drill can be used repeatedly until it becomes blunt and ineffective, producing a significant increase in temperature [11, 13]. Since the sharpness of the drill bit is one of the most important factors when considering the temperature increase, to minimize this surgical trauma well-sharpened drills are recommended [13, 22–24]. In a previous study SEM analysis evidenced manufacturing defects in new drills which increased in number and deteriorated with use [9, 14]. These defects influence the cutting efficiency, favoring heat and bone microcrack generation, and reduce the time when the reused drills can be considered sharp enough. Considerations about heat generation and wear with some macrostructural bur components (e.g., cutting lips, rake angle, flute, and helix angle) have been extensively reported. Also microstructural components of the bur surface can influence heat generation and wear.

The aim of this study was to investigate accurately the surface morphology of surgical bone drills through the confocal microscopy and by using multivariate and multidimensional statistical analysis, in order to assess roughness parameters able to predict the evolution of tribological phenomena linked to heat development, wear, and corrosion phenomena occurring in clinical use.

2. Material and Methods

Implant drills approximately 2.0 mm in diameter were selected because they usually represent one of the first bone drills to be used for implant site preparation, drilling both cortical and cancellous bone.

The following implant bone drills made by five manufacturers were analyzed:

(1) Straumann (Straumann AG, Waldenburg, Switzerland) 2.2 mm in diameter (for short, A)

(2) Nobel Biocare (Nobel Biocare AB, Goteborg, Sweden) 2.0 mm in diameter (for short, B)

(3) Xive Implant System (Friadent GmbH, Mannheim, Germany) 2.0 mm in diameter (for short, C)

(4) Global D (French) 2.5 mm in diameter (for short, D)

(5) Sweden & Martina (Padova, Italy) 2.5 mm in diameter (for short, E)

The rugosimetric survey was carried out through a Leica DCM 3D confocal microscope with white light laser interferometry, which makes it possible to study the surface finish of the drills in high resolution. More specifically, confocal microscopy allows the reconstruction through several optical sections, without any physical contact with parts, of complex 3D surfaces that cannot be analyzed otherwise [25]. Using, for example, contact profilometers, filtering was then carried out, based on the choice of cut-off, in order to separate the roughness profile from the waviness profile (or geometric shape). On the basis of preliminary performed measurements and extraction of primary profiles, according to the international standard ISO 4287 [26], since the acquired profile seemed to be quite periodic, P_{sm} (i.e., spacing parameters obtained by the primary profile) was chosen as the parameter to determine the appropriate value of the cut-off length. Moreover, since, in our case, the above-mentioned parameter, P_{sm}, is very close to the boundary value of 0.04 mm, which separates two different cut-off values applicable, i.e., 0.08 mm and 0.25 mm, both cut-off values were taken into account in determining the roughness and waviness profiles and relative parameters. The filtering operation was carried out with a robust Gaussian filter. For each manufacturer, three bone drills were employed. For each filtering operation, three profiles parallel to the acquisition direction and three perpendicular to the acquisition direction were extracted. In this way, the parameters prescribed by ISO 4287-1997 [26] were obtained, accordingly described below.

The distortions due to the ends of the profile and the finite length of the profile were minimized by removing a portion of profile at the beginning (run-up) and at the end of profile (run-down) and by applying a minimum number of cut-offs in the measured profile (evaluation length), namely, three.

Surface texture can be described in quantitative terms by means of a certain number of parameters. All of these parameters represent different aspects of the surface, such as roughness, waviness, and shape. In order to predict the behavior of a component during its normal use, it is necessary to quantify the surface characteristics. This is possible through the parameters mentioned below. They can be classified into amplitude, spacing, and hybrid parameters, in particular, (i) amplitude parameters: R_p, R_v, R_z, R_c, R_t, R_a, R_q, R_{sk}, R_{ku} [26]; (ii) material ratio parameters: R_{mr} ($c = 1 \mu m$ below the highest peak), R_{dc} (p = 5%, q = 95%) [26]; (iii) spacing parameters: primary profile, PS_m [27]; (iv) hybrid parameters: R_{sk}, R_{ku}.

The best known and commonly used parameter is R_a, defined as the arithmetical mean of the absolute values of the profile deviations from the mean line of the roughness profile [26]. This is an amplitude parameter that is useful for preliminary analysis of the surface finish. R_a is used as a global evaluation of the roughness amplitude on a profile. It does not say anything on the spatial frequency of the

irregularities or the shape of the profile. R_a is meaningful for random surface roughness (stochastic) machined with tools that do not leave marks on the surface, such as sand blasting, milling, and polishing. Since the aim of the paper was to assess surface parameters that are related to phenomena such as heat generation, wear, and corrosion, our attention also turned to hybrid parameters: R_{sk} and R_{ku}. R_{sk} parameter was chosen because it represents the profile asymmetry with respect to the mean line. When it is positive, the profile is more pronounced toward the peaks. By contrast, when it is negative the profile is more pronounced toward the valleys. That said, the greater the distance from zero, the more asymmetric the profile. The second parameter, R_{ku}, was chosen because it is an index of the shape of the peaks and more specifically their "tailness"; i.e., the higher the value, the more pronounced the peaks.

These parameters, according to the consideration made also by Karl Niklas Hansson and Stig Hansson in their work [28], represent in our case the best indicators for the phenomena involved. In a first step, multifactorial statistical analysis was performed starting from a hypothesis-free perspective. This implies that no "outcome" variables based on clinical experience were selected because the aim was to identify potential associations that might have been overlooked before.

Therefore, all variables were tried in the analysis. The approach was performed by using discriminant analysis (DA). The aim is to statistically distinguish between the five groups of makers. To distinguish between the groups, a collection of discriminating variables that measure the characteristics on which the groups are expected to differ were selected (i.e., all the above-mentioned parameters). The mathematical objective of DA is to weight and linearly combine the discriminating variables in some fashion so that the groups are forced to be as statistically distinct as possible. The statistical theory of DA assumes that the discriminating variables have a multivariate normal distribution and that they have equal variance-covariance matrices within each group. In practice, the technique is very robust and these assumptions need not be strongly adhered to. DA attempts to do this by forming one or more combinations of discriminating variables (i.e., discriminant functions) such as

$$D_i = d_{i1}Z_{i2} + d_{i2}Z_2 + \cdots + d_{ip}Z_p, \quad i = 1, \ldots, n \quad (1)$$

where n is the number of discriminant functions, D_i is the score on discriminant function i, the d's are the weighting coefficients, and Z's are the standard values of the p discriminating variables used in the analysis. That said, the functions, based on the weight of d's coefficients, are formed in such a way as to maximize the separation between the groups and to minimize the distance within each group. Once the discriminant functions have been derived, the research objectives of DA, i.e., analysis and classification, are pursued [29].

In a second step the mean difference of variables selected by DA between each pair of manufacturers was examined; for more details see [30]. The multiple comparisons of mean difference between continuous variables were examined by

using Dunnett's test. The level at which results were defined as being statistically significant was set at a P≤0.05. The calculations were performed using IBM SPSS Statistics, v.20.0 software (IBM Corp., Armonk, NY, USA).

3. Results and Discussion

3.1. The image of each bone drill and 3D details of the surfaces extracted from the five manufacturers' implant bone drills after leveling and filling points is shown in Figure 1.

The 3D surface reported below each bone drill represents the area taken from the surface that possesses minor isolated peaks, naturally present due to the complexity of the surface acquisitions by means of the confocal microscope. Therefore, to avoid as much irregularity as possible, a portion of the $500x500\mu m^2$ of the acquired areas was considered. These Areas of Interest (AoI) have been chosen to perform as better as possible the comparative analysis among the bone drills considering, for a given drill, the surface portion that embraces part of its cylindrical external surface, near the cutting edges.

Naturally, comparative analysis has been performed taking into account every cutting edge for each drilling tool, which are at least two, to enrich the experimental data for the statistical analysis and to obtain more accurate results (Figure 2).

Preliminary, it should be noted that no significant differences were found for the various cut-offs along the transversal direction.

3.2. Robust Gaussian filter 0.08mm was used for the extraction of the roughness profiles parallel to the bone drill axis. The variables extracted through DA analysis ordered were as follows, according to the relative decreasing weight: R_q, R_z, R_{mr}, R_{ku}, P_{sm}, R_{sk}. Figure 3 shows the cluster distribution of five manufacturers according to the canonical discriminant functions. In general, the closeness of the group centroids, marked with ■, to territorial lines suggests that the separation between all groups is not very strong. The centroids summarize the group locations in the "reduced" space defined by the discriminant functions.

The average values for each manufacturer and model parameter, for the cut-off = 0.08mm, are reported in Table 1. The last column reports the significant difference between manufacturers for each parameter.

In particular, R_q is defined as the root mean square deviation of the assessed profile. It corresponds to the standard deviation of the height distribution, defined on the sampling length. R_q provides the same information as R_a (arithmetic mean deviation of the assessed profile), but in a more accurate way since it is less sensitive to variations due to isolated peaks that affect the measure. The higher the dispersion, the greater the nonuniformity of the surface. Contextually, D represents the worst case, having the highest data dispersion. R_z parameter is the maximum height of the profile defined on the sampling length, evaluated as the mean distance from the 10 highest peaks and the 10 deepest valleys. Although being less accurate than R_q, this parameter also represents a valid
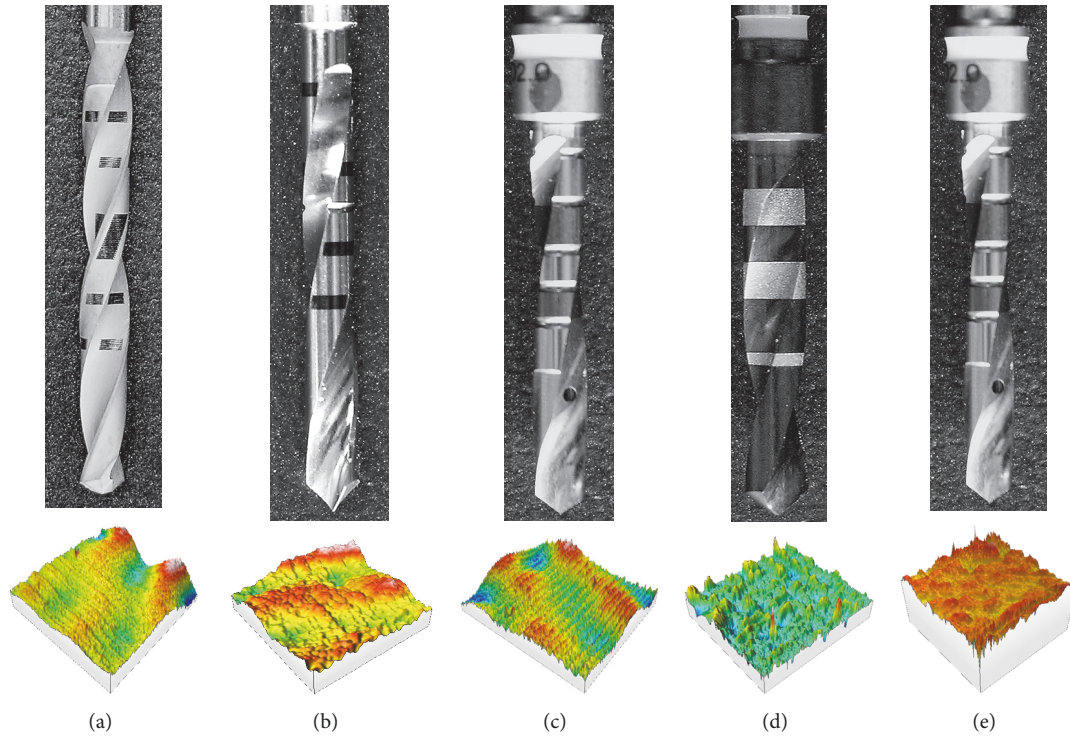
FIGURE 1: Top from left to right image of implant bone drill: (a), (b), (c), (d), (e); bottom corresponding reconstruction 3D of AoI.

TABLE 1: Crosstab manufacturer versus mean model parameters, significant difference, cut-off 0.08mm.

Manufacturer versus model parameter	A	B	C	D	E	Significant difference
R_q	0.10	1.01	0.77	8.61	2.17	A-B, A-C, A-D, B-D, C-D, E-D
R_z	0.38	2.85	1.965	21.405	3.80	A-B, A-C, A-D, A-E, B-D, C-D, E-D
R_{mr}	99.00	33.27	4.17	1.37	1.53	A-B, A-C, A-D, A-E
R_{ku}	2.73	3.00	1.97	3.43	1.73	A-E, B-E, C-D, D-E
P_{sm}	28.00	76.67	190.00	53.67	101.50	A-B, A-C, A-E, B-C, C-D, C-E
R_{sk}	-0.05	-0.46	0.58	0.46	-0.18	A-C, A-D, B-C, B-D, C-E

outcome variable, since it does not consider regular profiles with isolated peaks. Also, it is frequently used to check whether the profile has protruding peaks that might affect static or sliding contact function. In fact, this result has been confirmed from the values reported on the table, agreeing with the considerations made for R_q. R_{mr}, defined as the ratio of the material length $Ml(c)$ of a profile curve element to the evaluation length at the sectioning level c (whether as % or μm), enforces indications about the tailness of the profile, expressed as a ratio among vacancies and material confined in a defined virtual surface. In this case, more than a simple roughness indicator, this parameter offers an indication of the drill's integrity, and hence it is reasonable to take it into account in light of the evaluations explained herein. The previously defined R_{sk} and R_{ku} hybrid parameters represent the best indicators for the subject of this work: according to the definitions given above, it is preferable to have profiles with negative values of R_{sk}, since they are characterized by a valley-shaped morphology, which is an advantage regarding heat generation and wear phenomena due to lower shear contacts with bones. In this context, bone drills corresponding to cases A, B, and E are the more preferable.

Different considerations have to be made for parameter R_{ku}. It is well known that for values of this parameter less than 3, profile peaks are more likely to be round-shaped. Vice versa, when values are greater than 3, peaks are more likely to be pronounced. Standing on the results, cases C and E are the best since round-shaped edges of the bone drill's surfaces are preferable since they guarantee a longer tool life and a better quality of hole circularity, given that peaks can be more easily damaged during the cutting action. Naturally, this aspect is also related to the above-mentioned heat and wear phenomena.

3.3. Robust Gaussian filter 0.25mm was used for the extraction of roughness profiles parallel to the bone drill axis.

TABLE 2: Crosstab manufacturer versus mean model parameters, significant difference, cut-off 0.25mm.

Manufacturer versus model parameter	A	B	C	D	E	Significant difference
Rv	0.32	1.35	4.56	11.20	3.52	A-B, A-C, A-D, A-E, B-C, B-D, B-E, C-D, D-E
Ra	0.15	1.77	1.98	4.80	2.32	A-B, A-C, A-D, A-E, C-D, C-E, E-D
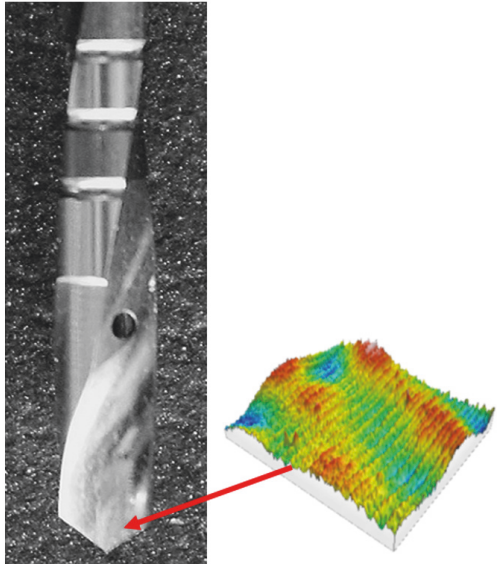
FIGURE 2: Close-up of AoI showing the location where the measurements were performed.

FIGURE 4: Cluster distribution of five manufacturers.

FIGURE 3: Cluster distribution of five manufacturers.

The variables extracted through DA analysis are ordered according to the relative decreasing weight as follows: R_v and R_a.

Figure 4 shows the cluster distribution of five manufacturers according to the canonical discriminant functions.

The average values for each manufacturer and model parameter and for the cut-off = 0.25mm are reported in Table 2. In the last column is reported the significant difference between manufacturers for each parameter.

As depicted in the table, R_a is highlighted as a key parameter. According to the discussion about the previous case, it is still a valid parameter, especially being the most widely used. This result also validates the goodness of the simulation methodology adopted. On the other hand, the R_v parameter deserves special consideration. More specifically, according to its definition as the maximum valley depth along a considered profile, it could not be considered as a global indicator of surface quality because it refers to isolated singularities, i.e., valleys. However, this result remains interesting since other tribological phenomena are related to this parameter, i.e., corrosion. In fact, the presence of a consistent number of deep valleys on a surface is more vulnerable to the effects of sterilization procedures [1, 12, 16], triggering localized corrosion phenomena like pitting. Based on these considerations, D represents again the worst case.

4. Conclusions

The study observed that the surface micromorphology, influencing the contact area between the drill and bone, can be considered as a factor that contributes to heat, wear, and corrosion phenomena due to material friction and corrosion resistance through several surface texture indicators. Not only the design, but also the micromorphology of the cutting surface directly contacting bone plays a key role in the cutting power and wear trend. The result of this research also showed considerable differences in the parameters examined

in the implant drills present on the market, depending on the particular surface aspect to be analyzed in terms of its clinical impact.

Conflicts of Interest

The authors declare that they have no conflicts of interest.

References

[1] O. F. L. Allsobrook, J. Leichter, D. Holborow, and M. Swain, "Descriptive study of the longevity of dental implant surgery drills," *Clinical Implant Dentistry and Related Research*, vol. 13, no. 3, pp. 244–254, 2011.

[2] H. Oh, B. Kim, H. Kim, I. Yeo, U. Wikesjö, and K. Koo, "Implant drill characteristics: thermal and mechanical effects of two-, three-, and four-fluted drills," *The International Journal of Oral & Maxillofacial Implants*, vol. 32, no. 3, pp. 483–488, 2017.

[3] G. Singh, V. Jain, and D. Gupta, "Comparative study for surface topography of bone drilling using conventional drilling and loose abrasive machining," *Proceedings of the Institution of Mechanical Engineers, Part H: Journal of Engineering in Medicine*, vol. 229, no. 3, pp. 225–231, 2015.

[4] V. Gupta, P. M. Pandey, R. K. Gupta, and A. R. Mridha, "Rotary ultrasonic drilling on bone: a novel technique to put an end to thermal injury to bone," *Proceedings of the Institution of Mechanical Engineers, Part H: Journal of Engineering in Medicine*, vol. 231, no. 3, pp. 189–196, 2017.

[5] E. M. Sartori, É. H. Shinohara, D. Ponzoni, L. E. M. Padovan, L. Valgas, and A. L. Golin, "Evaluation of deformation, mass loss, and roughness of different metal burs after osteotomy for osseointegrated implants," *Journal of Oral and Maxillofacial Surgery*, vol. 70, no. 11, pp. e608–e621, 2012.

[6] C. Ercoli, P. D. Funkenbusch, H.-J. Lee, M. E. Moss, and G. N. Graser, "The influence of drill wear on cutting efficiency and heat production during osteotomy preparation for dental implants: a study of drill durability," *The International Journal of Oral & Maxillofacial Implants*, vol. 19, no. 3, pp. 335–349, 2004.

[7] N. Oliveira, F. Alaejos-Algarra, J. Mareque-Bueno, E. Ferrés-Padró, and F. Hernández-Alfaro, "Thermal changes and drill wear in bovine bone during implant site preparation. A comparative in vitro study: twisted stainless steel and ceramic drills," *Clinical Oral Implants Research*, vol. 23, no. 8, pp. 963–969, 2012.

[8] M. Sumer, A. F. Misir, N. T. Telcioglu, A. U. Guler, and M. Yenisey, "Comparison of heat generation during implant drilling using stainless steel and ceramic drills," *Journal of Oral and Maxillofacial Surgery*, vol. 69, no. 5, pp. 1350–1354, 2011.

[9] L. F. S. Pires, B. Tandler, N. Bissada, and S. Duarte, "Comparison of heat generated by alumina-toughened zirconia and stainless steel burs for implant placement," *The International Journal of Oral & Maxillofacial Implants*, vol. 27, no. 5, pp. 1023–1028, 2012.

[10] K. Koo, M. Kim, H. Kim, U. M. Wikesjö, J. Yang, and I. Yeo, "Effects of implant drill wear, irrigation, and drill materials on heat generation in osteotomy sites," *Journal of Oral Implantology*, vol. 41, no. 2, pp. e19–e23, 2015.

[11] R. K. Pandey and S. S. Panda, "Drilling of bone: a comprehensive review," *Journal of Clinical Orthopaedics and Trauma*, vol. 4, no. 1, pp. 15–30, 2013.

[12] G. C. B. Mendes, L. E. M. Padovan, P. D. Ribeiro-Júnior, E. M. Sartori, L. Valgas, and M. Claudino, "Influence of implant drill materials on wear, deformation, and roughness after repeated drilling and sterilization," *Implant Dentistry*, vol. 23, no. 2, pp. 188–194, 2014.

[13] W. Allan, E. D. Williams, and C. J. Kerawala, "Effects of repeated drill use on temperature of bone during preparation for osteosynthesis self-tapping screws," *British Journal of Oral and Maxillofacial Surgery*, vol. 43, no. 4, pp. 314–319, 2005.

[14] S. C. Möhlhenrich, A. Modabber, T. Steiner, D. A. Mitchell, and F. Hölzle, "Heat generation and drill wear during dental implant site preparation: systematic review," *British Journal of Oral and Maxillofacial Surgery*, vol. 53, no. 8, pp. 679–689, 2015.

[15] A. Scarano, A. Piattelli, B. Assenza et al., "Infrared thermographic evaluation of temperature modifications induced during implant site preparation with cylindrical versus conical drills," *Clinical Implant Dentistry and Related Research*, vol. 13, no. 4, pp. 319–323, 2011.

[16] A. N. Porto, Á. H. Borges, A. Semenoff-Segundo et al., "Effect of repeated sterilization cycles on the physical properties of scaling instruments: a scanning electron microscopy study," *Journal of International Oral Health*, vol. 7, no. 5, pp. 1–4, May 2015.

[17] G. E. Chacon, D. L. Bower, P. E. Larsen, E. A. McGlumphy, and F. M. Beck, "Heat production by 3 implant drill systems after repeated drilling and sterilization," *Journal of Oral and Maxillofacial Surgery*, vol. 64, no. 2, pp. 265–269, 2006.

[18] Y. Reingewirtz, S. Szmukler-Moncler, and B. Senger, "Influence of different parameters on bone heating and drilling time in implantology," *Clinical Oral Implants Research*, vol. 8, no. 3, pp. 189–197, 1997.

[19] C. H. Jacob, J. T. Berry, M. H. Pope, and F. T. Hoaglund, "A study of the bone machining process-Drilling," *Journal of Biomechanics*, vol. 9, no. 5, pp. 343–IN5, 1976.

[20] L. S. Matthews and C. Hirsch, "Temperatures measured in human cortical bone when drilling," *The Journal of Bone and Joint Surgery*, vol. 54, no. 2, pp. 297–308, 1972.

[21] T. Staroveski, D. Brezak, and T. Udiljak, "Drill wear monitoring in cortical bone drilling," *Medical Engineering & Physics*, vol. 37, no. 6, pp. 560–566, 2015.

[22] A. Pirjamalineisiani, N. Jamshidi, M. Sarafbidabad, and N. Soltani, "Assessment of experimental thermal, numerical, and mandibular drilling factors in implantology," *British Journal of Oral and Maxillofacial Surgery*, vol. 54, no. 4, pp. 400–404, 2016.

[23] R. M. Jochum and P. A. Reichart, "Influence of multiple use of Timedur," *Clinical Oral Implants Research*, vol. 11, no. 2, pp. 139–143, 2000.

[24] U. Lekholm, "Clinical procedures for treatment with osseointegrated dental implants," *The Journal of Prosthetic Dentistry*, vol. 50, no. 1, pp. 116–120, 1983.

[25] V. Niola, G. Nasti, and G. Quaremba, "A problem of emphasizing features of a surface roughness by means the discrete wavelet transform," *Journal of Materials Processing Technology*, vol. 164-165, pp. 1410–1415, 2005.

[26] ISO 4287, Geometrical Product Specifications (GPS)—Surface texture: Profile method—Terms, definitions and surface texture parameters, 1997.

[27] ISO 3274, Geometrical Product Specifications (GPS)—Surface texture: Profile method—Nominal characteristics of contact (stylus) instruments, 1996.

[28] S. Hansson and K. N. Hansson, "The effect of limited lateral resolution in the measurement of implant surface roughness: a computer simulation," *Journal of Biomedical Materials Research Part A*, vol. 75, no. 2, pp. 472–477, 2005.

[29] N. H. Nie, C. H. Hull, J. G. Jenkins et al., *SPSS*, Mc Graw Hill, 2nd edition, 1975.

[30] H. Tinsley and S. Brown, Eds., *Handbook of Applied Multivariate Statistics and Mathematical Modeling*, Academic Press, 1st edition, 2000.

Clinical Study

Clinical Relevance of Bone Density Values from CT Related to Dental Implant Stability: A Retrospective Study

Vincenzo Bruno [iD],[1] **Cesare Berti** [iD],[2] **Carlo Barausse,**[2] **Mauro Badino,**[3]
Roberta Gasparro [iD],[4] **Daniela Rita Ippolito,**[5] **and Pietro Felice**[2]

[1]*Department of Biomedical and Specialty Surgical Sciences, Unit of Prosthesis, University of Ferrara,*
 Via Borsari 46, 44121 Ferrara, Italy

[2]*Department of Biomedical and Neuromotor Sciences, Unit of Periodontology and Implantology, University of Bologna,*
 Via San Vitale 59, 40125 Bologna, Italy

[3]*Private Practice, Vicolo Carceri 10, 10064 Pinerolo, Torino, Italy*

[4]*Department of Neuroscience, Reproductive Sciences and Odontostomatology, Unit of Oral Surgery and Implantology,*
 University of Naples, Via Pansini 5, Edificio 14, 80131 Naples, Italy

[5]*Department of Biomedical and Neuromotor Sciences, Unit of Orthodontics, University of Bologna,*
 Via San Vitale 59, 40125 Bologna, Italy

Correspondence should be addressed to Cesare Berti; cesare.berti@studio.unibo.it

Purpose. The majority of the techniques used to assess the primary implant stability are subjective and empirical and can be used during or after the surgery. The aim of this study is to evaluate the bone density prior to surgery, in order to give recommendations to the clinician about the best surgical technique and the type of implant which is needed. *Materials and Methods.* A surgeon operated on 75 patients for 269 implants over the period 2010–2014. He required a CT to plan the surgery and he documented the type, the diameters, and the lengths of the implants, the insertion torque, and the ISQ values. At a later stage another clinician measured bone density and cortical thickness. We endeavoured to get the most accurate superimposition between the implants placed by the surgeon and those placed by the clinician. *Results.* In maxilla ISQ showed a significant positive correlation with HU values detected for coronal-buccal ($r = 0.302$; $p = 0.020$) and middle-lingual ($r = 0.295$; $p = 0.023$). Torque showed a positive correlation with cortical bone thickness at the middle of the ridge ($\rho = 0.196$; $p = 0.032$). *Conclusion.* It is important to take into consideration the Hounsfield Units and the cortical thickness as predictive parameters during the preoperative assessment, with regard to the choice of the implant type as well as the surgical technique.

1. Introduction

Osseointegration underlies contemporary implantology and it occurs in a primary and secondary level [1]. The primary implant stability can be defined as the "biometric stability immediately after implant insertion" [2], a mechanical phenomenon that is related to the local bone quality and quantity, to the implant geometry (i.e., length, diameter, and type), and to the placement technique used (i.e., relation between drill size and implant size, whether a pretapped or self-tapped implant is used). The primary implant stability has always represented one of the essential prerequisites for performing

and maintaining osseointegration [3], for it prevents micromovement and the formation of fibrous scar tissue at the time of implant loading. Unfortunately, the majority of techniques for testing implant stability are widely empirical and subjective; moreover they evaluate the bone quality during or after (RFA and Periotest) the implant surgery [4]. All these methods are useful in evaluating the osseointegration, but no objective information on bone quality has been given prior to the preparation of the osteotomy [5, 6]. Moreover, according to Degidi et al. [7]: "the primary implant stability prediction is not good enough to prevent mistakes when using for example an immediate loading technique". A method, which is proven
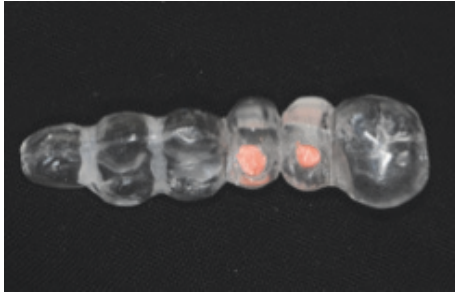
FIGURE 1: A radiological template with gutta-percha marks.

FIGURE 2: A panoramic view from CT with the radiological template in situ.

FIGURE 3: Some slices of the CT.

to be objective and valid to assess the bone density prior to surgery, is to utilize the HU value measured on CT images [8–10]. The aim of this prospective study is to evaluate the bone density prior to surgery, in order to give recommendations to the clinician about the best surgical technique and the type of implant which is needed. Thanks to this information, the clinician could be able to obtain the best primary implant stability, essential to obtain a long-term success, even in those cases where the bone is not particularly dense; this includes pertinent information regarding the diameter, the length, and the type of implant. In this study, the correlation between the Hounsfield Units (5 values around the implant) from the Computerized Tomography, the width of the cortical bone (3 values around the implant neck), and the final insertion torque and the resonance frequency (ISQ) were all evaluated.

2. Materials and Methods

2.1. Enrollment of Patients. An experienced implantologist had consecutively enrolled 75 patients for 269 implants over the period 2010–2014. He required a conventional multislice computed tomography (CT) to assess bone quantity and to ensure that there was sufficient bone to perform surgery without the need of a bone augmentation procedure, prior to implant placement. The reason we used CT was that at the time we were unable to use cone beam computed tomography. All patients gave written informed consent and the guidelines of the Declaration of Helsinki were observed.

2.2. Baseline Measurement. Alginate impressions were taken and diagnostic casts were fabricated (Vel-Mix Die Stone, Kerr Corporation, Washington, DC). A transparent template by using a clear acrylic resin (ProBase Cold; IvoclarVivadent AG, Schaan, Liechtenstein), based on the wax up, was constructed and gutta-percha marks were inserted along the axis of the teeth to be replaced (Figure 1). A CT was obtained with the template placed in situ (Figures 2 and 3). All CTs were performed using identical settings which were applied for all patients: 120 kV, 90 mAs, 0.5 mm slice thickness, and 0.3 mm slice increment. Data was stored in Dicom format. These Dicom files were loaded in a planning software (NobelClinician, Nobel Biocare AB, Goteborg, Sweden), which included 3D reconstruction and drawing of the reference curve. This procedure allowed for localization of the osteotomy sites related to the gutta-percha marks
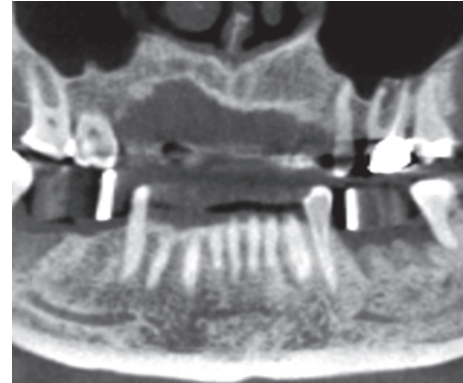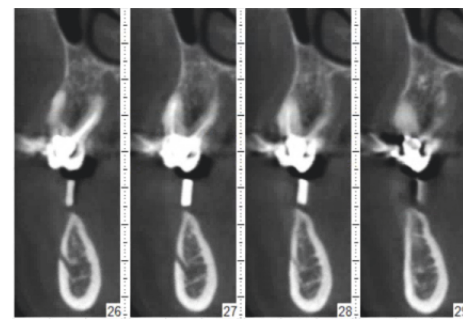
and, therefore, the corresponding cross-sectional CT slices. The surgeon planned the implant(s) (Nobel Replace Select Tapered, Nobel Active, Nobel Replace Select Straight, Nobel Replace Groovy, Nobel Speedy, Branemark Groovy), including the length and diameter, and selected an implant model, from the NobelClinician implant library, and was/were finally placed at the corresponding site(s). The surgeon, at that time, did not take any other measurements (Figure 4).

2.3. Surgical Procedures. The template was modified with holes in the implant positions to perform a precise surgery. Preoperative antibiotics were given orally 1 day prior to surgery and were continued for another 5 days, every 12 hours, prescribing amoxicillin, 1 g. The surgery was performed using a full thickness mucoperiosteal flaps which were raised under local anaesthesia. A 2 mm diameter twist drill was used, under profuse isotonic saline irrigation, to prepare the initial full depth channel at the implant site. The sequence of tapered drill of the length and the diameter chosen was then used to shape the osteotomy site, always using profuse irrigation. Finally, implants were inserted without the use of the irrigation.

2.4. Data Collection. The surgeon proceeded with the surgery using the modified template, documenting the diameters and the lengths of the implants, and the insertion torque (20,
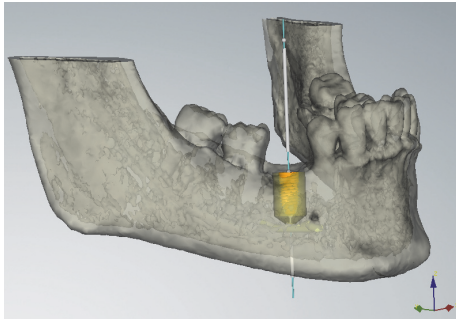
FIGURE 4: The implant planned by the surgeon in the NobelClinician software selected from the implant.
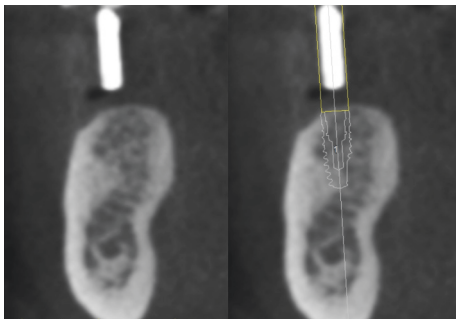
FIGURE 5: Superimposition between the gutta-percha mark and the implant placed by the clinician.

35, 45, and more than 45 Ncm) until the implant reached its final position. Finally, the Resonance Frequency Analysis (RFA) was recorded using the wireless device (Ostell ISQ Instrument, Integration diagnostics AB, Sävedalen, Sweden), measuring the ISQ values in four different directions consisting of the mesial, distal, lingual, and buccal which calculated the mean ISQMean, for 109 implants.

2.5. Measurements of Bone Density and Cortical Thickness. The measurements of bone density and cortical thickness were obtained by another clinician to avoid any bias, using the SIMPLANT® software. This clinician was not aware of other parameters except for the diameter, the lengths, the type of implants used, and their position. The measurements were carried out at a later stage than the surgery. The clinician simulated the implants' position by using, as reference points, the same gutta-percha marks—the same which the surgeon had used in order to plan the surgery and find the best implant site for each patient; that way, we endeavoured to get the most accurate superimposition between the implants placed by the surgeon and those placed by the clinician, so as to study bone density and cortical thickness (Figure 5). The assessment was made at 5 points on every slice: coronal-buccal (HU1), middle-buccal (HU2), middle at the apex (HU3), middle-lingual (HU4), and coronal-lingual (HU5) (Figures 6(a) and 6(b)). The Hounsfield Units (HU) values were recorded separately, and they were calculated as the arithmetical means of an area measuring 60 mm^2

for each of the five spots around the implant which we examined (Figure 7). Additionally, the cortical thickness was calculated at sites of the implant–bone contact: lingual (C1) and buccal (C2), including the middle of the ridge (C3). The measurements of cortical thickness were carried out as material measures around the implant neck (Figures 8(a) and 8(b)). The clinician selected the implants from the SIMPLANT® implant library, using the type of implants and the same diameter and length that the surgeon chooses for the surgery.

2.6. Statistical Analysis. A sample size calculation was conducted. The primary outcome on which the calculation was based was the difference in mean torque among the different implant types. Given $\alpha = 0.05$, $\beta = 0.80$, a medium effect size ($f = 0.25$), 6 groups, and an additional 15% samples compared to the corresponding parametric test, the minimum sample required was determined to be 249. All data analyses were carried out according to a pre-established analysis plan. The implant was the statistical unit of the analyses. A dentist with expertise in statistics analyzed the data without knowing the group allocation. Data were summarized using frequencies (for nominal-level variables), means, and standard deviations (for continuous data). Independent t-tests and Mann–Whitney tests were used to examine the differences, respectively, in ISQ and torque between genders and implant location (anterior or posterior). One-way ANOVAs and Kruskal Wallis tests explored the differences in ISQ and torque among subjects with different smoking habits. Relationships between ISQ and continuous variables (age, bone density according to the Hounsfield scale, cortical bone thickness, implant length, and implant diameter) were assessed by using the Pearson Product-moment correlation. A Spearman's Rank Order correlation was run to determine the relationship between torque and continuous variables. Differences in ISQ among different implant types were investigated through a One-way ANOVA. To control for the continuous variables which had shown a significant correlation with ISQ an ANCOVA was used; a two-way ANOVA was conducted to examine the effect on ISQ of nominal variables which had shown significant differences in ISQ together with implant type. A Kruskal Wallis test was used to investigate the differences in torque among different implant types. Pairwise comparisons were performed by using the Mann–Whitney U test with Bonferroni correction (maxilla: adjusted α level = 0.003; mandible: adjusted α level = 0.005). Ordinal regressions were used to analyze the effect of the interaction between type of implant and the variables which had shown a significant correlation with torque. All statistical analyses were conducted using the Statistical Package for Social Sciences Software (IBM Corp. Released 2012. IBM SPSS Statistics for Windows, Version 21.0. Armonk, NY: IBM Corp). $p < 0.05$ was set as the level for statistical significance.

The data that support the findings of this study are available on request from the corresponding author. The data are not publicly available due to privacy reasons.

TABLE 1: Patient and intervention characteristics.

Number of patients	75
Mean age ± SD (range)	60.31 ± 12.57 (23–80) years
Females	40 (53.3%)
Smokers	12 (16.0%)
smoking ≤ 10 cigarettes	4 (5.3%)
smoking > 10 cigarettes	8 (10.7%)
# Implants	269
# Patients receiving 1 implant	10 (13.3%)
# Patients receiving 2 implant	22 (29.3%)
# Patients receiving 3 implant	10 (13.3%)
# Patients receiving 4 implant	13 (17.3%)
# Patients receiving 5 implant	5 (6.7%)
# Patients receiving 6 implant	7 (9.3%)
# Patients receiving 7 implant	4 (5.3%)
# Patients receiving 8 implant	1 (1.3%)
# Patients receiving 10 implant	3 (4.0%)
Implant length (mean ± SD)	13.08 ± 1.71 mm
Implant diameter (mean ± SD)	4.36 ± 0.64 mm
Implant type	
Nobel Replace Select Tapered	145 (53.9%)
Nobel Active	40 (14.9%)
Nobel Replace Select Straight	23 (8.6%)
Nobel Replace Groovy	12 (4.5%)
Nobel Speedy	43 (16.0%)
Brånemark Groovy	6 (2.2%)
Dental arch of implant insertion	
Maxilla	149 (55.4%)
Mandible	120 (44.6%)
Implant placement zone	
Anterior (canine - canine)	64 (23.8%)
Posterior (premolars and molars)	205 (76.2%)

SD: standard deviation.

3. Results

Seventy-five patients were enrolled in the study. The main baseline patient characteristics are presented in Table 1. No significant differences were found in ISQ according to patient characteristics (sex, age, and smoking habits) nor in maxilla nor in mandible ($p > 0.05$). Torque in mandible showed a significant negative correlation with age ($\rho = -0.236$; $p = 0.009$). Concerning the bone characteristics (implant location, bone density according to the Hounsfield scale, and cortical bone thickness), in maxilla ISQ showed a significant positive correlation with HU values detected for coronal-buccal ($r = 0.302$; $p = 0.020$) and middle-lingual ($r = 0.295$; $p = 0.023$). In mandible a significant difference was found between anterior and posterior implant location both in ISQ (anterior: 66.04; posterior: 72.22; mean difference: −6.182; 95% CI of the difference: −10.033 to −2.331; $p = 0.002$) and in torque (anterior: 1.81±1.05; posterior: 2.47±0.98; $p = 0.006$). Moreover torque showed a positive correlation with cortical bone thickness at the middle of the ridge ($\rho = 0.196$; $p = 0.032$). With respect to implant characteristics, a statistically

significant correlation was found between ISQ and implant length in maxilla ($r = 0.316$; $p = 0.015$) and between torque and implant length both in maxilla ($\rho = 0.216$; $p = 0.008$) and in mandible ($\rho = -0.318$; $p < 0.001$). A significant correlation between torque and implant diameter was found both in maxilla ($\rho = 0.172$; $p = 0.036$) and in mandible ($\rho = 0.370$; $p < 0.001$) whereas no significant correlations existed between ISQ and implant diameter ($p > 0.05$). No significant differences were found in ISQ among the different implant types (Table 2), even after controlling for the variables that had shown a significant correlation with ISQ ($p > 0.05$; Tables 3 and 4). No statistically significant interactions between the effects on torque of implant type and each variable that had shown a significant correlation with torque were found ($p > 0.05$). In maxilla Nobel Active implants showed a significantly higher torque than Nobel Replace Select Straight implants, Nobel Replace Groovy implants, and Nobel Speedy implants; in mandible Nobel Replace Select Tapered implants had a significantly higher torque than Replace Select Straight implants (Table 5).

4. Discussion

Several published methods are suggested for the assessment of bone quality, but many of these have shown a deficiency in the objectivity [6, 11, 12], because they are dependent upon the practitioner and/or can only be used during or after surgery [4]. Percussion and manual testing assess the implant stability by judging the presence of any mobility by a gentle application of a soft rotational force to the implant and abutment complex by the use of an appropriate screwdriver. They are widely practised clinical techniques, but there is little evidence in the literature supporting these concepts [12]. Radiographic examination is the most commonly used technique in clinical practice [13]. The implant is monitored at 6 and 12 months and every year thereafter in order to identify any marginal bone loss and perifixtural radiolucencies. Unfortunately, radiographs have a poor diagnostic ability for detection of perifixtural radiolucency due to their limited discriminatory acuity [14] and they show a two-dimensional image, while the implant/bone interface is a three-dimensional area; moreover, it is difficult to use a standard technique to ensure good reproducibility [15]. The insertion torque records the torque required to place the implant, it provides important information about the local bone quality and maybe about primary stability; indeed several authors have reported that the insertion torque measurements can be used to determine primary stability [16–20]. Removal torque is a technique that involves measuring the peak torque necessary to shear the interface between the implant surface and the surrounding bone, with a manual torque gauge; this test has been criticized as being destructive method and it is mostly used only in experiments [21]. Another method can be used after the implant placement is the Periotest® (Siemens AG, Bensheim, Germany) [22], which consists of percussing implant surface with a handheld probe containing an electromagnetically driven metal pellet; the mobility is assessed by the measurement of the contact time between the metal hammer and the surface under test. The sensitivity of Periotest to clinical
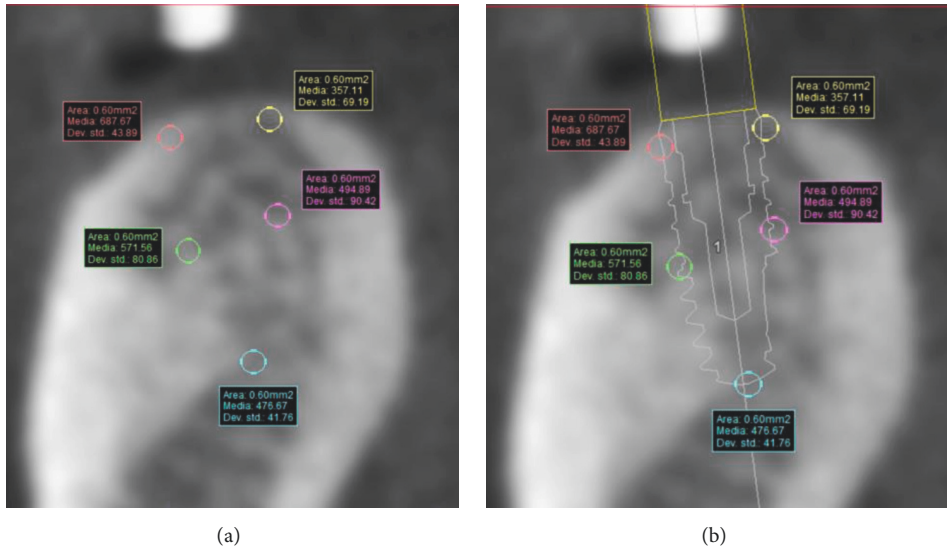
FIGURE 6: (a) The five points where to measure the Hounsfield Units and (b) in relation to implant.

FIGURE 7: HU values detected as the arithmetical means of an area measuring 60 mm^2.
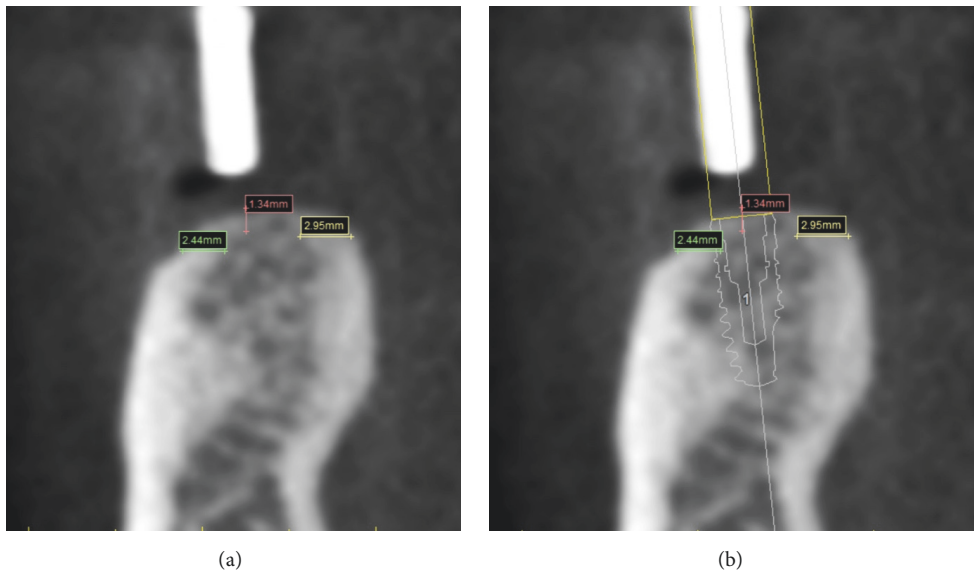
FIGURE 8: The three lines designed to measure the Cortical Thickness and (b) in relation to implant.

variables such as striking position and hand piece angulation limited the application of the instrument as a definitive clinical diagnostic tool, to be used; the values of this method are also influenced by the implant and abutment lengths [5]. With the advent of Resonance Frequency Analysis, there is an objective method for stability testing [23]: it analyses the resonance frequency of a transducer attached to an implant fixture or abutment [24]. The most recent version of Resonance Frequency Analysis is wireless, where a metal rod is connected to the implant by means of a screw connection

Table 2: ISQ comparison among implant types.

	ISQ (N; mean ± SD)	p value[*]
Maxilla		
Nobel Replace Select Tapered	12; 66.17 ± 7.16	
Nobel Active	19; 63.42 ± 9.53	
Nobel Replace Select Straight	4; 65.50 ± 11.96	0.201
Nobel Replace Groovy	3; 76.00 ± 5.29	
Nobel Speedy	21; 64.81 ± 7.13	
Mandible		
Nobel Replace Select Tapered	30; 72.20 ± 5.94	
Nobel Active	2; 66.00 ± 4.24	
Nobel Replace Select Straight	9; 67.22 ± 4.76	0.134
Nobel Speedy	9; 70.44 ± 7.99	

N: number; SD: standard deviation; [*]one-way ANOVA.

Table 3: Maxilla: ISQ comparison among implant types controlling for continuous variables which showed a significant correlation with ISQ (ANCOVA).

	p value (Implant type)	p value (covariate)
HU1 (coronal-buccal)	0.283	0.040
HU4 (middle-lingual)	0.558	0.157
Implant length	0.059	0.003

(Osstell ISQ instrument). This is a consistent and noninvasive technique to establish clinically relevant information about the state of the implant–bone interface at any stage of the treatment or at follow-up examinations [25]. In this study we evaluated the correlations between diameter and implants lengths, HU values, and cortical thickness with ISQ and the insertion torque (both objective parameters to assess the primary implant stability [26, 27]) in order to evaluate the bone density prior to surgery and give recommendations to the surgeon about the best surgical technique and about the type of implant; this was suggested by Salimov et al. [28], who explored the efficacy of bone density values by evaluating its correlation with the implant stability param- eters, including insertion torque value and the Resonance Frequency Analysis, finding a correlation, however with the limit of a clinical study on just 17 patients. We carried out the present study using preexisting CTs because, at the time of treating these patients (2010–2014), we were unable to use CBCT. Moreover, being not able at the time to acquire any CTs in our private practice, patients were simply referred, so different CT machines were used. Anyway, there is a significant correlation between primary implant stability and gray density values detected not only by cone beam (CBCT), but also by conventional multislice computed tomography (CT). In any case, CBCT is nowadays preferable because of lower radiation dose and costs, as stated by Arisan et al. [29]; as a consequence we have planned to publish our results with CBCT, once we reach a suitable number of patients with adequate follow-ups. In our study we found that the cortical bone thickness in the middle of the ridge showed a

positive correlation with torque, and it could be considered in an agreement with the conclusions of other studies [30, 31] on the importance of cortical thickness as a predictive factor of primary implant stability. Additionally, it could be interesting to highlight that crestal cortical bone thickness depends on the region of the jawbone. The thickness shows the highest values in posterior mandible and the lower in posterior maxilla: that leads us to pay close attention to implant placement in the posterior maxilla region in order to obtain a good primary implant stability [32]. The present study also found a significant positive correlation between ISQ and the HU values detected for coronal-buccal and middle-lingual in maxilla, according to Turkyilmaz et al. [9], which found statistically significant correlations between ISQ and bone density, expressed in HU values. Moreover, we found that the posterior implant location in mandible showed higher values of both ISQ and torque than the anterior implant location in the same jaw. This difference is statistically significant, but it is in contrast with literature; this could be explained by the fact that the majority of the implants have been placed in premolars and molars area. ISQ values showed a significant correlation with implants length in maxilla, but no correlations with implants diameter have been found in this study. Those results are partially in contrast with Fuster-Torres et al. [8]: they did not find significative correlation between the implant length and ISQ. The difference in results could be probably explained in view of the limited sample size of that study. No significant differences were also found in ISQ among the different implant types and among the patient characteristics (sex, age, and smoking habits) nor in maxilla nor in mandible. Moreover, in the present study torque showed a significant correlation between implant length and implant diameter both in maxilla and in mandible. Nobel Active implants showed a significantly higher torque than Nobel Replace Select Straight implants in maxilla, Nobel Replace Groovy implants, and Nobel Speedy implants. In mandible Nobel Replace Select Tapered implants had a significantly higher torque than Nobel Replace Select Straight implants. Finally, torque in mandible showed a significant negative correlation with age, unlike other studies [9, 33] which recorded higher torque values in older patients. This

Table 4: Mandible: ISQ comparison among implant types and implant location.

	Nobel Replace Select Tapered	Nobel Active	Nobel Replace Select Straight	Nobel Speedy	2-way ANOVA
Anterior	64.75 ± 0.96	-	66.25 ± 4.86	67.13 ± 9.90	0.383 (type: 0.396; loc: 0.012)
Posterior	73.35 ± 5.53	66.00 ± 4.24	68.00 ± 5.10	73.10 ± 5.86	
Total	72.20 ± 5.94	66.00 ± 4.24	67.22 ± 4.76	70.44 ± 7.99	

Data are presented as Mean ± Standard deviation; 2-way ANOVA: Two-Way ANOVA with implant type and implant location as independent variables; Two-Way ANOVA results are reported as significance of implant type-implant location interaction (Main effects p value).

Table 5: Torque comparison among implant types.

	Torque (N; mean ± SD)	p value[*]
Maxilla		
Nobel Replace Select Tapered	53; 1.68 ± 1.31	
Nobel Active	38; 2.42 ± 1.03	
Nobel Replace Select Straight	14; 1.21 ± 0.80	<0.001[#§^]
Nobel Replace Groovy	10; 1.00 ± 1.05	
Nobel Speedy	28; 1.54 ± 0.92	
Brånemark Groovy	6; 1.00	
Mandible		
Nobel Replace Select Tapered	92; 2.52 ± 0.99	
Nobel Active	2; 3.00	
Nobel Replace Select Straight	9; 1.44 ± 0.53	<0.001[ϛ]
Nobel Replace Groovy	2; 3.00	
Nobel Speedy	15; 1.93 ± 1.03	

N: number; SD: standard deviation; [*]Kruskal Wallis test. Significant post hoc comparisons: [#]Nobel Active versus Nobel Replace Select Straight; [§]Nobel Active versus Nobel Replace Groovy; [^]Nobel Active versus Nobel Speedy; [ϛ]Nobel Replace Select Tapered versus Nobel Replace Select Straight.

fact could be a result of the small difference in age between the patients who have been considered in this study (mean age was 60.31 ± 12.57 years).

5. Conclusion

The results of this study suggest that the bone density values (as measured in HU), which were obtained from the CT, could be utilized as predictive parameters during the preoperative assessment when correlated to the primary implant stability (ISQ), especially for the HU values detected for coronal-buccal and middle-lingual. Diameter and implants lengths do not seem to have had correlation to the primary implant stability (ISQ), except for implants lengths in maxilla. Moreover, the results suggest that the cortical thickness, especially in the middle of the ridge, which was measured from the CT, could be utilized as predictive parameter during the preoperative assessment when correlated to the primary implant stability (insertion torque). Subsequently, it is important to take into consideration the Hounsfield Units and the cortical thickness, with regard to the choice of the implant type as well as the surgical technique.

Conflicts of Interest

The authors declare that they have no conflicts of interest and this research did not receive funding.

References

[1] A. N. Natali, E. L. Carniel, and P. G. Pavan, "Investigation of viscoelastoplastic response of bone tissue in oral implants press fit process," *Journal of Biomedical Materials Research Part B: Applied Biomaterials*, vol. 91, no. 2, pp. 868–875, 2009.

[2] F. Javed and G. E. Romanos, "The role of primary stability for successful immediate loading of dental implants. A literature review," *Journal of Dentistry*, vol. 38, no. 8, pp. 612–620, 2010.

[3] N. Lioubavina-Hack, N. P. Lang, and T. Karring, "Significance of primary stability for osseointegration of dental implants," *Clinical Oral Implants Research*, vol. 17, no. 3, pp. 244–250, 2006.

[4] P. Johansson and K. G. Strid, "Assessment of bone quality from placement resistance during implant surgery," *The International Journal of Oral & Maxillofacial Implants*, vol. 9, pp. 279–288, 1994.

[5] N. Meredith, "Assessment of implant stability as a prognostic determinant," *International Journal of Prosthodontics*, vol. 11, no. 5, pp. 491–501, 1998.

[6] G. Alsaadi, M. Quirynen, K. Michiels, R. Jacobs, and D. Van Steenberghe, "A biomechanical assessment of the relation between the oral implant stability at insertion and subjective bone quality assessment," *Journal of Clinical Periodontology*, vol. 34, no. 4, pp. 359–366, 2007.

[7] M. Degidi, G. Daprile, and A. Piattelli, "Determination of primary stability: a comparison of the surgeon's perception and objective measurements," *The International Journal of Oral & Maxillofacial Implants*, vol. 25, no. 3, pp. 558–561, 2010.

[8] M. Á. Fuster-Torres, M. Peñarrocha-Diago, D. Peñarrocha-Oltra, and M. Peñarrocha-Diago, "Relationships between bone density values from cone beam computed tomography, maximum insertion torque, and resonance frequency analysis at implant placement: a pilot study," *The International Journal of Oral & Maxillofacial Implants*, vol. 26, no. 5, pp. 1051–1056, 2011.

[9] I. Turkyilmaz, T. F. Tözüm, C. Tumer, and E. N. Ozbek, "Assessment of correlation between computerized tomography values of the bone, and maximum torque and resonance frequency values at dental implant placement," *Journal of Oral Rehabilitation*, vol. 33, no. 12, pp. 881–888, 2006.

[10] Y.-D. Song, S.-H. Jun, and J.-J. Kwon, "Correlation between bone quality evaluated by cone-beam computerized tomography and implant primary stability," *The International Journal of Oral & Maxillofacial Implants*, vol. 24, no. 1, pp. 59–64, 2009.

[11] U. Lekholm and G. Zarb, "Patient selection and preparation," in *Tissue-Integrated Prostheses: Osseointegration in Clinical Dentistry*, P.-I. Brånemark, G. A. Zarb, and T. Albrektsson, Eds., pp. 199–209, Quintessence, Chicago, Ill, USA, 1985.

[12] B. Friberg, L. Sennerby, N. Meredith, and U. Lekholm, "A comparison between cutting torque and resonance frequency measurements of maxillary implants: A 20-month clinical study," *International Journal of Oral and Maxillofacial Surgery*, vol. 28, no. 4, pp. 297–303, 1999.

[13] K. Gröndahl and U. Lekholm, "The Predictive Value of Radiographic Diagnosis of Implant Instability," *The International Journal of Oral & Maxillofacial Implants*, vol. 12, no. 1, pp. 59–64, 1997.

[14] J. G. Caton and C. J. Kowalski, "Primate model for testing periodontal treatment procedures: II. Production of contralaterally similar lesions," *Journal of Periodontology*, vol. 47, no. 9, pp. 506–510, 1976.

[15] S. Sundén, K. Gröndahl, and H.-G. Gröndahl, "Accuracy and precision in the radiographic diagnosis of clinical instability in Brånemark dental implants," *Clinical Oral Implants Research*, vol. 6, no. 4, pp. 220–226, 1995.

[16] P. Maló, B. Friberg, G. Polizzi, F. Gualini, T. Vighagen, and B. Rangert, "Immediate and early function of Brånemark System® implants placed in the esthetic zone: A 1-year prospective clinical multicenter study," *Clinical Implant Dentistry and Related Research*, vol. 5, no. 1, pp. 37–46, 2003.

[17] L. V. Bogaerde, G. Pedretti, P. Dellacasa, M. Mozzati, and B. Rangert, "Early function of splinted implants in maxillas and posterior mandibles using brånemark system® machined-surface implants: An 18-month prospective clinical multicenter study," *Clinical Implant Dentistry and Related Research*, vol. 5, no. 1, pp. 21–28, 2003.

[18] P.-O. Östman, M. Hellman, and L. Sennerby, "Direct implant loading in the edentulous maxilla using a bone density-adapted surgical protocol and primary implant stability criteria for inclusion," *Clinical Implant Dentistry and Related Research*, vol. 7, no. 1, pp. S60–S69, 2005.

[19] K. Akça, A. M. Kökat, A. Cömert, M. Akkocaoğlu, I. Tekdemir, and M. C. Çehreli, "Torque-fitting and resonance frequency analyses of implants in conventional sockets versus controlled bone defects in vitro," *International Journal of Oral and Maxillofacial Surgery*, vol. 39, no. 2, pp. 169–173, 2010.

[20] V. Bruno, D. O'Sullivan, M. Badino, and S. Catapano, "Preserving soft tissue after placing implants in fresh extraction sockets in the maxillary esthetic zone and a prosthetic template for interim crown fabrication: A prospective study," *Journal of Prosthetic Dentistry*, vol. 111, no. 3, pp. 195–202, 2014.

[21] C. Johansson and T. Albrektsson, "Integration of screw implants in the rabbit: A 1-yr follow-up of removal torque of titanium implants," *The International Journal of Oral & Maxillofacial Implants*, vol. 2, no. 2, pp. 69–75, 1987.

[22] K. Derhami, J. F. Wolfaardt, G. Faulkner, and M. Grace, "Assessment of the periotest device in baseline mobility measurements of craniofacial implants," *The International Journal of Oral and Maxillofacial Implants*, vol. 10, no. 2, pp. 221–229, 1995.

[23] N. Meredith, *On the clinical measurement of implantstability and osseointegration, [Ph.D. thesis]*, Department of Biomaterials, University of Göteborg, 1997.

[24] N. Meredith, D. Alleyne, and P. Cawley, "Quantitative determination of the stability of the implant-tissue interface using resonance frequency analysis," *Clinical Oral Implants Research*, vol. 7, no. 3, pp. 261–267, 1996.

[25] L. Sennerby and N. Meredith, "Implant stability measurements using resonance frequency analysis: biological and biomechanical aspects and clinical implications," *Periodontology 2000*, vol. 47, no. 1, pp. 51–66, 2008.

[26] A. Beer, A. Gahleitner, A. Holm, M. Tschabitscher, and P. Homolka, "Correlation of insertion torques with bone mineral density from dental quantitative CT in the mandible," *Clinical Oral Implants Research*, vol. 14, no. 5, pp. 616–620, 2003.

[27] F. S. Lages, D. W. Douglas-de Oliveira, and F. O. Costa, "Relationship between implant stability measurements obtained by insertion torque and resonance frequency analysis: A systematic review," *Clinical Implant Dentistry and Related Research*, pp. 1–8, 2017.

[28] F. Salimov, U. Tatli, M. Kürkçü, M. Akoglan, H. Öztunç, and C. Kurtoglu, "Evaluation of relationship between preoperative bone density values derived from cone beam computed tomography and implant stability parameters: a clinical study," *Clinical Oral Implants Research*, vol. 25, no. 9, pp. 1016–1021, 2014.

[29] V. Arisan, Z. C. Karabuda, H. Avsever, and T. Özdemir, "Conventional Multi-Slice Computed Tomography (CT) and Cone-Beam CT (CBCT) for Computer-Assisted Implant Placement. Part I: Relationship of Radiographic Gray Density and Implant Stability," *Clinical Implant Dentistry and Related Research*, vol. 15, no. 6, pp. 893–906, 2013.

[30] I. Miyamoto, Y. Tsuboi, E. Wada, H. Suwa, and T. Iizuka, "Influence of cortical bone thickness and implant length on implant stability at the time of surgery—Clinical, prospective, biomechanical, and imaging study," *Bone*, vol. 37, no. 6, pp. 776–780, 2005.

[31] J. Merheb, N. Van Assche, W. Coucke, R. Jacobs, I. Naert, and M. Quirynen, "Relationship between cortical bone thickness or computerized tomography-derived bone density values and implant stability," *Clinical Oral Implants Research*, vol. 21, no. 6, pp. 612–617, 2010.

[32] Y.-C. Ko, H.-L. Huang, Y.-W. Shen, J.-Y. Cai, L.-J. Fuh, and J.-T. Hsu, "Variations in crestal cortical bone thickness at dental implant sites in different regions of the jawbone," *Clinical Implant Dentistry and Related Research*, vol. 19, no. 3, pp. 440–446, 2017.

[33] I. Turkyilmaz, C. Tumer, E. N. Ozbek, and T. F. Tözüm, "Relations between the bone density values from computerized tomography, and implant stability parameters: a clinical study of 230 regular platform implants," *Journal of Clinical Periodontology*, vol. 34, no. 8, pp. 716–722, 2007.

Research Article

Does Adding Silver Nanoparticles to Leukocyte- and Platelet-Rich Fibrin Improve Its Properties?

Hooman Khorshidi [iD],[1] **Pardis Haddadi** [iD],[1] **Saeed Raoofi** [iD],[1]
Parisa Badiee [iD],[2] **and Ali Dehghani Nazhvani**[3]

[1]*Department of Periodontology, School of Dentistry, Shiraz University of Medical Sciences, Shiraz, Iran*
[2]*Professor Alborzi Clinical Microbiology Research Center, Shiraz University of Medical Sciences, Shiraz, Iran*
[3]*Department of Oral & Maxillofacial Pathology, Biomaterial Research Center, School of Dentistry,*
 Shiraz University of Medical Sciences, Shiraz, Iran

Correspondence should be addressed to Pardis Haddadi; phaddadi@sums.ac.ir and Parisa Badiee; badieep@gmail.com

Objectives. Leucocyte- and platelet-rich fibrin (L-PRF) membrane can be used in various regenerative treatments. In the case of classical heterologous membrane exposure, microorganisms can be colonized on it and jeopardize the success of treatment. The aim of this study was to compare the antibacterial, mechanical, and histologic characteristics of the L-PRF membrane before and after the addition of silver nanoparticles (SNP). *Materials and Method.* This study was performed on 10 volunteer men aged 25-35 years. 20 ml whole bloods were collected from each person and L-PRFs were made by routine and SNP modified method. Mechanical, antibacterial, and histological properties were evaluated. *Results.* The antibacterial efficacy of L-PRF and nanosilver-modified L-PRF was presented as *Klebsiella pneumonia* had growth on the L-PRF membrane after 12 hours. After 24 hours, *Klebsiella pneumonia* and *Streptococcus viridans* had growth on L-PRF and only *Klebsiella pneumonia* had growth on SNP-L-PRF. The tensile strength and stiffness were significantly higher in the SNP-L-PRF. Precipitation of the SNPs was patchy in the outer layers and quite homogeneous in the inner core. *Conclusion.* Modification of L-PRF with SNP improves the mechanical properties and antibacterial activity of the L-PRF. It can play an important role in regenerative procedures.

1. Introduction

Guided tissue regeneration (GTR) and guided bone regeneration (GBR) are surgical techniques that aim to reconstruct the damaged periodontal tissues which are lost due to periodontal lesions and to regain the alveolar bone, lost due to tooth extraction or periodontal disease [1]. These methods employ various membranes to cover the bone and periodontal ligament and temporarily separate them from the epithelium and gingival connective tissue [2].

Regenerative potential of platelets was first introduced in the 1970s, just when they were found to contain growth factors responsible for increasing the collagen production, cell mitosis, blood vessels growth, and induction of cell differentiation [3]. The platelets were increasingly used in

tissue regeneration over time. The platelet-rich fibrin can be used in various regenerative treatments to accelerate the healing and improve the regeneration procedure [4]. It can also be used as a scaffold in tissue engineering [5].

Nowadays, there are several techniques to obtain the high concentration of platelets, each of which results in a specific product that is unique in terms of biology and performance. These methods are generally classified into four groups based on their fibrin and leucocyte content: pure platelet-rich plasma (P-PRP), leucocyte- and platelet-rich plasma (L-PRP), pure platelet-rich fibrin (P-PRF), and leucocyte- and platelet-rich fibrin (L-PRF) [6].

The chemical and physical properties of the membrane can influence the ultimate outcome of GBR and GTR [7]. The tensile strength of the tissue or the material which is

sutured affects the success of suturing and the clinical results of wound healing [8]. Meanwhile, the membrane stiffness and presence of stiff material influence the distribution of mechanical forces over the surrounding tissues [9]. Generally, the better the mechanical properties of the membrane provide the better support for regenerative treatments.

Among the mentioned methods for the preparation of high platelet concentrations, the L-PRF results in the formation of a strong fibrin matrix which can remodel slowly in the tissue, and if pressed, it turns to a strong membrane with better mechanical properties like tensile strength [6, 10]. In this technique, the patient's venous blood is centrifuged within an anticoagulant-free tube at low speed. Consequently, the L-PRF is formed in the middle between red blood cells in the bottom and plasma layer in the above [11].

The most frequent postoperative complication of different regenerative techniques is the membrane exposure to the oral cavity, in which case, oral cavity microorganisms can colonize on the membrane and jeopardize the success of treatment [12]. It results in higher risk of infection and poor bone healing even in healthy individuals. Reinforcing the membranes' antimicrobial properties with inorganic materials can improve the treatment results. Inorganic antimicrobial materials have been more appreciated recently due to their safety and stability.

One of the substances widely used today in various medical fields is silver nanoparticle (SNP). It has been shown that these particles have high biocompatibility and also have favorable properties, including antimicrobial properties [13]. Studies reported the effect of these materials on a wide spectrum of gram-negative and gram-positive bacteria as well as antibiotic-resistant species. Additionally, their antifungal and antiviral effects were proven [12]. The purpose of this study was to compare the antibacterial, mechanical, and histologic characteristics of the L-PRF membrane before and after the addition of SNPs.

2. Materials and Method

This study was performed on 10 volunteers selected on the basis of their availability. The inclusion criteria were male sex and age range of 25-35 years. The exclusion criteria were the history of the known systemic diseases, history of anticoagulant drugs assumption, smoking, use of any medication within the last three months, and lack of satisfaction.

2.1. Preparing SNP Suspension.
To obtain a uniform suspension, 0.1 gr nanosilver powder with particles sized <100 nm (Sigma Aldrich; USA), along with 1 cc normal saline, was poured into the tube and sonicated at 200 W for 2 minutes in a sonicator device [14].

2.2. Blood Samples Collection.
In this experimental study, after obtaining informed consent approved by the Ethics Committee of Shiraz University of Medical Sciences (code# 14866), 19 ml venous blood was taken from the subjects. Then, 10 ml of the obtained blood sample was poured into a dry sterile tube and the remaining 9 ml in addition to 1 ml of SNP

suspension was poured into another tube and gently shook with hand to achieve a uniform 1% concentration.

2.3. Making L-PRF and SNP Modified L-PRF.
The previously mentioned tubes were centrifuged at 2700 rpm for 12 minutes to produce original L-PRF (Intra-Spin, Intra-Lock); the only CE and FDA cleared system for the preparation of L-PRF [15]. The fibrin clot containing platelets was formed in the middle of the tubes, with the red blood cells lying at the bottom and the plasma on the top. The fibrin clots were removed from the tubes and separated from the underlying layers. The clots were placed on the metal grid in XPression Box (Intra-Lock). The metal lid was placed over the samples for 10 minutes to form them under pressure. They were used to evaluate the antimicrobial properties.

Prior to evaluation of the mechanical properties, the samples needed to be equalized in terms of shape and size. Thus, a plexiglass mold was prepared as inspired by Alston's method [16]. The mold was dog-bone-shaped of 2-mm thickness all over and 2-mm width in the middle. This part was the weakest area for stress accumulation and rupture.

2.4. Evaluation of Antimicrobial Characteristics.
1 ml unstimulated saliva was collected in sterile tube from three volunteers and mixed for 3ml saliva pool. They were requested to avoid eating and drinking within the two preceding hours. To evaluate the microflora of saliva pool, it was cultured on blood agar (Liofilchem; Italy) and Thioglycolate broth (Merck; Germany). Each fibrin membrane was divided into smaller pieces and incubated with 1 ml of saliva pool at 37°C for 24 hours.

After incubation, each piece was rinsed three times with sterile normal saline, placed on the shaker for 30 seconds, and centrifuged for 1 minute to remove the surrounding saliva, so as to solely evaluate the microbial biofilm formed on the sample. Then, 500 μl of the RPMI 1640 medium (Sigma; St. Louis, Missouri) was poured over the samples and incubated at 37°C for 12 and 24 hours. After incubation periods, 200 μl of media was poured in 96 well plates and evaluated by Elisa Reader device (Thermolabsystem, Multiskan Ascent, Finland) at 578 nm. Positive and negative controls in this study were the saliva cultured in RPMI and RPMI medium, respectively [17]. The isolated microorganisms were identified by using API 20 E (BioMerieux), Optochin test, and biliary solution.

2.5. Evaluation of the Mechanical Properties.
The tensile test was done by using the Universal testing machine (Zwick/Roell; 2020, Germany). The sample was fixed in the device. The tensile force was applied at 2mm/min speed, while the stress-strain curve was being simultaneously drawn by the Test Expert II software. The force was applied until the sample was torn from the thin middle part. The test finished as the sample ruptured. Then, the curve was used to measure the samples' tensile strength, toughness, and stiffness.

2.6. Evaluation of Histological Properties.
The remaining pieces of the membranes were fixed in 10% formalin for 24

(a)   (b)   (c)
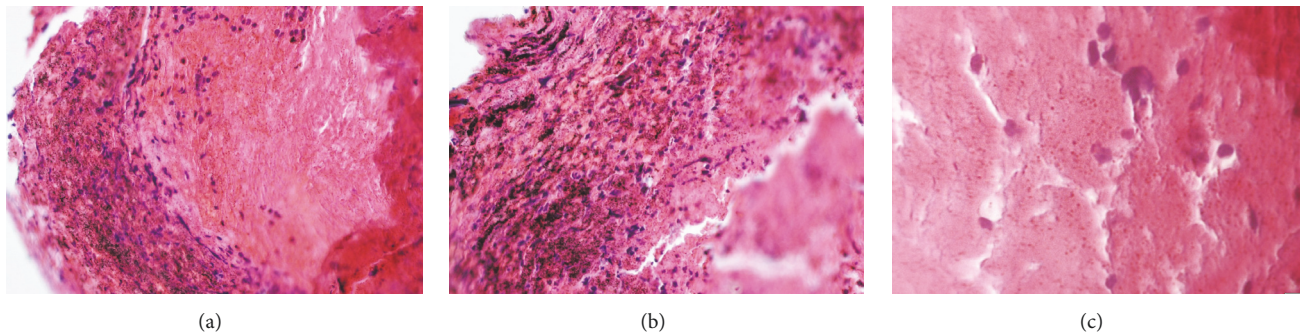
FIGURE 1: Microscopic sections show silver nanoparticles all over the membrane ((a), 100X); in outer layers they were more densely seated in the fibrin meshwork ((b), 200X) compared with the inner layers. Precipitation of the AgNPs was patchy in outer layers and quite homogeneous in inner layers ((c), 400X). Leukocytes were also denser in outer layers than inner layers (H&E staining).

hours to be subjected to H&E staining and evaluated with the light microscope.

2.7. Statistical Data Analysis. The obtained data was entered into Microsoft Excel software to find the area under the curve (toughness) and the slope (stiffness). The tensile strength of the samples was calculated by dividing the maximum force leading to membrane rupture by their cross-section area (4 mm^2). Paired t-test was used to compare these values between the two types of membranes and $P < 0.05$ was considered to be statistically significant.

3. Results

3.1. Antimicrobial Properties. The *Streptococcus viridans* and *Klebsiella pneumoniae* species were isolated from the primary saliva pool culture. After 12 hrs incubation of membrane in RPMI 1640, the turbidity (absorbance) of medium (negative control) at 578 nm wavelength was equal to the SNP modified L-PRF membrane, whereas in the L-PRF membrane the turbidity was higher which indicated the growth of some microorganisms. Identification of the isolated species indicated the growth of *K. pneumoniae* on the L-PRF membrane after 12 hours. After 24 hours, the SNP modified L-PRF revealed the presence of *K. pneumonia*, while the L-PRF showed both *K. pneumoniae* and *S. viridans*.

3.2. Mechanical Properties

3.2.1. Tensile Strength. The mean tensile strength was 0.154±0.05 MPa in L-PRF membrane samples and 0.435±0.19 MPa in L-PRF samples modified by SNPs, being statistically significantly higher in the latter ($P = 0.01$).

3.2.2. Stiffness. The mean stiffness value was 0.009 ± 0.004 MPa in L-PRF and 0.05 ± 0.02 MPa in L-PRF membranes modified by SNPs, being significantly higher in the latter ($P = 0.01$).

3.2.3. Toughness. The mean toughness was measured to be 63.8 ± 22.4 J/mm^3 in L-PRF and 74.29 ± 35.1 J/mm^3 in SNP modified L-PRF. Although the toughness was higher in

nanosilver group, the difference was not statistically significant ($P = 0.4$)

3.3. Histological Properties. Evaluating the microscopic sections, the silver nanoparticles were observed all over the membrane, but in the outer layers they were more densely attached to the fibrin strands compared with the inner layers. Precipitation of the SNPs was patchy in the outer layers and quite homogeneous in the inner layers. Moreover, the leukocytes were denser in the outer layers than in the inner layers (Figures 1(a), 1(b), and 1(c)).

4. Discussion

In the present study, the tensile strength, stiffness, and antibacterial activity were significantly higher in the SNP modified L-PRF membranes than the L-PRF group. The membrane's mechanical properties were improved as a result of adding SNPs to the L-PRF and its array in the fibrin matrix. The microscopic assessment of the samples showed that the SNPs were more densely mixed with the fibrin strands in the outer layers than the inner layers. Furthermore, their precipitation was patchy in the outer layer but quite homogenous in the inner layers. This may justify the improved mechanical properties of the L-PRF membrane modified by SNPs. Yet, further studies by an electron microscope are suggested to investigate more details.

The mechanical values measured in L-PRF group were in line with the study by Khorshidi et al. who reported that, among the techniques used for making high concentrations of platelets, the L-PRF technique created more favorable mechanical properties like better tensile strength. Hence, it had better clinical handling and could be a more suitable membrane for periodontal regenerative surgical procedures. [10].

The different mechanical properties observed in different methods of making PRF and L-PRF can be due to the differences in polymerization stages, as well as the different densities of fibrin matrix and different fibrinogen concentrations [10]. The tensile strength of the tissue or the material that is sutured affects the success of suturing and the clinical result of wound healing. Thus in clinical use, the membranes

with higher tensile strength are more tear resistant and bear greater applied forces [8].

The membrane produced in this study offered better mechanical properties besides maintaining its molecular properties. L-PRF can be a biologic scaffold and a reservoir for the growth factors in tissue regeneration. This fibrin increases the proliferation, migration, and differentiation of human bone marrow stem cells [18]. It also causes the expression of extracellular phosphorylated protein kinase and osteoprotegerin in osteoblasts and considerably affects the bone regeneration [19].

On the other side, the most common postoperative complication of regenerative surgeries is the membrane exposure, in which case, the oral cavity microorganisms can be colonized on the membrane and jeopardize the success of treatment [12]. Certainly, it results in increased infection risk and poor bone repair. Thus, reinforcing the antimicrobial feature of membranes can contribute to the improvement of the treatment outcome.

The SNPs are highly biocompatible and have favorable properties such as antimicrobial property [13]. Despite the several proposed theories, controversy exists regarding the mechanism of action of SNPs on microbes [20]. Silver nanoparticles can adhere to the cell membrane of the bacteria and make it porous, which consequently changes the permeability of the cell membrane and causes cell death [21].

A number of studies claimed that the contact between the silver nanoparticles and bacteria forms free radicals which can damage the bacterial cell membrane and cause bacterial death through increasing the permeability [12]. It was also announced that the Ag ions released from the nanoparticles could interfere with the thiol group of enzymes and deactivate them [22].

Several studies showed that these materials can influence a wide spectrum of gram-negative and gram-positive bacteria and also antibiotic-resistant species. They have also been proven to have antifungal and antiviral effects [12]. Bone cement reinforced with nanosilver can destroy different bacteria such as *Staphylococcus epidermidis*, methicillin-resistant *Staphylococcus epidermidis*, and methicillin-resistant *Staphylococcus aureus*, in vitro [17].

Adding SNPs to oral mouthwashes considerably reduced the growth of *Streptococcus mutans* compared with antibiotics and chlorhexidine [23]. In endodontic treatments, application of different concentrations of SNPs in combination with MTA and CEM had shown an antibacterial effect against *Escherichia coli, Enterococcus faecalis, Candida albicans,* and *Actinomyces* spp. [24]. The membrane designed in the present study succeeded to offer suitable antimicrobial properties like the previously mentioned studies.

Viridans group *Streptococcus* (VGS) is a heterogeneous group of organisms with six main subgroups and at least 30 different strains. Functioning as the normal flora of the body or pathogens, they can cause delay or failure in the healing of the surgical site. The VGS include gram-positive catalase-negative coccus with chain morphology in microscopic evaluation [25]. They are among the species whose interspecies genetic changes result in increased antibiotic resistance [12].

Klebsiella is an anaerobic facultative gram-negative non-motile bacillus, the commonest type of which is *K. pneumonia*. It inhabits the oral cavity of healthy individuals sporadically and can cause oral infections in cases such as nosocomial infection, poor oral hygiene, alcohol overuse, leukemia, weak immune system, and extensive dental caries [26].

In the current study, the membrane modified by SNPs showed no VGS growth after neither 12 nor 24 hours; however, it had no effect on *K. pneumonia*.

5. Conclusion

In the present study, modification of L-PRF by SNPs yielded a product which can help prevent the growth of a great family of bacteria (VGS) on the surgical sites and its consequences. This membrane not only has biological advantages, but also offers better mechanical properties including higher tensile strength, stiffness, and toughness compared with the traditional membrane.

Conflicts of Interest

The authors declare that there are no conflicts of interest regarding the publication of this article.

Acknowledgments

References

[1] G. Pellegrini, G. Pagni, and G. Rasperini, "Surgical approaches based on biological objectives: GTR versus GBR techniques," *International Journal of Dentistry*, vol. 2013, Article ID 521547, 13 pages, 2013.

[2] A. Sculean, D. Nikolidakis, and F. Schwarz, "Regeneration of periodontal tissues: combinations of barrier membranes and grafting materials—biological foundation and preclinical evidence: a systematic review," *Journal of Clinical Periodontology*, vol. 35, no. 8, pp. 106–116, 2008.

[3] V. R. Kumar and G. Gangadharan, "Platelet rich fibrin in dentistry: a review of literature," *International Journal of Medicine*, vol. 3, no. 2, 2015.

[4] A. B. Castro, N. Meschi, A. Temmerman et al., "Regenerative potential of leucocyte- and platelet-rich fibrin. Part A: intrabony defects, furcation defects and periodontal plastic surgery. A systematic review and meta-analysis," *Journal of Clinical Periodontology*, vol. 44, no. 1, pp. 67–82, 2017.

[5] D. M. Dohan, J. Choukroun, A. Diss et al., "Platelet-rich fibrin (PRF): a second-generation platelet concentrate. Part II: platelet-related biologic features," *Oral Surgery, Oral Medicine, Oral Pathology, Oral Radiology, and Endodontology*, vol. 101, no. 3, pp. E45–E50, 2006.

[6] D. M. Dohan Ehrenfest, L. Rasmusson, and T. Albrektsson, "Classification of platelet concentrates: from pure platelet-rich plasma (P-PRP) to leucocyte- and platelet-rich fibrin (L-PRF)," *Trends in Biotechnology*, vol. 27, no. 3, pp. 158–167, 2009.

[7] S.-B. Lee, J.-S. Kwon, Y.-K. Lee, K.-M. Kim, and K.-N. Kim, "Bioactivity and mechanical properties of collagen composite membranes reinforced by chitosan and β-tricalcium phosphate," *Journal of Biomedical Materials Research Part B: Applied Biomaterials*, vol. 100, no. 7, pp. 1935–1942, 2012.

[8] D. M. Marturello, M. S. Mcfadden, R. A. Bennett, G. R. Ragetly, and G. Horn, "Knot security and tensile strength of suture materials," *Veterinary Surgery*, vol. 43, no. 1, pp. 73–79, 2014.

[9] L. N. Melek, "Tissue engineering in oral and maxillofacial reconstruction," *Tanta Dental Journal*, vol. 12, no. 3, pp. 211–223, 2015.

[10] H. Khorshidi, S. Raoofi, R. Bagheri, and H. Banihashemi, "Comparison of the Mechanical Properties of Early Leukocyte- and Platelet-Rich Fibrin versus PRGF/Endoret Membranes," *International Journal of Dentistry*, vol. 2016, Article ID 1849207, 7 pages, 2016.

[11] D. M. Dohan, M. Del Corso, and J.-B. Charrier, "Cytotoxicity analyses of Choukroun's platelet-rich fibrin (PRF) on a wide range of human cells: The answer to a commercial controversy," *Oral Surgery, Oral Medicine, Oral Pathology, Oral Radiology, and Endodontology*, vol. 103, no. 5, pp. 587–593, 2007.

[12] J. Zhang, Q. Xu, C. Huang, A. Mo, J. Li, and Y. Zuo, "Biological properties of an anti-bacterial membrane for guided bone regeneration: an experimental study in rats," *Clinical Oral Implants Research*, vol. 21, no. 3, pp. 321–327, 2010.

[13] L. Ge, Q. Li, M. Wang, J. Ouyang, X. Li, and M. M. Q. Xing, "Nanosilver particles in medical applications: synthesis, performance, and toxicity," *International Journal of Nanomedicine*, vol. 9, no. 1, pp. 2399–2407, 2014.

[14] E.-A. Jun, K.-M. Lim, K. Kim et al., "Silver nanoparticles enhance thrombus formation through increased platelet aggregation and procoagulant activity," *Nanotoxicology*, vol. 5, no. 2, pp. 157–167, 2011.

[15] D. M. Dohan Ehrenfest, N. R. Pinto, A. Pereda et al., "The impact of the centrifuge characteristics and centrifugation protocols on the cells, growth factors, and fibrin architecture of a leukocyte- and platelet-rich fibrin (L-PRF) clot and membrane," *Platelets*, vol. 24, pp. 1–14, 2017.

[16] S. M. Alston, K. A. Solen, A. H. Broderick, S. Sukavaneshvar, and S. F. Mohammad, "New method to prepare autologous fibrin glue on demand," *Translational Research*, vol. 149, no. 4, pp. 187–195, 2007.

[17] V. Alt, T. Bechert, P. Steinrücke et al., "An in vitro assessment of the antibacterial properties and cytotoxicity of nanoparticulate silver bone cement," *Biomaterials*, vol. 25, no. 18, pp. 4383–4391, 2004.

[18] Y.-H. Kang, S. H. Jeon, J.-Y. Park et al., "Platelet-rich fibrin is a bioscaffold and reservoir of growth factors for tissue regeneration," *Tissue Engineering Part A*, vol. 17, no. 3-4, pp. 349–359, 2011.

[19] I.-C. Chang, C.-H. Tsai, and Y.-C. Chang, "Platelet-rich fibrin modulates the expression of extracellular signal-regulated protein kinase and osteoprotegerin in human osteoblasts," *Journal of Biomedical Materials Research Part A*, vol. 95, no. 1, pp. 327–332, 2010.

[20] S. Prabhu and E. K. Poulose, "Silver nanoparticles: mechanism of antimicrobial action, synthesis, medical applications, and toxicity effects," *International Nano Letters*, vol. 2, no. 1, article 32, 2012.

[21] I. Sondi and B. Salopek-Sondi, "Silver nanoparticles as antimicrobial agent: a case study on *E. coli* as a model for gram-negative bacteria," *Journal of Colloid and Interface Science*, vol. 275, no. 1, pp. 177–182, 2004.

[22] Y. Matsumura, K. Yoshikata, S. Kunisaki, and T. Tsuchido, "Mode of bactericidal action of silver zeolite and its comparison with that of silver nitrate," *Applied and Environmental Microbiology*, vol. 69, no. 7, pp. 4278–4281, 2003.

[23] A. Kariminik and M. Motaghi, "Evaluation of Antimicrobial susceptibility pattern of Streptococcus mutans isolated from dental plaques to chlorhexidine, nanosil and common antibiotics," *International Journal of Life Sciences*, vol. 9, pp. 18–21, 2015.

[24] N. Jonaidi-Jafari, M. Izadi, and P. Javidi, "The effects of silver nanoparticles on antimicrobial activity of ProRoot mineral trioxide aggregate (MTA) and calcium enriched mixture (CEM)," *Journal of Clinical and Experimental Dentistry*, vol. 8, no. 1, pp. e22–e26, 2016.

[25] C. D. Doern and C.-A. Burnham, "It's not easy being green: the viridans group streptococci, with a focus on pediatric clinical manifestations," *Journal of Clinical Microbiology*, vol. 48, no. 11, pp. 3829–3835, 2010.

[26] F. F. Lopes, L. C. Souza, M. P. Macedo et al., "Oral cavity as respiratory pathogens reservoir associated with ventilator-associated pneumonia," *Oral Surgery, Oral Medicine, Oral Pathology, Oral Radiology, and Endodontology*, vol. 124, no. 2, article e149, 2017.

Clinical Study

The Influence of the Crown-Implant Ratio on the Crestal Bone Level and Implant Secondary Stability: 36-Month Clinical Study

Jakub Hadzik [ID],[1,2] **Maciej Krawiec,**[1] **Konstanty Sławecki,**[1] **Christiane Kunert-Keil** [ID],[3]
Marzena Dominiak,[1] **and Tomasz Gedrange** [ID] [1,3]

[1]*Department of Dental Surgery, Wroclaw Medical University, ul. Krakowska 26, 50-425 Wrocław, Poland*
[2]*Department of Oral Implantology, Wroclaw Medical University, ul. Krakowska 26, 50-425 Wrocław, Poland*
[3]*Department of Orthodontics, Technische Universität Dresden, Carl Gustav Carus Campus, Fetscherstr. 74, 01307 Dresden, Germany*

Correspondence should be addressed to Jakub Hadzik; jakub.hadzik@umed.wroc.pl

Introduction. When the era of dental implantology began, the pioneers defined some gold standards used in dental prosthetics treatment for implant-supported restorations. Referring to traditional prosthetics, it was taken for granted that the length of an implant placed in the alveolar bone (the equivalent of the root) should exceed the length of the superstructure. *Aim of the Study.* The aim of the study was to determine whether implant length and the crown-to-implant (C/I) ratio influence implant stability and the loss of the surrounding marginal bone and whether short implants can be used instead of sinus augmentation procedures. *Material and Methods.* The patients participating in the study ($n = 30$) had one single tooth implant, a short (OsseoSpeed™ L6 Ø4 mm, Implants) or a regular implant (OsseoSpeed L11 and L13 Ø4 mm, DENTSPLY Implants), placed in the maxilla. The evaluation was based on clinical and radiological examination. The crown-to-implant ratio was determined by dividing the length of the crown together with the abutment by the length of the implant placed crestally. Mean crown-to-implant ratios were calculated separately for each group and its correlation with the MBL (marginal bone loss) and stability was assessed. The authors compared the correlation between the C/I ratio values, MBL, and secondary implant stability. *Results.* Positive results in terms of primary and secondary stability were achieved with both (short and conventional) implants. The MBL was low for short and conventional implants being 0.34 ± 0.24 mm and 0.22 ± 0.46 mm, respectively. No significant correlation was found between the C/I ratio and secondary stability as well as the C/I ratio and the marginal bone loss. *Conclusions.* Short implants can be successfully used to support single crowns. The study has revealed no significant differences in the clinical performance of prosthetic restorations supported by short implants. Clinical trial registration number is NCT03471000.

1. Introduction

The crown-to-root (C/R) ratio is commonly used by dental clinicians to qualify a tooth for a fixed dental crown. It is believed that a proper C/R is one of the key factors in achieving a long-term prognosis in prosthetic rehabilitation [1–3]. The importance of a proper C/R ratio may be explained by the biomechanical concept of a class I lever, so when a disproportionate C/R ratio occurs, the periodontium is more susceptible to injury due to heavy occlusal forces. This phenomenon was studied, for example, by McGuire and Nunn in a prospective study on predicting tooth loss for periodontal patients [4]. There are no strict guidelines for a

C/R ratio, but when a periodontium is healthy the optimal C/R ratio for a fixed crown is considered 1 : 2 or less [1, 5].

When the era of dental implantology began, clinicians started using certain guidelines associated with natural teeth for the implant-supported fixed crowns. It was taken for granted that the length of an implant placed in the alveolar bone (the equivalent of the root) part should exceed the length of the superstructure.

Many studies have shown that the success of implant osseointegration is considerably dependent on its surface and it has been proven that osteoblastic cells adhere more quickly to rough surfaces [6–8]. Many methods for increasing the dental implant roughness were described; one of them

is the the sandblasted and acid-etched surface created by the combination of sand-blasting and acid-etching is the most relevant and most commonly used method, and its significance has been documented in numerous studies [9–11].

Before implant surface modifications were widely recognized in the literature, in case of insufficient bone volume, augmentation procedures had been the only solution to ensure sufficient bone volume [12]. In the maxilla, in cases with vertical dimension deficiency, the augmentation in the maxillary sinus prior to the planned implantation is often necessary to obtain sufficient bone volume to stabilize a dental implant. Many biomaterials (including autografts, allografts, xenografts, and alloplasts) may be successfully used in these techniques, but sinus lift procedures feature the risk of complications, such as the perforation of the Schneiderian membrane (7–30% depending on the used technique and instruments) [13–15].

The indisputable progress and improvement of the implant surface enabled implant length reduction while still maintaining proper stability and functionality. Short implants could be used in cases where traditional implants preceded by the grafting procedure were the only solution. Furthermore, the implant surface modification also made it possible to stop following the guidelines used in traditional prosthetics. The barrier to maintaining a proper crown-to-implant (C/I) ratio was exceeded. A considerable number of studies addressed the issue of implant length as a predictor of implant survival, but they achieved inconclusive results. However, it has been pointed out that the excessive C/I ratio could impair long-term implant survival [16].

On the other hand, the recent literature indicates very promising results and argues that short implants may safely replace regular implants; however, due to their sophisticated surface, short implants remain stable when loaded with a crown longer than the implant itself [17–19].

The aim of the study was to check whether the crown-implant ratio influences the secondary implant stability and the marginal bone level [MBL] in implants loaded with single nonsplinted crowns. It was also assessed whether the use of increased C/I ratios for short implants would be as successful as for long implants proceeded by maxillary sinus augmentation with a xenograft.

2. Material and Methods

For the purpose of unifying the nomenclature in the manuscript, authors use the word superstructure for the prosthetic crown with the abutment.

2.1. Experimental Design. This prospective study was conducted based on clinical and radiographic examination. The study protocol was approved by the local ethical commission (Bioethics Committee at Wroclaw Medical University, approval number KB 427/201). All patients gave two written consents: the first was general consent to have dental implants placed, and the other consent involved the participation in the study. The study has been conducted in full compliance with the Declaration of Helsinki. The primary protocol of the study assumed a larger group of patients; however, only 30 patients were included in this long follow-up period. Other patients because of long evaluation period resigned from participation in the project; others because of poor compliance were excluded from the project.

The evaluation in this study group of patients incorporated 30 adults (10 males, 20 females), with a mean age of 45.5 years, who had DENTSPLY implants placed at the Department of Dental Surgery at Wroclaw Medical University. The patients who met the inclusion criteria were divided at random (by drawing lots) into two groups according to the method of treatment provided.

Group 1 (G1; $n = 15$ patients) had conventional dental implants (OsseoSpeed L11 Ø4 mm and L13 Ø4 mm) [DENTSPLY Implants, Waltham, MA, USA] placed, preceded by the sinus lift procedure from a lateral window approach with the application of the xenogeneic bone graft Geistlich Bio-Oss® [Geistlich AG, Wolhusen, Switzerland]. The lateral window approach sinus lift surgery was performed 6 weeks prior to the implant placement by the same surgeon.

Group 2 (G2; $n = 15$ patients) had short implants (OsseoSpeed L6 mm Ø4 mm) [DENTSPLY Implants, Waltham, MA, USA] placed without sinus lift and augmentation procedure.

2.2. Inclusion and Exclusion Criteria. Nonsmoking patients with no systemic or local diseases were qualified.
Additional inclusion criteria were as follows:

 (i) Minimal apicocoronal height of the alveolar ridge of 6 mm in the region of the implant insertion in the presurgical qualification

 (ii) Minimal width of the alveolar ridge of 6-7 mm in the region of interest

 (iii) HKT (height of the keratinized tissue) higher than 2 mm

 (iv) API ≤ 35 (Approximal Plaque Index)

 (v) PI ≤ 25. (Plaque Index)

 (vi) Bone Type III or D2 were included in the study

 (vii) No graft procedures in the area of interest

In both groups, D2 (Misch) was the radiologically and clinically assessed bone density based on presurgery CT scans and intrasurgery clinical evaluation. The surgical procedure was performed under the same conditions and by the same medical team with induced local anesthesia. All patients were instructed to rinse their mouths with 0.12% chlorhexidine solution (twice a day until suture removal) and to take the prescribed antibiotics and analgesics (Augmentin 1,0 in tabl. One dose at one hour before the surgery and then 5 days after implant placement 1,0 g every 12 hours). In addition patients in Group 1 where the sinus floor was elevated received additional antibiotic therapy when the surgery was performed (Augmentin 1,0 in tabl. One dose at one hour before the surgery and then 5 days after implant placement 1,0 g every 12 hours). Nonresorbable sutures were removed 7–14 days after the implant placement. In all cases,

final restorations were manufactured and cemented with resin based semipermanent cement 6 months after implant placement. All implants in this study were loaded with single nonsplinted crowns.

CBCT (Cone Beam Computed Tomography) [Galileos® D3437, Sirona Dental, Germany] and RVG [Visualix® eHD, Gendex Dental Systems, USA] were taken for each implant analyzed and measured to assess the crown-implant ratio. The initial CBCT and RVG taken immediately after the implant placement (T0) and CBCT and RVG radiographs taken after 36 month (T1) were used to assess the marginal bone level changes. The loss of the marginal bone was measured based on the CBCT image and using a standard RVG periapical X-ray done with the use of a straight angle technique with a positioner. The CBCT image offers transrectal views so the measurement can be made around the implant. On the periapical X-ray, the bone level was measured on the mesial and distal site of the implant and the mean values were calculated. The measuring points on CBCT were located around the implant (4 points around each mesial, distal, buccal, and palatal) and the mean values were calculated. To indicate the value in millimeters, in each case the radiological measurement was calibrated with the previously known length of the implant. Then the mean value of the measurements from both CBCT and RVG was calculated and these mean values were presented in the manuscript.

For Periotest®, measured in PVT Periotest Values [Periotest Classic, Medizintechnik Gulden, Germany] examination was performed to assess secondary implant stability after 36 months. In all cases, the Periotest evaluation was conducted in the same manner. Each implant was evaluated at 4 different location points, each with a different direction of the excitation: 2 points at the buccal (45 degrees from the mesiobuccal direction, 90 degrees from the buccal direction, both at the half the height of the supragingival part of the crown) and similarly on the palate, each excitation place was evaluated 3 times. The mean was calculated for all evaluation points for each implant.

The crown-to-implant ratio was determined by dividing the length of the superstructure (crown and the abutment) by the length of the implant that was placed crestally (Figures 1 and 2). Mean crown-to-implant ratios were calculated separately for each group and its correlation with the MBL (MBL = marginal bone loss) and implant stability was evaluated. The authors compared the correlation between the range of C/I ratio values, the MBL, and secondary implant stability, respectively.

2.3. Statistical Analysis. The statistical analysis was performed using GraphPad Prism 6 software [GraphPad Software, Inc., USA]. Spearman's rho test was used to measure correlation. All data were given as means ± standard deviation (SD). $P < 0.05$ was considered statistically significant.

3. Results

The evaluation of implant stability with Periotest after 36 months (T1) yielded good results of secondary implant stability in both groups (G1 and G2: 0.93 ± 3.39 PTV and
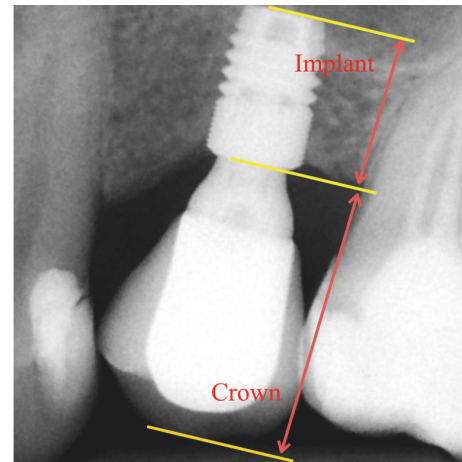
FIGURE 1: Periapical digital radiograph of a short implant (Astra Tech implant system™ OsseoSpeed TX 4.0 S; Ø4 mm, 6 mm long). The C/I ratio measurement method is presented. Radiological status 36 months after implant placement.
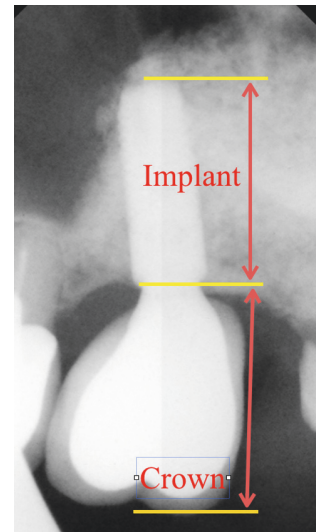
FIGURE 2: Periapical digital radiograph of a regular implant (Astra Tech implant system OsseoSpeed TX 4.0 S; Ø4 mm, 11 mm long). The C/I ratio measurement method is presented. Radiological status 36 months after implant placement.

1.0 ± 2.7 PTV). The marginal bone level loss was low and similar in both groups (G1 and G2: 0.22 ± 0.46 mm and 0.34 ± 0.24 mm). No significant difference in the MBL between short and regular implants was found (Table 1).

The average C/I ratio in G1 was 1.063 and in G2 1.69 (Table 2). No significant correlation between the C/I ratio and the secondary stability was found as well as for the C/I ratio and the marginal bone loss (Table 3).

4. Discussion

There is still some controversy over the definition of a short implant. According to Tawil and Younan, an implant

TABLE 1: Marginal bone level loss. T0 compared to T1. Mean value ± SD.

	Group 1	Group 2	Wilcoxon test
T0 versus T1	0.22 ± 0.46 mm	0.34 ± 0.24 mm	$P = 0.1229$

TABLE 2: Correlations between C/I ratio: secondary stability and C/I ratio: marginal bone level loss.

Correlation	C/I ratio: secondary stability	C/I ratio: marginal bone level loss
r	−0.04	0.32
Test	Spearman	Spearman
Significance	No	No

TABLE 3: Crown-implant ratio (C/I) after 36 months (T1).

Group 2	C/I Ratio	Group 1	C/I Ratio
min	1.36	min	0.68
max	1.97	max	1.65
Mean	1.679	Mean	1.063
SD	0.2129	SD	0.293
Median	1.69	Median	1.05

of ≤10 mm is considered short [20], whereas Nisand and Renouard define the one with a designed intrabony length of ≤8 mm as short and a device with a designed intrabony length of ≤5 mm as extra short [21]. In our study, the implants with a length of 11 or 13 mm were considered regular, whereas 6 mm dental implants were considered short. The study only used single crown restorations for both G1 and G2. Splinting the crowns when examining the impact of the C/I ratio would change the distribution of forces and, consequently, the results would be disturbed. The determination of the marginal bone level (MBL) was based on radiographic measurements after 36 months. The marginal bone level loss was low and similar in both tested groups. No significant difference in the MBL between short and conventional implants was found, as well as no correlation between the MBL and the C/I ratio. Furthermore, the correlation between the C/I and implant stability was reported not to be statistically significant. These results may correspond with a majority of the C/I ratio studies arguing that the crown-to-root ratio guidelines associated with natural teeth should not be directly applied when planning implant-supported single tooth restoration.

The recent literature shows that the crown-to-implant ratio has no major impact on the clinical performance of implants and may be successfully applied [19, 22–24]. In the systematic review by Blanes it was found that the C/I ratios of implant-supported reconstructions do not influence peri-implant crestal bone loss [22]. Mangano et al. studied 68 short dental implants over a period of 5 years with different C/I ratios. No significant differences were found in the survival rate, prevalence of biological complications, and prosthetic complications between the groups with $C/I \geq 2$ and $C/I < 2$ [24]. Those findings correspond to ours. We have found no correlation between the C/I ratio and the MBL. Schulte et al. analyzed retrospectively 889 single tooth implants from 294 patients and put forward that the

crown-to-root ratio guidelines associated with natural teeth should not be applied to a potential implant site or an existing implant restoration [19]. Schneider et al. in a 5-year retrospective investigation demonstrated that the C/I ratio did not influence the clinical performance of implants supporting single crown restorations in the posterior segments of the jaw [23]. However, a significant negative association between the crown-implant ratio and the marginal bone loss was described in the literature as well. The systematic review by Garaicoa-Pazmiño et al. revealed that the C/I ratio of implant-supported restorations has an effect on the peri-implant marginal bone level [25]. Malchiodi et al. achieved similar results in his study. These authors analyzed 259 short dental implants in 136 patients over a period of 36 months. They observed a significant correlation between the clinical C/I ratio and the crestal bone loss. The peri-implant bone loss was significantly increased for implants with the $C/I \geq 2$ [26]. The study by Nunes et al. evaluated 118 implants from 59 patients, where 30 implants presented the $C/I \leq 2$ and 88 implants the $C/I > 2$. The authors revealed a weak inverse but insignificant correlation between the C/I ratio and the MBL [27]. They concluded that implant-supported fixed prostheses with the C/I ratio of >2 have a negative impact on the MBL. Anitua et al. managed to demonstrate that the use of a cantilever for prosthetic rehabilitation had a negative impact on the MBL. When the cantilever was used, the MBL was increased considerably by 238%. In contrast, when the cantilever was not used, the MBL is independent from the C/I ratio [28]. Using the finite element method, it was demonstrated that the stress concentration and stress distribution increase with the height of the crown [29, 30]. As the C/I ratio increased twice, the von Mises stresses rose by about 47%. At the C/I ratio of 2/1, the highest stresses were observed around the implant neck [29].

The improper placement of a dental implant and, consequently, the improper direction of the occlusive forces may

lead to increased stress and strain distribution on the bone around the dental implants; therefore, the marginal bone loss and recession of the soft tissues may occur [31–33]. However, the authors of the study gave the proper location of the implants careful thought, and thus none of these occurred.

Authors have presented only one scenario for the use of short implants, which seems to be the very common clinical situation. Maxillary molars are most often prematurely lost in maxilla. Due to loss of bone volume and maxillary sinus expansion, bone conditions often do not allow for placing regular length implants. This is a clinically important since here short implants are an alternative to regenerative treatment such as sinus lift procedures that can feature the risk of complications. According to Oikarinen et al. who studied over 400 patients the available bone height in the posterior maxilla in 38% of cases is at least 6 mm [34]; this is just enough bone volume to consider short dental implant without supportive regenerative treatment. The loading with nonsplinted crowns is also groundbreaking and clinically relevant since many previous studies like Cannizzaro et al. [35], Esposito et al. [36], and Pistilli et al. [37] evaluate splinted crowns in similar conditions; however, Guljé et al. [38] and Thoma et al. [39] have presented good clinical outcome with nonsplinted short implants in maxilla.

Of course, the lack of single tooth in the maxilla is not the only indication for the short implants. They can successfully be used to avoid regeneration procedures in a atrophic mandible; among many studies over this issue also our research group Hadzik et al. presented successful application of short dental implants to replace two missing molars in atrophic mandible [40]. The literature shows many more fine examples of common clinical situations where short implants are used to avoid less predictable and difficult regenerative treatments combined with regular implants. These implants have been described by Esposito et al. as effective in rehabilitation of fully edentulous atrophic maxilla [41]; Maló et al. has presented a short-term outcome study with successful immediate loading of short implants in edentulous maxilla using all-on-4 concept [42].

5. Conclusion

In conclusion, due to the fact that no negative impact of the lowered C/I ratio on the marginal bone level and implant stability was found, we came to the conclusion that short implants may be successfully used to support a single crown. The clinical performance of short implants is comparable to regular implants. Both treatment modalities can be considered in the atrophic posterior maxilla; however short implants may be more favourable regarding short-term patient morbidity.

Data Availability

The authors declare that they are in possession of complete data on the basis of which the results presented in the manuscript have been developed. The authors will make the data available to interested parties if necessary.

Conflicts of Interest

DENTSPLY Implants, the manufacturer of the dental implants used in this study, provided this trial with dental implants *(Astra Tech Grant no. D-2010-34)*. However, the data is the possession of the authors and the sponsor did not interfere with the course of the trial or in the publication of its results whatsoever. The authors declare no other conflicts of interest that could have influenced outcomes of this manuscript.

References

[1] H. Schillingburg, S. Hobo, L. Whitsett, R. Jacobi, and S. Brackett, *Fundamentals of fixed prostodontics*, Quintessence, CHI, IL, USA, 1997.

[2] R. E. Jung, B. E. Pjetursson, R. Glauser, A. Zembic, M. Zwahlen, and N. P. Lang, "A systematic review of the 5-year survival and complication rates of implant-supported single crowns," *Clinical Oral Implants Research*, vol. 19, no. 2, pp. 119–130, 2008.

[3] Y. Grossmann and A. Sadan, "The prosthodontic concept of crown-to-root ratio: A review of the literature," *Journal of Prosthetic Dentistry*, vol. 93, no. 6, pp. 559–562, 2005.

[4] M. K. McGuire and M. E. Nunn, "Prognosis versus actual outcome. III. The effectiveness of clinical parameters in accurately predicting tooth survival," *Journal of Periodontology*, vol. 67, no. 7, pp. 666–674, 1996.

[5] S. Rosenstiel, M. Land, and J. Fujimoto, *Contemporary fixed prosthodontics*, vol. 29, Elsevier, STL, MO, USA, 2014.

[6] D. L. Cochran, P. V. Nummikoski, F. L. Higginbottom, J. S. Hermann, S. R. Makins, and D. Buser, "Evaluation of an endosseous titanium implant with a sandblasted and acid-etched surface in the canine mandible: radiographic results," *Clinical Oral Implants Research*, vol. 7, no. 3, pp. 240–252, 1996.

[7] Z. Schwartz, C. H. Lohmann, J. Oefinger, L. F. Bonewald, D. D. Dean, and B. D. Boyan, "Implant surface characteristics modulate differentiation behavior of cells in the osteoblastic lineage," *Advances in Dental Research*, vol. 13, pp. 38–48, 1999.

[8] L. Gaviria, J. P. Salcido, T. Guda, and J. L. Ong, "Current trends in dental implants," *Journal of the Korean Association of Oral and Maxillofacial Surgeons*, vol. 40, no. 2, p. 50, 2014.

[9] D. Buser, N. Broggini, M. Wieland et al., "Enhanced bone apposition to a chemically modified SLA titanium surface," *Journal of Dental Research*, vol. 83, no. 7, pp. 529–533, 2004.

[10] M. M. Bornstein, P. Valderrama, A. A. Jones, T. G. Wilson, R. Seibl, and D. L. Cochran, "Bone apposition around two different sandblasted and acid-etched titanium implant surfaces: a histomorphometric study in canine mandibles," *Clinical Oral Implants Research*, vol. 19, no. 3, pp. 233–241, 2008.

[11] F. Schwarz, M. Herten, M. Sager, M. Wieland, M. Dard, and J. Becker, "Histological and immunohistochemical analysis of

initial and early osseous integration at chemically modified and conventional SLA titanium implants: preliminary results of a pilot study in dogs," *Clinical Oral Implants Research*, vol. 18, no. 4, pp. 481–488, 2007.

[12] M. Chanavaz, "Maxillary sinus: anatomy, physiology, surgery, and bone grafting related to implantology–eleven years of surgical experience (1979–1990)," *Journal of Oral Implantology*, vol. 16, no. 3, pp. 199–209, 1990.

[13] D. Schwartz-Arad, R. Herzberg, and E. Dolev, "The prevalence of surgical complications of the sinus graft procedure and their impact on implant survival," *Journal of Periodontology*, vol. 75, no. 4, pp. 511–516, 2004.

[14] S. S. Wallace, Z. Mazor, S. J. Froum, S.-O. Cho, and D. P. Tarnow, "Schneiderian membrane perforation rate during sinus elevation using piezosurgery: clinical results of 100 consecutive cases," *International Journal of Periodontics and Restorative Dentistry*, vol. 27, no. 5, pp. 413–419, 2007.

[15] F. Heinemann, T. Mundt, R. Biffar, T. Gedrange, and W. Goetz, "A 3-year clinical and radiographic study of implants placed simultaneously with maxillary sinus floor augmentations using a new nanocrystalline hydroxyapatite," *Journal of Physiology and Pharmacology*, vol. 60, 8, pp. 91–97, 2009.

[16] S. Winkler, H. F. Morris, and S. Ochi, "Implant survival to 36 months as related to length and diameter," *Annals of Periodontology*, vol. 5, no. 1, pp. 22–31, 2000.

[17] R. J. Blanes, J. P. Bernard, Z. M. Blanes, and U. C. Belser, "A 10-year prospective study of ITI dental implants placed in the posterior region. II: influence of the crown-to-implant ratio and different prosthetic treatment modalities on crestal bone loss," *Clinical Oral Implants Research*, vol. 18, no. 6, pp. 707–714, 2007.

[18] H. Birdi, J. Schulte, A. Kovacs, M. Weed, and S.-K. Chuang, "Crown-to-implant ratios of short-length implants," *Journal of Oral Implantology*, vol. 36, no. 6, pp. 425–433, 2010.

[19] J. Schulte, A. M. Flores, and M. Weed, "Crown-to-implant ratios of single tooth implant-supported restorations," *Journal of Prosthetic Dentistry*, vol. 98, no. 1, pp. 1–5, 2007.

[20] G. Tawil and R. Younan, "Clinical evaluation of short, machined-surface implants followed for 12 to 92 months," *The International Journal of Oral & Maxillofacial Implants*, vol. 18, no. 6, pp. 894–901, 2003.

[21] D. Nisand and F. Renouard, "Short implant in limited bone volume," *Periodontology 2000*, vol. 66, no. 1, pp. 72–96, 2014.

[22] R. J. Blanes, "To what extent does the crown-implant ratio affect the survival and complications of implant-supported reconstructions? A systematic review," *Clinical Oral Implants Research*, vol. 20, supplement 4, pp. 67–72, 2009.

[23] D. Schneider, L. Witt, and C. H. F. Hämmerle, "Influence of the crown-to-implant length ratio on the clinical performance of implants supporting single crown restorations: A cross-sectional retrospective 5-year investigation," *Clinical Oral Implants Research*, vol. 23, no. 2, pp. 169–174, 2012.

[24] F. Mangano, I. Frezzato, A. Frezzato, G. Veronesi, C. Mortellaro, and C. Mangano, "The effect of crown-to-implant ratio on the clinical performance of extra-short locking-taper implants," *The Journal of Craniofacial Surgery*, vol. 27, no. 7, pp. 675–681, 2016.

[25] C. Garaicoa-Pazmiño, F. S.-L. Del Amo, A. Monje et al., "Influence of crown/implant ratio on marginal bone loss: A systematic review," *Journal of Periodontology*, vol. 85, no. 9, pp. 1214–1221, 2014.

[26] L. Malchiodi, A. Cucchi, P. Ghensi, D. Consonni, and P. F. Nocini, "Influence of crown-implant ratio on implant success

rates and crestal bone levels: a 36-month follow-up prospective study," *Clinical Oral Implants Research*, vol. 25, no. 2, pp. 240–251, 2014.

[27] M. Nunes, R. F. Almeida, A. C. Felino, P. Malo, and M. D. A. Nobre, "The influence of crown-to-implant ratio on short implant marginal bone loss," *The International Journal of Oral & Maxillofacial Implants*, vol. 31, no. 5, pp. 1156–1163, 2016.

[28] E. Anitua, L. Piñas, and G. Orive, "Retrospective study of short and extra-short implants placed in posterior regions: influence of crown-to-implant ratio on marginal bone loss," *Clinical Implant Dentistry and Related Research*, vol. 17, no. 1, pp. 102–110, 2015.

[29] D. Cinar and P. Imirzalioglu, "The effect of three different crown heights and two different bone types on implants placed in the posterior maxilla: Three-dimensional finite element analysis," *The International Journal of Oral & Maxillofacial Implants*, vol. 31, no. 2, pp. e1–e10, 2016.

[30] N. R. Vootla, S. C. Barla, V. H. C. Kumar, H. Surapaneni, S. Balusu, and S. Kalyanam, "An evaluation of the stress distribution in screw retained implants of different crown implant ratios in different bone densities under various loads-A FEM study," *Journal of Clinical and Diagnostic Research*, vol. 10, no. 6, pp. ZC96–ZC101, 2016.

[31] M. Dominiak and T. Gedrange, "New Perspectives in the Diagnostic of Gingival Recession," *Advances in Clinical and Experimental Medicine*, vol. 23, no. 6, pp. 857–863, 2014.

[32] M. Zietek, T. Gedrange, and M. Mikulewicz, "Mikulewicz: Long term evaluation of biomaterial application in surgical treatment of periodontosis," *Journal of Physiology and Pharmacology*, vol. 59, 5, pp. 81–86, 2008.

[33] D. Yazicioglu, B. Bayram, Y. oguz, D. Cinar, and S. Uckan, "Stress distribution on short implants at maxillary posterior alveolar bone model with different bone-to-implant contact ratio: finite element analysis," *Journal of Oral Implantology*, 2012.

[34] K. Oikarinen, A. M. Raustia, and M. Hartikainen, "General and local contraindications for endosseal implants - an epidemiological panoramic radiograph study in 65-year-old subjects," *Community Dentistry and Oral Epidemiology*, vol. 23, no. 2, pp. 114–118, 1995.

[35] G. Cannizzaro, P. Felice, M. Leone, P. Viola, and M. Esposito, "Early loading of implants in the atrophic posterior maxilla: lateral sinus lift with autogenous bone and Bio-Oss versus crestal mini sinus lift and 8-mm hydroxyapatite-coated implants. A randomised controlled clinical trial," *European Journal of Oral Implantology*, vol. 2, no. 1, pp. 25–38, 2009.

[36] M. Esposito, G. Pellegrino, R. Pistilli, and P. Felice, "Rehabilitation of postrior atrophic edentulous jaws: prostheses supported by 5 mm short implants or by longer implants in augmented bone? One-year results from a pilot randomised clinical trial," *European Journal of Oral Implantology*, vol. 4, pp. 21–30, 2011.

[37] R. Pistilli, P. Felice, G. Cannizzaro et al., "Posterior atrophic jaws rehabilitated with prostheses supported by 6 mm long 4 mm wide implants or by longer implants in augmented bone. One-year post-loading results from a pilot randomised controlled trial," *European Journal of Oral Implantology*, vol. 6, pp. 359–372, 2013.

[38] F. L. Guljé, G. M. Raghoebar, A. Vissink, and H. J. Meijer, "Single crowns in the resorbed posterior maxilla supported by either 6-mm implants or by 11-mm implants combined with sinus floor elevation surgery: a 1-year randomised controlled trial," *European Journal of Oral Implantology*, vol. 7, pp. 247–255, 2014.

[39] D. S. Thoma, R. Haas, M. Tutak, A. Garcia, G. P. Schincaglia, and C. H. F. Hämmerle, "Randomized controlled multicentre study comparing short dental implants (6 mm) versus longer dental implants (11–15 mm) in combination with sinus floor elevation procedures. Part 1: demographics and patient-reported outcomes at 1 year of loading," *Journal of Clinical Periodontology*, vol. 42, no. 1, pp. 72–80, 2015.

[40] J. Hadzik, U. Botzenhart, M. Krawiec et al., "Comparative evaluation of the effectiveness of the implantation in the lateral part of the mandible between short tissue level (TE) and bone level (BL) implant systems," *Annals of Anatomy - Anatomischer Anzeiger*, vol. 213, pp. 78–82, 2017.

[41] M. Esposito, C. Barausse, R. Pistilli, G. Sammartino, G. Grandi, and P. Felice, "Short implants versus bone augmentation for placing longer implants in atrophic maxillae: One-year post-loading results of a pilot randomised controlled trial," *European Journal of Oral Implantology*, vol. 8, no. 3, pp. 257–268, 2015.

[42] P. Maló, M. A. de Araújo Nobre, A. V. Lopes, and R. Rodrigues, "Immediate loading short implants inserted on low bone quantity for the rehabilitation of the edentulous maxilla using an All-on-4 design," *Journal of Oral Rehabilitation*, vol. 42, no. 8, pp. 615–623, 2015.

Research Article

Biomimetic Implant Surface Functionalization with Liquid L-PRF Products: In Vitro Study

Marco Lollobrigida (iD),[1] **Manuela Maritato,**[2] **Giuseppina Bozzuto,**[3] **Giuseppe Formisano,**[3] **Agnese Molinari,**[3] **and Alberto De Biase** (iD)[1]

[1]*Department of Oral and Maxillofacial Sciences, Sapienza University of Rome, Rome, Italy*
[2]*Private Practice, Rome, Italy*
[3]*National Centre of Drug Research and Evaluation, Istituto Superiore di Sanità, Rome, Italy*

Correspondence should be addressed to Marco Lollobrigida; marcolollobrigida@virgilio.it

Objective. Platelet-rich fibrin (PRF) clots and membranes are autologous blood concentrates widely used in oral surgical procedures; less is known, however, about the liquid formulations of such products. The aim of this in vitro study is to assess the behavior of different implant surfaces when in contact with two liquid leucocyte- and platelet-rich fibrin (L-PRF) products. *Methods*. Six commercial pure titanium discs, of 9.5 mm diameter and 1.5 mm thickness, were used. Three of these samples had a micro/nano-rough surface; three were machined. Three different protocols were tested. Protocols involved the immersion of the samples in (1) a platelets, lymphocytes, and fibrinogen liquid concentrate (PLyF) for 10 minutes, (2) an exudate obtained from L-PRF clots rich in fibronectin and vitronectin for 5 minutes, and (3) the fibronectin/vitronectin exudate for 2 minutes followed by immersion in the PLyF concentrate for further 8 minutes. After these treatments, the samples were fixed and observed using a scanning electron microscope (SEM). *Results*. Under microscopic observation, (1) the samples treated with the PLyF concentrate revealed a dense fibrin network in direct contact with the implant surface and a significant number of formed elements of blood; (2) in the samples treated with the fibronectin/vitronectin exudates, only a small number of white and red blood cells were detectable; and (3) in samples exposed to the combined treatment, there was an apparent increase in the thickness of the fibrin layer. When compared to the machined surface, the micro/nano-rough samples showed an overall increased retention of fibrin, leading to a thicker coating. *Conclusions*. Liquid L-PRF products promote the formation of a dense fibrin clot on micro/nano-rough implant surfaces in vitro. The adjunctive treatment of surfaces with the fibronectin/vitronectin exudate could provide support to contact of the fibrin with the surface, though it is not essential for the clot formation. Further studies are necessary to better elucidate the properties and benefits of liquid L-PRF products.

1. Introduction

Implant supported oral rehabilitation has increasingly improved the treatment options for edentulous patients, reporting high long-term survival and success rates [1, 2]. However some clinical conditions can affect osseointegration, significantly reducing the success rate of dental implants. An increased rate of implant loss has been reported in irradiated patients [3], in patients receiving bisphosphonates [4], and in individuals with severe periodontal disease [5]. In these patients, implant failures can occur at an early stage of

peri-implant bone healing, thus suggesting a role for local factors. One fundamental phase of the healing process is the formation of a stable fibrin clot in contact with the implant surface to provide a provisional scaffold for the migration of differentiating osteogenic cells towards the implant surface [6]. This has led to the development of surfaces with specific micro- and nanotopographies and biomimetic characteristics to promote fibrin adhesion and improve osseointegration. If, on the one hand, dental implants with surface micro-topography have become a standard of care, on the other very few brands commercially offer micro-nano-textured surfaces,

whilst biomimetic approaches for implant functionalization are still not available for clinical use. These treatments generally involve immobilization of specific peptides on the implant surface during the production process. Another possible approach involves functionalizing the implant surface with the patient's autologous blood immediately before placement.

Today, platelet concentrates include several biologic products, commonly referred to as platelet-rich plasma (PRP) and platelet-rich fibrin (PRF), used to facilitate and promote wound healing. Specific formulations also include leucocyte- and platelet-rich fibrin (L-PRF) products [7]. Platelet concentrates are obtained through the centrifugation of a whole blood sample, discarding red blood cells and concentrating the components of use for therapeutic purposes, that is, fibrinogen, fibrin, platelets, growth factors, leukocytes, and other circulating cells [8, 9]. By pressing the fibrin clots obtained through the centrifugation, an exudate is formed which is rich in growth factors and serum proteins, including fibronectin and vitronectin [10]. These play an important role in cell adhesion and migration into the fibrin clot [11]. Liquid concentrates rich in platelets, lymphocytes, plasma proteins, and fibrinogen can also be obtained by shorter blood centrifugation. This plasma fibrinogen concentrate can be collected before coagulation and used for local delivery of growth factors similarly to the clots. Compared to PRF clots however, less is known as to the properties and the potential applications of liquid PRF products.

Although platelet concentrates are widely used in bone regeneration procedures, their role in relation to implant osseointegration remains poorly investigated. The purpose of this in vitro study was thus to evaluate the effects of treating rough and smooth implant surfaces with two liquid leucocyte- and platelet-rich fibrin (L-PRF) products.

2. Materials and Methods

2.1. Liquid Platelet Concentrate and Exudate Preparation. Blood samples (9 cc each) were collected in 6 red cap vacuum tubes (IntraSpin™, Intra-Lock International, Boca Raton, FL) to obtain the L-PRF clots and two white cap vacuum tubes (IntraSpin, Intra-Lock International, Boca Raton, FL) to produce the liquid concentrate. The total of 8 test tubes was then placed within the centrifuge (IntraSpin, Intra-Lock International, Boca Raton, FL) at opposing positions to balance the rotor (Figure 1(a)). After 3 minutes of centrifugation at 2700 rpm, the process was stopped and the 2 white tubes were removed, and the centrifuge restarted for a remaining period of 9 minutes. 3 cc of liquid (PLyF concentrate) was taken from the top of test tubes with the white caps (Figure 1(b)). After a total of 12 (3 + 9) minutes of centrifugation at 2700 rpm, the L-PRF clots were removed from the test tubes. The red layer containing the red blood cells was gently separated using a sterile instrument. The clots were then placed on a sterile metal grid and compressed under the weight of a sterile metal plate (Figure 1(c)), without applying any manual pressure (Xpression™ Kit, Intra-Lock International, Boca Raton, FL). After 5 minutes the L-PRF membranes were formed and the expressed exudate rich in

fibronectin and vitronectin was collected at the base of the metal box (Figure 1(d)).

2.2. Treatment of Titanium Discs. Twelve sterile commercial pure titanium discs (ASTM Grade 4) of 9.5 mm diameter and 1.5 mm thickness were used for this study. Six discs had a rough fractal nanosurface (Ossean® surface, Intra-Lock International, Boca Raton, FL, USA) and six a machined surface. The discs were then divided into three separate groups using a multiwell cell culture plate: four discs, two machined and two rough (P_R and P_L), were immersed in the PLyF concentrate for 10 minutes; four discs, two machined and two rough (E_R and E_L), were immersed in the fibronectin and vitronectin exudate for 5 minutes; four discs, two machined and two rough (EP_R and EP_L), were first immersed in the fibronectin and vitronectin exudate for 2 minutes and then in the PLyF liquid for 8 minutes. The samples were then fixed with 2% glutaraldehyde in 0.1 M cacodylate buffer (pH 7.4) and successively analyzed using a field emission gun scanning electron microscope (FEG-SEM) (Inspect FTM, FEI Company, Hillsboro, OR, USA) at different magnifications and an acceleration voltage of 10 kV.

3. Results

On microscopic analysis, the P_R samples revealed a high-density, small-meshed fibrin network (Figures 2(a)–2(d)). A significant number of red blood cells, white blood cells, and platelets were also observed, both in contact with the disc surface and within the fibrin network. The fibrin clot was of variable thickness and direct contact between the fibrin network and the implant surface could be observed. Partial detachment of the fibrin from the titanium surface was also noted in some areas of the sample.

In samples P_L a wide-meshed fibrin network was observed (Figures 2(e)–2(h)). As compared to P_R, the fibrin layer had a reduced thickness with few contact points between the fibrin and the implant surface. Similarly to P_R samples, a number of blood cells and platelets were trapped in the fibrin network.

In samples E_R (Figures 3(a)–3(d)) and E_L (Figures 3(e)–3(h)) no significant biologic process could be observed. Few white and red blood cells could be identified in contact with surface irregularities.

Similarly to what was observed in the P_R samples, a dense, small-meshed fibrin layer had formed on the EP_R discs (Figures 4(a)–4(d)). Compared to P_R, a greater quantity of fibrin had formed and a relatively higher number of formed blood elements were also detected within the fibrin clot. Several areas showed partial or total detachment of the fibrin layer from the surface, probably occurring during the fixation process.

Finally, the EP_L samples were covered with a wide-meshed fibrin network with several formed blood elements (Figures 4(e)–4(h)). Compared to EP_R, the fibrin layer on EP_L showed a reduced thickness in all the observed areas. Similarly to P_L, few direct contacts between the fibrin network and the implant surface were identified.

(a)

(b)

(c)

(d)
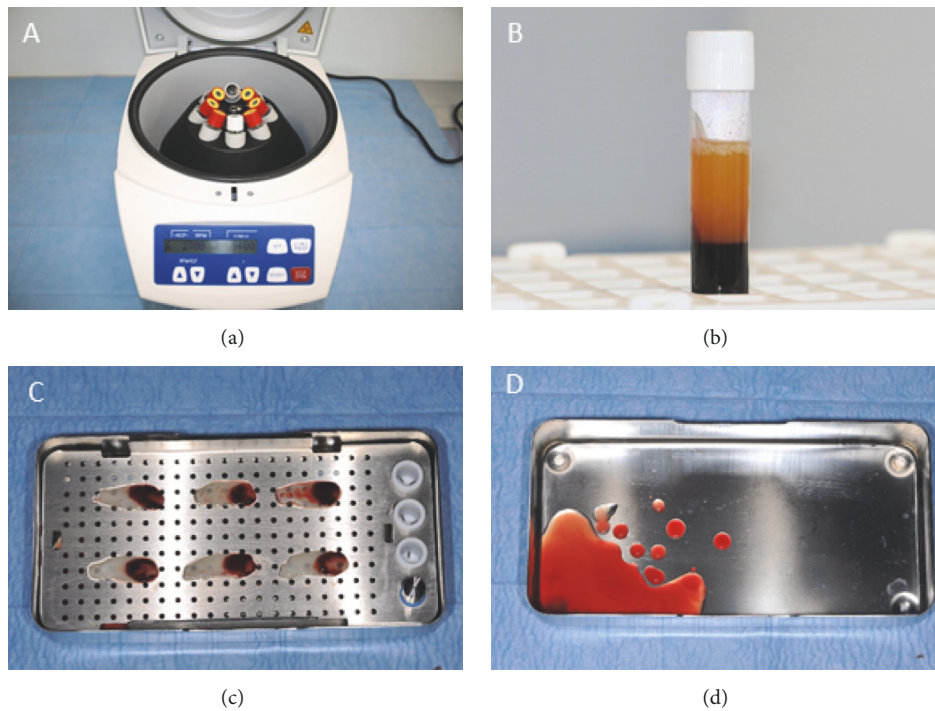
Figure 1: L-PRF products preparation. (a) The centrifuge used for the study with the vacutainer tubes in place. (b) PLyF concentrate on the top of the white vacutainer. (c) L-PRF membranes obtained after compression of the clots. (d) Exudate rich in fibronectin and vitronectin derived from membranes compression.

(a)

(b)

(c)

(d)

(e)

(f)

(g)

(h)
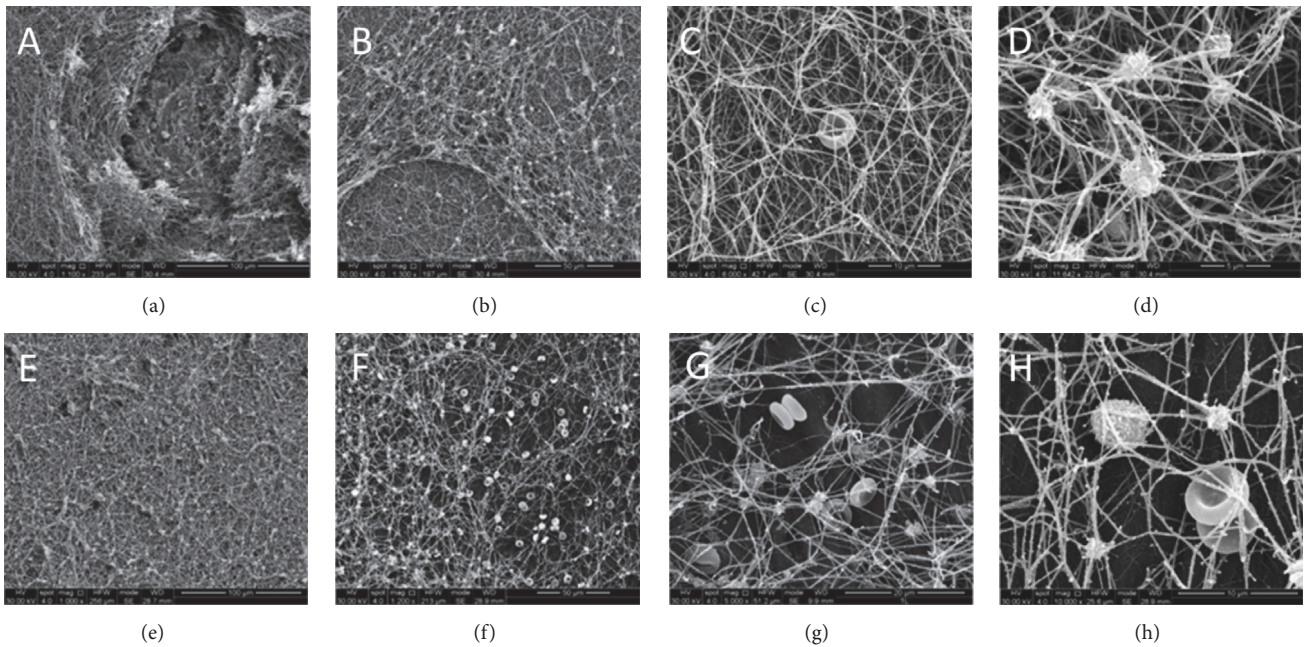
Figure 2: SEM images of titanium samples after immersion in the PLyF concentrate for 10 minutes. (a–d) Samples with rough surface (P_R). (e–h) Samples with machined surface (P_L). A dense fibrin network has formed on the surfaces with abundant thrombocytes, erythrocytes, and leukocytes.

(a)　　　　(b)　　　　(c)　　　　(d)

(e)　　　　(f)　　　　(g)　　　　(h)
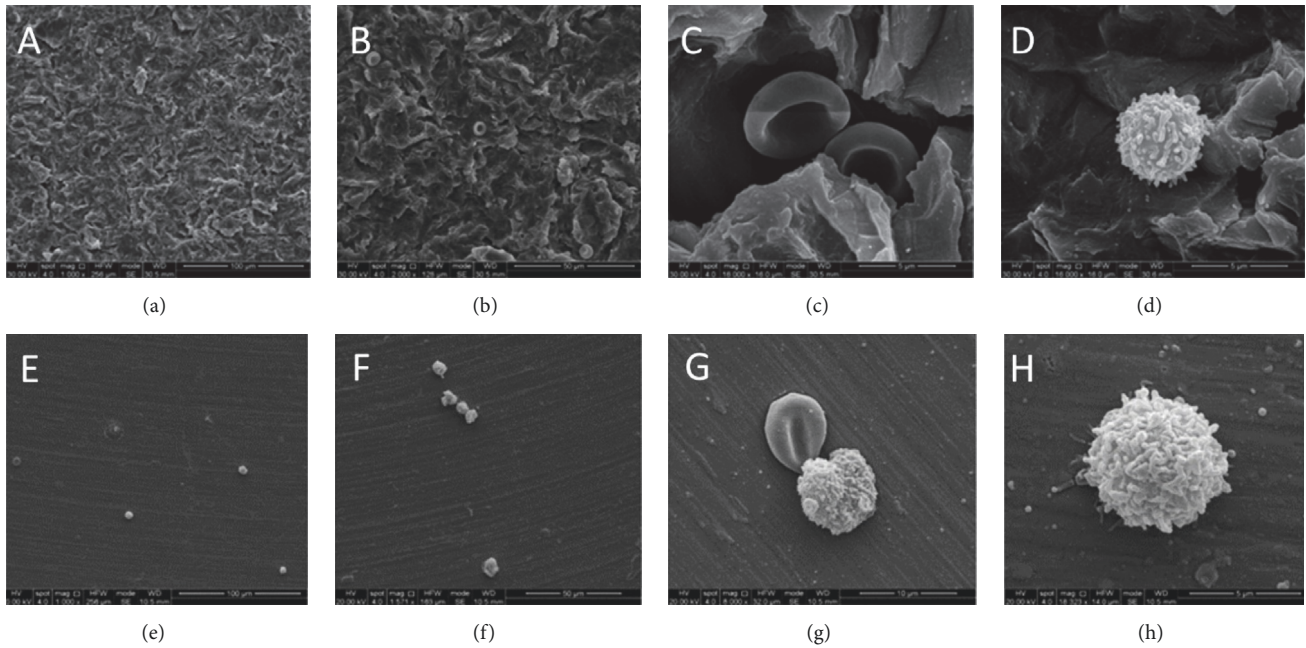
FIGURE 3: SEM images of titanium samples after immersion in the fibronectin and vitronectin exudate for 5 minutes. (a–d) Samples with rough surface (E_R). (e–h) Samples with machined surface (E_L). Scarce erythrocytes and leukocytes can be clearly detected on both the surfaces.

(a)　　　　(b)　　　　(c)　　　　(d)

(e)　　　　(f)　　　　(g)　　　　(h)
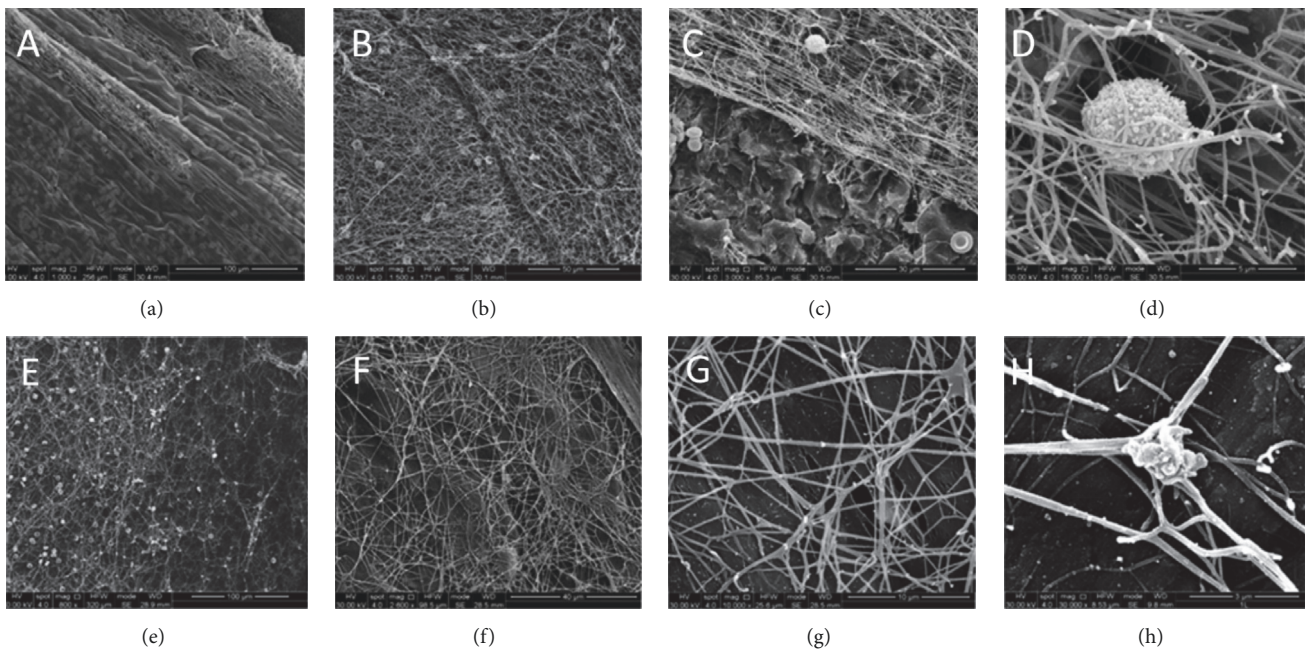
FIGURE 4: SEM images of titanium samples after immersion in the fibronectin and vitronectin exudate for 2 minutes and then in the PLyF concentrate for further 8 minutes. (a–d) Samples with rough surface (EP_R). (e–h) Samples with machined surface (EP_L). Compared to P_R and P_L samples, a major quantity of fibrin has formed on the surfaces.

4. Discussion

The results of this study have shown that the contact of a micro/nano-rough implant surface with a liquid blood concentrate allows formation of a stable fibrin layer containing platelets and leucocytes. SEM micrographs have also suggested that fibrin clot formation may be further supported by adjunctive pretreatment of samples with an exudate containing fibronectin and vitronectin.

Platelet concentrates have been used widely in several branches of medicine to improve repair of soft tissue. In recent years, particular attention has been given to the

potential for interaction between platelet concentrates and bone healing. In an experimental rat model of femoral fracture, Dülgeroglu and Metineren [12] observed increased bone formation after 28 days of healing when PRF clots were applied to bone. Similarly, Nagata et al. [13] observed significantly increased bone formation in surgically created bone defects in rat calvaria treated with a combination of autogenous bone graft and platelet-rich plasma. In 2003, Schlegel et al. [14] tested the potential of PRP in artificial peri-implant bone defects in a dog model without conclusive results. Most recent research has focused on the use of PRF to enhance bone regeneration and osseointegration. PRF has proven effective in bone regeneration of peri-implant defects in both animal [15, 16] and human clinical studies [17, 18]. In a histometric study in rabbits, Öncü et al. [19] evaluated the effect on osseointegration of placing L-PRF within implant beds and implant prewetting in L-PRF clots before placement. The authors report increases in the rate and the amount of new bone formation in the experimental group compared to the control, especially in the early healing stages. In a histologic study in dogs, Neiva et al. [20] evaluated the effects of L-PRF around immediately placed implants with two different surfaces, micro/nano-rough surface (Ossean™ surface) and dual-etched. The authors reported a significantly increased bone formation by combining Ossean surface with L-PRF concluding that micro/nano-rough surface and L-PRF have a synergistic effect on peri-implant bone healing.

In the present study a different approach has been developed, consisting in soaking the titanium samples in a liquid platelet concentrate obtained after 3 minutes of centrifugation. The theoretical advantage of liquid concentrates instead of PRF clots is that fibrin polymerization occurs in direct contact with the implant surface. As demonstrated by the SEM images, fibrin can establish numerous contacts with the implant surface, providing a biologic coating. Although various efforts are being made to improve osseointegration by mechanisms such as implant surface coating, the most important biological event is the fibrin clot formation around the implant. The quality and stability of the fibrin clot are, in fact, a prerequisite for mesenchymal stem cell migration and differentiation into the osteoblast lineage and subsequent contact osteogenesis. From this perspective, L-PRF concentrates provide all the key agents necessary for the early stages of osseointegration: fibrin, platelets (and related growth factors), and leukocytes.

Bone healing is also influenced by a number of molecules including fibronectin and vitronectin. During the early healing phase, fibronectin is incorporated into the fibrin matrix affecting distinct platelet functions (adhesion aggregation, activation), as well as cell migration into the forming provisional matrix [21, 22]. Similarly, once incorporated into the fibrin clot vitronectin supports platelet adhesion and aggregation and, at later stages, contributes to cell adhesion to the extracellular matrix [23]. Based on this, some authors have proposed fibronectin and vitronectin-coated implants to enhance osseointegration [24–26]; despite some positive results obtained in vitro, however, the complexity and cost of such surface treatments have limited their widespread use. In this study, a simpler approach, consisting in soaking the

surfaces in the L-PRF-derived products, has been adopted. In the case of the fibronectin/vitronectin exudate, protein adsorption occurs as a result of van der Waals forces or electrostatic interactions similarly to what happens in vivo. Moreover, in adjunction to the autologous origin of adsorbed molecules, the advantage of this procedure is that it is applicable during surgery [27].

The use of PRF preparations for the biomimetic coating of dental implants can promote peri-implant bone healing also through the local delivery of growth factors and proteins [28]. Various growth factors, including platelet-derived growth factor (PDGF) and transforming growth factor beta (TGF-β), are secreted by local platelet degranulation. Growth factors act as modulators of cellular activity, inducing specific responses in all phases of bone repair [29] and promoting angiogenesis [30]. From this perspective, PRF products may have an osteopromotive effect during peri-implant bone healing when associated with a nanotextured surface [31, 32]. Indeed, the specific L-PRF formulation used in this study could further support the healing process, participating in the initial inflammatory response. However the role of leukocytes contained in PRF still has to be elucidated.

Considering these properties, PRF products may find application in patients with impaired bone healing capacity, for example, those who have undergone radiation therapy. In these patients, osseointegration is negatively affected as a result of the hypocellular, hypovascular, and hypoxic tissue environment [33], with an increased risk of failure particularly in the maxilla and in grafted sites [34]. These products could also prove beneficial in immediate implant placement after extraction, to stimulate fibrin clot formation in the gap between the alveolar bone and the implant surface, in guided bone regeneration procedures with simultaneous implant placement [35], and in the regeneration of peri-implant defects [36]. However, rather than as hitherto described in the literature, this study proposes use of liquid L-PRF instead of clots in order to enhance direct contact of the fibrin layer with the implant surface, obtaining an immediate biofunctionalization of the surface.

5. Conclusion

This study represents a preliminary evaluation of surface treatment with liquid L-PRF products, with the main limitations being a small number of samples and the qualitative nature of the observations. The study results indicate that treatment of implant surfaces with liquid PRF leads to the formation of a stable and dense fibrin layer in direct contact with the implant surface, thus providing a biomimetic autologous coating. Compared to machined surfaces, the micro/nano-rough samples were found to be more retentive, leading to thicker coatings. Adjunctive treatment with the L-PRF clot exudate containing fibronectin and vitronectin seems to promote greater fibrin adhesion and formation when in combination with the liquid platelet concentrate. There is a need for additional studies to better elucidate the potential benefits of liquid PRF in enhancing osseointegration, particularly in those patients for whom implant therapies still encounter increased risk of failure.

Data Availability

All data analyzed during this study are available from the corresponding author on reasonable request.

Conflicts of Interest

The authors declare that there are no conflicts of interest regarding the publication of this article.

References

[1] V. Moraschini, L. A. D. C. Poubel, V. F. Ferreira, and E. D. S. P. Barboza, "Evaluation of survival and success rates of dental implants reported in longitudinal studies with a follow-up period of at least 10 years: a systematic review," *International Journal of Oral and Maxillofacial Surgery*, vol. 44, no. 3, pp. 377–388, 2015.

[2] P. Simonis, T. Dufour, and H. Tenenbaum, "Long-term implant survival and success: a 10-16-year follow-up of non-submerged dental implants," *Clinical Oral Implants Research*, vol. 21, no. 7, pp. 772–777, 2010.

[3] L. Chambrone, J. Mandia, J. A. Shibli, G. A. Romito, and M. Abrahao, "Dental implants installed in irradiated jaws: A systematic review," *Journal of Dental Research*, vol. 92, no. 12, 2013.

[4] N.-R. de-Freitas, L.-B. Lima, M.-B. de-Moura, C.-D. Veloso-Guedes, P.-C. Simamoto-Júnior, and D. de-Magalhães, "Bisphosphonate treatment and dental implants: A systematic review," *Medicina Oral Patología Oral y Cirugía Bucal*, vol. 21, no. 5, Article ID 20920, pp. e644–e651, 2016.

[5] M. V. Olmedo-Gaya, F. J. Manzano-Moreno, E. Cañaveral-Cavero, J. De Dios Luna-Del Castillo, and M. Vallecillo-Capilla, "Risk factors associated with early implant failure: A 5-year retrospective clinical study," *Journal of Prosthetic Dentistry*, vol. 115, no. 2, pp. 150–155, 2016.

[6] J. E. Davies, "Understanding peri-implant endosseous healing," *Journal of Dental Education*, vol. 67, no. 8, pp. 932–949, 2003.

[7] D. M. Dohan Ehrenfest, L. Rasmusson, and T. Albrektsson, "Classification of platelet concentrates: from pure platelet-rich plasma (P-PRP) to leucocyte- and platelet-rich fibrin (L-PRF)," *Trends in Biotechnology*, vol. 27, no. 3, pp. 158–167, 2009.

[8] T. Bielecki and D. M. Dohan Ehrenfest, "Platelet-Rich Plasma (PRP) and Platelet-Rich Fibrin (PRF): surgical adjuvants, preparations for in situ regenerative medicine and tools for tissue engineering," *Current Pharmaceutical Biotechnology*, vol. 13, no. 7, pp. 1121–1130, 2012.

[9] D. M. Dohan Ehrenfest, I. Andia, M. A. Zumstein, C.-Q. Zhang, N. R. Pinto, and T. Bielecki, "Classification of platelet concentrates (Platelet-Rich Plasma-PRP, Platelet-Rich Fibrin-PRF) for topical and infiltrative use in orthopedic and sports medicine: current consensus, clinical implications and perspectives," *Muscle, Ligaments and Tendons Journal*, vol. 4, no. 1, pp. 3–9, 2014.

[10] D. M. D. Ehrenfest, "How to optimize the preparation of leukocyte- and platelet-rich fibrin (L-PRF, Choukroun's technique) clots and membranes: introducing the PRF Box," *Oral Surgery, Oral Medicine, Oral Pathology, Oral Radiology, and Endodontology*, vol. 110, no. 3, pp. 275–278, 2010.

[11] R. Pankov and K. M. Yamada, "Fibronectin at a glance," *Journal of Cell Science*, vol. 115, no. 20, pp. 3861–3863, 2002.

[12] T. C. Dülgeroglu and H. Metineren, "Evaluation of the effect of platelet-rich fibrin on long bone healing: An experimental rat model," *Orthopedics*, vol. 40, no. 3, pp. e479–e484, 2017.

[13] M. J. H. Nagata, M. Messora, N. Pola et al., "Influence of the ratio of particulate autogenous bone graft/platelet-rich plasma on bone healing in critical-size defects: a histologic and histometric study in rat calvaria," *Journal of Orthopaedic Research*, vol. 28, no. 4, pp. 468–473, 2010.

[14] K. A. Schlegel, F. R. Kloss, P. Kessler, S. Schultze-Mosgau, E. Nkenke, and J. Wiltfang, "Bone conditioning to enhance implant osseointegration: An experimental study in pigs," *The International Journal of Oral & Maxillofacial Implants*, vol. 18, no. 4, pp. 505–511, 2003.

[15] K.-I. Jeong, S.-G. Kim, J.-S. Oh et al., "Effect of platelet-rich plasma and platelet-rich fibrin on peri-implant bone defects in dogs," *Journal of Biomedical Nanotechnology*, vol. 9, no. 3, pp. 535–537, 2013.

[16] E.-S. Jang, J.-W. Park, H. Kweon et al., "Restoration of peri-implant defects in immediate implant installations by Choukroun platelet-rich fibrin and silk fibroin powder combination graft," *Oral Surgery, Oral Medicine, Oral Pathology, Oral Radiology, and Endodontology*, vol. 109, no. 6, pp. 831–836, 2010.

[17] A. Simonpieri, J. Choukroun, M. D. Corso, G. Sammartino, and D. M. D. Ehrenfest, "Simultaneous sinus-lift and implantation using microthreaded implants and leukocyte- and platelet-rich fibrin as sole grafting material: a six-year experience," *Implant Dentistry*, vol. 20, no. 1, pp. 2–12, 2011.

[18] B. Hamzacebi, B. Oduncuoglu, and E. E. Alaaddinoglu, "Treatment of peri-implant bone defects with platelet-rich fibrin," *International Journal of Periodontics and Restorative Dentistry*, vol. 35, no. 3, pp. 415–422, 2015.

[19] E. Öncü, B. Bayram, A. Kantarcı, S. Gülsever, and E.-E. Alaaddinoğlu, "Posıtıve effect of platelet rich fibrin on osseointegration," *Medicina Oral Patología Oral y Cirugía Bucal*, vol. 21, no. 5, Article ID 21026, pp. e601–e607, 2016.

[20] R. F. Neiva, L. F. Gil, N. Tovar et al., "The synergistic effect of leukocyte platelet-rich fibrin and micrometer/nanometer surface texturing on bone healing around immediately placed implants: An experimental study in dogs," *BioMed Research International*, vol. 2016, Article ID 9507342, 2016.

[21] W. S. To and K. S. Midwood, "Plasma and cellular fibronectin: Distinct and independent functions during tissue repair," *Fibrogenesis & Tissue Repair*, vol. 4, no. 1, article no. 21, 2011.

[22] E. A. Lenselink, "Role of fibronectin in normal wound healing," *International Wound Journal*, vol. 12, no. 3, pp. 313–316, 2015.

[23] Y.-P. Wu, H. J. Bloemendal, E. E. Voest et al., "Fibrin-incorporated vitronectin is involved in platelet adhesion and thrombus formation through homotypic interactions with platelet-associated vitronectin," *Blood*, vol. 104, no. 4, pp. 1034–1041, 2004.

[24] S. Kim, W. C. Myung, J. S. Lee et al., "The effect of fibronectin-coated implant on canine osseointegration," *Journal of Periodontal & Implant Science*, vol. 41, no. 5, pp. 242–247, 2011.

[25] T. A. Petrie, C. D. Reyes, K. L. Burns, and A. J. García, "Simple application of fibronectin-mimetic coating enhances osseointegration of titanium implants," *Journal of Cellular and Molecular Medicine*, vol. 13, no. 8B, pp. 2602–2612, 2009.

[26] A. Cacchioli, F. Ravanetti, A. Bagno, M. Dettin, and C. Gabbi, "Human vitronectin-derived peptide covalently grafted onto titanium surface improves osteogenic activity: A pilot in vivo study on rabbits," *Tissue Engineering Part: A*, vol. 15, no. 10, pp. 2917–2926, 2009.

[27] R. Tejero, E. Anitua, and G. Orive, "Toward the biomimetic implant surface: biopolymers on titanium-based implants for bone regeneration," *Progress in Polymer Science*, vol. 39, no. 7, pp. 1406–1447, 2014.

[28] D. M. Dohan Ehrenfest, T. Bielecki, R. Jimbo et al., "Do the fibrin architecture and leukocyte content influence the growth factor release of platelet concentrates? An evidence-based answer comparing a pure Platelet-Rich Plasma (P-PRP) gel and a leukocyte- and Platelet-Rich Fibrin (L-PRF)," *Current Pharmaceutical Biotechnology*, vol. 13, no. 7, pp. 1145–1152, 2012.

[29] V. Devescovi, E. Leonardi, G. Ciapetti, and E. Cenni, "Growth factors in bone repair," *La Chirurgia degli Organi di Movimento*, vol. 92, no. 3, pp. 161–168, 2008.

[30] M. S. Gaston and A. H. R. W. Simpson, "Inhibition of fracture healing," *Journal of Bone and Joint Surgery Series: B*, vol. 89, no. 12, pp. 1553–1560, 2007.

[31] W. F. Zambuzzi, E. A. Bonfante, R. Jimbo et al., "Nanometer scale titanium surface texturing are detected by signaling pathways involving transient FAK and Src activations," *PLoS ONE*, vol. 9, no. 7, Article ID e95662, 2014.

[32] C. Marin, R. Granato, M. Suzuki, J. N. Gil, A. Piattelli, and P. G. Coelho, "Removal torque and histomorphometric evaluation of bioceramic grit-blasted/acid-etched and dual acid-etched implant surfaces: an experimental study in dogs," *Journal of Periodontology*, vol. 79, no. 10, pp. 1942–1949, 2008.

[33] R. E. Marx and R. P. Johnson, "Studies in the radiobiology of osteoradionecrosis and their clinical significance," *Oral Surgery, Oral Medicine, Oral Pathology, Oral Radiology, and Endodontology*, vol. 64, no. 4, pp. 379–390, 1987.

[34] N. Nooh, "Dental implant survival in irradiated oral cancer patients: a systematic review of the literature," *The International Journal of Oral & Maxillofacial Implants*, vol. 28, no. 5, pp. 1233–1242, 2013.

[35] R. J. Miron, G. Zucchelli, M. A. Pikos et al., "Use of platelet-rich fibrin in regenerative dentistry: a systematic review," *Clinical Oral Investigations*, vol. 21, no. 6, pp. 1913–1927, 2017.

[36] D. P. S Patil, D. M. Bhongade, D. P. Dhadse, and D. P. Bajaj, "Management of Peri-Implantitis with PRF as a Sole Grafting Material: A Case Report," *Scholars Journal of Dental Sciences*, vol. 3, no. 7, pp. 204–206, 2016.

Research Article

Effect of Hypoxia-Inducible Factor 1α on Early Healing in Extraction Sockets

Hyun-Chang Lim (ID),[1] **Daniel S. Thoma,**[1] **Mijeong Jeon,**[2] **Je-Seon Song** (ID),[2]
Sang-Kyou Lee,[3] **and Ui-Won Jung** (ID)[4]

[1]*Clinic for Fixed and Removable Prosthodontics and Dental Material Science, University of Zurich, Zurich, Switzerland*
[2]*Department of Pediatric Dentistry, Oral Science Research Center, College of Dentistry, Yonsei University, Seoul, Republic of Korea*
[3]*Department of Biotechnology, College of Life Science and Biotechnology, Yonsei University, Seoul, Republic of Korea*
[4]*Department of Periodontology, Research Institute for Periodontal Regeneration, College of Dentistry,*
 Yonsei University, Seoul, Republic of Korea

Correspondence should be addressed to Ui-Won Jung; drjew@yuhs.ac

The aim of the present study was to investigate the effect of hypoxia-inducible factor 1α (HIF1A) on the early healing (4 weeks) of extraction sockets exhibiting partial loss of the labial bone. Two extraction sockets of the maxillary incisors from each of six dogs were assigned to two treatment modalities: deproteinized bovine bone mineral (i) with 10% collagen (DBBM-C) soaked with HIF1A and covered by a collagen membrane (CM) (HIF group) or (ii) treated with DBBM-C only and covered by a CM (control group). Microcomputed tomography revealed some degree of collapse of the labial contour. The totally augmented volume and new bone volume did not differ significantly between two groups ($P > 0.05$). The histological analysis revealed that the apical area of the socket was mostly filled with newly formed bone, while there was less newly formed bone in the coronal area and incomplete cortex formation. The histomorphometric analysis revealed that the area of newly formed bone was significantly larger in the HIF group than the control group (12.16 ± 3.04 versus 9.48 ± 2.01 mm^2, $P < 0.05$), while there was no significant intergroup difference in the total augmented area. In conclusion, even though DBBM-C soaked with HIF1A enhanced histomorphometric bone formation, this intervention did not demonstrate superiority in preventing ridge shrinkage compared to DBBM-C alone. Clinical relevance of these findings should be further studied.

1. Introduction

The interest in counteracting ridge shrinkage has increased in recent years [1], which has led to detailed investigations of so-called alveolar ridge preservation (ARP) using a variety of protocols and biomaterials [2]. A gold standard has yet to be established, even though many preclinical and clinical studies have demonstrated that ARP reduces ridge shrinkage compared to a naturally healed socket [1].

Previous clinical studies regarding ARP have generally used a healing period after ARP of more than 3 months before implant placement [3]. Although such period was used to ensure maturation of newly formed hard tissue, ARP may delay the overall treatment time [4]. A systematic review also suggested that ARP procedures might not be able to accelerate or keep up with natural healing [3].

Another criticism of ARP is the possibility of further augmentation at the time of implant placement [1], which is mainly due to ARP not completely preventing ridge shrinkage. Moreover, most clinical studies have targeted sockets with minimal destruction, with even further augmentation sometimes being reported [5]. It is reasonable to suspect that further augmentation is more likely for damaged sockets.

Enhancers for bone formation may be required in practical applications to address the above-mentioned issues. Bone morphogenetic protein-2, platelet-derived growth factor, and enamel matrix derivative have previously been utilized [6–8], but their effects have been somewhat unclear.

The establishment of a vascular network precedes the formation of mineralized tissue. Insufficient vascularity will inevitably interrupt the nutritional and metabolic supply, leading to compromised healing [9]. Hypoxia-inducible factor 1α (HIF1A) is able to stimulate angiogenesis by activating genes encoding proangiogenic factors [10, 11] and enhance new bone formation and bone mineral density [12–14]. Such angiogenic-osteogenic coupling has been tested in bone fracture, osteoporosis, and distraction osteogenesis models [12, 13, 15–17], suggesting that HIF1A has potential in bone tissue engineering. However, to the best of the present authors' knowledge, HIF1A has yet to be investigated in the field of ARP.

Previously, Jeon et al. (2017) induced HIF1A overexpression using novel protein transduction domain (PTD; Hph-1-GAL4, ARVRRRGPRRR) and demonstrated that PTD-induced HIF1A increased angiogenesis [18]. PTD is composed of short amino acid sequences of less than 30 bp and can penetrate the plasma membrane [19, 20], and thus it has been considered effective for delivering proteins, DNA/RNA, drugs, and biological factors to target cells [21]. The osteogenic potential of HIF1A assisted by PTD could be useful for addressing the above-described long and delayed healing and probability of further augmentation.

The aim of the present study was to investigate the effect of HIF1A on healing of sockets exhibiting partial loss of the labial bone plate at the early stage in dogs.

2. Materials and Methods

2.1. Animals. Six male beagle dogs weighing 10–12 kg were used for the present study (Gukje, Pocheon, Korea). An individual cage under standard laboratory condition was allowed for each dog. Daily monitoring by a veterinarian was provided throughout the study. The protocol for the animal experiments was approved by the Institutional Animal Care and Use Committee of Yonsei Medical Center, Seoul, Korea (IACUC Approval No. 2013-0317-4).

2.2. Study Design. Bilateral maxillary incisors (teeth #102 and #202) were chosen as the recipient sites. After extracting the teeth, a bone defect was created on the labial socket wall (4 mm wide and 6 mm high). The extraction sockets were randomly assigned to the following two groups: (i) treatment with deproteinized bovine bone mineral with 10% collagen (DBBM-C; Bio-Oss® Collagen, Geistlich Pharma, Wolhusen, Switzerland) soaked with 0.2 ml of HIF1A (4 μg of HIF1A DNA was mixed with 100 μg of Hph-1-GAL4 at room temperature for 15 min, and 0.2-ml aliquots of the solutions were used) and covered by a collagen membrane (CM; Bio-Gide®, Geistlich Pharma) (HIF group) or (ii) treatment with DBBM-C soaked with saline and covered by a CM (control group).

2.3. Experimental Materials: HIF1A and Hph-1-G4D. HIF1A was generated and Hph-1-G4D (GAL4-DBD) was purified as described by [18]. In brief, *Homo sapiens* HIF1A (NCBI Reference Sequence: NM_001530.3) was amplified using the polymerase chain reaction (PCR). The PCR product was inserted into the pEGFPN1 plasmid vector (Invitrogen, Carlsbad, CA, USA) using restriction enzyme NheI (Takara Bio, Otsu, Japan) at 5′ termini and KpnI (Takara Bio) at 3′ termini of the PCR fragment. The DNA of G4D combined with Hph-1 was transformed with *Escherichia coli* BL-21 Star (DE3) pLysS (Invitrogen). The recombinant proteins were subsequently mixed with SP Sepharose Fast Flow (GE Healthcare, Milwaukee, WI, USA) and Hph-1-G4D protein was eluted. The eluted proteins were desalted using PD-10 Sephadox B-25 (Amersham Pharmacia Biotech, Piscataway, NJ, USA) with 10% glycerol phosphate-buffered saline (Sigma-Aldrich, St Louis, MO, USA).

2.4. Animal Surgery. General anesthesia was induced by a subcutaneous injection of atropine (Kwangmyung Pharmaceutical, Seoul, Korea) and an intravenous injection of xylazine (Rompun, Bayer Korea, Seoul, Korea) and Zoletil (Virbac, Carros, France). Tracheal intubation for enflurane inhalation (Gerolan, Choongwae Pharmaceutical, Seoul, Korea) was performed. Surgical sites were locally anesthetized using 2% lidocaine HCl (Huons, Seoul, Korea).

Two vertical incisions were made at the mesial line angle of the mesial tooth and distal line angle of the distal tooth, and a sulcular incision was performed. Teeth #102 and #202 were carefully extracted, and defects were created on the labial aspect of the socket using a high-speed bur. Either DBBM-C soaked with HIF1A or DBBM-C soaked with saline (depending on the group allocation) was placed to fill the labial defect and the upper portion of the socket. DBBM-C was gently packed against the lingual wall and lightly squeezed between the lateral walls of the socket. Condensation into the apical direction was minimally performed. No labial overcorrection was performed. The defect and socket entrance were then covered by a CM. Primary flap closure was obtained through a periosteal releasing incision (Figure 1).

Antibiotic (20 mg/kg cefazoline, Yuhan, Seoul, Korea) was administered intramuscularly for 3 days postoperatively. The surgical wounds were disinfected daily using chlorhexidine (Bukwang, Seoul, Korea), and the animals were fed a soft diet throughout the healing period. After 4 weeks of healing, the dogs were euthanized by an overdose injection of pentobarbital sodium (90–120 mg/kg).

2.5. Microcomputed Tomography Analysis. The block sections of the experimental sites were harvested and immersed in 5% formic acid for 14 days. A microcomputed tomography (micro-CT) scan was performed (SkyScan 1072, SkyScan, Aartselaar, Belgium) at a resolution of 35 μm (achieved using 100 kV and 100 μA), and the acquired data were reconstructed with NRecon software (version 1.6.8.0, SkyScan, Kontich, Belgium).

2.5.1. Volumetric Measurements. The binarization was conducted using the grayscale threshold values defined by ranging 115–225 for bone substitute and 69–115 for new bone. The following parameters were measured: total volume (TV) of the volume of interest, volume of newly formed bone (NV), and volume of residual bone substitute material (RV).

(a)   (b)   (c)   (d)
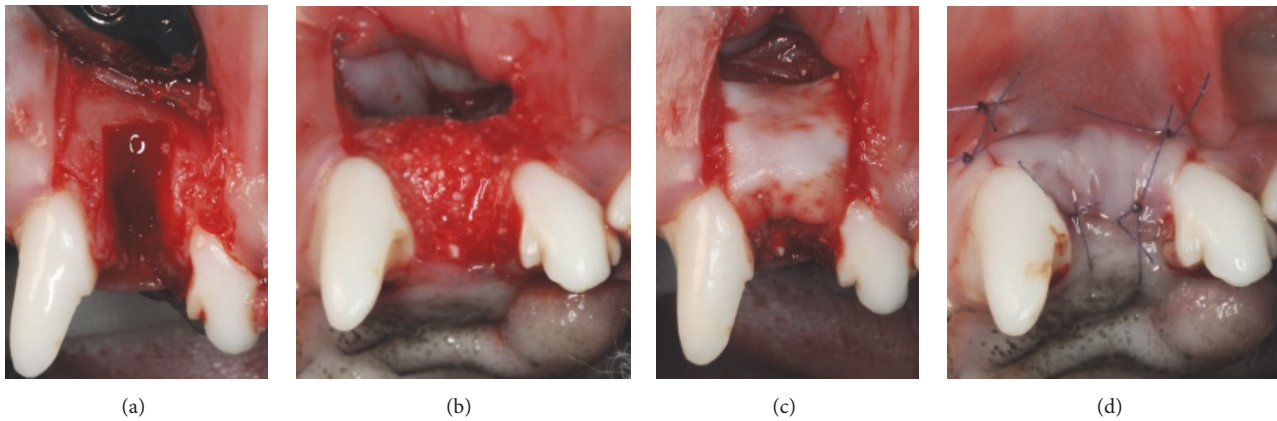
FIGURE 1: Clinical photographs of the surgical procedures. (a) Extraction and defect creation (4 mm wide and 6 mm high), (b) placement of either demineralized bovine bone mineral with 10% collagen (DBBM-C) soaked with hypoxia-inducible factor 1α (HIF1A) or DBBM-C only in the defect and the upper part of the socket, (c) coverage of the defect using a collagen membrane, and (d) primary flap closure.

(a)   (b)
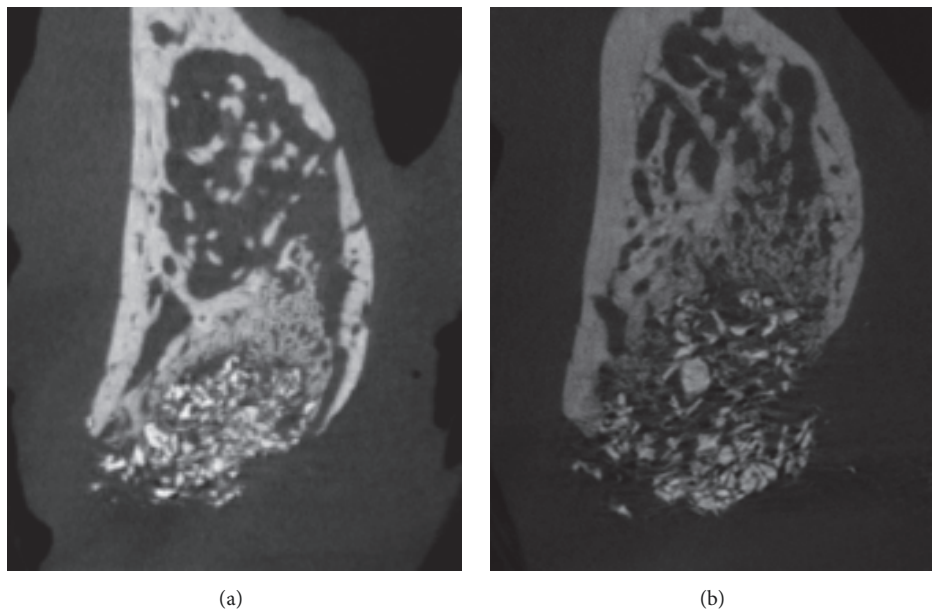
FIGURE 2: Representative microcomputed tomography (micro-CT) images: (a) control group and (b) HIF group.

2.5.2. Linear Measurements.

The linear measurements were based on the assumption that the lingual plate of the socket would exhibit minimal resorption. A vertical reference line was drawn along the long axis in the center of each recipient socket, and perpendicular lines to this vertical reference were drawn at 1, 3, and 5 mm below the lingual crest. The horizontal width was determined at each of these levels, defined as HW_1, HW_3, and HW_5.

2.6. Histological Processing and Histomorphometric Analysis.

The resected specimens were then decalcified, trimmed, and embedded in paraffin. The blocks were sectioned serially in $5\,\mu$m thickness perpendicular to the long axis of the socket. The central-most section was chosen for histological and histomorphometric analyses. Hematoxylin/eosin and Masson's trichrome staining were performed. The histological slides were scanned using digital slide scanner (Panoramic 250 Flash III, 3DHISTECH, Budapest, Hungary) and observed through CaseViewer (version 2.1, 3DHISTECH). The histomorphometric analysis was performed using CaseViewer (version 2.1, 3DHISTECH) and Photoshop CS6 (Adobe, CA, USA) by a single experienced investigator (H.C.L.) who was blinded to the group assignment.

The histomorphometric measurements were performed for both the entire augmented area and three rectangular regions of interest (ROIs) within the augmented area (each of size 2.0 mm^2) set up by dividing the entire augmented area into three equal areas, defined as the coronal$_{1/3}$, middle$_{1/3}$, and apical$_{1/3}$ areas. The following parameters were measured (Figure 2): (i) total augmented area including new bone, residual material, and nonmineralized tissue (TA), (ii) area of newly formed bone (NB), and (iii) area of residual bone

(a)

(b)

(c)
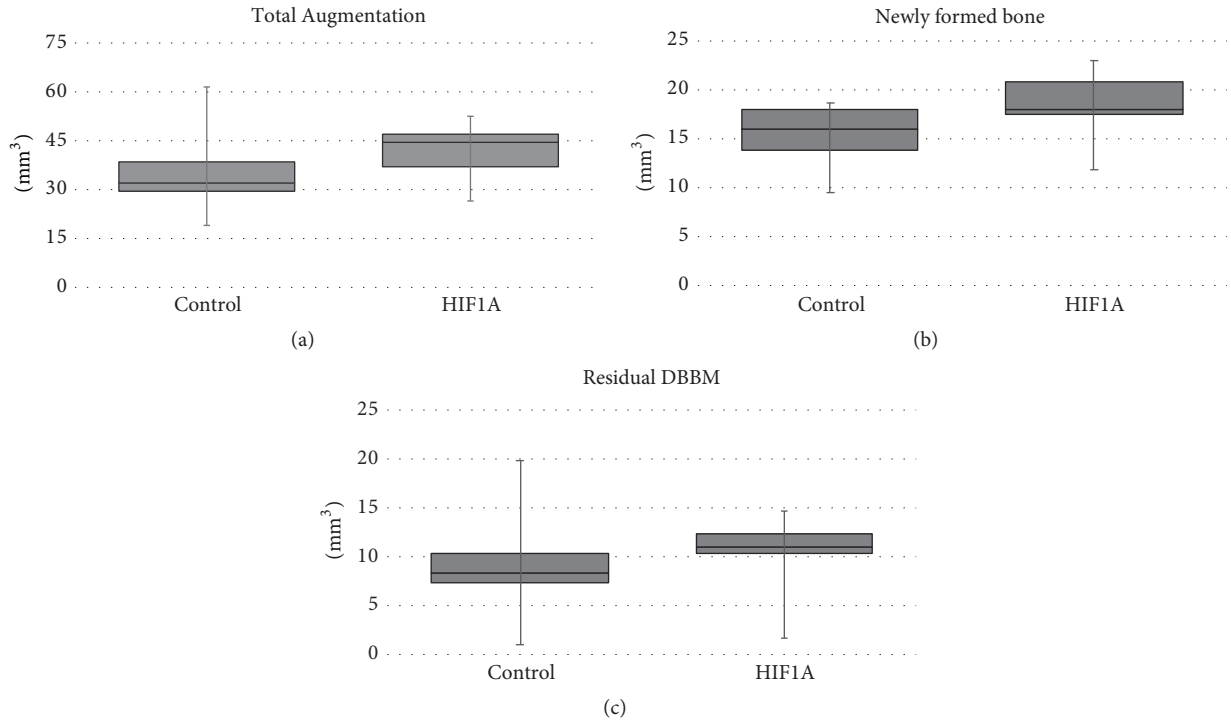
FIGURE 3: Parameters measured in the microcomputed tomography analysis: (a) total augmented volume (TV), (b) volume of newly formed bone (NV), and (c) volume of residual bone substitute material (RV). None of these parameters differed significantly between the two groups.

substitute material (RM). The number of blood vessels (BV) was measured in each ROI.

2.7. Statistics. Statistical analyses were performed using a commercially available statistical package (SPSS 21.0, SPSS, Chicago, IL, USA). Data are presented as mean ± SD values. Shapiro-Wilk tests were used to check if the data conformed to a normal distribution, and then a paired t-test or the Wilcoxon signed-ranked test was applied. The cutoff for statistical significance was set at $P < 0.05$.

3. Results

3.1. Clinical Findings. Clinical healing was uneventful in all experimental animals. No adverse reaction such as pus discharge or swelling was observed.

3.2. Micro-CT Analysis. The labial contour at the coronal level of the socket generally shrunk in both the HIF and control groups. This tendency became pronounced from the margin of the defect to the labial crest. DBBM particles predominated in the upper half of the socket, with a small amount of newly formed bone between these particles. Some of the DBBM particles were displaced and scattered. Fewer DBBM particles were present in the lower half of the socket, with newly formed bone mostly occupying the space. Newly formed bone could still be differentiated from the socket wall due to its low radiopacity (Figure 2).

The horizontal width did not differ significantly between the HIF and control groups at any level ($P > 0.05$): HW_1

TABLE 1: Microcomputed tomographic data.

	Control	HIF1A	P value
TV (mm^3)	35.48 ± 14.43	41.58 ± 9.34	0.300
NV (mm^3)	15.27 ± 3.47	18.29 ± 3.94	0.120
RV (mm^3)	9.17 ± 6.14	10.18 ± 4.47	0.685

Data are expressed as mean ± SD; TV, total volume of the volume of interest; NV, the volume of newly formed bone; RV, the volume of residual bone substitute material.

was 5.79 ± 0.67 versus 5.47 ± 0.54 mm, HW_2 was 6.71 ± 0.71 versus 6.70 ± 0.68 mm, and HW_3 was 7.80 ± 0.50 versus 7.97 ± 0.58 mm.

TV and NV were larger in the HIF group than the control group (41.58 ± 9.34 versus 35.48 ± 14.43 mm^3 and 18.29 ± 3.94 versus 15.27 ± 3.47 mm^3, resp.), but there was no significant intergroup difference ($P > 0.05$). RV also did not differ significantly between the HIF and control groups (10.18 ± 4.47 versus 9.17 ± 6.14 mm^3, $P > 0.05$) (Figure 3, Table 1).

3.3. Histological Observations. At the coronal level of the ridge, the labial contour generally showed shrinkage in both groups, which started from the apical margin of the dehiscence defect. In contrast, the palatal bone plate remained almost unaffected. Most of the coronal area of the sockets was filled with DBBM. Some DBBM particles placed in the outermost area of the dehiscence defect were displaced and scattered in a few specimens (Figures 4 and 5).

The pattern of new bone formation was similar in the two groups, but the amount of newly formed bone appeared to

FIGURE 4: Histological views of the control group (Masson's trichrome stain). (a) Overall view of the alveolus. (b, c, d) High-magnification images of the boxed areas in the alveolus. *Newly formed bone; black arrow, residual bone substitute material.

be greater in the HIF group. New bone formation generally appeared to start from preexisting socket walls. There were finger-shaped projections of newly formed bone from the palatal, apical, and remaining labial socket walls. In the apical area, there were few DBBM particles, with it being filled by newly formed bone with osteocytes and reversal lines. Various amounts of DBBM particles were observed in the middle and coronal areas in both groups, but there appeared to be more particles in the control group. Newly formed bone and provisional matrix were observed on the DBBM particles in those areas (Figures 4 and 5).

Vascular structures of varying sizes were observed throughout the socket. Some blood vessels formed around the DBBM particles, but there were very few blood vessels around the particles in the outermost coronal part of the socket.

3.4. Histomorphometric Analysis. TA did not differ significantly between the HIF and control groups (26.38 ± 3.88 versus 26.05 ± 3.21 mm^2, $P > 0.05$). NB was significantly larger in the HIF group than the control group (12.16 ± 3.04 versus 9.48 ± 2.01 mm^2, $P = 0.042$). RM was larger in the control group (3.22 ± 2.22 mm^2) than the HIF group (1.69 ± 1.55 mm^2), but there was no significant intergroup difference (Figure 6, Table 2).

TABLE 2: Histomorphometric data of the entire socket.

	Control	HIF1A	P value
TA (mm^2)	26.05 ± 3.21	26.38 ± 3.88	0.886
NB (mm^2)	9.48 ± 2.01	12.16 ± 3.04	0.042
RM (mm^2)	3.22 ± 2.22	1.69 ± 1.55	0.080

Data are expressed as mean $\pm$ SD; TA, total augmented area including new bone, residual material, and nonmineralized tissue; NB, the area of newly formed bone; RM, the area of residual bone substitute material.

In all ROIs (coronal$_{1/3}$, middle$_{1/3}$, and apical$_{1/3}$ areas), NB and BV were larger in the HIF group than the control group, but there was no significant intergroup difference ($P > 0.05$). RM in all ROIs did not differ significantly between the HIF and the control group ($P > 0.05$) (Table 3).

4. Discussion

This study investigated whether or not HIF1A enhanced bone formation in extraction sockets exhibiting partial loss of the labial bone plate. Following 4 weeks of healing, it was demonstrated that (i) the histomorphometric amount of newly formed bone was significantly greater in the HIF group
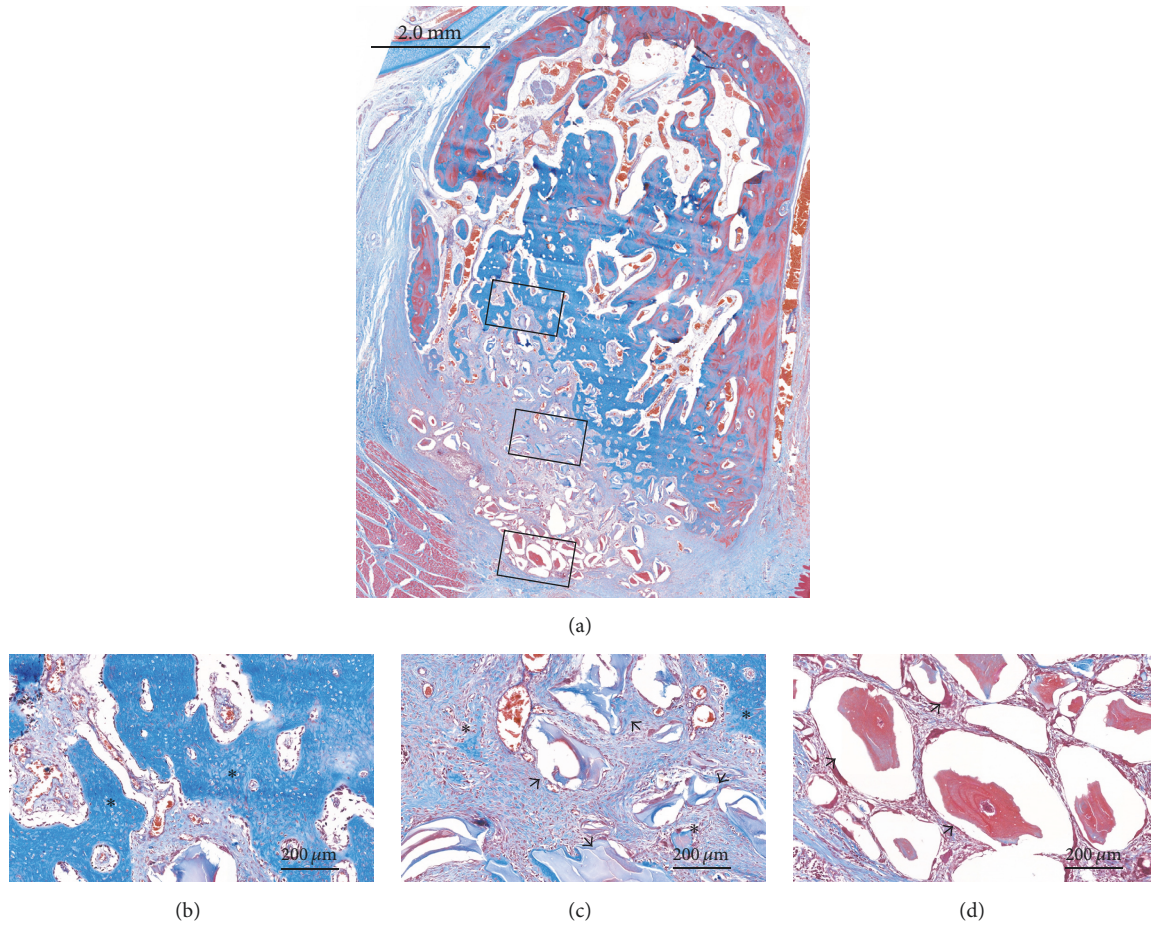
(a)

(b)

(c)

(d)
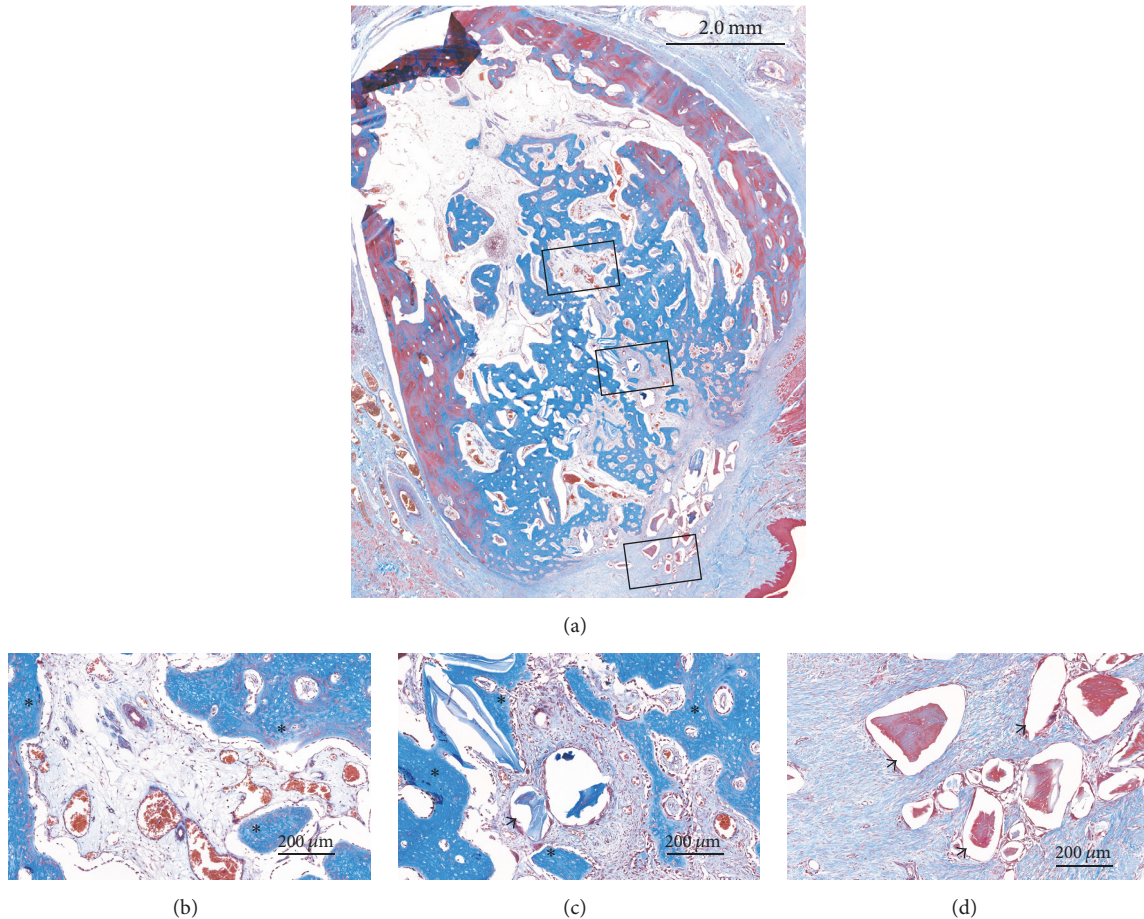
Figure 5: Histological views of the HIF group (Masson's trichrome stain). (a) Overall view of the alveolus. (b, c, d) High-magnification images of the boxed areas in the alveolus. *Newly formed bone; black arrow, residual bone substitute material.

Table 3: Histomorphometric data of the three regions of interest (ROIs) within the socket.

	Control	HIF1A	P value
NB (mm^2)			
Coronal$_{1/3}$	0.46 ± 0.50	0.67 ± 0.39	0.463
Middle$_{1/3}$	0.65 ± 0.49	1.01 ± 0.19	0.204
Apical$_{1/3}$	1.01 ± 0.42	1.08 ± 0.27	0.767
RM (mm^2)			
Coronal$_{1/3}$	0.66 ± 0.42	0.26 ± 0.31	0.141
Middle$_{1/3}$	0.33 ± 0.30	0.07 ± 0.11	0.080
Apical$_{1/3}$	0.00 ± 0.01	0.06 ± 0.14	0.655
BV (n)			
Coronal$_{1/3}$	26.17 ± 11.70	30.33 ± 10.11	0.320
Middle$_{1/3}$	28.67 ± 8.31	36.50 ± 10.09	0.108
Apical$_{1/3}$	29.00 ± 13.91	31.50 ± 16.17	0.207

Data are expressed as mean ± SD. The dimension of each ROI was 2.0 mm^2. NB, the area of newly formed bone; RM, the area of residual bone substitute material; BV, the number of blood vessels.

than the control group and (ii) the shrinkage of the labial contour was comparable in the two groups.

Many preclinical and clinical studies have investigated ARP [2, 22]. The results of previous studies appeared to be quite promising, but some disadvantages were also found, such as long healing periods after ARP and the possibility of further augmentation at the time of implant placement [4, 5]. Considering that angiogenesis always precedes osteogenesis, HIF1A might be one solution for overcoming these obstacles. Previous studies found that disruption of HIF1A in the osteoblasts led to thinner and less-vascularized bone [14] and that HIF1A injection enhanced gap healing following distraction osteogenesis [15]. These findings support angiogenic-osteogenic coupling by HIF1A. In line with those studies, the present study found greater new bone formation in the HIF group than the control group based on both histomorphometry (12.16 ± 3.04 versus 9.48 ± 2.01 mm^2) and micro-CT (18.29 ± 3.94 versus 15.27 ± 3.47 mm^3) analyses, although the difference was statistically significant only in the histomorphometric analysis.

However, irrespective of new bone formation, both groups showed shrinkage of the coronal area of the socket and with no significant difference in the resultant width. This result might be consistent with those from a previous comparison of ARP for different protocols (only DBBM, DBBM + CM, DBBM + rhBMP-2) with natural healing in sockets with the buccal bone removed [23]. Even though those authors found a significant intergroup difference in new

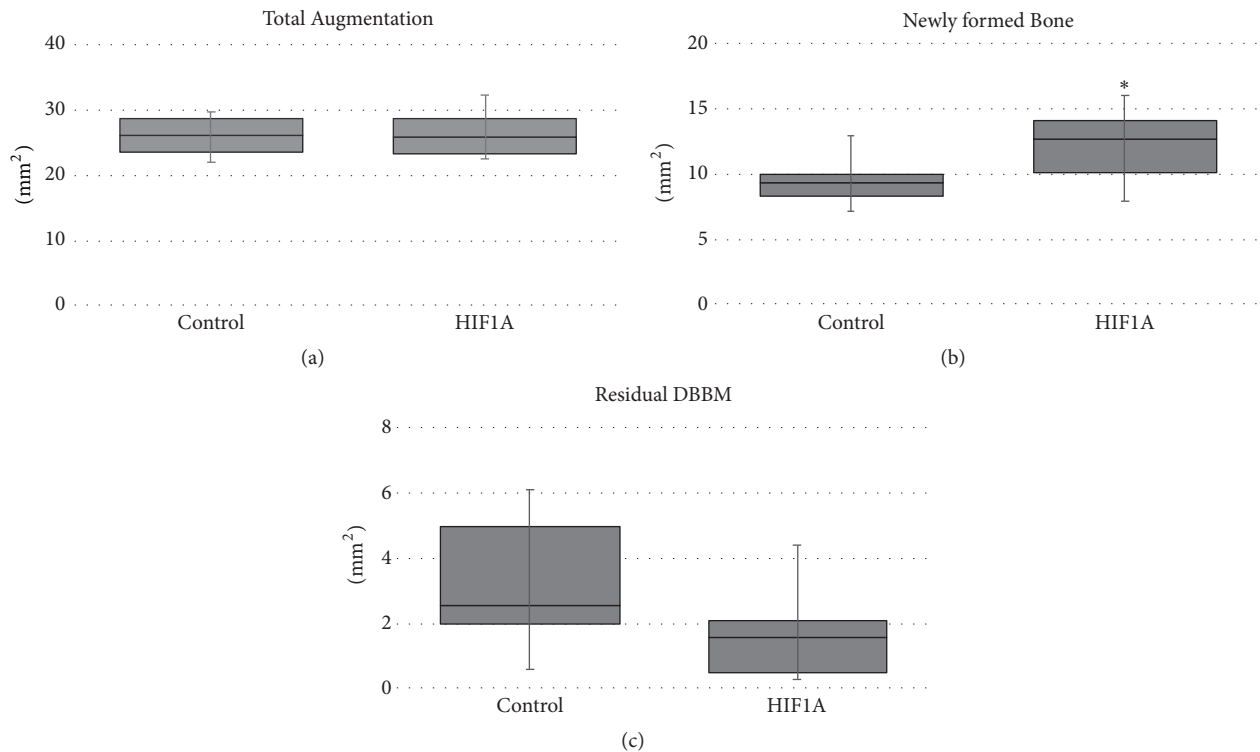FIGURE 6: Parameters measured in the histomorphometric analysis: (a) total augmented area (TA), (b) area of newly formed bone (NB), and (c) area of residual bone substitute material (RM). *Significantly different compared to the control group.

bone formation, there was no difference in ridge shrinkage (approximately 20%) in the coronal area of ARP-received sockets. The addition of a barrier membrane and enhancers might improve the healing process from a histological point of view compared to simply filling the socket with bone substitute, but the maintenance of ridge dimension might not fulfill the expectations of clinicians.

In all of the present histological specimens, no cortex formation was observed in the labial area and the outermost part of the coronal area of the socket mainly consisted of DBBM particles. This healing pattern can be compared with the findings of De Santis et al. (2011) using the same recipient sites (canine maxillary incisors) [24]. They immediately placed external-type implants in extraction socket with a dehiscence defect on the labial aspect, performed guided bone regeneration with either autogenous bone or DBBM and a CM, and histologically examined the specimens after 8 and 16 weeks of healing. Those authors found that DBBM particles were located above the new alveolar crest of the defect and were not incorporated with bone matrix after 8 weeks, but the particles became in close contact with newly formed bone after 16 weeks. It can therefore be conjectured that DBBM particles located in the outermost part of the coronal area would be incorporated into the bone volume over time. A recent preclinical study also demonstrated that the above-mentioned immature tissue was capable of being modeled into bone tissue for implant placement during the early healing period after ARP [4]. However, it is disappointing that cortex formation still requires a sufficient healing time even when HIF1A is used.

It was expected that HIF1A would increase angiogenesis in the socket. BV was slightly higher in the HIF group than the control group, but there was no significant intergroup difference. This observation might be explained by several factors. First, during the surgery, DBBM-C was stabilized by squeezing into the dehiscence defect, but some scattering and displacement of the DBBM particles were observed in the histology and micro-CT analyses. This might have been due to uncontrolled pressure from the labial side, resorption of the collagen component in the DBBM-C, and no apical securement causing micromotion in the graft, since it was demonstrated that micromotion during the early healing period could favor fibrous tissue that lacks blood vessels [25]. Second, no delivery protocol for applying HIF1A has been verified in medium-sized and large animals. Jiang et al. (2016) locally injected two different doses of HIF1A (10 and 20 μg) and saline daily into a distraction osteogenesis model in rabbit and found that the 20 μg dose led to the highest mineralization [15]. The present study is the first to utilize DBBM-C for carrying HIF1A and Hph-1-G4D, and so further investigations are required.

One of the particularly interesting findings in the present study is related to the apical healing in both groups. During the surgery, DBBM-C was placed mainly in the labial defect area and the upper portion of the socket, and so the apical area received only a small amount of DBBM-C. After 4 weeks, there was abundant bone formation in the apical area, in contrast to the middle and coronal areas where most of the DMMB-C had been placed. This is in line with previous studies showing a complete filling of woven bone

in the healing of nongrafted sockets at 4 weeks after tooth extraction [26, 27] and less woven bone formation in the socket filled with bone substitute material [28]. Clinically, these observations may question the necessity of apical filling. It has been clearly demonstrated that the most-susceptible area for ridge resorption following extraction is confined to the coronal area of the socket [29]. The area below the middle of the socket could remain stable without ARP, and so focused filling with a bone substitute material into the upper part of the socket may be feasible option for ARP.

The labial bone plates of the anterior teeth are prone to defects resulting from periodontal disease and trauma due to its natural thinness. In the present study, we therefore selected anterior teeth and tried to simulate sockets with defects by creating a dehiscence-type defect on the labial wall. Also, considering that immediate or early implant placement might be more straightforward than ARP for a socket with intact walls, the current model may be more relevant to many clinical situations. However, it should be noted that the present study used an acute type of defect, because the healing capacity differs between sockets with chronic pathologies and intact sockets [30].

The present study used both histomorphometric and micro-CT data to evaluate the effects of HIF1A. Although the general trends of newly formed bone were similar in these two types of analysis, statistically significant results were only detected in histomorphometry. The trend was somewhat opposite for residual bone substitute material. This kind of discrepancy was also previously noted [31]. Micro-CT analyses sometimes appear to be less sensitive because they require different ranges of grayscale values to be chosen for various tissues, and when a bone substitute is mixed with living bone tissue, the grayscale range for the bone substitute could overlap that for bone tissue. Care is therefore needed when interpreting the results from both types of analysis.

5. Conclusion

In conclusion, new bone formation was enhanced histomorphometrically when using DBBM-C with HIF1A compared to DBBM-C alone in sockets exhibiting partial loss of the labial bone plate. However, clinical relevance of this difference should be carefully interpreted due to small amount of difference and short healing period. Moreover, DBBM-C with HIF1A was not superior to DBBM-C alone in preventing ridge shrinkage in the coronal part of the socket.

Conflicts of Interest

The authors declare that they have no conflicts of interest.

Acknowledgments

References

[1] G. Avila-Ortiz, S. Elangovan, K. W. O. Kramer, D. Blanchette, and D. V. Dawson, "Effect of alveolar ridge preservation after tooth extraction: a systematic review and meta-analysis," *Journal of Dental Research*, vol. 93, no. 10, pp. 950–958, 2014.

[2] F. Vignoletti, P. Matesanz, D. Rodrigo, E. Figuero, C. Martin, and M. Sanz, "Surgical protocols for ridge preservation after tooth extraction. A systematic review," *Clinical Oral Implants Research*, vol. 23, no. 5, pp. 22–38, 2012.

[3] V. De Risi, M. Clementini, G. Vittorini, A. Mannocci, and M. De Sanctis, "Alveolar ridge preservation techniques: A systematic review and meta-analysis of histological and histomorphometrical data," *Clinical Oral Implants Research*, vol. 26, no. 1, pp. 50–68, 2015.

[4] D. S. Thoma, N. Naenni, G. I. Benic, F. Muñoz, C. H. F. Hämmerle, and R. E. Jung, "Effect of ridge preservation for early implant placement – is there a need to remove the biomaterial?" *Journal of Clinical Periodontology*, vol. 44, no. 5, pp. 556–565, 2017.

[5] N. Mardas, A. Trullenque-Eriksson, N. MacBeth, A. Petrie, and N. Donos, "Does ridge preservation following tooth extraction improve implant treatment outcomes: a systematic review: group 4: therapeutic concepts & methods," *Clinical Oral Implants Research*, vol. 26, no. 11, pp. 180–201, 2015.

[6] E. A. Alkan, A. Parlar, B. Yildirim, and B. Sengüven, "Histological comparison of healing following tooth extraction with ridge preservation using enamel matrix derivatives versus Bio-Oss Collagen: A pilot study," *International Journal of Oral and Maxillofacial Surgery*, vol. 42, no. 12, pp. 1522–1528, 2013.

[7] Y.-J. Kim, J.-Y. Lee, J.-E. Kim, J.-C. Park, S.-W. Shin, and K.-S. Cho, "Ridge preservation using demineralized bone matrix gel with recombinant human bone morphogenetic protein-2 after tooth extraction: A randomized controlled clinical trial," *Journal of Oral and Maxillofacial Surgery*, vol. 72, no. 7, pp. 1281–1290, 2014.

[8] B. S. McAllister, K. Haghighat, H. S. Prasad, and M. D. Rohrer, "Histologic evaluation of recombinant human platelet-derived growth factor-BB after use in extraction socket defects: a case series," *International Journal of Periodontics and Restorative Dentistry*, vol. 30, no. 4, pp. 365–373, 2010.

[9] Y. Gao, C. Li, H. Wang, and G. Fan, "Acceleration of bone-defect repair by using A-W MGC loaded with BMP2 and triple point-mutant HIF1α-expressing BMSCs," *Journal of Orthopaedic Surgery and Research*, vol. 10, no. 1, article no. 83, 2015.

[10] M. Bosch-Marce, H. Okuyama, J. B. Wesley et al., "Effects of aging and hypoxia-inducible factor-1 activity on angiogenic cell mobilization and recovery of perfusion after limb ischemia," *Circulation Research*, vol. 101, no. 12, pp. 1310–1318, 2007.

[11] M. P. Simon, R. Tournaire, and J. Pouyssegur, "The angiopoietin-2 gene of endothelial cells is up-regulated in hypoxia by a HIF binding site located in its first intron and by the central factors GATA-2 and Ets-1," *Journal of Cellular Physiology*, vol. 217, no. 3, pp. 809–818, 2008.

[12] R. Stewart, J. Goldstein, A. Eberhardt, G. T.-M. Gabriel Chu, and S. Gilbert, "Increasing vascularity to improve healing of a segmental defect of the rat femur," *Journal of Orthopaedic Trauma*, vol. 25, no. 8, pp. 472–476, 2011.

[13] C. Wan, S. R. Gilbert, Y. Wang et al., "Activation of the hypoxia-inducible factor-1alpha pathway accelerates bone regeneration," *Proceedings of the National Academy of Sciences of the United States of America*, vol. 105, no. 2, pp. 686–691, 2008.

[14] Y. Wang, C. Wan, L. Deng et al., "The hypoxia-inducible factor α pathway couples angiogenesis to osteogenesis during skeletal development," *The Journal of Clinical Investigation*, vol. 117, no. 6, pp. 1616–1626, 2007.

[15] X. Jiang, Y. Zhang, X. Fan, X. Deng, Y. Zhu, and F. Li, "The effects of hypoxia-inducible factor (HIF)-1α protein on bone regeneration during distraction osteogenesis: an animal study," *International Journal of Oral and Maxillofacial Surgery*, vol. 45, no. 2, pp. 267–272, 2016.

[16] X. Liu, Y. Tu, L. Zhang, J. Qi, T. Ma, and L. Deng, "Prolyl hydroxylase inhibitors protect from the bone loss in ovariectomy rats by increasing bone vascularity," *Cell Biochemistry and Biophysics*, vol. 69, no. 1, pp. 141–149, 2014.

[17] W. Zhang, G. Li, R. Deng, L. Deng, and S. Qiu, "New bone formation in a true bone ceramic scaffold loaded with desferrioxamine in the treatment of segmental bone defect: A preliminary study," *Journal of Orthopaedic Science*, vol. 17, no. 3, pp. 289–298, 2012.

[18] M. Jeon, Y. Shin, J. Jung et al., "HIF1A overexpression using cell-penetrating DNA-binding protein induces angiogenesis in vitro and in vivo," *Molecular and Cellular Biochemistry*, vol. 437, no. 1-2, pp. 99–107, 2017.

[19] C. de Coupade, A. Fittipaldi, V. Chagnas et al., "Novel human-derived cell-penetrating peptides for specific subcellular delivery of therapeutic biomolecules," *Biochemical Journal*, vol. 390, no. 2, pp. 407–418, 2005.

[20] M. Veldhoen, A. I. Magee, M. N. Penha-Goncalves, and B. Stockinger, "Transduction of naive CD4 T cells with kinase-deficient Lck-HIV-Tat fusion protein dampens T cell activation and provokes a switch to regulatory function," *European Journal of Immunology*, vol. 35, no. 1, pp. 207–216, 2005.

[21] C. Denicourt and S. F. Dowdy, "Protein transduction technology offers novel therapeutic approach for brain ischemia," *Trends in Pharmacological Sciences*, vol. 24, no. 5, pp. 216–218, 2003.

[22] R. E. Wang and N. P. Lang, "Ridge preservation after tooth extraction," *Clinical Oral Implants Research*, vol. 23, no. s6, pp. 147–156, 2012.

[23] J.-S. Lee, J.-S. Jung, G.-I. Im, B.-S. Kim, K.-S. Cho, and C.-S. Kim, "Ridge regeneration of damaged extraction sockets using rhBMP-2: an experimental study in canine," *Journal of Clinical Periodontology*, vol. 42, no. 7, pp. 678–687, 2015.

[24] E. De Santis, D. Botticelli, F. Pantani, F. P. Pereira, M. Beolchini, and N. P. Lang, "Bone regeneration at implants placed into extraction sockets of maxillary incisors in dogs," *Clinical Oral Implants Research*, vol. 22, no. 4, pp. 430–437, 2011.

[25] P. Aspenberg, S. Goodman, S. Toksvig-Larsen, L. Ryd, and T. Albrektsson, "Intermittent micromotion inhibits bone ingrowth. Titanium implants in rabbits," *Acta Orthopaedica*, vol. 63, no. 2, pp. 141–145, 1992.

[26] M. G. Araújo and J. Lindhe, "Dimensional ridge alterations following tooth extraction. An experimental study in the dog," *Journal of Clinical Periodontology*, vol. 32, no. 2, pp. 212–218, 2005.

[27] G. Cardaropoli, M. Araújo, and J. Lindhe, "Dynamics of bone tissue formation in tooth extraction sites: An experimental study in dogs," *Journal of Clinical Periodontology*, vol. 30, no. 9, pp. 809–818, 2003.

[28] J. Lindhe, M. G. Araújo, M. Bufler, and B. Liljenberg, "Biphasic alloplastic graft used to preserve the dimension of the edentulous ridge: An experimental study in the dog," *Clinical Oral Implants Research*, vol. 24, no. 10, pp. 1158–1163, 2013.

[29] R. E. Jung, A. Philipp, B. M. Annen et al., "Radiographic evaluation of different techniques for ridge preservation after tooth extraction: a randomized controlled clinical trial," *Journal of Clinical Periodontology*, vol. 40, no. 1, pp. 90–98, 2013.

[30] J.-H. Kim, C. Susin, J.-H. Min et al., "Extraction sockets: erratic healing impeding factors," *Journal of Clinical Periodontology*, vol. 41, no. 1, pp. 80–85, 2014.

[31] D. S. Thoma, H.-C. Lim, V. M. Sapata, S. R. Yoon, R. E. Jung, and U.-W. Jung, "Recombinant bone morphogenetic protein-2 and platelet-derived growth factor-BB for localized bone regeneration. Histologic and radiographic outcomes of a rabbit study," *Clinical Oral Implants Research*, vol. 28, no. 11, pp. e236–e243, 2017.

Research Article

Effect of Semelil, an Herbal Selenium-Based Medicine, on New Bone Formation in Calvarium of Rabbits

Amir Alireza Rasouli-Ghahroudi,[1] **Amirreza Rokn,**[1] **Mohammad Abdollahi** [ID],[2] **Fatemeh Mashhadi-Abbas,**[3] **and Siamak Yaghobee** [ID][1]

[1]*Department of Periodontics and Dental Implant Research Center, School of Dentistry, Tehran University of Medical Sciences, Tehran, Iran*
[2]*Toxicology and Disease Group, Pharmaceutical Sciences Research Center and Department of Toxicology and Pharmacology, Faculty of Pharmacy, Tehran University of Medical Sciences, Tehran, Iran*
[3]*Oral Maxillofacial Pathology Department, School of Dentistry, Shahid Beheshti University of Medical Sciences, Tehran, Iran*

Correspondence should be addressed to Siamak Yaghobee; s_yaghobee@yahoo.com

Background. This study aims to analyze the effect of Semelil, an herbal selenium-based medicine, on osteogenesis in rabbit calvarium defects. *Methods.* Four identical bony defects (8 mm) were created in the calvarium of 16 New Zealand male rabbits and filled randomly with xenogenic bone substitute material (Bio-Oss®) and semelil herbal drug (ANGIPARS™). One site was filled with Bio-Oss (B); the second site was treated with ANGIPARS (A); the third site was treated with ANGIPARS + Bio-Oss (AB); and the fourth site was left as untreated control (C) and defects were left unfilled. Rabbits were randomly divided into two groups ($n = 8$) and sacrificed at four and eight weeks. Percentage of new bone formation, type of the newly formed bone, percentage of the remaining xenograft biomaterial, and foreign body reaction (FBR) were evaluated via histological and histomorphometric analyses. *Results.* The percentage of new bone formation was significantly different among four groups. The highest effect was observed in AB, followed by A, B, and C groups, respectively. The difference in the mean percentage of new bone formation between four and eight weeks was significant for all four groups ($P < 0.001$). Regarding bone formation, the interaction effect of A and B was significant at four ($P < 0.001$) and eight weeks ($P = 0.002$). ANGIPARS alone and in presence of Bio-Oss enhanced new bone formation at both four and eight weeks ($P < 0.001$). The mean amount of new bone formation was significantly different at four and eight weeks in groups C ($P = 0.008$), A ($P < 0.001$), B ($P < 0.001$), and AB ($P = 0.003$). FBR was not observed in any group. *Conclusion.* Semelil may be useful as an adjunct to conventional osteoconductive materials in order to enhance osteogenesis.

1. Introduction

Bone graft materials have extensive clinical applications in medicine and dentistry [1]. Most manufacturers claim to produce bone grafts with suitable physical, chemical, and biological properties [2]. Clinicians have always been in search for high-standard biomaterials to achieve a regenerative and reconstructive procedure. Autogenous bone is often referred as the gold standard for regenerative and reconstructive procedures due to its optimal biological properties. Autogenous bone grafts (ABGs) may be procured from the iliac crest, mandibular symphysis, ribs, and tibia orcalvarium [3]. The

biological mechanisms involved in new bone formation at reconstructed sites include osteoinduction, osteoconduction, and osteogenesis [4, 5]. Autogenoueos bone has all of these characteristics. In most cases, all the three mechanisms are involved in the process of bone regeneration. In fact, osteogenesis does not occur completely in the absence of osteoconductive and osteoinductive mechanisms. In other words, simultaneous presence of the three following requirements is necessary to achieve osteogenesis: (A) presence of osteoblasts or cells with the potential for differentiation into bone forming cells; (B) presence of osteoinductive stimuli to initiate the differentiation of mesenchymal cells to osteoblasts; and

(C) presence of an osteoconductive environment to form a scaffold for growth and proliferation of preosteoblastic cells and their differentiation into osteoblasts for new bone formation. Autogenous bone has some disadvantages and complications specially unpredictable outcome, postoperative infection, inadequate quantity, the need for an extra donor site, patient discomfort, donor site morbidity, and graft resorption [4–6]. A biomaterial possessing the three aforementioned properties would be most ideal.

To overcome these limitations, alternative biomaterials have been developed. Bone graft materials available in the market are mostly osteoconductive rather than osteoinductive or osteogenic. To date, most previous studies conducted on bovine bone products like Bio-Oss have shown that this graft material is biocompatible and mainly osteoconductive. Bio-Oss is inorganic bovine bone mineral and is known as a gold standard bone substitute. Its organic content has been chemically removed and thus can be used in hosts after sterilization [7, 8].

Semelil (ANGIPARS) is a recently marketed herbal medicine produced from the extract of *Melilotus Officinalis* (yellow sweet clover), which belongs to the Fabaceae Legume Family. ANGIPARS has been recently introduced as an effective medicine for treatment of diabetic foot ulcer [9]. It facilitates wound healing, improves the quality of the repair tissue at the wound site, and decreases the rate of recurrence [10]. This product has minimal toxicity and not only decreases wound size but also improves microvascularization of tissues [11, 12]. It also contains variable amounts of selenium, urea, fructose, sodium phosphoglycerol, 7-hydroxycoumarine, and flavonoids, which have potent antioxidant and neuroprotective properties. Since angiogenesis is a key factor in bone formation and the main mechanism of action of ANGIPARS is via angiogenesis and increasing the tissue blood flow and oxygenation [8], we hypothesized that ANGIPARS may be able to enhance osteogenesis. Therefore, the present study was undertaken to assess the efficacy of ANGIPARS in combination with or without Bio-Oss in new bone formation at the site of bone defects in rabbit calvarium.

2. Materials and Methods

This experimental animal study was approved by the Ethics Committee of Tehran University of Medical Sciences with the code number of 91-03-69-14897. Maintenance and care of experimental animals complied with the internationally accepted guidelines for the care and use of laboratory animals. Sixteen healthy white New Zealand male rabbits with a mean weight of 2.5 kg were used. Of 16, 8 were sacrificed at four weeks and the rest at 8 weeks. The sample size was calculated according to the previous study by Rokn et al. [13] considering 80% power and 95% confidence interval (CI). Animals were kept in the animal room of the Faculty of Pharmacy in separate cages on a uniform standard feeding regimen for two weeks prior to the experiment. Semelil (ANGIPARS) was generously delivered by the ParsRoos Co. (Tehran, Iran). Bio-Oss bone substitute (0.25 mm–1 mm granules) was purchased from Geislitch Pharma AG (Wolhusen, Switzerland).

2.1. *Surgical Procedure.* Animals were anesthetized via intramuscular injection of 2% xylazine and 10% ketamine. The calvarium was scrubbed with 7% Betadine for 5 minutes and the fur on the surgical site was shaved. After preparation and draping, the area was scrubbed with 7% Betadine for 5 minutes. Using #15 scalpel, a 10 cm craniocaudal incision was made and a mucoperiosteal flap was elevated using a periosteal elevator (Figure 1(a)). To standardize the location of defects, anatomical landmarks were used, including the occipital process and the craniocaudal suture. Using a low-speed hand piece and a trephine bur with an internal diameter of 7 mm and an external diameter of 8 mm, four identical circular defects (two in the frontal and two in the parietal bone) were created in the calvarium under copious saline irrigation (Figures 1(b) and 1(c)). Three types of materials were used to fill three of the defects: (1) ANGIPARS (A), (2) Bio-Oss with a particle size of 250 to 1000 μm (B), and (3) ANGIPARS plus Bio-Oss (AB). The fourth defect was left unfilled and considered as the control. To eliminate bias in defect location, the sequence of the filling of the defects, two in frontal bone and two in parietal bone, was varied as follows. In the first rabbit, the defects were treated randomly with the three aforementioned materials and the fourth defect was left unfilled as the control. Then these positions were changed rotationally (clockwise) for the other rabbits (Figure 1(d)). All locations were recorded on charts. Following placement of the materials, the periosteum and the calvarial skin were then sutured with 4.0 vicryl (Ethicon, Somerville, NJ, USA) and 3.0 nylon (Ethicon, Somerville, NJ, USA), respectively (Figures 1(e) and 1(f)). Animals were transferred to a room with 37°C temperature for recovery and 0.1 ml of ketoprofen was administered daily for three days to control pain and swelling. 0.6 ml of enrofloxacin (Baytril, Bayer Corp., Shawnee, KS, USA) was also administered subcutaneously for 5 days. Of the 16 rabbits that were operated, eight (group 1) were sacrificed randomly after four and the remaining eight (group 2) after eight weeks by injection of 2 mL sodium thiopental into their marginal auricular venules. The calvarium was resected using a saw and fixed in 10% buffered formalin for histological analysis (Figure 1).

2.2. *Laboratory Phases.* Specimens were separately stored in 10% formalin for two weeks for complete fixation and were then immersed in 10% nitric acid solution for one week. They were evaluated daily during this time period to control decalcification. Specimens were then immersed in 20% lithium carbonate for neutralization. The defects were then sectioned from their longest diameter horizontally and coded by a three-digit code. The left digit indicated the evaluation time point (4 or 8 weeks), the middle digit indicated the respective rabbit (number 1 to 8), and the right digit indicated the respective defect [AB (ANGIPARS + Bio-Oss), A (ANGIPARS), B (Bio-Oss), and C (control)]. Paraffin embedded blocks were routinely prepared; 3 μm slices were sectioned for hematoxyline and eosin (H & E) staining and further histolgical/histomorphometric analyses.

2.3. *Histological and Histomorphometric Analyses.* Specimens were observed under a light microscope (BX-41, Olympus,
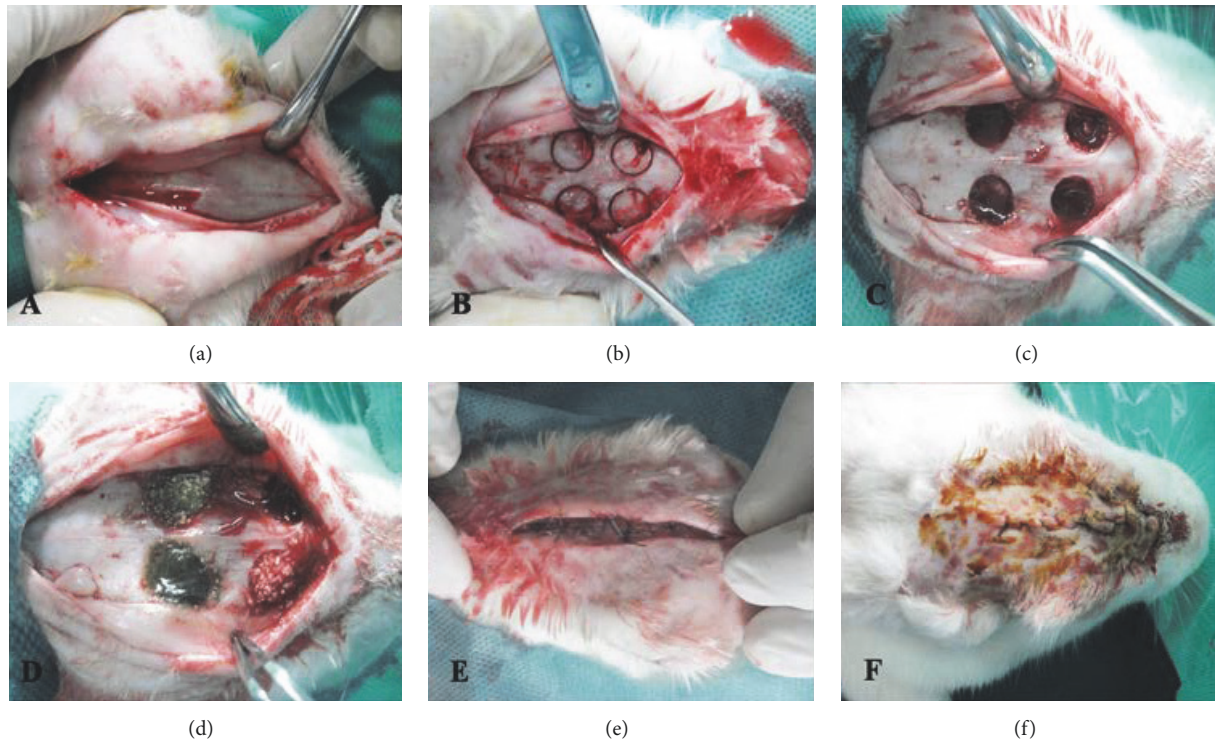
(a)   (b)   (c)

(d)   (e)   (f)

Figure 1: *Surgical Procedure*. (a) 10 cm craniocaudal incision was made and a mucoperiosteal flap was elevated (b, c). Four identical circular defects (8 mm in diameter, two in the frontal and two in the parietal bone) were created in the calvarium using a trephine bur (d). The defects were filled with ANGIPARS, ANGIPARS plus Bio-Oss, and Bio-Oss alone and the other one is left empty (e, f). The periosteum and the calvarial skin were then sutured with 4.0 vicryl (Ethicon, Somerville, NJ, USA) and 3.0 nylon (Ethicon, Somerville, NJ, USA) sutures, respectively.

Japan) by a pathologist blinded to the coding of specimens. The following parameters were evaluated in the specimens and scored.

2.3.1. Foreign Body Reaction (FBR). This phenomenon was determined based on the presence of giant cells and granulomatous reaction at ×40 magnification. Presence of FBR was categorized as follows:

    Score 0: 0 foci

    Score 1: 0–10 foci

    Score 2: 10–20 foci

    Score 3: More than 20 foci

2.3.2. Bone Vitality. This parameter was determined based on the presence of osteocytes inside trabecular bone lacunae at ×40 magnification and categorized as vital or non-vital.

2.3.3. Type of Newly Formed Bone (NFB). Order and orientation of collagen fibers in the NFB were evaluated under polarized light at ×40 magnification. A type of NFB was categorized as follows:

    Score I: woven bone alone

    Score II: both lamellar and woven bone

    Score III: lamellar bone alone

    Score IV: osteoid formation

2.3.4. Percentage of NBF. This measurement defines the percentage of the entire defect occupied by the NFB. To calculate the percentage of new bone formation, histological sections were photographed at ×40 magnification via a digital camera (E8400, Nikon, Japan). Using Iranian histomorphometric software version 1 (SBMU, Tehran, Iran), the mean percentage of areas occupied by bone was calculated.

2.3.5. Percentage of Remaining Biomaterial. This defines the percentage of total defect occupied by Bio-Oss particles. To calculate this variable, digital photographs were obtained of H&E stained histological slides at ×40 magnification and the mean percentage of areas occupied by the biomaterial was calculated using the Iranian histomorphometric analysis software version 1.

2.3.6. Location of Osteogenesis in Defects

    Grade 1: central

    Grade 2: marginal

    Grade 3: central and marginal

2.4. Statistical Analysis. The quantitative variables were reported as mean and standard deviation and as raw number and percentage. To compare qualitative data among the four groups (A, B, AB, and C), Fisher's Exact test was used. To analyze the effect of application of Bio-Oss and ANGIPARS

TABLE 1: Percentage and type of the NFB in examined defects.

Group	Time/NFB type					
	4 weeks			8 weeks		
	Lamellar	Woven	Woven-Lamellar	Lamellar	Woven	Woven-Lamellar
Control	0	100% (8)	0	75% (6)	12.5% (1)	12.5% (1)
Bio-Oss	0	100% (8)	0	75% (6)	0	12.5% (2)
AngiPars	0	0	100% (8)[a]	62.5% (5)	0	37.5% (3)
AngiPars + Bio-Oss	0	0	100% (8)[a]	100% (8)	0	0

[a] At four weeks in the ANGIPARS groups (alone or combined), lamellar bone formation was observed. The percentage of new bone formation at the center and margin of each defect is shown in Table 2.

TABLE 2: The mean percentage and standard deviation of NFB at the center and margin of defects.

	Mean %NFB (standard deviation)			
	4 weeks		8 weeks	
	Center	Margin	Center	Margin
Control	5.87 (7.05)	21.67 (1.79)	22.08 (13.20)	31.72 (6.23)
Bio-Oss	14.56 (5.29)	33.90 (5.42)	35.93 (8.60)	51.19 (6.11)
ANGIPARS	20.15 (8.96)	33.42 (4.15)	43.75 (6.57)	53.64 (6.31)
ANGIPARS + Bio-Oss	22.64 (9.54)	35.50 (5.65)	41.60 (11.58)	61.57 (7.65)

Although the most bone formation is observed in combination with ANGIPARS and Bio-Oss in the fourth week especially in center of the defect. ANGIPARS alone was more effective than Bio-OSS alone in both 4 and 8 weeks.

on quantitative variables, including new bone formation, two-way ANOVA was used. Student's t-test was applied when the interaction effect of the two factors was significant. The distribution of percentage of the remaining biomaterial was not normal. Thus, the effect of the two factors was analyzed using Mann Whitney U test, separately. $P < 0.05$ was considered statistically significant.

3. Results

During the postoperative period, none of the animals were lost. Eight of the rabbits were sacrificed randomly at four weeks and the remaining eight at eight weeks, 16 Bio-Oss, 16 ANGIPARS plus Bio-Oss, 16 ANGIPARS, and 16 empty defects were evaluated. The FBR was not observed in any specimen. Giant cells or granulomatous reaction were not seen in any defect. All the NFB in defects was vital.

At four weeks, lamellar bone was not seen in any defect while woven-lamellar bone was only seen in A and AB groups (Figure 2). At eight weeks, all defects in AB group were of lamellar bone (Figure 3) (Table 1). According to Fisher's exact test, the difference in the type of the NFB at four and eight weeks was significant in the control ($P = 0.001$), Bio-Oss ($P < 0.001$), ANGIPARS ($P = 0.02$), and ANGIPARS + Bio-Oss ($P < 0.001$) groups.

The percentage of total NBF is demonstrated in Table 3. According to two-way ANOVA, the interaction effects of materials in defects are shown in Table 3.

Based on t-test, the mean percentage of NBF between four and eight-week time points was significant in the control ($P < 0.001$), B ($P < 0.001$), A ($P < 0.001$), and A + B ($P < 0.001$) groups.

3.1. Percentage of Remaining Biomaterial. At four weeks, in group B, the mean, maximum, and minimum percentages of remaining Bio-Oss biomaterials were 23.15, 26.75, and 6.90, respectively. At eight weeks, these rates were 4.16, 10.58, and 1.05, respectively. In group AB, the mean, maximum, and minimum percentage of remaining BioOss were 23.40, 28.33, and 4.44, respectively, at four weeks and 7.29, 9.87, and 2.13, respectively, at eight weeks. The change was statistically significant at four ($P < 0.001$) and eight ($P < 0.001$) weeks.

3.2. Location of Bone Formation in the Defects. Based on Fisher's exact test, the difference in location of bone formation was significant at four ($P = 0.008$) but not significant at eight weeks ($P = 1.00$) among groups. At four weeks, four specimens in group C only demonstrated marginal bone formation. The remaining samples showed bone formation at the center and the margins. At eight weeks, only one specimen in group C did not show bone formation at the center. The remaining specimens demonstrated bone formation at the center and the margins.

4. Discussion

Many techniques have been recently introduced to enhance bone regeneration [14]. A bone substitute is necessarily required to enhance bone regeneration and healing in bony defects. Autogenous bone graft as the gold standard technique is mainly associated with donor site morbidity, graft resorption, limited quantity, and patient discomfort [15, 16]. One solution is to use bone substitute materials alone as an osteoconductive scaffold for regeneration of bone filling defect [17]. Thus, demand for nonautogenous bone grafts is

TABLE 3: The interaction effect of ANGIPARS and Bio-Oss on NFB.

			NFB in four weeks		NFB in eight weeks	
			Mean ± SD	P value	Mean ± SD	P value
(1)	Presence of Bio-Oss	Presence of ANGIPARS	31.34 ± 3.28[a]	0.005	54.93 ± 6.02	0.004
		Absence of ANGIPARS	26.44 ± 2.55		46.11 ± 4.20	
(2)	Absence of Bio-Oss	Presence of ANGIPARS	29.00 ± 2.31	<0.001	5.37 ± 5.36	<0.001
		Absence of ANGIPARS	16.30 ± 2.36		30.25 ± 2.43	
(3)	Presence of ANGIPARS	Presence of Bio-Oss	31.34 ± 3.28	0.12	54.93 ± 6.02	0.13
		Absence of Bio-Oss	29.00 ± 2.31		50.37 ± 5.36	
(4)	Absence of ANGIPARS	Presence of Bio-Oss	26.44 ± 2.55	<0.001	46.11 ± 4.20	<0.001
		Absence of Bio-Oss	16.30 ± 2.36		30.25 ± 2.43	

[a]As demonstrated, ANGIPARS has more synergic effect than BiO-Oss on NBF. *Row 1*. In presence of Bio-Oss, ANGIPARS showed a significant synergism effect on NBF both in 4 and 8 weeks even in the absence of Bio-Oss. *Row 2*. Even in absence of Bio-Oss, presence of ANGIPARS showed a significant effect on NBF in both 4 and 8 weeks. *Row 3*. In presence of ANGIPARS, Bio-Oss had no significant synergic effect on NBF in both 4 and 8 weeks. *Row 4*. In absence of ANGIPARS, Bio-Oss showed a significant effect on NBF in both 4 and 8 weeks.

(a)

(b)

(c)

(d)

FIGURE 2: Bone formation at 4 weeks in samples at ×40 magnification (black arrow = regenerated bone; blue arrow = remaining grafting material). (a) Control, (b) Bio-Oss sample, (c) ANGIPARS, and (d) ANGIPARS plus Bio-Oss. As shown, the most trabecular bone pattern was seen in ANGIPARS plus Bio-Oss group.

increasing due to availability, ease of storage, and sterility [18–20].

Our study is the first animal study to assess the efficacy of Semelil (ANGIPARS) in osteogenesis alone and in combination with Bio-Oss, a popular bone graft substitute, in order to assess if this material can promote bone formation. Systemic application of ANGIPARS has no adverse effect on bone formation [21]. Results of an animal study showed that, during the study period, no significant difference existed in biochemical or hematologic parameters between the test and control groups. Evidence shows that ANGIPARS is well tolerated and has no adverse effects on the function of body organs in subacute and chronic toxicity tests [22].

In the current study, the efficacy of ANGIPARS with and without Bio-Oss for bone regeneration in experimentally created defects was compared in rabbit calvarium. Rabbit
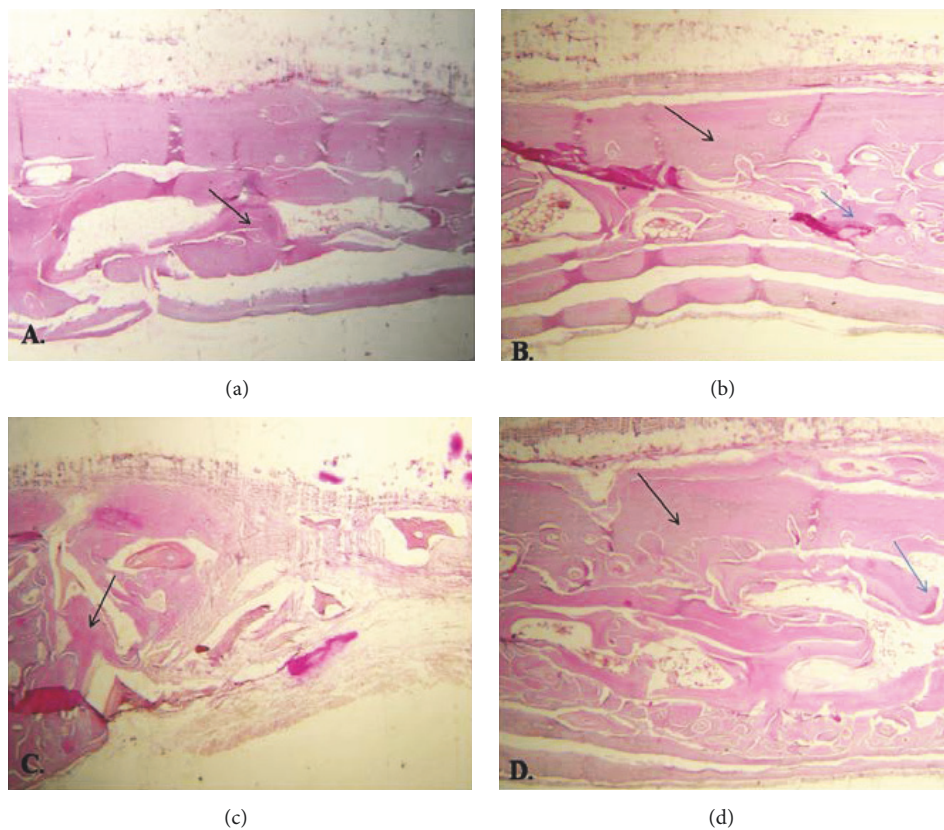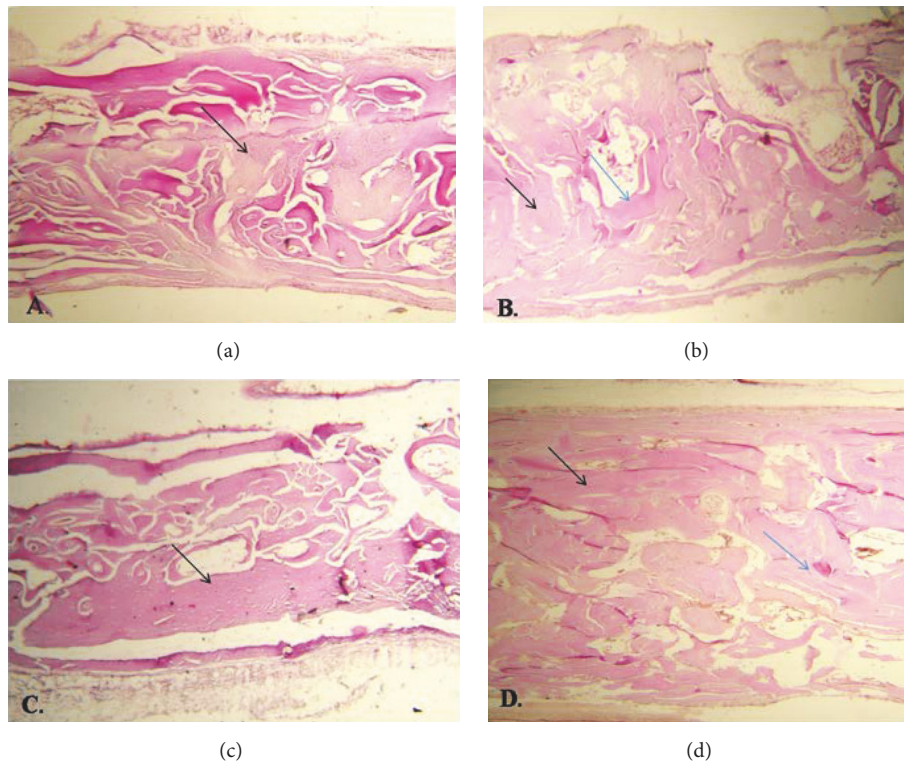
(a)

(b)

(c)

(d)

Figure 3: Bone formation at 8 weeks in samples at ×40 magnification (black arrow = regenerated bone; blue arrow = remaining grafting material). (a) Control, (b) Bio-Oss sample, (c) ANGIPARS, and (d) ANGIPARS plus Bio-Oss. As observed, the most trabecular bone pattern was seen in ANGIPARS plus Bio-Oss group.

cranial defects are the first choice as a bone model for bone grafting and bone regeneration studies because they provide adequate bone marrow that facilitates bone formation [23, 24]. The cranium of a rabbit is larger than that of rats and a greater number of defects can be created in a rabbit calvarium. Therefore, the duration of surgery, the costs, and the visual errors can be decreased. The bone remodeling phase occurs three times faster in rabbits than in humans [24–28]. Thus, two- to four-week recovery period is considered adequate for evaluation of the early response. Eight weeks or longer time intervals can be considered for evaluation of the delayed phase of healing, that is, suture closure, biomaterial resorption, bone remodeling, or rate of bone regeneration [24–28].

Although, in the experimental defects, osteogenesis was noted in the 8 mm control defects, it was significantly less than that of other groups. This finding may be due to the suturing of the thick periosteum of the rabbit calvarium over the experimental defects, mimicking the effect of guided bone regeneration (GBR). Bone regeneration is the basis of GBR. In this process, the blood clot is stabilized, defect space is maintained, and the surgical site does not undergo mechanical loading [29, 30]. Accordingly, NBF was significantly higher in groups A, B, and AB at four and eight weeks than that of group C. This demonstrated the positive effect of experimental materials used in our study. Thus, we believe that creating four circular defects (8 mm in diameter) in rabbit calvarium

provides a suitable model for evaluation of the healing phase and comparison of the efficacy of different materials simultaneously in order to decrease individual variations in experimental studies. Results obtained in such conditions can better be generalized to human periodontal lesions because, in the clinical setting, periodontal bone defects around teeth usually have dimensions smaller than 8 mm [31–33].

In the current study, a significant difference was observed regarding the overall percentage of NBF at both four and eight weeks in the following order from the highest to the lowest: AB > A > B > C. However, assessment of NBF at the center of defects revealed the following order: AB > A > B > C and A > AB > B > C at four and eight weeks, respectively.

Previous studies have demonstrated that Bio-Oss is a osteoconductive biocompatible graft material that can promote bone formation [13, 31, 32]. Lindhe et al. demonstrated that percentage of Bio-Oss particles decreased over time indicating their replacement with host bone in the long term [20]. In the current study, NBF in the Bio-Oss group was significantly higher than in the control group, which is in accordance with the aforementioned studies. However, there are some studies reporting that Bio-Oss is resistant to resorption and its particles may remain in the graft site up to four years [32]. Khorsand et al. found no significant difference in this regard between the Bio-Oss and control groups at four, six, and eight weeks [34]. In the current study, ANGIPARS alone significantly increased NBF in both the

center and margins of defects compared to the Bio-Oss and control groups. Melilotus, coumarin, and flavonoids are the main constituents of ANGIPARS. It has been demonstrated that coumarin and vitamin K products increase osteogenic markers, that is, osteocalcin and alkaline phosphatase (ALP), and probably decrease urinary calcium and secretion of hydroxy proline (bone loss markers) [21].

Tang et al. demonstrated that a coumarin derivative stimulates NBF following local subcutaneous injection into the calvarium and could increase the biomechanical bone strength. It also increased osteoblastic differentiation under in vitro conditions via the bone morphogenetic protein-2 (BMP-2) and Wnt/β-catenin signaling pathways. BMP-2 bonds to receptors on the surface of bone cells and phosphorylates SMAD 1/5/8; as a result, some specific bone genes are expressed [35]. Ostholeinhibits bone resorption by its estrogen-like effects on ovariectomized rats, facilitates osteoid formation and mineralization [36, 37]. Chen et al. (2005) indicated the positive effects of flavonoids on improving bone strength, enhancing bone cell proliferation, and osteogenic differentiation of mesenchymal stem cells [38]. Xiao et al. (2014) demonstrated that flavonoids stimulated the proliferation and differentiation of preosteoblasts. Flavonoids significantly enhanced cell proliferation, activated ALP, and increased the expression of osteoprotegerin mRNA (OPG/RANKL) in mouse osteosarcoma cells [39].

Although a higher overall bone formation was found in the AB group during study. Assessment of the center of defects revealed a higher bone formation in this area in group A at the end of the course of study. These findings emphasize the direct effect of ANGIPARS on bone formation and its ability to enhance NBF when applied alone or in combination with Bio-Oss.

The authors believe that higher rate of osteogenesis in the ANGIPARS and ANGIPARS plus Bio-Oss groups may be attributed to the effect of 7-hydroxy coumarin and flavonoids as the main constituents of ANGIPARS. A possible mechanism is the increased expression of BMP-2 and its effect on proliferation and differentiation of preosteoblastic cells at the defect site. According to a study by Gao et al. (2013), appropriate concentrations of 7-methoxy-8-isopentyl coumarin not only increase cell proliferation but also induce the differentiation of periodontal ligament progenitor cells like the mesenchymal stem cells [40].

In our study, at both four and eight weeks, both ANGI-PARS groups (A and/or AB) demonstrated higher formation of lamellar bone. This may be attributed to the presence of coumarins in ANGIPARS. Coumarins can induce the secretion of extracellular matrix, increase the uptake of calcium by the matrix, and enhance collagen type I secretion by increasing ALP activity in the cells, the matrix, and the formation of osteoblastic vesicles leading to mineralization [40] which could enhance the speed of bone maturation.

According to a study by Lin et al. (2014), BMP-2 enhances the proliferation and differentiation of mesenchymal stem cells and bone regeneration [41]. Since coumarins and flavonoids are the main constituents of ANGIPARS, they may induce osteogenesis via BMP-2, signaling pathways, which cause enhanced bone remodeling and maturation of defects

filled with ANGIPARS. Studies have demonstrated that Bio-Oss is an osteoconductive bone substitute with the surface porosities that provide a suitable matrix for osteogenic cells that promote bone formation [13, 31, 32]. Thus, it is suggested that Bio-Oss combined with ANGIPARS can be a suitable composite graft material that not only increases the amount of NBF but also improves the quality and maturation of the NFB.

In this study, all the NFB in all defects was vital with no FBR. FBR or giant cells were not seen in the Bio-Oss defects; this is in line with some previous studies demonstrating that Bio-Oss is a biocompatible material that does not cause FBR [31, 32, 42, 43]. In contrast, other previous studies have shown presence of osteoclasts at the Bio-Oss graft area [42–44]. In a study by Rokn et al., all the defects in the Bio-Oss group showed mild FBR at four and eight weeks [33, 45]. Tapety et al. in a similar study on rabbits reported the presence of osteoclasts at 14 days in the Bio-Oss group [46]; this is not in line with the current study results. Literature review shows that flavonoids are capable of causing osteo-clastic apoptosis and preventing bone loss [12, 47]. Moreover, coumarin has inhibitory effects on phagocytic activity and subsequent production of nitric oxide and metabolism by phagocytes [12]. Since ANGIPARS contains variable amounts of coumarin and flavonoid compounds, the authors believe that osteoclastic apoptosis caused by flavonoids and the inhibitory effects of coumarin can neutralize the FBR in ANGIPARS groups [8]. Besides, Bao et al. found that some of the ANGIPARS constituents can inhibit osteoclastogenesis by decreasing the resorption capacity of osteoclasts [48].

In our study, biomaterial remnants were assessed in the Bio-Oss groups (B and AB). This percentage was slightly (but not significantly) higher in the AB compared to the B group. A previous study demonstrated that *Magnolia Officinalis* decreased the number of leukocytes and polymorphonuclear cells in wounds and, subsequently, inhibited acute inflammation with its anti-inflammatory effect [12]. Considering the anti-inflammatory properties of ANGIPARS and consequent prevention of osteoclastic activity, this material can prevent Bio-Oss resorption; thus, the percentage of remaining biomaterials is expected to be higher in the AB group.

The current study showed that ANGIPARS not only promoted bone formation alone but also had a synergistic effect on both formation and maturation of new bone when applied along with Bio-Oss. It may be a suitable adjunct to confer osteogenic properties to materials like Bio-Oss, which are osteoconductive and space maintaining. Future human studies and clinical trials are required to assess the efficacy of ANGIPARS alone or as an adjunct to Bio-Oss and other conventionally used bone graft substitutes in the clinical setting.

5. Conclusion

Within the limitations of this animal study, ANGIPARS may be further examined as an adjunct to Bio-Oss for the purpose of enhancing bone healing and augmentation of bony defects.

Conflicts of Interest

The authors declare no conflicts of interest.

Acknowledgments

References

[1] S. P. Avera, W. A. Stampley, and B. S. McAllister, "Histologic and clinical observations of resorbable and nonresorbable barrier membranes used in maxillary sinus graft containment," *The International Journal of Oral & Maxillofacial Implants*, vol. 12, no. 1, pp. 88–94, 1997.

[2] P. Habibovic, M. C. Kruyt, M. V. Juhl et al., "Comparative in vivo study of six hydroxyapatite-based bone graft substitutes," *Journal of Orthopaedic Research*, vol. 26, no. 10, pp. 1363–1370, 2008.

[3] M. A. Rawashdeh and H. Telfah, "Secondary alveolar bone grafting: the dilemma of donor site selection and morbidity," *British Journal of Oral and Maxillofacial Surgery*, vol. 46, no. 8, pp. 665–670, 2008.

[4] S. E. Lynch, *Tissue Engineering: Applications in Oral And Maxillofacial Surgery And Periodontics*, 2008.

[5] A. Stavropoulos, L. Kostopoulos, J. R. Nyengaard, and T. Karring, "Deproteinized bovine bone (Bio-Oss) and bioactive glass (Biogran) arrest bone formation when used as an adjunct to guided tissue regeneration (GTR): an experimental study in the rat," *Journal of Clinical Periodontology*, vol. 30, no. 7, pp. 636–643, 2003.

[6] J. E. Zins and L. A. Whitaker, "Membranous versus endochondral bone: implications for craniofacial reconstruction," *Plastic and Reconstructive Surgery*, vol. 72, no. 6, pp. 778–785, 1983.

[7] G. Iezzi, A. Scarano, C. Mangano, B. Cirotti, and A. Piattelli, "Histologic results from a human implant retrieved due to fracture 5 years after insertion in a sinus augmented with anorganic bovine bone," *Journal of Periodontology*, vol. 79, no. 1, pp. 192–198, 2008.

[8] A. Scarano, G. Pecora, M. Piattelli, and A. Piattelli, "Osseointegration in a sinus augmented with bovine porous bone mineral: histological results in an implant retrieved 4 years after insertion. A case report," *Journal of Periodontology*, vol. 75, no. 8, pp. 1161–1166, 2004.

[9] S. Bakhshayeshi, S. Madani, M. Hemmatabadi, R. Heshmat, and B. Larijani, "Effects of semelil (ANGIPARS™) on diabetic peripheral neuropathy: A randomized, double-blind placebo-controlled clinical trial," *DARU Journal of Pharmaceutical Sciences*, vol. 19, no. 1, pp. 65–70, 2011.

[10] M. Mousavi-Jazi, H. Aslroosta, A. R. Moayer, M. Baeeri, and M. Abdollahi, "Effects of Angipars on oxidative inflammatory indices in a murine model of periodontitis," *DARU Journal of Pharmaceutical Sciences*, vol. 18, no. 4, pp. 260–264, 2010.

[11] K. Asres, S. Gibbons, E. Hana, and F. Bucar, "Anti-inflammatory activity of extracts and a saponin isolated from Melilotus elegans," *Die Pharmazie*, vol. 60, no. 4, pp. 310–312, 2005.

[12] L. Pleşca-Manea, A. E. Pârvu, M. Pârvu, M. Taǎmaş, R. Buia, and M. Puia, "Effects of Melilotus officinalis on acute inflammation," *Phytotherapy Research*, vol. 16, no. 4, pp. 316–319, 2002.

[13] A. R. Rokn, M. A. Khodadoostan, G. A. A. R. Rasouli et al., "Bone formation with two types of grafting materials: A histologic and histomorphometric study," *The Open Dentistry Journal*, vol. 5, no. 1, pp. 96–104, 2011.

[14] C. B. Lopes, M. T. T. Pacheco, L. Silveira Jr., J. Duarte, M. C. T. Cangussú, and A. L. B. Pinheiro, "The effect of the association of NIR laser therapy BMPs, and guided bone regeneration on tibial fractures treated with wire osteosynthesis: Raman spectroscopy study," *Journal of Photochemistry and Photobiology B: Biology*, vol. 89, no. 2-3, pp. 125–130, 2007.

[15] O. R. Beirne, "Comparison of complications after bone removal from lateral and medial plates of the anterior ilium for mandibular augmentation," *International Journal of Oral and Maxillofacial Surgery*, vol. 15, no. 3, pp. 269–272, 1986.

[16] E. Nystrom, K. E. Kahnberg, and J. Gunne, "Bone grafts and Brånemark implants in the treatment of the severely resorbed maxilla: a 2-year longitudinal study," *Implant Dentistry*, vol. 8, no. 1, pp. 45–53, 1993.

[17] H. Burchardt, "The biology of bone graft repair," *Clinical Orthopaedics and Related Research*, vol. 174, pp. 28–42, 1983.

[18] E. Kauschke, E. Rumpel, J. Fanghänel, T. Bayerlein, T. Gedrange, and P. Proff, "The in vintro viability and growth of fibroblasts cultured in the presence of different bone grafting materials (NanoBone® and Straumann Bone Ceramic®)," *Folia Morphologica*, vol. 65, no. 1, pp. 37–42, 2006.

[19] R. Haas, K. Donath, M. Födinger, and G. Watzek, "Bovine hydroxyapatite for maxillary sinus grafting: comparative histomorphometric findings in sheep," *Clinical Oral Implants Research*, vol. 9, no. 2, pp. 107–116, 1998.

[20] J. Lindhe, D. Cecchinato, M. Donati, C. Tomasi, and B. Liljenberg, "Ridge preservation with the use of deproteinized bovine bone mineral," *Clinical Oral Implants Research*, vol. 25, no. 7, pp. 786–790, 2014.

[21] S. Hasani-Ranjbar, Z. Jouyandeh, M. Qorbani, M. Hemmatabadi, and B. Larijani, "The effect of semelil (angipars®) on bone resorption and bone formation markers in type 2 diabetic patients," *DARU Journal of Pharmaceutical Sciences*, vol. 20, no. 1, article no. 84, 2012.

[22] M. Abdollahi, B. Farzamfar, P. Salari et al., "Evaluation of acute and sub-chronic toxicity of Semelil (ANGIPARS™), a new phytotherapeutic drug for wound healing in rodents," *DARU Journal of Pharmaceutical Sciences*, vol. 16, no. 1, pp. 7–14, 2008.

[23] E. Newman, A. S. Turner, and J. D. Wark, "The potential of sheep for the study of osteopenia: current status and comparison with other animal models," *Bone*, vol. 16, no. 4, pp. S277–S284, 1995.

[24] S. Castañeda, R. Largo, E. Calvo et al., "Bone mineral measurements of subchondral and trabecular bone in healthy and osteoporotic rabbits," *Skeletal Radiology*, vol. 35, no. 1, pp. 34–41, 2006.

[25] S. Xu, K. Lin, Z. Wang et al., "Reconstruction of calvarial defect of rabbits using porous calcium silicate bioactive ceramics," *Biomaterials*, vol. 29, no. 17, pp. 2588–2596, 2008.

[26] S. C. S. X. B. Cavalcanti, C. L. Pereira, R. Mazzonetto, M. de Moraes, and R. W. F. Moreira, "Histological and histomorphometric analyses of calcium phosphate cement in rabbit calvaria," *Journal of Cranio-Maxillo-Facial Surgery*, vol. 36, no. 6, pp. 354–359, 2008.

[27] J. Torres, F. M. Tamimi, I. F. Tresguerres et al., "Effect of solely applied platelet-rich plasma on osseous regeneration compared to Bio-Oss: a morphometric and densitometric study on rabbit calvaria," *Clinical Implant Dentistry and Related Research*, vol. 10, no. 2, pp. 106–112, 2008.

[28] J. Sohn, J. Park, Y. Um et al., "Spontaneous healing capacity of rabbit cranial defects of various sizes," *Journal of Periodontal & Implant Science*, vol. 40, no. 4, pp. 180–187, 2010.

[29] E. Calciolari, N. Mardas, X. Dereka, N. Kostomitsopoulos, A. Petrie, and N. Donos, "The effect of experimental osteoporosis

on bone regeneration: part 1, histology findings," *Clinical Oral Implants Research*, 2016.

[30] A. N. Silva Júnior, A. L. B. Pinheiro, M. G. Oliveira, R. Weismann, L. M. Pedreira Ramalho, and R. Amadei Nicolau, "Computerized morphometric assessment of the effect of low-level laser therapy on bone repair: an experimental animal study," *Journal of Clinical Laser Medicine & Surgery*, vol. 20, no. 2, pp. 83–87, 2002.

[31] P. Valentini and D. J. Abensur, "Maxillary sinus grafting with anorganic bovine bone: A clinical report of long-term results," *The International Journal of Oral & Maxillofacial Implants*, vol. 18, no. 4, pp. 556–560, 2003.

[32] T. Berglundh and J. Lindhe, "Healing around implants placed in bone defects treated with Bio-Oss: an experimental study in the dog," *Clinical Oral Implants Research*, vol. 8, no. 2, pp. 117–124, 1997.

[33] A. A. Rasouli Ghahroudi, A. R. Rokn, K. A. M. Kalhori et al., "Effect of low-level laser therapy irradiation and Bio-Oss graft material on the osteogenesis process in rabbit calvarium defects: A double blind experimental study," *Lasers in Medical Science*, vol. 29, no. 3, pp. 925–932, 2014.

[34] A. Khorsand, A. A. Rasouli Ghahroudi, P. Motahhari, M. Rezaei Rad, and Y. Soleimani Shayesteh, "Histological evaluation of Accell Connexus® and Bio-Oss® on quality and rate of bone healing: a single blind experimental study on rabbit's calvarium," *Journal of Dentistry*, vol. 9, no. 2, pp. 116–127, 2012.

[35] D. Tang, W. Hou, Q. Zhou et al., "Osthole stimulates osteoblast differentiation and bone formation by activation of β-catenin-BMP signaling," *Journal of Bone and Mineral Research*, vol. 25, no. 6, pp. 1234–1245, 2010.

[36] X. X. Li, I. Hara, and T. Matsumiya, "Effects of osthole on postmenopausal osteoporosis using ovariectomized rats; comparison to the effects of estradiol," *Biological & Pharmaceutical Bulletin*, vol. 25, no. 6, pp. 738–742, 2002.

[37] F. Meng, Z. Xiong, Y. Sun, and F. Li, "Coumarins from *Cnidium monnieri* (L.) and their proliferation stimulating activity on osteoblast-like UMR106 cells," *Die Pharmazie*, vol. 59, no. 8, pp. 643–645, 2004.

[38] K. M. Chen, B. F. Ge, H. P. Ma, X. Y. Liu, and M. H. Bai, "a flavonoid from the herb Epimedium enhances the osteogenic differentiation of rat primary bone marrow stromal cells," *Pharmazie*, vol. 60, no. 12, pp. 939–942, 2005.

[39] H.-H. Xiao, C.-Y. Fung, S.-K. Mok et al., "Flavonoids from Herba epimedii selectively activate estrogen receptor alpha (ERα) and stimulate ER-dependent osteoblastic functions in UMR-106 cells," *The Journal of Steroid Biochemistry and Molecular Biology*, vol. 143, pp. 141–151, 2014.

[40] L.-N. Gao, Y. An, M. Lei et al., "The effect of the coumarin-like derivative osthole on the osteogenic properties of human periodontal ligament and jaw bone marrow mesenchymal stem cell sheets," *Biomaterials*, vol. 34, no. 38, pp. 9937–9951, 2013.

[41] Z. Lin, J.-S. Wang, L. Lin et al., "Effects of BMP2 and VEGF165 on the osteogenic differentiation of rat bone marrow-derived mesenchymal stem cells," *Experimental and Therapeutic Medicine*, vol. 7, no. 3, pp. 625–629, 2014.

[42] C. Slotte and D. Lundgren, "Augmentation of calvarial tissue using non-permeable silicone domes and bovine bone mineral: An experimental study in the rat," *Clinical Oral Implants Research*, vol. 10, no. 6, pp. 468–476, 1999.

[43] M. Piattelli, GA. Favero, A. Scarano, and G. Orsini, "Bone reactions to anorganic bovine bone (Bio-Oss) used in sinus augmentation procedures: a histologic long-term report of 20 cases in humans," *The International Journal of Oral & Maxillofacial Implants*, vol. 14, no. 6, pp. 835–840, 1999.

[44] H. Schliephake, M. Dard, H. Planck, H. Hierlemann, and A. Jakob, "Guided bone regeneration around endosseous implants using a resorbable membrane vs a PTFE membrane," *Clinical Oral Implants Research*, vol. 11, no. 3, pp. 230–241, 2000.

[45] A. Rokn, AR. Ghahroudi, A. Mesgarzadeh, A. Miremadi, and S. Yaghoobi, "Evaluation of stability changes in tapered and parallel wall implants: a human clinical trial," *Journal of Dentistry*, vol. 8, no. 4, pp. 186–200, 2011.

[46] F. I. Tapety, N. Amizuka, K. Uoshima, S. Nomura, and T. Maeda, "A histological evaluation of the involvement of Bio-Oss® in osteoblastic differentiation and matrix synthesis," *Clinical Oral Implants Research*, vol. 15, no. 3, pp. 315–324, 2004.

[47] J.-F. Zhang, G. Li, C.-L. Meng et al., "Total flavonoids of Herba Epimedii improves osteogenesis and inhibits osteoclastogenesis of human mesenchymal stem cells," *Phytomedicine*, vol. 16, no. 6-7, pp. 521–529, 2009.

[48] L. Bao, L. Qin, L. Liu et al., "Anthraquinone compounds from Morinda officinalis inhibit osteoclastic bone resorption in vitro," *Chemico-Biological Interactions*, vol. 194, no. 2-3, pp. 97–105, 2011.

Research Article

Elucidation on Predominant Pathways Involved in the Differentiation and Mineralization of Odontoblast-Like Cells by Selective Blockade of Mitogen-Activated Protein Kinases

Jia Tang [iD] [1] **and Takashi Saito** [iD] [2]

[1]*Division of Biochemistry, Department of Oral Biology, School of Dentistry, Health Sciences University of Hokkaido, Hokkaido, Japan*
[2]*Division of Clinical Cariology and Endodontology, Department of Oral Rehabilitation, School of Dentistry, Health Sciences University of Hokkaido, Hokkaido, Japan*

Correspondence should be addressed to Jia Tang; tangjia@hoku-iryo-u.ac.jp

Aim. To analyze the effect of three mitogen-activated protein kinase (MAPK) inhibitors, namely, SB202190 (p38 inhibitor), SP600125 (JNK inhibitor), and PD98059 (ERK inhibitor) in Dex-stimulated MDPC-23 cell differentiation and mineralization. *Methods*. Experiment was divided into five groups, control (cells without Dex and inhibitors treatment), Dex (cells with Dex treatment but without inhibitors), Dex + SB202190, Dex + SP600125, and Dex + PD98059. Cell differentiation was assessed by alkaline phosphatase (ALP) activity assay and real time RT-PCR. Cell mineralization was investigated by alizarin red staining. *Results*. Exposure to SB202190 (20 μM) significantly decreased the mineral deposition in Dex-treated cells as demonstrated by alizarin red staining. Treatment of SP600125 (20 μM) attenuated the mineralization as well, albeit at a lower degree as compared to SB202190 (20 μM). Similarly, SB202190 (20 μM) completely abrogated the ALP activity stimulated by Dex at six days in culture, while no changes were observed with regard to ALP activity in SP600125 (20 μM) and PD98059 (20 μM) treated cells. The upregulation of bone sialoprotein (BSP), ALP, and osteopontin (OPN) in Dex challenged cells was completely inhibited by SB202190. *Conclusion*. Blockade of p38-MAPK signaling pathway resulted in significant inhibition of ALP activity, mineralization, and downregulation of osteogenic markers. The data implicated that p38 signaling pathway plays a critical role in the regulation of MDPC-23 cells differentiation and mineralization.

1. Introduction

Both bone and dentine are mineralized tissues, meaning their formation is defined by mineral crystal deposition onto organic matrix (mostly type I collagen) produced by osteoblasts or odontoblasts. Disorders that interrupt the normal mineralization process of the two tissues lead to abnormal phenotype, which seriously impair the life quality of people. For instance, osteogenesis imperfecta (OI) is a typical bone disease caused by the mutations in type I collagen; the patients tend to suffer bone fractures when subjected to only minor trauma. Another example is rickets, a defective mineralization of bone due to the lack of phosphates at the epiphyseal growth plate and mineralizing bone surfaces [1]. On the other hand, unlike bone, dentine becomes accessible

to external environment with increase of time, which put it at higher risk of bacterial infection or injury. As the sensory center-dental pulp is just beneath dentine, loss of dentine not only destroys the integrity of a tooth but also deprived the pulp of a complete and healthy structural support. Therefore, elucidation on the underlying mechanism during the process of dentine mineralization is of profound importance for the development of novel dentin regeneration reagents.

Mitogen-activated protein kinases (MAPKs) are a family of conserved serine/threonine protein kinases, which contribute to a variety of cellular activities, such as proliferation [2], differentiation, migration, apoptosis, senescence [3], and stress response [4]. Typical MAPKs members include extracellular signal regulated kinase (ERK1/2 or p44/42),

c-Jun N-terminal kinases 1-3 (JNK1-3), and p38 isoforms (p38α, β, γ, and δ). Since its discovery nearly three decades ago [5], MAPKs have been revealed as key players in osteoblast and odontoblast commitment and differentiation [6–9]. Based on the findings, it is thus proposed by researchers that targeting the MAPKs may offer a novel therapeutic approach for regeneration of hard tissue [10, 11].

Under the *in vitro* condition, osteoblast or odontoblast-like cells do not spontaneously undergo mineralization in the absence of any extra induction factors. When grown in the presence of synthetic glucocorticoid dexamethasone (Dex), ascorbic acid (AA), and β-glycerophosphate (β-GP), cells differentiate and produce mineralizing nodules over time [12]. Specifically, AA increases the production of collagen matrix [13]; β-GP acts as a source of inorganic phosphate ions [14]; Dex, a synthetic glucocorticoid, exhibits potent osteogenic and mitogenic effect [15]. In the preliminary study using the three reagents, we observed that Dex (10 nM, 100 nM) accelerated mineralization of MDPC-23 cell in the presence of β-GP (10 mM). The potent influence of Dex in the mineralization of MDPC-23 cell prompted us to study the potential signaling pathways that might be involved. To elucidate the effect of the three MAPKs in the differentiation and mineralization process stimulated by Dex, we used commercially available pharmacological inhibitors specific to p38 (SB202190), JNK (SP600125), and ERK (PD98059) to treat the cells prior to the addition of Dex stimulant. Cell differentiation and mineralization were analyzed.

2. Materials and Methods

2.1. Cell Culture. Rat odontoblast-like cell line (MDPC-23 cell) [16] was generously provided by Professor Jacques E. Nör (University of Michigan). The cells are cultured in Dulbecco's modified eagle's medium (DMEM, D5796, Sigma) supplemented with 5% heat-inactivated fetal bovine serum (FBS, 10270-106, Gibco) at 37°C in a humidified atmosphere and 5% CO_2. Cells were plated at the density of 1×10^4/mL and 1.25×10^4/mL in 24-well (Tissue culture treated polystyrene, Iwaki) and 12-well plates (Tissue culture treated polystyrene, Falcon), respectively. Mineralization reagent including β-GP (10 mM) (191-02042, Wako), AA (50 μg/mL) (013-19641, Wako), and Dex (100 nM) (D2915, Sigma) in DMEM (5% FBS) was added on day five, when cells reached confluence.

2.2. Mineralization Assay. To investigate the calcific deposition in response to three MAP kinase inhibitors, MDPC-23 cell were inoculated in 24-well plate at the density of 1×10^4/mL and cultured for five days in DMEM supplemented with 5% FBS ($n = 3$). On day five, cells were challenged with the three inhibitors (SB202190, SP600125, and PD98059) (Cell Signaling Technology) for 2 h in serum free DMEM. Inhibitors containing media were replaced with mineralization inducing media including β-GP, AA, and Dex. Control wells represent cells treated by both β-GP and AA, but without Dex. On day eight, the mineralization was observed by alizarin red staining and quantified using cetylpyridinium chloride (CPC) (C0732-100G, Sigma-Aldrich) extraction method. Briefly, cell monolayer was gently washed by

phosphate-buffered saline (PBS) (10010049, Gibco) and fixed in 10% formalin neutral buffer solution (060-01667, Wako) at room temperature for 20 min. Afterwards, the monolayer was rinsed by distilled water once prior to staining by 200 μL alizarin red s (1%, w/v, pH 4.1 in water) (011-01192, Wako) per well. The cells were incubated with alizarin red s solution at room temperature for about 5 min. Extra dye was discarded, and the wells were washed quickly with distilled water for four to five times and after that washed with distilled water for 2 h with gentle shaking until the water became transparent. The mineralization nodules were visualized by an inverted camera (Canon) in a digital photograph system (Funakoshi). For quantification of staining, 800 μL CPC (10%, w/v, in water) was poured to each well, and the plates were incubated at 37°C for 2 h. After incubation, the transparent CPC solution turned into purple and was transferred into 96-well plate (200 μL/well) for absorbance reading at 570 nm.

2.3. ALP Activity. The cells were maintained in 12-well plate at the initial seeding concentration of 1.25×10^4/mL (2 mL media/well) for five days. On day five, the three inhibitors were added to cells for 2 h. After incubation with the inhibitors, media were aspirated and replaced by mineralization inducing media (β-GP, AA, and Dex). Cells were cultured for another day and lysed by 0.1% Triton-X-100 (T8787, Sigma) and sonicated on ice for 10 min at day six. The cell lysates were centrifuged and supernatant was collected for ALP activity assay and protein quantification. Specifically, before conducting the ALP assay (LabAssay™ ALP, Code number 291-58601, Wako), the collected supernatant was diluted by 100 times in ultrapure water. In parallel, standard solution was prepared by series dilution of 0.5 mmol/L p-nitrophenol (0, 0.0625, 0.125, 0.25, and 0.5 mmol/L). The reaction mixture was constituted by 20 μL of the diluted samples or standard solution and 100 μL of the p-nitrophenylphosphate substrate. Prior to incubation, the mixture was thoroughly mixed using plate mixer for 1 min. After incubation under 37°C for 15 min, the reaction was terminated by addition of 0.2 mol/L sodium hydroxide. Absorbance was read at 405 nm. The calculated ALP activity was divided by protein concentration, which was quantified using Pierce BCA assay kit, to avoid the influence of protein amount variation.

2.4. Real Time RT-PCR. Cells were seeded into 12-well plate at the initial density of 1.25×10^4/mL. On day five, cells were exposed to the three inhibitors (20 μM) for 2 h; mineralization reagent was added after inhibition treatment on the same day. On day seven, total RNA was purified from cells in 12-well plate ($n = 3$) using Trizol® reagent (Invitrogen, Carlsbad, CA, USA) according to manufacturer's instruction. The concentration of RNA was determined using a Nanodrop 2000 spectrophotometer (Thermo Fisher Scientific, Wilmington, DE, USA). One microgram purified RNA was treated with RNase inhibitor and reverse transcribed into complementary DNA (cDNA) in a 20 μL reaction system by the Moloney Murine Leukemia Virus (M-MLV) reverse transcriptase (1 μg RNA; DNase and RNase free
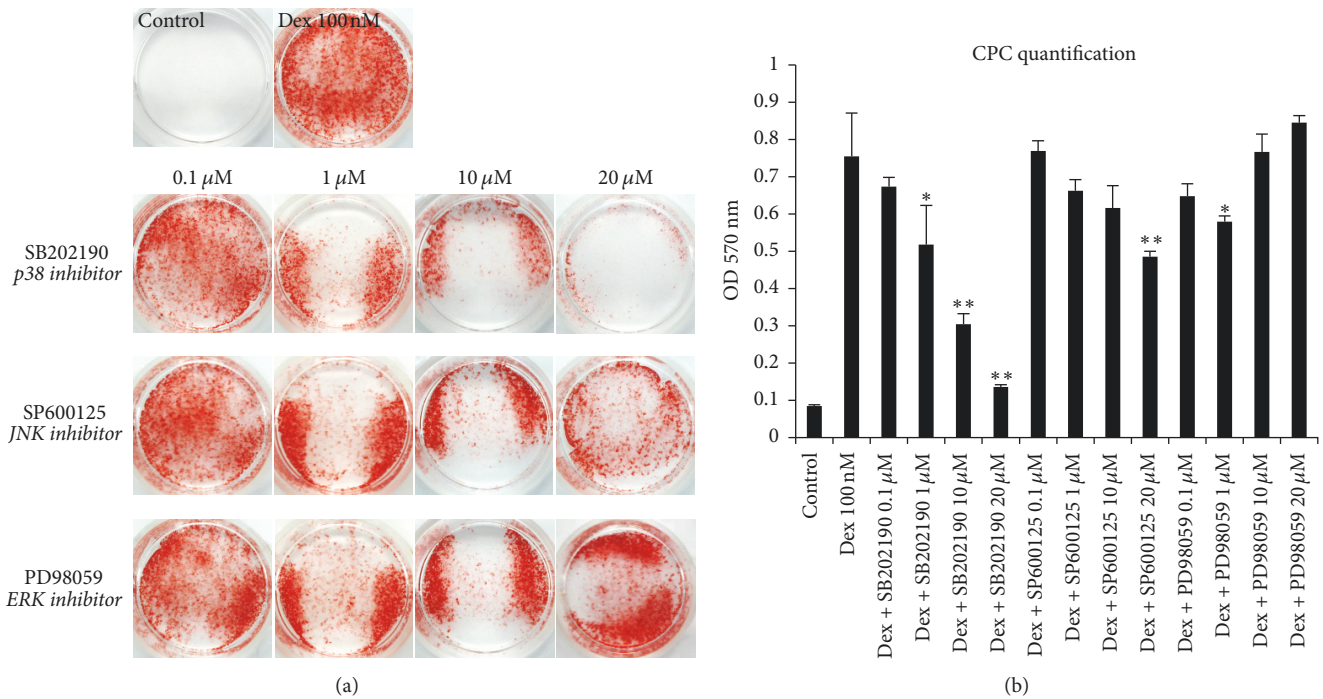
(a)

(b)

FIGURE 1: *Effects of blockade of p38, JNK, or ERK activation on mineralizing nodules formation.* Cells were cultured in control medium (β-GP and AA) or mineralization medium (β-GP, AA, and Dex) or mineralization medium supplemented with SB202190, SP600125, or PD98059. Alizarin red staining was performed on day eight as described under Materials and Methods Section 2.2. Addition of Dex significantly accelerated mineralization, as staining was hardly observable in control containing only β-GP and AA (a). SB202190 inhibits mineralization in a concentration-dependent manner ((a) and (b)). SP600125 slightly attenuates the mineralization at the concentration of 20 μM. PD98059 (1 μM) marginally decreased the mineralization, while PD98059 in the other concentration groups did not impact it (*$p < 0.05$; **$p < 0.01$; differences were given out as compared to Dex group).

water; 1 μL Oligo (dT) (18418-012, Invitrogen); 4 μL dNTP mixture (2.5 mM each, 4030, TaKaRa); 1 μL RNase inhibitors (40 U/μL) (Cat#2313A, TaKaRa); 4 μL 5x first strand buffer (Invitrogen, Carlsbad, CA, USA); 2 μL 0.1 M dithiothreitol (DTT, Invitrogen); 1 μL Moloney Murine Leukemia Virus (M-MLV) enzyme (200 U/μL) (REF 28025-013, Invitrogen)). Following the synthesis of cDNA, real time PCR was carried out in a LightCycler Nano® (Roche) system using FastStart Essential DNA Probes Master (2x) (Roche). Target gene expression was normalized by housekeeping gene β-actin. The mean value for the control group was taken to be 100% of mRNA expression and served as a reference. The detailed information for primers and real time PCR reaction conditions are listed in Table 1. The SYBR green amplification reaction consisted in an initial denaturation of 10 min at 95°C, followed by 50 cycles of 15 s at 95°C (denaturation), 30 s at annealing temperature (see Table 1 for each set of primer), and 30 s at 72°C (extension). The $2^{-\Delta\Delta Ct}$ method was used to calculate relative gene expression.

2.5. Statistical Analysis.
Data are presented as average ± standard deviation (SD). The statistical analysis of differences among the groups was analyzed by post hoc Tukey HSD test at a 5% level of significance.

3. Results

3.1. Mineralization Assay.
The potential effect of the three inhibitors on calcific deposition in MDPC-23 cell was explored using alizarin red staining. The staining photograph (Figure 1(a)) showed that 2 h exposure to SB202190, the p38 inhibitor, leads to a significant reduction of mineral deposition stimulated by Dex; the mineralization of cells treated by SB202190 decreased in a concentration-dependent manner (Figure 1(b)). Particularly, a concentration of 20 μM almost completely blocked the mineral deposition of cells (optical density 0.14 ± 0.01 versus 0.09 ± 0.00 of control, $p <$ 0.01). On the other hand, although SP600125 exhibited mineralization inhibition activity, the influence was much weaker as compared to SB202190: SP600125 (20 μM) (optical density: 0.49 ± 0.02) only inhibits 35% of the mineralization induced by Dex (0.76 ± 0.12). With regard to the cells treated by PD98059, slight decrease of mineralization was observed in the group of 1 μM (0.58 ± 0.02 versus 0.76 ± 0.12 in Dex group, $p < 0.01$). No statistical differences were found between Dex group and the other PD98059 (0.1, 10, and 20 μM) groups.

3.2. ALP Activity.
The ALP activity was markedly augmented by Dex at the concentration of 100 nM (1.52 ±

TABLE 1: Primers information.

| Gene name	Forward	Backward	Fragment size (bp)	Annealing temperature (°C)
BSP (NM_012587.2)	CTGCTTTAATCTTGCTCTG	CCATCTCCATTTTCTTCC	211	55
ALP (NM_013059.1)	GGAAGGAGGCAGGATTGACCAC	GGGCCTGGTAGTTGTTGTGAGC	338	55
OPN (NM_012881.2)	TTTCCCTGTTTCTGATGAACAGTAT	CTCTGCTTATACTCCTTGGACTGCT	228	55
Npnt (XM_008761543.1)	CTCAAAGCTGTGTGCCAACC	TTGTGGCTTGATGATCCGGG	178	59.9
Runx-2 (NM_001278484.2)	CCACAGAGCTATTAAAGTGACAGTG	AACAAACTAGGTTTAGAGTCATCAAGC	87	55
DMP-1 (NM_203493.3)	CGTTCCTCTGGGGGCTGTCC	CCGGGATCATCGCTCTGCATC	577	62
BMP-4 (NM_012827.2)	CAGGGCCAACATGTCAGGAT	TGGCGACGGCAGTTCTTATT	188	59.9
COL1A1 (NM_053304.1)	AGAATATGTATCACCAGACG	CAGCTGATTTCTCATCATAG	224	43
OCN (NM_013414.1)	AGCTCAACCCAATTGTGAC	AGCTGTGCCGTCCATACTTT	190	55
ITGA1 (NM_030994.2)	TCAACGTTAGCCTCACCGTC	CAGGGATCGTCTCATTGGCA	396	59.9
ITGA3 (XM_0037509072.2)	GAAAGGCTGACCGACGACTA	TGCGTGGTACTTGGGCATAA	108	66
ITGA5 (NM_001108118.1)	GAAGGGACGAGGAGTCAGTGTG	TGAATGGTGCTGCACTGGAT	127	66
ITGAV (XM_008762000.1)	ATAAAGCGCGGATGGCAAAG	CTCACCCGAAGATAGGCGAC	213	64.9
ITGB1 (NM_017022.2)	ACAAGAGTGCCGTGACAACT	AGCTTGATTCCAAGGGTCCG	325	59.9
ITGB5 (NM_147139.2)	CACGGTCCATCATCTCTCGG	CATGGAGAGGGAGAGGTCCA	281	62.8
β-actin (NM_031144.3)	AACCCTAAGGCCAACAGTGAAAG	TCATGAGGTAGTCTGTGAGGT	241	53
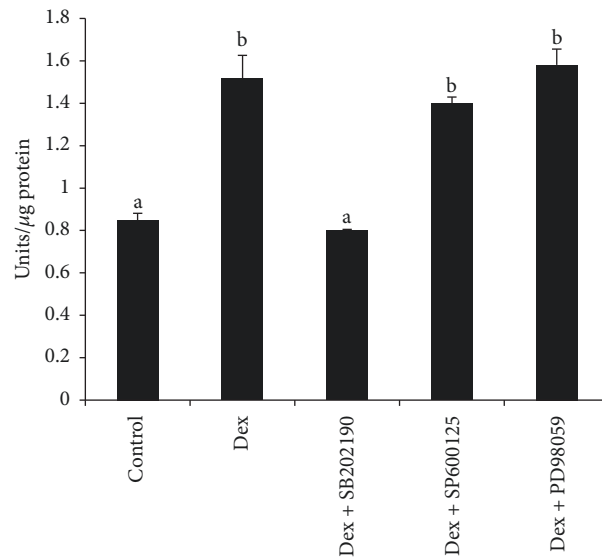
FIGURE 2: *Inhibition of ALP activity by SB202190 in MDPC-23 cell.* ALP activity on day six was determined as described under Materials and Methods. The results represent average ± SD of cultures ($n = 4$). ALP activity in cultured treated with SP600125 (20 μM) or PD98059 (20 μM) alone was similar to those of Dex group. On the contrary, treatment of cells using SB202190 completely inhibited the ALP activity stimulated by Dex (a-b indicate significant differences between different characters, $p < 0.01$).

0.11 units/μg protein versus 0.85 ± 0.03 units/μg protein of control, $p < 0.01$) (Figure 2). This upregulation of was completely hindered by the addition of SB202190 (20 μM) (0.80 ± 0.01 units/μg protein). The addition of SP600125 (1.40 ± 0.03 units/μg protein) or PD98059 (1.58 ± 0.07 units/μg protein) did not impact the ALP activity stimulated by Dex.

3.3. Real Time RT-PCR. Gene expression of BSP, ALP, OPN, nephronectin (Npnt), runt-related transcription factor 2 (Runx-2), dentine matrix protein-1 (DMP-1), bone morphogenetic protein-4 (BMP-4), collagen I (COL-1), and osteocalcin (OCN) were assessed by real time RT-PCR (Figure 3). Among those, BSP (3.33 ± 0.19-fold), ALP (2.47 ± 0.15-fold), and OPN (1.40 ± 0.01-fold) were significantly promoted by Dex; concomitantly, the upregulation of the three genes was completely impeded by SB202190 (20 μM). On the contrary, exposure to SP600125 (20 μM) further boosted the expression of BSP (5.36 ± 0.87-fold), while it did not affect ALP and OPN expression as compared to Dex group. Moreover, PD98059 (20 μM) slightly upregulated ALP (3.06 ± 0.05-fold) and OPN (1.82 ± 0.13-fold) compared to Dex. There was no change in relation to the expression of BSP after inclusion of PD98059. Expression of Npnt (a newly discovered extracellular matrix protein) was significantly promoted by Dex (1.62 ± 0.03-fold). SB202190 and SP600125 did not affect the expression of Npnt, but PD98059 slightly enhanced its expression (1.97 ± 0.11-fold). mRNA expression of Runx-2 was marginally higher in Dex group (1.09 ± 0.01-fold) than control. Similarly, SB202190 repressed its expression while both SP600125 and PD98059 upregulated it compared to Dex group. For the rest of four genes, all were downregulated by Dex treatment, remarkably, and OCN expression level was inhibited to nearly 50% in Dex group. The expression profile of the four genes modulated by the three inhibitors was similar, with

SB202190 downregulating and the other two upregulating the expression.

To further characterize the mRNA expression of integrins, the well-established cell surface receptors for a number of extracellular proteins, total six types of integrins (integrin alpha 1 (ITGA1), integrin alpha 3 (ITGA3), integrin alpha 5 (ITGA5), integrin alpha v (ITGAV); integrin beta 1 (ITGB1) and integrin beta 5 (ITGB5)) were evaluated by real time RT-PCR (Figure 4). Among the four alpha integrins, ITGA3 was markedly enhanced by Dex (1.80 ± 0.06 fold); the upregulation was not altered by incorporation of SB202190 (1.70 ± 0.15-fold) but was further strengthened by SP600125 (2.33 ± 0.14-fold) and PD98059 (2.10 ± 0.04-fold). Expression of both ITGA1 (0.75 ± 0.00-fold) and ITGAV (0.80 ± 0.00-fold) was marginally retarded by Dex, while that of ITGA5 was unchanged in Dex group compared to control. Two beta integrins (ITGB1 and ITGB5) were slightly promoted by Dex. In agreement with the above noted trend, SB202190 inhibited the expression of ITGA1, ITGA5, ITGAV, ITGB1, and ITGB5 while SP600125 and PD98059 enhanced them.

4. Discussion

Although the activation of MAPKs has been associated with osteo/odontoblast differentiation and mineralization, it is unclear as to which pathway plays a predominant role. In the present study, to clarify the underlying signal pathways involved in the differentiation and mineralization stimulated by Dex, we used three MAPK inhibitors to investigate their respective effects in a series of cell behavior. SB202190, a pyridinyl imidazole, is cell permeable and highly selective inhibitor of p38α and β isoforms. It shares structure similarity with another p38 inhibitor-SB203580 and is usually used as an alternative to SB203580. The specificity of SB202190
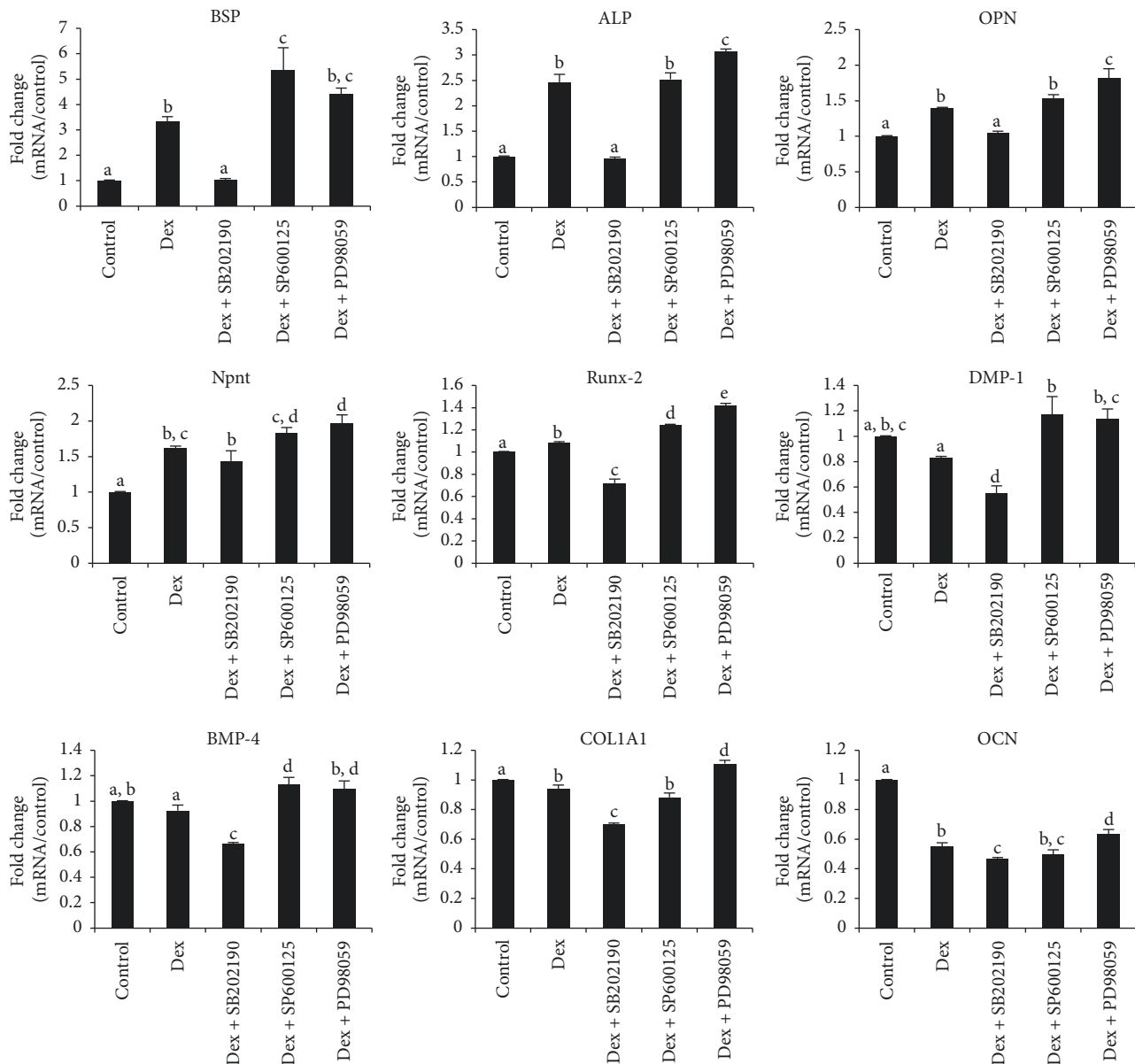
FIGURE 3: *Gene expression profile of osteogenesis related markers in culture containing SB202190, SP600125, or PD98059*. MDPC-23 cells were cultured as described in Materials and Methods. Total RNA was isolated on day seven and analyzed by reverse-transcription PCR with the indicated primers illustrated in Table 1. Control means cells cultured in the presence of β-GP and AA, without Dex or any inhibitors. Dex group means cells maintained in β-GP, AA, and Dex, without any inhibitors. The concentration for the three inhibitors was unified to be 20 μM (a–e indicate significant differences between different characters in each panel, $p < 0.01$).

toward p38 pathway was revealed by its low half maximal inhibitory concentration (IC_{50}) and failure to affect other protein kinases [17]. SP600125 is a novel selective JNK1/2/3 inhibitor, which causes inhibition of phosphorylation of c-Jun. Its IC_{50} toward JNK1/2/3 was found to be as low as 1/272 of the value on ERK2 or p38β, indicating SP600125 was highly specific for JNK [18]. PD98059 binds to inactive forms of MEK1 and prevents activation by upstream activators such as c-Raf [19]. In the comparative study that compares 28 types of commercially available kinases inhibitors, PD98059 stands out by its superior specificity: it did not show any

inhibition activity at a concentration of 50 μM, by which concentration ERK was inhibited [17]. The concentration of each inhibitor used in the present experiment was based on recommendations from the manufacturer. It was suggested that the working concentration for SB202190, SP600125, and PD98059 is 5–20 μM, 25–50 μM, and 5–50 μM, respectively. To avoid causing cytotoxicity, we selected the lowest maximal working concentration from SB202190 (20 μM) for the experiment.

Maintenance of a health pulp is a longstanding issue and of critical importance, as teeth devitalized by root canal
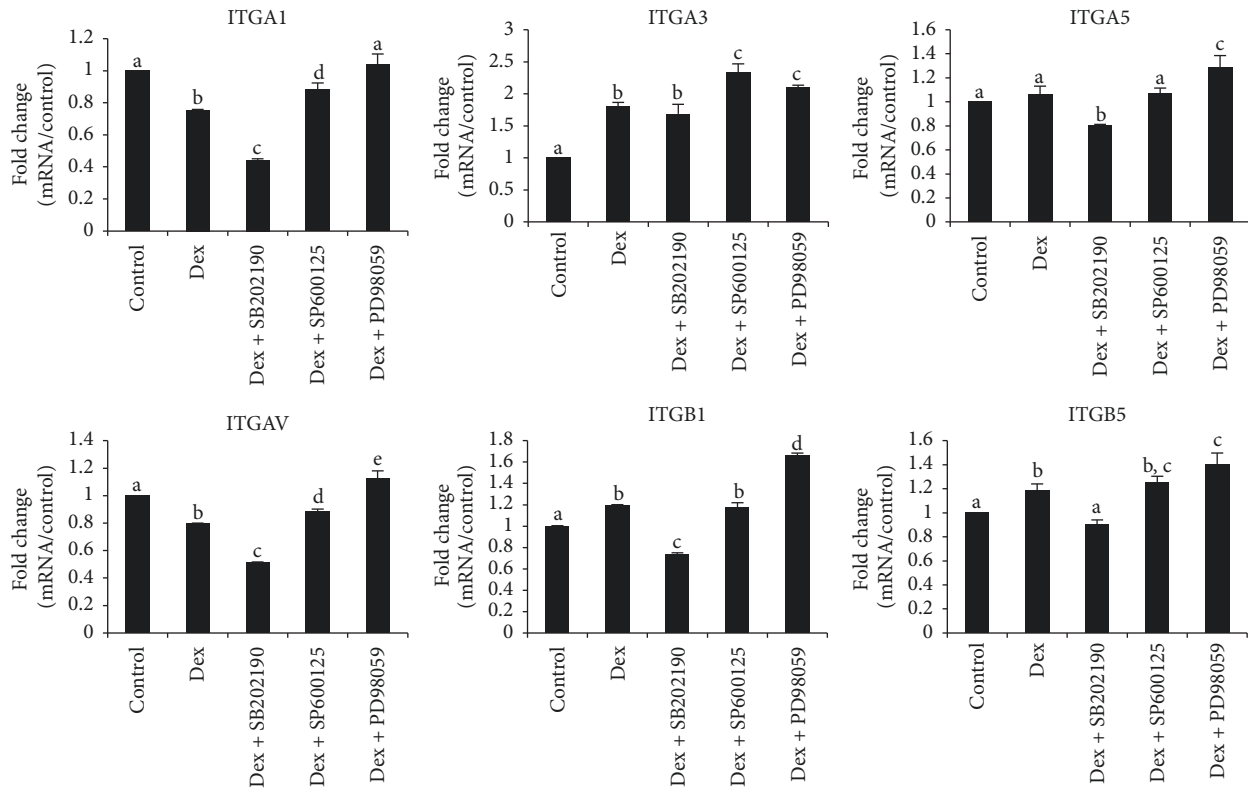
FIGURE 4: *Gene expression profile of integrins in culture containing SB202190, SP600125, or PD98059.* MDPC-23 cells were cultured in the same way as Figure 3. Total RNA was isolated on day seven and analyzed by reverse-transcription PCR with the indicated primers illustrated in Table 1. Control means cells cultured in the presence of β-GP and AA, without Dex or any inhibitors. Dex group means cells maintained in β-GP, AA, and Dex, without any inhibitors. The concentration for the three inhibitors was unified to be 20 μM (a–e indicate significant differences between different characters in each panel, $p < 0.01$ except for $p < 0.05$ between Dex and Dex + PD98059 in ITGA3 panel; $p < 0.05$ between Dex and Dex + SP600125 in ITGAV panel; $p < 0.05$ between control and Dex in ITGB5 panel).

treatment become more vulnerable and prone to structural failure over time. Odontoblasts share some common features with osteoblasts: both of them secrete extracellular matrix that undergoes mineralization [20, 21]. Nevertheless, the uniqueness of the former lies in the fact that they are trapped at the periphery of dental pulp and produce reparative dentine in case of attrition, deep caries, or injury. The implications of tooth devitalization have driven significant interest in research with regard to the development of bioactive materials that facilitate the regeneration of damaged pulp tissue by harnessing the capacity of dental pulp for self-repair. Recently, there are a large number of *in vitro* and *in vivo* studies that investigated the relevant role of p38, JNK, and ERK throughout the osteoblast/odontoblast differentiation process, from mesenchymal stem cells to fully committed anabolic osteoblast/odontoblast-like cell lines. For example, p38 phosphorylation was increased in an *in vitro* caries model established by addition of *Streptococcus mutans* in MDPC-23 cell [22]. Importantly, although ERK was activated in parallel with p38 MAPK in the differentiation of primary calvarial osteoblast, inhibition of ERK did not affect osteoblast differentiation in terms of ALP activity and mineral deposition, while inhibition of p38 significantly

suppressed the ALP activity and mineralization [23]. On the other hand, JNK signal pathway was noted to be required for late stage differentiation in both MC3T3-E1 cells and primary calvarial osteoblasts, as demonstrated by a significant inhibition of OCN and BSP expression [24]. Phosphorylation of p38, JNK, and ERK was increased by fucoidan, a type of polysaccharide, during the differentiation process of human alveolar bone marrow mesenchymal stem cells, but it was found that osteogenic differentiation induced by fucoidan was inhibited by SP600125 and PD98059 but not SB203580 (another type of p38 inhibitor) [25]. More recently, a study using calcium hydroxide, the commonly used pulp capping material, in dental pulp stem cells (DPSCs) has revealed p38, JNK, and ERK are all responsible for enhanced differentiation in DPSCs [26].

Here, we showed that inhibition of p38 signaling pathway by SB202190 interfered with the differentiation and mineralization process of the MDPC-23 cell. ALP activity, an important parameter for evaluating initiation but not progression of osteoblast/odontoblast differentiation, was completely blocked by this p38 inhibitor; in comparison, the treatment of SP600125 and PD98059 did not alter the ALP activity as compared to Dex group, reflecting that ALP

activity upregulation stimulated by Dex was predominantly regulated via p38 signaling pathway, neither JNK nor ERK pathways.

Next, real time RT-PCR was conducted to assess multiple hard tissue forming genes. In contradiction to the results presented by Kim et al. [25], it was found that expression of BSP, ALP, and OPN, three classical osteogenesis markers, was completely inhibited in cell treated with SB202190 but not SP600125 or PD98059. The discrepancy may be caused by different cell type and stimulant used for osteogenic induction. Npnt, recently reported to be able to induce the differentiation of MDPC-23 cell into an odontoblast-like phenotype [27], was upregulated by Dex at the concentration of 100 nM to 1.6-fold more than control; its expression was unaffected by the treatment with neither SB202190 nor SP600125, but that PD98059 slightly enhanced it. The observation denoted that some other signal pathways are involved in the Dex-mediated upregulation of Npnt. Indeed, a recent work demonstrated that Wnt/β-catenin signaling pathway is responsible for the activation of Npnt by Wnt3a in MC3T3-E1 cell [28]. Whether the same signaling pathway is required in Dex-induced Npnt expression awaits further investigation. Marginal upregulation of Runx-2 (or core-binding factor subunit alpha-1, CBF-α1) was detected and that inhibition of p38 downregulated the expression, while inhibition of JNK and ERK upregulates it. This correlates well with a study by Lee et al. [29], who showed that strong induction of Runx-2 using a p38 activator (anisomycin) was blocked by the addition of SB203580 (a specific p38 inhibitor). This further demonstrated that p38 signaling pathway is positively involved in the regulation of Runx-2 expression. DMP-1, an acidic protein found in mineral phase of vertebrates and invertebrates, is a key regulatory protein of odontogenesis [30]. We found that p38 inhibition led to a significant reduction of DMP-1 expression, while JNK and ERK inhibition enhanced it. Previously, it was reported that downregulation of DMP-1 in KN-3 cell (rat incisors dental papilla derived cell line) initiated by interferon-γ (IFN-γ), a proinflammatory cytokine, was achieved through the phosphorylation of p38 MAPK [31]. BMP-4 is a potent inducer for odontoblast differentiation [32], it is shown that there was no change in terms of the gene expression for DMP-1 and BMP-4 upon treatment by Dex. Since BSP, ALP, and OPN are well-established osteogenic factors, the data denoted Dex may induce the transdifferentiation of MDPC-23 cells into osteoblast. Similarly, the inhibition of BMP-4 and COL1A1 by SB202190 indicated that gene expression of both may be partially regulated via the p38 signaling pathway. Indeed, Tan et al. [33] found that the upregulation of BMP-4 activated by CCN3 was abrogated by p38 and JNK inhibitors. COL1A1, the gene encoding alpha chain of type I collagen, was inhibited by exposure to SB202190 and promoted by PD98059, denoting that this gene is regulated by p38 and ERK signaling pathway and unaffected by JNK. Finally, the OCN expression was significantly downregulated by Dex, although there was slight reduction of expression in SB202190 group, and the difference was not evident, suggesting that some other signaling pathways might be involved.

As cell matrix is regulated to a large extent by surface receptors such as integrin, we further expanded our investigation to analyze the gene expression of integrin stimulated by Dex and MAPK inhibitors. Thus far, there are 24 known integrins. We characterized six subtypes of integrin (ITGA1, ITGA3, ITGA5, and ITGAV and ITGB1 and ITGB5) by real time RT-PCR. ITGB1, a ubiquitously expressed integrin, was promoted. Indeed, *in vivo* ITGB1 knockout mice were found to exhibit delayed eruption of molars, indicating that it was indispensable for the tooth development [34]. Among the four alpha integrins, only ITGA3 was significantly promoted by Dex, and SB202190 did not impact the expression of ITGA3, denoting that p38 is not involved in the regulation of ITGA3 expression. There was no change in terms of ITGA5 expression after exposure to Dex, but ITGA1 and ITGAV were downregulated. Furthermore, SB202190 markedly downregulates the expression of ITGA1, ITGA5, ITGAV, ITGB1, and ITGB5. In contrast, SP600125 and PD98059 significantly enhanced the expression of all the integrins. It is thus suggested that Dex induced an altered integrin expression pattern, which were further changed by the exposure to MAPK inhibitors.

Dentine undergoes continuous matrix deposition. Odontoblasts are cells that line the periphery of the pulp and responsible for dentine matrix secretion and mineralization. In the case of injury, certain signaling pathways in odontoblasts are activated by inflammatory factors to initiate wound healing process. Among various pathways inside a cell, MAPKs are a family of enzymes that are implicated in a series of processes. Here, we established the mineralization and differentiation model in MDPC-23 cell by stimulating it with Dex and identified the signaling pathways of switching odontoblasts from quiescent state to active secretion state. We selected three specific MAPKs inhibitors and clarified their effects when added to cell culture media. The results, which correlate well with previous literatures, underline a critical role of p38 in the regulation of differentiation and mineralization in MDPC-23 cell. Qin et al. examined differentiation of human dental pulp cells into odontoblasts using bone morphogenetic protein-2 (BMP-2) and detected enhanced phosphorylation of p38α; moreover, knock-down of this pathway inhibited ALP activity and mineralization and suppression of p38α attenuated odontoblastic differentiation [35]. Another comparative study of early and late stage odontoblasts suggested that p38 was intensively expressed by early stage odontoblasts and disappeared in late stage odontoblasts, denoting that it was involved in the primary dentine formation [36]. Interestingly, Yu et al. purified human dentin matrix proteins cocktail and added them to bone marrow-derived mesenchymal stem cells to find that both ERK and p38 were phosphorylated, and inhibition of this two pathways simultaneously suppressed mineralization and gene expression of osterix and DSPP [37]. It is hence should be pointed out that, due to the differences in stimulants, cell types, and experiment design, the potential effects of p38, JNK, and ERK reported in literatures are not always the same, sometimes even contradictory. One should thus be careful to interpret the data in published literatures.

In the present work, we used Dex as a mineralization inducer to establish an *in vitro* differentiation model in MDPC-23 cell and compared the effects of three specific inhibitors to p38, JNK, and ERK. Despite the limitations of the current experiment, it is suggested that p38 signaling pathway emerges to be an important member in the regulation of differentiation and mineralization of MDPC-23 cell.

5. Conclusion

To summarize, analysis of the data presented by the current study demonstrated that addition of Dex into the mineralization media accelerated differentiation and mineralization in MDPC-23 cell and that inhibition of the MAPK pathways (p38, JNK, and ERK) identified SB202190, a specific p38 MAPK inhibitor completely blocked the ALP activity, expression of osteogenesis markers including BSP, ALP, and OPN, and mineralization. As shown above, there are several studies on Dex-induced signaling via MAPKs regulating osteogenic differentiation and mineralization in other cell types; however, none has reported those effects in odontoblast-like cell. Benefit from the current work provides a possible rationale for future work to use small-molecule activators toward p38 as a treating modality for induction of hard tissue formation in dental pulp lesion.

Conflicts of Interest

The authors declare that there are no conflicts of interest in relation to the publication of the article.

Acknowledgments

References

[1] C. J. Elder and N. J. Bishop, "Rickets," *The Lancet*, vol. 383, no. 9929, pp. 1665–1676, 2014.

[2] Z. Wei and H. T. Liu, "MAPK signal pathways in the regulation of cell proliferation in mammalian cells," *Cell Research*, vol. 12, no. 1, pp. 9–18, 2002.

[3] Y. Sun, W. Z. Liu, T. Liu, X. Feng, N. Yang, and H. F. Zhou, "Signaling pathway of MAPK/ERK in cell proliferation, differentiation, migration, senescence and apoptosis," *Journal of Receptors and Signal Transduction*, vol. 35, pp. 600–604, 2015.

[4] N. J. Darling and S. J. Cook, "The role of MAPK signalling pathways in the response to endoplasmic reticulum stress," *Biochimica et Biophysica Acta (BBA) - Molecular Cell Research*, vol. 1843, no. 10, pp. 2150–2163, 2014.

[5] J. Avruch, "MAP kinase pathways: The first twenty years," *Biochimica et Biophysica Acta (BBA) - Molecular Cell Research*, vol. 1773, no. 8, pp. 1150–1160, 2007.

[6] T. Zhou, S. Guo, Y. Zhang, Y. Weng, L. Wang, and J. Ma, "GATA4 regulates osteoblastic differentiation and bone remodeling via p38-mediated signaling," *Journal of Molecular Histology*, vol. 48, no. 3, pp. 187–197, 2017.

[7] J.-H. Son, B.-S. Park, I.-R. Kim et al., "A novel combination treatment to stimulate bone healing and regeneration under hypoxic conditions: photobiomodulation and melatonin," *Lasers in Medical Science*, vol. 32, no. 3, pp. 533–541, 2017.

[8] S. M. Woo, K. J. Seong, S. J. Oh et al., "17β-Estradiol induces odontoblastic differentiation via activation of the c-Src/MAPK pathway in human dental pulp cells," *The International Journal of Biochemistry & Cell Biology*, vol. 93, no. 6, pp. 587–595, 2015.

[9] W. Qin, P. Liu, R. Zhang et al., "JNK MAPK is involved in BMP-2-induced odontoblastic differentiation of human dental pulp cells," *Connective Tissue Research*, vol. 55, no. 3, pp. 217–224, 2014.

[10] Q. Li, M. S. Valerio, and K. L. Kirkwood, "MAPK Usage in Periodontal Disease Progression," *Journal of Signal Transduction*, vol. 2012, Article ID 308943, 17 pages, 2012.

[11] J. A. C. de Souza, C. Rossa Junior, G. P. Garlet, A. V. B. Nogueira, and J. A. Cirelli, "Modulation of host cell signaling pathways as a therapeutic approach in periodontal disease," *Journal of Applied Oral Science*, vol. 20, no. 2, pp. 128–138, 2012.

[12] J. Tang and T. Saito, "Dexamethasone stimulates nephronectin expression and mediates mineralization in MDPC-23 cell via Akt/mTOR signaling pathway," *Biology, Engineering and Medicine*, vol. 2, no. 3, pp. 1–6, 2017.

[13] S. Murad, D. Grove, K. A. Lindberg, G. Reynolds, A. Sivarajah, and S. R. Pinnell, "Regulation of collagen synthesis by ascorbic acid," *Proceedings of the National Acadamy of Sciences of the United States of America*, vol. 78, no. 5, pp. 2879–2882, 1981.

[14] C.-H. Chung, E. E. Golub, E. Forbes, T. Tokuoka, and I. M. Shapiro, "Mechanism of action of β-glycerophosphate on bone cell mineralization," *Calcified Tissue International*, vol. 51, no. 4, pp. 305–311, 1992.

[15] F. Langenbach and J. Handschel, "Effects of dexamethasone, ascorbic acid and β-glycerophosphate on the osteogenic differentiation of stem cells in vitro," *Stem Cell Research & Therapy*, vol. 4, no. 5, article 117, 2013.

[16] C. T. Hanks, D. Fang, Z. Sun, C. A. Edwards, and W. T. Butler, "Dentin-specific proteins in MDPC-23 cell line," *European Journal of Oral Sciences*, vol. 106, supplement 1, pp. 260–266, 1998.

[17] S. P. Davies, H. Reddy, M. Caivano, and P. Cohen, "Specificity and mechanism of action of some commonly used protein kinase inhibitors," *Biochemical Journal*, vol. 351, no. 1, pp. 95–105, 2000.

[18] Z. Han, D. L. Boyle, L. Chang et al., "c-Jun N-terminal kinase is required for metalloproteinase expression and joint destruction in inflammatory arthritis," *The Journal of Clinical Investigation*, vol. 108, no. 1, pp. 73–81, 2001.

[19] K. Yeung, P. Janosch, B. McFerran et al., "Mechanism of suppression of the Raf/MEK/extracellular signal-regulated kinase pathway by the Raf kinase inhibitor protein," *Molecular and Cellular Biology*, vol. 20, no. 9, pp. 3079–3085, 2000.

[20] S. Chen, J. Gluhak-Heinrich, Y. H. Wang et al., "Runx2, osx, and dspp in tooth development," *Journal of Dental Research*, vol. 88, no. 10, pp. 904–909, 2009.

[21] T. Komori, "Regulation of bone development and extracellular matrix protein genes by RUNX2," *Cell and Tissue Research*, vol. 339, no. 1, pp. 189–195, 2010.

[22] S. Simon, A. J. Smith, A. Berdal, P. J. Lumley, and P. R. Cooper, "The MAP kinase pathway is involved in odontoblast stimulation via p38 phosphorylation," *Journal of Endodontics*, vol. 36, no. 2, pp. 256–259, 2010.

[23] Y. Hu, E. Chan, S. X. Wang, and B. Li, "Activation of p38 mitogen-activated protein kinase is required for osteoblast differentiation," *Endocrinology*, vol. 144, no. 5, pp. 2068–2074, 2003.

[24] T. Matsuguchi, N. Chiba, K. Bandow, K. Kakimoto, A. Masuda, and T. Ohnishi, "JNK activity is essential for Atf4 expression and late-stage osteoblast differentiation," *Journal of Bone and Mineral Research*, vol. 24, no. 3, pp. 398–410, 2009.

[25] B. S. Kim, H.-J. Kang, J.-Y. Park, and J. Lee, "Fucoidan promotes osteoblast differentiation via JNK- and ERK-dependent BMP2-Smad 1/5/8 signaling in human mesenchymal stem cells," *Experimental & Molecular Medicine*, vol. 47, no. 1, article no. e128, 2015.

[26] L. Chen, L. Zheng, J. Jiang et al., "Calcium Hydroxide–induced Proliferation, Migration, Osteogenic Differentiation, and Mineralization via the Mitogen-activated Protein Kinase Pathway in Human Dental Pulp Stem Cells," *Journal of Endodontics*, vol. 42, no. 9, pp. 1355–1361, 2016.

[27] J. Tang and T. Saito, "Nephronectin Stimulates the Differentiation of MDPC-23 Cells into an Odontoblast-like Phenotype," *Journal of Endodontics*, vol. 43, no. 2, pp. 263–271, 2017.

[28] M. Ikehata, A. Yamada, N. Morimura et al., "Wnt/β-catenin signaling activates nephronectin expression in osteoblasts," *Biochemical and Biophysical Research Communications*, vol. 484, no. 2, pp. 231–234, 2017.

[29] K.-S. Lee, S.-H. Hong, and S.-C. Bae, "Both the Smad and p38 MAPK pathways play a crucial role in Runx2 expression following induction by transforming growth factor-β and bone morphogenetic protein," *Oncogene*, vol. 21, no. 47, pp. 7156–7163, 2002.

[30] Y. Lu, L. Ye, S. Yu et al., "Rescue of odontogenesis in Dmp1-deficient mice by targeted re-expression of DMP1 reveals roles for DMP1 in early odontogenesis and dentin apposition in vivo," *Developmental Biology*, vol. 303, no. 1, pp. 191–201, 2007.

[31] A. Nakagawa, T. Okinaga, W. Ariyoshi, T. Morotomi, C. Kitamura, and T. Nishihara, "Effects of Interferon-γ on odontoblastic differentiation and mineralization of odontoblast-like cells," *The Inflammation and Regeneration*, vol. 35, no. 4, pp. 210–217, 2015.

[32] D. Seki, N. Takeshita, T. Oyanagi et al., "Differentiation of odontoblast-like cells from mouse induced pluripotent stem cells by pax9 and bmp4 transfection," *Stem Cells Translational Medicine*, vol. 4, no. 9, pp. 993–997, 2015.

[33] T.-W. Tan, Y.-L. Huang, J.-T. Chang et al., "CCN3 increases BMP-4 expression and bone mineralization in osteoblasts," *Journal of Cellular Physiology*, vol. 227, no. 6, pp. 2531–2541, 2012.

[34] K. Saito, E. Fukumoto, A. Yamada et al., "Interaction between fibronectin and β1 integrin is essential for tooth development," *PLoS ONE*, vol. 10, no. 4, Article ID e0121667, 2015.

[35] W. Qin, Z. M. Lin, R. Deng et al., "p38a MAPK is involved in BMP-2-induced odontoblastic differentiation of human dental pulp cells," *International Endodontic Journal*, vol. 45, no. 3, pp. 224–233, 2012.

[36] S. Simon, A. J. Smith, P. J. Lumley et al., "Molecular characterization of young and mature odontoblasts," *Bone*, vol. 45, no. 4, pp. 693–703, 2009.

[37] Y. Yu, L. Wang, J. Yu et al., "Dentin matrix proteins (DMPs) enhance differentiation of BMMSCs via ERK and P38 MAPK pathways," *Cell and Tissue Research*, vol. 356, no. 1, pp. 171–182, 2014.